Remote sensing of aboveground and belowground function in grassland ecosystems

A thesis submitted to the University of Manchester
for the degree of Doctor of Philosophy
in the Faculty of Humanities

2023

Alexandra H Hamer

School of Environment, Education and Development

LIST OF CONTENTS

Word count = 49, 489

LIST OF TABLES

LIST OF FIGURES

LIST OF ACRONYMS

AOP = airborne observation platform

C = carbon

CHL = chlorophyll

CV = coefficient of variation

CWM = community weighted mean

EVI = enhanced vegetation index

F:B = fungi to bacteria ratio

GAI = global aridity index

LDMC = leaf dry matter content

LES = leaf economics spectrum

MAP = mean annual precipitation

MAT = mean annual temperature

MSAVI = modified soil adjusted vegetation index

MSE = mean square error

MSI = multispectral instrument

N = nitrogen

NDMI = normalised difference moisture index

NDVI = normalised difference vegetation index

NEON = National Ecological Observatory Network

NIR = near infra-red

NLCD = national land cover definition

OOB = out of box

PCA = principal components analysis

PLFA = phospholipid fatty acid

PLSR = partial least squares regression

RE = red edge

RF = random forest

RMSE = root mean square error

SAVI = soil adjusted vegetation index

SLA = specific leaf area

SWIR = short wave infra-red

ABSTRACT

Grasslands are one of the most extensive biomes on Earth, are integral to global biogeochemical cycling, and are directly depended upon by human societies for food and fuel. Important functions of grassland ecosystems include carbon storage, biomass production and nutrient cycling, which are driven by closely interlinked grassland plant and soil communities. Measuring and monitoring these communities across large spatial extents is vital in order to understand and predict the impacts of climate and land-use changes which affect grasslands currently and are forecast into the future. However, current field-based methods are intensive and time-consuming to carry out, and therefore limited in their spatial and temporal coverage. Remote sensing technologies including imagery from airborne and satellite platforms have transformed capabilities to measure the biosphere at large scales. However, grassland ecosystems are under-represented in remote sensing research, and the application of remote sensing to belowground ecosystem functions remains relatively unexplored. The aim of this thesis is to investigate how remote sensing data can be used to retrieve important information about the above- and belowground portions of grassland ecosystems, across large spatial extents. This aim is achieved by pairing *in-situ* soil and plant community data from large-scale ecological monitoring networks with hyperspectral and multispectral imagery from airborne and satellite platforms, to answer three specific research objectives. 1) to predict variation in soil microbial communities from airborne hyperspectral imagery, 2) to retrieve community-level plant functional traits from multispectral satellite data and 3) to predict ecosystem multifunctionality using long-term (decadal) timeseries of satellite-derived vegetation indices. All objectives are addressed using observations from varied natural grassland communities distributed at continental and global scales. The results of the three research chapters demonstrate that soil microbial communities, in particular microbial community structure, can be retrieved with high accuracy (up to R^2 0.68, NRMSE 9%) from hyperspectral sensing. Satellite multispectral data was able to retrieve variation in 13 out of 20 foliar traits, in some cases with comparable accuracy to recent hyperspectral mapping (up to R^2 0.76, NRMSE 12%). The ability of satellite systems to facilitate a multitemporal perspective on the ecosystem was valuable for predicting ecosystem multifunctionality, where past vegetation dynamics and stability have important legacy effects on contemporary functioning. Overall, the thesis shows that remote sensing technologies have the potential to contribute to understanding of above- and belowground grassland functions by capturing ecological properties of the vegetation surface which are not able to be measured in the field, and by expanding the spatial and temporal scales across which relationships can be found. Remote sensing should be incorporated into the design of future large-scale ecological monitoring efforts, with a view to understanding and preserving grassland ecosystem functions for the future.

DECLARATION

No portion of the work referred to in the thesis has been submitted in support of an application for another degree or qualification of this or any other university or other institute of learning.

COPYRIGHT STATEMENT

ACKNOWLEDGEMENTS

The road has been long. Thanks to all the wonderful people who have helped me along the way.

Harriet and Dan, my companions at the beginning.

My cohort and peers for all the fun in our first PhD year. Gizem, Sarah, Sam, Beth, Adam, Ksenia, Simon, Timna, Dael, Oskar, Adam, Liz. The ecology lab group, especially Debbie and Chris.

The Weirdos for being such a beautiful, welcoming cult. And for the parties.

Furrowed Brow: Richey, Cristy, Ryan, Meg and Evie. For all the madness and the laughs.

The Abbertonians, babes, goats. Andy, Rhys, Aristeidis, Angelika, Ruth and Olivia. For the mojitos and the garden parties and cards round the table. For being a family, with all the love and the drama and getting through the rough years.

Joe and Sarah for the time in their lovely house on Sydney Road.

The Leaders: Nicholas, Susie, Fawei, Huda, Ellio, Lara.

The yoga teachers for all their strength and wisdom. Sarah, Sue, Viktor, Kelly, Lianne and most of all Dana.

The Old Abbey Taphouse, The Peer Hat, Bottle & Barrel & Bank Vault.

Colleagues old and new. Special mention to Jonny, Emma, Pete, Andy and Morgan.

Wonderful friends old and new. Richard, the best brother I could ask for. The queens Poppy and Chloe. Kind Tom, amazing Nick, fabulous Anna & Womba. It's such a pleasure to watch your lives unfolding alongside mine.

Beautiful, gentle and generous Casper.

All the rest, the auld lang syne-ers.

To my supervisors, of course. Richard, Tim and especially Angela, without whose hard work and patience and guidance nothing would have been possible.

Mum and Dad, to whom I owe everything.

Phoebe, my inspiration, my yardstick and my rock.

What an education it has been. To new adventures! Love is everywhere!

1. Introduction

1.1 Background

Grasslands are some of the most extensive and exploited ecosystems worldwide, integral to the subsistence of human societies, and under a plethora of climate and land-use pressures which act across continental and global spatial scales (Reinermann et al., 2020). In order to monitor and predict changes taking place in grasslands, understanding of both the above- and belowground portions of grassland ecosystems is necessary, because plant and soil communities together drive vital grassland functions. The study of aboveground-belowground links and feedbacks has become a major research theme in ecology (Bardgett, 2018), but is limited in scale by practical constraints of field sampling. Remote sensing is able to gather information about the surface of vegetation communities rapidly and in a spatially continuous manner across global scales, and so has great potential to contribute to grassland research.

Evidence from grasslands worldwide has shown that grassland soil communities, belowground and aboveground functions and whole-ecosystem multifunctionality can be predicted from plant community attributes which are measurable above ground including plant functional traits, productivity, diversity and phenology (de Vries, Manning, et al., 2012; Delgado-Baquerizo et al., 2018). There have been efforts to retrieve these vegetation properties from remote sensing data at a range of spatial scales and in different ecosystems worldwide; for example, productivity is routinely retrieved from remote sensing using vegetation indices (Pettorelli et al., 2005), whereas plant functional traits and diversity are more recent avenues of research interest, with promising early results (Cavender-Bares et al., 2020a). For the purpose of linking remote retrieval of vegetation properties to aboveground-belowground ecology, several key research gaps remain.

First, research explicitly linking remote sensing of the vegetation surface to belowground communities has been sparse. Though remote sensing data has been used in models of soil physical and chemical properties, such as soil carbon stocks (S. Liu et al., 2019; Wilson et al., 2017), there is increasing recognition that the dynamic populations of bacteria and fungi in soils are both key drivers of ecosystem functions at global scales and closely connected to plant communities at the surface (Bardgett & Van Der Putten, 2014). Recent work has demonstrated remarkably strong relationships between canopy imaging spectroscopy and the size, structure and functions of soil microbial communities in forest ecosystems (Madritch et al., 2014; Sousa et al., 2021), but it is not known to what extent these links may be found in grasslands.

Second, the use of multispectral satellite data to retrieve grassland functional traits. Grassland remote sensing to date has focused on the use of extremely detailed hyperspectral data, which has been used to retrieve grassland foliar traits at local to continental scales with success (Cavender-Bares et al., 2022; Van Cleemput et al., 2018; Z. Wang et al., 2019). Multispectral satellite data is of much coarser spectral and often spatial resolution, but has global spatial coverage and so has the most potential for assessing grassland functioning at global scales. Recent work has successfully retrieved foliar functional traits from multispectral Sentinel-2 data across tropical forest ecosystems (Aguirre-Gutiérrez et al., 2021), demonstrating that such data may also have potential in grasslands.

A key opportunity presented by the use of multispectral satellite data is its regular availability over long time periods, up to decades (Wulder et al., 2022). Relationships between plants, soils and reflectance are dynamic on multiple interacting timescales (Bardgett et al., 2005), for example throughout the course of a single growing season (R. Wang, Gamon, Montgomery, et al., 2016), up to the decades it takes to build up soil carbon pools (Millard & Singh, 2010). Multitemporal, multispectral timeseries of reflectance have been used to retrieve plant phenology (Dronova & Taddeo, 2022), and to improve remote assessments of community diversity in grasslands (Rossi et al., 2021), and therefore have great potential to contribute to the study of belowground ecosystems.

Third, remote sensing of grasslands has most often taken place across landscape scales and in the context of grassland management, with much less work taking place in diverse natural grasslands across broad ecoclimatic gradients. Globally, grassland ecosystems are extremely diverse in terms of their productivity, levels of vegetation density and coverage, and also in their relative composition of herbaceous and woody plant lifeforms, particularly marginal grasslands which are at the forefront of environmental change (Ratnam et al., 2011; Veldman et al., 2015). All of these factors can affect both modes of aboveground-belowground functioning (Grigulis et al., 2013) and the relationship between land surface spectral reflectance and ecological properties (Hacker et al., 2022), and so are likely to impact the ability of remote sensing to retrieve ecological functions (Cavender-Bares et al., 2022). Ecological studies have revealed relationships such as productivity-multifunctionality, and covariation of certain plant traits, to be generalisable across ecosystems worldwide (Borer et al., 2014; I. J. Wright et al., 2004), and it is important to identify the extent to which remote sensing is also able to identify patterns which are generalisable across global scales.

1.2 Thesis aims and objectives

The aim of this thesis is to investigate how remote sensing can be used to characterise aboveground and belowground functions of grasslands across large spatial extents.

This aim is achieved through the following research objectives.

1. To evaluate the extent to which soil microbial biomass, community structure and processes can be predicted from airborne imaging spectroscopy in grasslands and shrublands spanning broad ecoclimatic gradients. This builds on previous work which has demonstrated strong links between vegetation canopy spectroscopy and underlying soil microbial communities in forests (Madritch et al., 2014; Sousa et al., 2021).
2. To establish to what extent aboveground plant functional traits, including those which can represent soil communities and functions at the surface, can be retrieved in grasslands across large spatial extents from multispectral satellite data. This builds on previous work retrieving grassland foliar traits from airborne hyperspectral imagery (Z. Wang et al., 2019, 2020) and forest foliar traits from multispectral satellite imagery (Aguirre-Gutiérrez et al., 2021).
3. To identify the relationships between above- and belowground ecosystem functions, plant diversity and phenology across diverse natural grasslands at the global scale, and investigate whether these links can be used to predict grassland ecosystem multifunctionality from multitemporal satellite data. This builds on previous work demonstrating that ecosystem multifunctionality is associated with aboveground plant diversity across global grasslands (Hautier et al., 2018) and that plant diversity and ecosystem multi-functioning are linked to longer growing seasons, faster rates of green-up (Zaret et al., 2022) and greater phenological stability in managed grasslands (Weber et al., 2018), wetlands (Dronova et al., 2022) and forests (Paruelo et al., 2016) from different parts of the world.

1.3 Thesis structure

The thesis is structured around three separate research chapters (Chapters 3-5), each of which primarily addresses one of the research objectives along with some more specific objectives and hypotheses. Overall, the research chapters in this thesis present empirical

models between remote sensing imagery and field observations of above- and belowground grassland properties. Field-measured properties used in this thesis are sourced from large-scale ecological networks, the National Ecological Observatory Network (NEON) and the Nutrient Network (NutNet). Using secondary field data enabled the research to be completed without the planned fieldwork which was cancelled due to the COVID-19 pandemic, and enabled the scope of the work to be expanded to continental and global scales.

Chapter 3 addressed the first research objective using coincident soil microbial properties, aboveground plant traits and airborne hyperspectral imagery sourced from NEON. Data from 13 network field sites were used, representing grassland and shrubland ecosystems spanning a wide productivity gradient and distributed across North America. Random forest and partial least squares regression were used to predict variation in six soil properties representing the size, structure and functions of bacterial and fungal communities. The key outcomes of Chapter 3 are models of the soil microbial properties from field-measured plant traits, including variable importance scores identifying which plant traits are most closely linked to which soil properties (random forest), and models of soil microbial properties directly from canopy spectra (partial least squares regression).

To address the second objective, aboveground plant trait measurements from NEON were matched with coincident Sentinel-2 satellite imagery (Chapter 4). Eleven grassland sites were selected from the NEON network, distributed across North America and representing a range of grassland types, from homogenous pasture landscapes to those with a mixed matrix of herbaceous and woody vegetation. Random forest regression models of 20 plant functional traits were created using Sentinel-2 satellite bands, vegetation indices derived thereof, and ancillary climate and location variables as predictors. Sub-questions addressed the effects of grassland vegetation composition on the success of modelling traits from spectra, and the effect of temporal offset between field and satellite data sampling on model accuracy.

The third objective was addressed using ecosystem multifunctionality and species richness measured at 90 grassland sites distributed worldwide as part of the Nutrient Network, along with 30-year Landsat satellite timeseries (Chapter 6). The satellite timeseries were used to retrieve phenology metrics of the vegetation community at each site, including rate of growth and senescence, peak biomass, growing season length, and phenological stability over the 30-year period. Relationships between satellite-derived phenological properties, individual ecosystem properties, multifunctionality and diversity were characterised using Pearson's correlations, to explore whether ecosystem multifunctionality is detectable in the seasonal patterns of surface reflectance. To investigate the potential of satellite-derived phenology to predict ecosystem multifunctionality, phenological properties were used together along with

climate and location variables to predict ecosystem multifunctionality using random forest regression.

Each research chapter contains a background, detailed methodology and discussion specific to the chapter. The thesis literature review (Chapter 2) gives more detail about previous work which is relevant to all three research chapters and the overall aim of the thesis. Finally, evidence from across the three research chapters is brought together in the discussion and conclusion sections (Chapters 6 and 7), which draw out common themes and place the chapter conclusions in the context of the overall thesis objectives.

2. Literature review

2.1 The global importance of grassland ecosystem functioning

Grasslands cover up to 40% of the Earth's land surface, span a wide range of latitudes and support a multitude of natural and human systems (O'Mara, 2012; R. White et al., 2000). The ecosystem functions that take place in grasslands support services which are fundamental to human societies at local to global scales. Of these, three are considered to be crucial at the global scale. First, the production of aboveground biomass for food, fuel, fibre and supporting livestock (I. Ali et al., 2016; Reinermann et al., 2020; Svoray et al., 2013). Grasslands constitute 70% of the global agricultural area and so directly facilitate human subsistence (Reinermann et al., 2020). Second, the storage of carbon (C). Over 10% of the total biosphere C store is found in grasslands, and up to 98% of this is stored below ground in grassland soils (Eswaran et al., 1993; Jones & Donnelly, 2004). These C stocks are essential for maintaining the structure and quality of the soil, which enables grasslands to support plant life including crops, and are globally significant in terms of climate regulation (Bardgett, 2017; van der Putten et al., 2016). The third key function of grasslands is their role in the cycling of nutrients, particularly nitrogen (N) (Risch et al., 2019). When nutrient cycling is not maintained nutrients are leached from the system, resulting in decreased soil fertility and soil degradation, and causing ecological problems downstream if excessive levels of nutrients are introduced into natural ecosystems (de Vries, Bloem, et al., 2012; Wall et al., 2010).

There are a multitude of biologically-driven processes that operate together above- and belowground to provide ecosystem functions and services in grasslands (Bardgett & Van Der Putten, 2014). Photosynthesis and nutrient uptake by the vegetation community convert atmospheric carbon and mineral nutrients into organic forms, constituting plant growth (primary productivity). These organic materials are then transferred to the soil, both as litter inputs and as exudates from roots. Here, the soil biological community decompose organic structures, returning carbon to the atmosphere through respiration, making nutrients available for plant uptake through mineralization, or alternatively transforming the materials into more stable forms which will be stored in the soil (carbon and nutrient cycling). The composition and diversity of the plant and soil communities determines the rates at which these processes take place, and thus the overall functioning of the ecosystem.

While the dynamics of aboveground communities have been extensively studied in relation to ecosystem functions and services, the contribution of the belowground community has historically been overlooked. Recent work in ecology has sought to address this research gap (Delgado-Baquerizo et al., 2016; Guo et al., 2021; Legay et al., 2014; Pommier et al., 2018;

Van Der Heijden et al., 2008). However, as soil communities are under the ground and highly variable in time and space, assessment of their conditions and dynamics continues to present a challenge. Addressing this knowledge gap is a particularly urgent research priority given the multitude of pressures that are affecting grasslands worldwide.

Grasslands are one of the most exploited biomes worldwide due to their close links with human societies, but have historically been overlooked in terms of conservation priorities (Nerlekar & Veldman, 2020; Veldman et al., 2015). More than two-thirds of grasslands worldwide have been converted into anthropogenic ecosystems (Ellis & Ramankutty, 2008; Foley et al., 2005). Changing management regimes including intensification or abandonment of agricultural land (I. Aneece & Epstein, 2015; Tardy et al., 2015; Weber et al., 2018), and conservation or restoration efforts to anthropogenically reverse these processes (Fry et al., 2017; Tian et al., 2022) all have significant implications for aboveground and belowground grassland functioning. Grasslands are also dynamic ecosystems that can shift to forests or deserts with changing climatic conditions, and so are vulnerable to ongoing and predicted climate changes, such as rising temperatures and increased incidence and severity of drought, and associated indirect effects such as the range expansion of invasive species (Borer et al., 2017; Brooks et al., 2006; Eisenhauer & Scheu, 2008; Schirpke et al., 2017). Because soil communities and plant communities both respond to these pressures, as well as influencing each other, there is potential for varied and complex feedback mechanisms to be triggered, leading to consequences which are difficult to predict and may be unexpected (Baxendale et al., 2014). To predict and monitor how pressures impact grassland ecosystems across short and long timescales, it is important to be able to retrieve above- and belowground functions accurately, rapidly, and across large spatial extents.

2.2 The potential of remote sensing for large-scale monitoring of the biosphere

There is a need to study grasslands across large spatial scales. Experiments at the plot or site scale are important for isolating effects and identifying mechanisms and processes that take place under certain conditions, but the findings may not be applicable to other sites and systems (Borer et al., 2014). In order to be able to predict ecosystem responses to pressures which act at regional or global spatial scales, such as climate changes, it is necessary to conduct ecological research across equivalent scales, incorporating a range of natural systems that are representative of the diversity of environments that are found in nature (Oehri et al., 2017; Reichstein et al., 2014). Only then can generally-applicable relationships be identified. In recognition of the need for joined-up, large-scale ecology are a number of continental and global ecological monitoring networks, such as the National Ecological Observatory Network (Kampe et al., 2010), and the Nutrient Network (Borer et al., 2014), and open databases such

as TRY (Gallagher et al., 2020; Kattge et al., 2011), which aim to collect or collate standardised reproducible datasets from a range of widely distributed ecosystems. These networks have provided valuable insights on the generality of key ecological relationships such as between productivity and diversity (Borer et al., 2017), response of ecosystems to widespread pressures such as nutrient additions (Leff et al., 2015), or covariation of plant functional properties worldwide (Díaz et al., 2016).

However, despite the large and growing scope of these networks, substantial gaps remain in sampling of vegetation and soil communities worldwide. The time and effort required to thoroughly sample across time and space results in clustered data points, with a geographical bias towards more easily accessible regions while more remote regions of the globe are under-represented (Anderson, 2018; Jetz et al., 2016). Gaps can be filled by interpolating between data points using abiotic factors such as climate and geological properties (Griffiths et al., 2011, 2016), but such approaches are of coarse spatial and temporal resolution, and unable to capture the dynamic nature of vegetation communities (Díaz et al., 2016; Moreno-Martínez et al., 2018). Remote sensing can generate data across large spatial extents and at spatial and temporal detail that is impossible to achieve using field-based measures; therefore there has been recent interest in the potential for remote sensing to be applied to global monitoring of the biosphere.

Remote sensing data captured from drones, planes and satellites enables many of the practical limitations of field sampling to be overcome, and therefore expands the spatial and temporal extent and detail with which environmental data can be gathered. Remote sensing data is spatially continuous, viewing the Earth's surface as a grid of pixels, which can range from millimetres to hundreds of metres in size. The spatially continuous nature of remotely sensed data makes it suitable for interpolating between point-based samples collected on the Earth's surface. It also makes it easy to increase or decrease the spatial detail of data and thus integrate or compare perspectives of ecosystems across multiple spatial scales (Davidson & Csillag, 2001; Helfenstein et al., 2022; Rossi et al., 2022). Remote sensing data has extensive coverage of the Earth and is therefore able to gather data on remote regions with ease (Aguirre-Gutiérrez et al., 2021), although data availability is constrained by other factors such as frequent cloud cover in tropical and polar regions. There is usually a trade-off between spatial extent or coverage and spatial and spectral detail when choosing remote sensing datasets. Spectroscopy or hyperspectral imagery captures large amounts of spectral detail which can be used to identify spectral absorption features associated with specific leaf chemicals, such as photosynthetic pigments (Gitelson et al., 2001, 2002; Ustin, Asner, et al., 2009), or phenolic compounds (Couture et al., 2016). Imaging spectroscopy has been used to capture plant functional traits and diversity in grasslands (Schweiger et al., 2018; Van Cleemput et al., 2018).

However, hyperspectral imaging systems are usually hosted on airborne platforms and used for plot and landscape-scale studies, and as such do not currently have the large-scale geographic coverage which is available from satellite remote sensing, although planned hyperspectral satellite missions are expected to change this in the near future (Pettorelli et al., 2018a).

Multispectral sensors found on satellite platforms have reduced spectral detail relative to hyperspectral sensors but are able to cover the entire globe with frequent return periods of up to one day, facilitating global-scale and multi-temporal studies. Different satellite sensors have various benefits; for example the recent Sentinel-2 multispectral instruments feature narrow bands in the red edge spectral region, specifically for retrieving vegetation properties (Clevers & Gitelson, 2013; Delegido et al., 2011), and the Landsat missions have a data archive spanning over 30 years and so facilitate long-term studies (Günal et al., 2021; Vermote et al., 2016; Wilson et al., 2017; Wulder et al., 2022). Satellite multispectral datasets have been used to create or enhance large-scale maps of many important environmental properties including plant traits (Aguirre-Gutiérrez et al., 2021; Butler et al., 2017; Moreno-Martínez et al., 2018), habitats (Tuanmu & Jetz, 2015) and productivity (Oehri et al., 2017; Wallis et al., 2019), among others (Meyer & Pebesma, 2022).

Historically, grasslands have been under-studied using remote sensing, compared to forest ecosystems, with remote sensing of grasslands often carried out from an agricultural or management perspective (I. Ali et al., 2016; Reinermann et al., 2020; Weber et al., 2018). Remote sensing of the belowground biosphere has also been relatively sparse, except for work modelling carbon stocks, which incorporates a significant belowground component (Bartholomeus et al., 2011; Schimel et al., 2015; Wilson et al., 2017), and some other recent efforts, such as linking satellite data to soil salinity (Günal et al., 2021) and nematode abundance (van den Hoogen et al., 2019). A growing body of research in ecology which links aboveground to belowground ecosystems, and predicts whole ecosystem functioning from proxies which can be assessed at the surface, may provide a link for remote sensing methodologies to extend to the belowground portion of the ecosystem.

The identity, diversity and functions of plant and soil organisms exert strong influences over each other within ecosystems (Wardle David A. et al., 2004). Understanding these ecological linkages has become a research focus in recent decades, and is now a major theme in terrestrial ecology (Bardgett, 2018). Specific plant and soil microorganism species form associations with one another, which can be mutually beneficial and are in many cases required for plant growth, for example the association of mycorrhizal fungi with plant root systems (Bradford et al., 2002; López-García et al., 2017; Van Der Heijden et al., 2008).

Relationships between co-occurring plant and soil organisms can also be antagonistic, for example the build-up in soils over time of microbial pathogens limit the growth of particular species with which they interact (Klironomos, 2002; Kulmatiski et al., 2008). These associations form the basis of plant-soil feedback mechanisms that influence species growth, competition and succession over time (Baxendale et al., 2014). At the community scale, relationships between plant and soil organisms can be understood not only through specific species-species interactions, but through other integrated aspects of the plant community such as diversity including species richness and evenness (De Deyn et al., 2011; Eisenhauer et al., 2010; Lange et al., 2015), presence or abundance of particularly influential species (Laughlin, 2011; Soliveres et al., 2016), and community-level functional traits (Cantarel et al., 2019; Grime, 1998; Lavorel et al., 2011; Lavorel & Grigulis, 2012; Legay et al., 2014).

2.3 Plant functional traits for linking aboveground and belowground ecology

Plant trait based approaches investigate how the functional properties of plants, such as growth rate, leaf area or root length, as opposed to their taxonomic identity are related to other components of the ecosystem, including belowground communities and functions (Bardgett, 2017; Delgado-Baquerizo et al., 2018; Funk et al., 2017). There are several benefits to the use of functional traits to understand the aboveground community. First, in determining the functional traits of plants that cause and respond to changes in the environment, soils, or other ecosystem components, the mechanisms that drive the links can begin to be identified (Legay et al., 2014). For example, traits facilitating rapid nitrogen uptake may enable plants to out-compete soil nitrogen-reducing bacteria for nutrients, and therefore explain the influence of plants on the composition of soil microbial communities (Moreau et al., 2015). Trait-based approaches can therefore help to answer the question of *why* above- and belowground communities form the spatial associations that are observed, and therefore how they may be expected to respond to environmental change, for example (Bardgett, 2017; Green et al., 2008). Second, trait-based approaches are sensitive to phenotypic variation that occurs between individuals of the same species (intraspecific) as well as between species (interspecific). Intraspecific variation can account for up to 30% of total biological variation observed within populations, and is therefore significant for ecosystem functioning and, at large scales, biogeochemical cycling (Albert et al., 2010; Siefert et al., 2015). Approaches to scaling-up functioning which use species mean trait values, for example aggregating to community-weighted means by species abundance (Grime, 1998), are not able to fully account for intraspecific variation, where direct trait-based approaches can (Funk et al., 2017). For this reason, trait-based approaches are more suitable than species-based approaches for assessing functioning over large spatial scales.

The best-established links between aboveground plant traits and soil communities are centred around leaf and whole-ecosystem economics, on a spectrum from exploitative to conservative resource use. Plant traits of a wide variety of species across the globe have been shown to have consistent associations with one another, described by the leaf economics spectrum (LES) (Reich, 2014; I. J. Wright et al., 2004). Traits which facilitate rapid photosynthesis, plant growth and nutrient uptake include high specific leaf area (SLA) and high leaf nutrient content, in particular nitrogen. These leaves covary to promote rapid growth at the expense of leaf longevity (exploitative), and the high-quality, nutrient-rich leaf litter is rapidly broken down by microbes in the soil. On the other end of the spectrum are higher values of traits which promote leaf longevity at the expense of growth rate (conservative), including robust complex structures such as lignin and other secondary metabolites, which are slow to decompose. These sets of associated, covarying plant traits, or trait syndromes, have been shown to be mirrored belowground in the size, structure and functioning of soil communities (Pérez-Ramos et al., 2012). High-quality litter, which is more readily decomposed, promotes the bacterial component of the soil microbial community as bacterial species are adapted to break down such material rapidly. Conversely, soil fungi are better adapted to decompose tough, lower-quality litter, so soil community structure with a higher biomass of fungi in relation to bacteria, or a higher F:B ratio, is associated with a conservative plant trait syndrome (de Vries, Manning, et al., 2012; Fry et al., 2018; Schellberg & Pontes, 2012).

The fast-slow economics of associated aboveground and belowground ecosystems are driven by factors including climate, geological or edaphic properties, and feedback mechanisms between the two communities (de Vries, Manning, et al., 2012; Delgado-Baquerizo et al., 2018). Plant and soil community economics have also been shown to drive ecosystem functions and services. For example, fast-cycling communities promote rapid turnover of carbon and nutrients, which reduces the provision of C and N retention in the soil in favour of greater productivity (Faucon et al., 2017; Grigulis et al., 2013; Lavorel, 2013; Lavorel et al., 2011; Lavorel & Grigulis, 2012). These associations between plant traits, soil communities and ecosystem functioning provide a pathway by which aboveground measurements of plant traits can be used to predict belowground ecosystems and whole-ecosystem functioning (de Vries, Manning, et al., 2012; Leff et al., 2018; Manning et al., 2015). This is particularly valuable given the challenging nature of measuring soil communities in the field, which highly variable across fine spatial and temporal scales, and given the potential of remote sensing to retrieve plant traits.

2.3.1 Remote sensing of plant functional traits

Spectral datasets are particularly suitable for application to trait-based approaches, because reflectance of light by vegetation is directly related to morphological and chemical traits as opposed to species identity (Lausch et al., 2018). There are a number of methods by which reflectance data can be used to retrieve plant traits. These include the development of spectral indices, where reflectance in specific portions of the spectrum, which are known to respond differently to certain leaf properties, are used to create a metric, which is then evaluated empirically using field data. Indices have been created to isolate and respond to many different foliar properties, in particular vegetation pigments (chlorophyll and carotene) (Clevers & Gitelson, 2013; Gitelson et al., 2002, 2006), water content (Gao, 1996) and total greenness or density. The most well-known vegetation index is the NDVI, which responds to vegetation greenness or density, and is widely used as a proxy measure of biomass and productivity (Pettorelli et al., 2005). Indices are designed to directly capture one aspect of the vegetation canopy, but can be used in combination as predictor variables for many associated ecosystem properties (A. M. Ali, Darvishzadeh, Skidmore, et al., 2017; Gaitán et al., 2013; Räsänen et al., 2021; Rivero et al., 2009; Tan et al., 2022; Tuanmu & Jetz, 2015). The covariation of many plant traits enables those that are not associated directly with particular spectral absorption features to be inferred by their covariation with those that do, termed constellation effects (Nunes et al., 2017).

There has been a recent move towards using more computationally-complex multivariate approaches which utilise the whole spectrum simultaneously, such as partial least squares regression (PLSR), to retrieve ecosystem properties. These are particularly powerful when used in combination with high-dimensionality hyperspectral data, and this combination of data and method have been used recently to retrieve foliar traits from grasslands, with success at landscape to continental scales (Homolová et al., 2013a; Van Cleemput et al., 2018; Z. Wang et al., 2019, 2020). The other key approach to retrieving foliar traits from remote sensing is radiative transfer models, which are physically-based as opposed to empirically-based, produce relationships that are more applicable across a range of ecosystems, but also require more known values to be inputted (Darvishzadeh *et al.*, 2011). Radiative transfer models are valuable but currently limited in the number of traits they can successfully retrieve and have generally been developed for forest ecosystems, although have been applied to grasslands with varying success (Pau et al., 2022; Rossi et al., 2020). There is great potential for spectral retrieval of plant traits to contribute to understanding and prediction of belowground and whole-ecosystem functioning in grasslands, however in order to realise this further research is needed in several key aspects.

First, there has been a significant bias towards forest ecosystems in remote sensing of plant traits, and much less is known about grasslands. Grasslands pose different challenges to forest ecosystems, due to small sizes of organisms relative to sensor resolution and therefore of mixing of species at sub-pixel scales, which has been found to decrease the strength of relationships at the leaf level (Hacker et al., 2022), compared to studies in forests where it is often possible to retrieve individual tree crowns from imagery (Aguirre-Gutiérrez et al., 2021; Schneider et al., 2017). In many grasslands, the vegetation surface at the spatial scale of remote sensing imagery (metres to tens of metres) is likely to include a mixture of herbaceous plants and isolated shrubs or trees (Reinermann et al., 2020), particularly at marginal grasslands or areas where active land cover change is taking place, and mixing of different plant life forms with different leaf structures and ecology can decrease the strength of relationships between spectra and vegetation properties (Hacker et al., 2022; House et al., 2003; Pau et al., 2022). Very few studies have been carried out retrieving traits across mixed grassland-woodland ecosystems (Z. Wang et al., 2020), despite the prevalence and importance (Ratajczak et al., 2012; Ratnam et al., 2011; Sexton et al., 2015; Y. Xu et al., 2022). Herbaceous and woody species differ in their physiology and ecology. For example, functional importance of leaves, stems and roots is not consistent among plant life-forms, and a whole-plant perspective, rather than just foliar traits, may be more appropriate in herbaceous communities where root exudates constitute a larger proportion of total inputs from above to belowground (De Long et al., 2019; Freschet et al., 2010; Funk & Cornwell, 2013; Laliberté, 2017; Poorter et al., 2014). Bare soil areas in imagery are also likely to be more prevalent at sub-pixel scales in grasslands than forest ecosystems, because of the lower density of vegetation overall (Hauser et al., 2021; Y. He et al., 2020; R. Wang et al., 2018a).

What work there is on trait retrieval in grasslands has been almost exclusively based on imaging spectroscopy or hyperspectral sensing, where extremely high levels of spectral detail are able to identify small absorption features associated with particular leaf properties (Homolová et al., 2013a; Obermeier et al., 2019; Van Cleemput et al., 2018; Z. Wang et al., 2019). Multispectral sensors have been demonstrated to retrieve foliar traits in forest ecosystems (Aguirre-Gutiérrez et al., 2021; Ma et al., 2019) and at very coarse resolution across mixed biomes globally (Butler et al., 2017; Moreno-Martínez et al., 2018). However, there have been very few attempts to retrieve grassland traits using multispectral remote sensing imagery, which is of coarser spatial and spectral resolution than hyperspectral imagery, but has a much greater global availability and coverage, and therefore has the most potential for trait retrieval at large geographic scales.

Finally, it isn't known to what extent the plant traits which are successfully retrieved from spectra are in common with those which are useful for retrieving belowground

properties. Ecology and remote sensing studies tend to have different sets of plant traits that are the focus of studies, based on which are the easiest to retrieve using field-based or spectral techniques. For example, chlorophyll content is one of the most common target traits in remote sensing due to its strong photosynthetic properties and therefore influence on reflectance (Croft et al., 2017; Kozhoridze et al., 2016; Ustin, Asner, et al., 2009). However, chlorophyll is not often included in the suite of traits used to investigate aboveground-belowground linkages in the field, so it is unknown to what extent this trait could represent belowground properties at the surface. Conversely, traits which are usually the focus in ecology, such as relative growth rate, vegetation height and structural properties like SLA and LDMC are not as clearly represented in an aerial perspective of the vegetation surface as they are from the ground and so are less often retrieved, although SLA has been more commonly modelled in recent years (A. M. Ali, Darvishzadeh, Skidmore, et al., 2017). This discrepancy could make it challenging to link the fields of remote sensing and ecology in this context, or alternatively could pose an opportunity for spectral data to make a unique contribution to the understanding of aboveground-belowground linkages. A significant portion of variation in soils remains unexplained by the set of plant traits which is usually and practicably measured in the field, leading authors to conclude that there are remaining, unmeasured traits that have influence belowground (Leff et al., 2018). Traits retrieved from remote sensing, for example pigments chlorophyll and carotene, could contribute additional explanatory power. Previous work linking soil properties directly to spectroscopy in aspen forests identified tannins as the most important linking foliar chemical (Madritch et al., 2014). However, tannins are not present in meaningful quantities in the leaves of herbaceous plants and so are unlikely to provide a link in grasslands (Bernays et al., 1989). Recent work across landscape scales in two grasslands identified leaf nitrogen and cellulose as important traits representing soil microbial biomass and functions, although the important traits were not the same in the two contrasting grassland sites studied (Cavender-Bares et al., 2022). Identifying which plant traits are both retrievable from spectra and useful for representing belowground conditions at the surface is an important objective towards linking understanding of grassland functions from the fields of remote sensing and ecology.

2.4 Aboveground productivity

Biomass production is one of the most important functions of grassland ecosystems, and drives the rates of other above- and belowground processes by determining the quantity of inputs from the aboveground to the belowground system, in the form of litter and root exudates. The quantity of aboveground biomass has been demonstrated to influence decomposition processes and microbial communities belowground. For example, plant

biomass has been shown to predict soil fungal communities more than plant diversity or community composition in an experimental grassland (Cline et al., 2018). Quantity of plant inputs belowground has also been found to be more influential than quality in a forest ecosystem (Lohbeck et al., 2015). The relative importance of litter quality and quantity may change across an ecosystem fertility gradient (Wardle David A. et al., 2004). In a comparison of two grasslands, quantity of aboveground inputs was more important for predicting soil communities in the infertile system, where overall quantity of inputs was low, and quality was more important in the productive system where the quantity of biomass ceased to be a limiting factor (Cavender-Bares et al., 2022).

Remote sensing is able to retrieve the productivity of ecosystems effectively. Many spectral indices capture the quantity of aboveground biomass, including the aforementioned NDVI and others for example which are tailored to dense or sparse vegetation environments (Oehri et al., 2017; Ren & Feng, 2015). Remote sensing indices of productivity are extensively used as proxies in models of other ecological properties (Delgado-Baquerizo et al., 2016; Pettorelli et al., 2005). Vegetation coverage is another productivity-related property retrievable from remote sensing and has been found to indicate belowground communities and biodiversity (Cavender-Bares et al., 2022; Hauser et al., 2021; Z. Wang et al., 2019). At the community level, productivity and trait syndromes are often studied together in ecology and remote sensing, because plant functional traits are drivers of productivity (Reich, 2014).

2.5 Plant diversity and ecosystem functioning

As well as individual plant functional traits, community-level trait syndromes and productivity, the diversity of plant functional traits in an ecosystem has strong implications for ecosystem functioning and ecosystem services (Lavorel, 2013). The taxonomic and functional diversity of aboveground plant communities can be considered important ecosystem properties or services in their own right, and are known to be positively associated with many other important above- and belowground functions (Maestre et al., 2012; Soliveres et al., 2016). The greater the range of functional attributes present in the plant community, the greater the ability at the community level to take advantage of spatial and temporal environmental niches, and therefore the more thorough and efficient the use of resources. Through this mechanism, plant diversity has been linked to higher levels of multiple ecosystem functions individually and simultaneously, termed multifunctionality, across a wide range of different ecosystems (Dooley et al., 2015; Lavorel, 2013; Lavorel et al., 2011; Schellberg & Pontes, 2012). Productivity in particular has been associated with greater plant diversity, and the productivity-diversity relationship has been explored among grasslands worldwide (Grace et al., 2016). Although there is a wealth of evidence to show that greater

plant diversity enhances productivity, the relationship between the two properties is not linear, with productivity often found to peak at intermediate levels of biodiversity (Fraser et al., 2015), and there is contrasting evidence in the literature (Adler et al., 2011; Cardinale et al., 2007; Knapp et al., 2014; Schittko et al., 2022; R. Wang, Gamon, Emmerton, et al., 2016). Plant diversity aboveground has been linked to diversity of soil microbial communities belowground, because inputs from different plant species provide suitable substrate for different soil microbes (Bardgett & Van Der Putten, 2014; Guo et al., 2021; Porazinska, Dorota L., Farrer, Emily C., Spasojevic , Marko J., 2018; Yang et al., 2018). Therefore, plant diversity represents another important aspect of the aboveground biosphere that can be used to infer belowground communities and functions from the surface.

There are many ways of assessing biodiversity in the plant community, and it is not clear which axes of diversity are the most important for linking aboveground and belowground ecosystems. Taxonomic, phylogenetic and functional diversity are all connected yet distinct axes of biological variation with implications for ecosystem functioning (Lausch et al., 2018). For example, the taxonomic identity of a plant determines the range of its functional traits but does not explain the intraspecific portion of functional variation which may be driven by short-term environmental factors (Funk et al., 2017). Taxonomic diversity is the most traditional metric for quantifying variation in the biological community, and is one of the Essential Biodiversity Variables that have been identified as conservation priorities globally (Jetz et al., 2019; Pereira et al., 2013). However, taxonomic diversity is subject to the same restraints as species-based approaches when compared with trait-based approaches; it is challenging to scale, does not account for within-species variation, and indirectly rather than directly drives ecosystem functioning. Plant trait-based approaches are more directly associated with functional diversity, which describes the variety of functional traits in the plant assemblage, as richness, evenness and dispersion (Legendre & Laliberté, 2010; Lepš et al., 2006; Schneider et al., 2017). All axes of diversity have multiple spatial components; alpha describes richness at the local scale or how many traits or species in the community, and beta describes spatial turnover of communities across the landscape. Both have been found to interactively drive ecosystem functioning (Albrecht et al., 2021; Hautier et al., 2018; K. He & Zhang, 2009; Jing et al., 2021; Pasari et al., 2013; Peng et al., 2022; Thompson et al., 2018; Zemunik et al., 2016). Remote sensing can contribute to assessments of aboveground biodiversity by capturing multiple axes of diversity simultaneously and by integrating relatively easily across multiple nested spatial scales.

2.5.1 Remote sensing of plant diversity and phenology

The potential to utilise remote sensing data to monitor biodiversity has received a lot of recent interest (Asner & Martin, 2016; Jetz et al., 2016; Pettorelli et al., 2014; R. Wang & Gamon, 2019). Because of the influence of plant functional traits on reflectance spectra, the diversity of spectra across time and space, termed spectral diversity, has been proposed as a proxy for the diversity of biological communities and their functions (Rocchini et al., 2011, 2021a; Rossi et al., 2021, 2022; Thouverai et al., 2021). Functional, taxonomic and phylogenetic axes of biodiversity are distinct but interlinked; remote sensing is able to integrate these different axes of biological variation, because all three influence the interactions of leaves and plant community surfaces with light (I. P. Aneece et al., 2017; Lausch et al., 2018; Schweiger et al., 2018). Therefore, the spectral diversity of ecosystems has been proposed as a metric of biodiversity in its own right, and has been used to explain variation in the productivity and belowground communities of grassland (Schweiger et al., 2018). Spectral diversity is calculated based on the dissimilarity of pixel-level reflectance profiles across space and time, where similar reflectance profiles are grouped into 'spectral species' which can be related to pixel-sized vegetation communities on the ground (Rocchini et al., 2018, 2021a; Rossi et al., 2022). Work characterising spectral diversity as a direct metric of biodiversity is in early stages and has to date focused on hyperspectral data (I. P. Aneece et al., 2017; Cavender-Bares et al., 2016, 2020b; R. Wang et al., 2018b) although see also (Ma et al., 2019; Rocchini et al., 2021a).

There is also a body of remote sensing research retrieving biodiversity of surface vegetation indirectly from multispectral data, utilising the close links between diversity, traits and productivity. The availability of multi-temporal multispectral data from satellites with a regular return period is particularly valuable for this purpose, as more diverse vegetation communities also maintain ecosystem functioning across time, promoting longer and more stable growing seasons. The mean and variability of satellite indices such as NDVI have been linked with some success to ground-based measures of species diversity (Mapfumo et al., 2016; Tan et al., 2022). As well as the overall variability in aboveground productivity or NDVI, satellite remote sensing data with a regular return period can be used to extract detailed temporal patterns of vegetation growth and senescence, termed phenology (Dronova & Taddeo, 2022). Phenology (productivity variation throughout a season) and phenological stability (phenological variation between seasons) have been shown to respond to the diversity of the plant community in wetland ecosystems (Dronova et al., 2022) and mixed ecosystems across Switzerland (Oehri et al., 2017). Greater biodiversity in the plant community is associated with longer growing seasons, greater stability of growing season timing between years, and faster rates of green-up (Zaret et al., 2022), all of which can be retrieved across large

extents from satellite timeseries. Previous work has utilised the phenology-biodiversity link to predict ecosystem functions and services in grassland and forest systems in the context of evaluating land management at landscape scales (Paruelo et al., 2016; Stumpf et al., 2020; Weber et al., 2018), but it is not known whether these findings can be replicated across diverse natural grasslands. Given the demonstrated correlations between biodiversity and belowground ecosystem functioning in grasslands worldwide (Hautier et al., 2018), there is an opportunity to apply remotely retrieved vegetation phenology to reveal patterns in whole-ecosystem functioning across diverse grasslands at large scales.

Close links between grassland functions above- and belowground mean that variation in belowground functioning, which is challenging to capture at large scales from field-based techniques, may be able to be retrieved from remote sensing. The functional traits of aboveground vegetation, and their temporal dynamics and diversity, are all properties which can be characterised using spectral data and are known to represent belowground and whole-ecosystem functions. However, there are many unknowns, in particular relating to which aboveground properties may best represent a link between spectra and soils in grasslands, being both valuable predictors of belowground conditions and well-retrieved from spectra. The current evidence is uneven; for example, grasslands dominate the ecological literature on aboveground-belowground linkages, yet remote sensing-based retrieval of grassland traits are relatively understudied, particularly using the multispectral datasets that are available across large geographic scales. These disparate research themes must be joined up in order to use remote sensing of the vegetation surface to infer variation in belowground functioning.

3. Plant traits link imaging spectroscopy to soil microbial communities in grasslands and shrublands across continental North America.

Abstract

Measuring the belowground biosphere across large spatial scales is an important research priority in the context of global-scale climate and land use changes, which impact soil microbial communities and associated biogeochemical cycles. Remote sensing methodologies, in particular imaging spectroscopy, have been shown to detect differences in belowground communities in forest ecosystems, because canopy foliar traits which are retrievable from spectral reflectance express patterns of the underlying soils belowground. However, these findings have yet to be replicated in varied natural grassland and shrubland ecosystems. This chapter addresses this research gap by linking imaging spectroscopy, plant traits and soil microbial properties at 13 grassland and shrubland sites across North America at the continental scale. Random forest and partial least squares regression are used to identify the extent to which plant traits and reflectance spectra can predict variation in soil microbial properties. Imaging spectroscopy was able to predict large amounts of variation in soil microbial properties (R^2 0.09 – 0.68, NRMSE 8 – 14%), and for microbial biomass and structure was a better predictor than plant traits measured *in situ*. Soil microbial community structure (F:B ratio), an important microbial property with implications for carbon storage and nutrient cycling, was the best-predicted soil property (R^2 0.68, NRMSE 8%). Plant traits indicative of leaf economics such as specific leaf area (SLA), along with less commonly studied foliar carotenoids, were identified as potential links between soils and reflectance. Other factors including quantity of biomass aboveground and the influence of bare soil were also inferred to influence the reflectance signal and likely contribute to the enhanced strength of spectral predictions. These results demonstrate the potential of imaging spectroscopy to predict variation in the belowground biosphere in grassland and shrubland ecosystems at continental scales, which is timely with respect to upcoming hyperspectral satellite missions and the ongoing pressures affecting the biosphere in the 21st century.

3.1 Introduction

Soil microbial communities are a key component of the belowground biosphere, and fundamental to global biogeochemical cycles (Bardgett & Van Der Putten, 2014). Monitoring soil microbes across large spatial extents is therefore an urgent priority in order to understand the impacts of climate and land use changes on soils and the implications for key ecosystem functions and services including carbon storage, nutrient cycling, and food and fuel production (Delgado-Baquerizo et al., 2017; Grigulis et al., 2013; Pommier et al., 2018). Grasslands and shrublands are particularly important with respect to these ecosystem services, being some of the most extensive and exploited ecosystems on Earth (O'Mara, 2012). *In-situ* measurement of soils – especially the microbial component – is a significant undertaking, and prohibitively time-consuming and complex at regional to global scales (Griffiths et al., 2011, 2016). However, our increasing understanding of the functional links between the belowground and aboveground portions of ecosystems may provide a pathway to estimate properties of soil microbial communities from the characteristics of the overlying vegetation surface; in particular, spectral characteristics which can be retrieved rapidly across large areas using remote sensing techniques.

Plant functional traits aboveground and soil bacteria and fungi populations belowground are linked by numerous mechanisms which act on different scales. At the scale of individual organisms, strong associations occur between particular plant and soil fungal species, which can be symbiotic or antagonistic. For example, mycorrhizal fungi associate directly with plant roots, where nutrients, water and carbohydrates are exchanged between the two organisms. The presence and abundance of mycorrhizal fungi therefore influences plant traits related to nutrient acquisition such as root morphology, nutrient allocations and nutrient-use efficiency, and these interactions occur between mycorrhizal fungi populations and the current plant community (De Deyn et al., 2011; Leff et al., 2018; Millard & Singh, 2010). Pathogenic relationships can also occur between specific plant and microbe species, which over time can alter plant traits related to defence, stress and resource allocation as populations of pathogenic microbes build up in the soil (Baxendale et al., 2014). More general (i.e. less species-specific) relationships occur between plant communities and saprophytic fungi, which decompose dead plant material inputted to the soil as litter and root exudates. The quantity and quality of litter inputs into soil, influenced by plant traits, determines the properties of the substrate available for saprophytic fungal populations and therefore their community size and composition. In turn, the rates of decomposition and nutrient cycling carried out by saprophytes influence plant functional traits related to nutrient availability and cycling. The quantity and composition of soil organic matter in the ecosystem is influenced by these feedback mechanisms across years and decades (Bardgett et al., 2005). The bacterial

component of soil microbial communities is particularly closely associated with the quality of soil organic matter, thereby being more influenced by historic vegetation communities and their legacy of carbon inputs than by the current vegetation in an ecosystem (Millard & Singh, 2010). Finally, plant and soil microbial communities may be associated through shared preferences for other environmental properties such as pH, moisture and nutrient levels. These properties are influenced over large extents and long timescales by climate and geology, and at smaller scales by feedbacks with the biosphere.

The associations between aboveground vegetation and belowground soil communities are largely driven by their two-way regulation of resources; plants determining the quantity and quality of resource inputs belowground, and soils the rate at which these inputs are transformed and stored (van der Putten et al., 2016; Wardle David A. et al., 2004). Between them, they determine the balance between biomass production and retention of carbon and nutrients in the ecosystem (Grigulis et al., 2013; Van Der Heijden et al., 2008). Theoretical and empirical evidence suggests that where plant communities are dominated by acquisitive traits which facilitate fast growth, such as high specific leaf area (SLA) and leaf nitrogen (N), soils are more fertile with faster rates of decomposition and nutrient cycling, and have a greater abundance of bacteria relative to fungi (Bardgett, 2017; Reich, 2014). These associations are termed leaf or ecosystem economics (Reich, 2014; I. J. Wright et al., 2004), have been found in diverse ecosystems across the globe, and recently been used to predict the size, structure and composition of soil microbial communities from aboveground plant traits at scales ranging from the individual plant to global datasets (de Vries, Manning, et al., 2012; Delgado-Baquerizo et al., 2018; Leff et al., 2018; Legay et al., 2014; Orwin et al., 2010). Trait-based approaches, as opposed to species-based approaches, offer a particular opportunity with respect to remote sensing, because they characterise the vegetation community as a continuous surface which can be scaled to the size of an image pixel, the smallest unit of measurement in remote sensing. Moreover, the physical traits of leaves, for example concentration of important photosynthetic pigments such as chlorophyll and carotenoids and their structure, directly influence their spectral reflectance patterns and therefore appearance in imagery (Funk et al., 2017; Lausch et al., 2018; Van Cleemput et al., 2018).

Remote sensing techniques are able to retrieve a variety of relevant plant functional traits from grassland and shrubland canopies at a range of scales (Thomson et al., 2021; Van Cleemput et al., 2018; Z. Wang et al., 2020). Imaging spectroscopy, also known as hyperspectral data, is especially useful because it records reflectance patterns to an extremely high level of spectral detail, which means that narrow absorption features responding to particular leaf components, such as carotenoids, lignin and tannins, can be identified (Couture et al., 2016; Gitelson et al., 2002; Kokaly et al., 2009; Nunes et al., 2017; A. Singh et al., 2015;

Ustin, Asner, et al., 2009; Z. Wang et al., 2020). The use of multivariate statistical techniques such as partial least squares regression has also improved modelling capabilities by fully exploiting the large amounts of data generated by hyperspectral systems (Pau et al., 2022; Schweiger et al., 2018; Van Cleemput et al., 2018). Different plant functional traits are often retrieved with varying levels of success, depending on their visibility in the spectral profile; for example photosynthetic pigments are generally more accurately retrieved than morphological traits such as SLA (Van Cleemput et al., 2018). This represents a mismatch in the selection of plant traits most successfully retrieved from spectroscopy in remote sensing studies and most strongly linked to belowground systems in ecology studies, where SLA is often the strongest predictor and pigments are rarely included (de Vries, Manning, et al., 2012). It remains relatively unexplored to what degree the *spectral* characteristics of aboveground vegetation might capture functional trait variation corresponding to belowground microbial communities.

Recent attempts to link canopy spectroscopy directly with soil properties in forest ecosystems have found remarkably strong relationships (Madritch et al., 2014; Sousa et al., 2021). A study on single-species aspen forests in North America found that canopy spectra from airborne imaging spectroscopy explained more variation in soil microbial activity than did foliar traits measured in the field (Madritch et al., 2014). The explanation for this finding is that, while reflectance spectra may not directly capture the pre-determined traits which can be sampled in the field and lab, there are many other axes of biological variation, including phylogenetic and functional variation, which influence spectral reflectance and may also respond to soil conditions, contributing additional explanatory power of the imagery (Lausch et al., 2018; Madritch et al., 2014; Schweiger et al., 2018). Relevant foliar traits which do not have characteristic absorption features may also be apparent in the reflectance signal via their close associations with other properties which do influence foliar reflectance, termed constellation effects (Couture et al., 2016; Nunes et al., 2017). Another recent study highlighted regions of the spectrum associated with carotenoids, leaf N, and water content as being important for the prediction of soil fungal communities from spectroscopy in mixed forests, for which they achieved very high prediction accuracies (Sousa et al., 2021). It is not well understood to what extent these promising findings may be replicated in non-forest ecosystems, where the size of the target organism relative to a single image pixel is likely to be much smaller. For example, in a grassland landscape the reflectance signal of a 1x1m pixel is influenced by multiple individuals, species and potentially higher-order classifications such as herbaceous plants and shrubs, depending on the heterogeneity of the site. Mixing of different plant lifeform types at sub-pixel scales can impact the relationship between spectra and traits, because the same physical trait may influence reflectance differently among different plant

lifeforms, depending on its ecological significance and covariation with other physiological properties (Hacker et al., 2022; Schweiger et al., 2018). Additionally, as with all community-level remote sensing there are other factors besides foliar traits which influence spectral reflectance; for example small-scale variations in topography, hydrology, or vegetation density, coverage and spatial arrangement and the influence of bare soil. Prevalence of bare soil in particular is more likely to impact reflectance in grasslands than in closed-canopy forests (Madritch *et al.*, 2020). The only previous study found linking spectroscopy, plant traits and soil communities in grassland ecosystems concluded that the productivity of the site was key to determine which properties of the vegetation community were relevant links between spectra and soils (Cavender-Bares et al., 2022). In the productive site, plant traits such as nitrogen and cellulose content were important, and in the unproductive grassland only vegetation coverage was an important link. It remains unknown how these differing controls may act across grasslands of varying productivity distributed at the continental scale.

The aim of this study is to evaluate whether soil microbial biomass, community structure and processes can be predicted from airborne imaging spectroscopy in grasslands and shrublands spanning broad ecoclimatic gradients. Further to this, we seek to establish the role of community-level plant traits in translating the belowground signal to surface reflectance. In order to do so, we use a subset of data from the National Ecological Observatory Network (NEON, www.neonscience.org), comprising 13 grassland and shrubland sites distributed across the US continent; a spatial extent of around 4500km. Specifically we aim to first determine the extent to which *in-situ* measured plant traits are related to belowground soil attributes and specifically which traits are most strongly associated with soil microbial community size, structure and functions. We then determine the extent to which imaging spectroscopy of grassland and shrubland surfaces can be used to characterise the same soil attributes, and compare the efficacy of *in-situ* and spectral approaches to retrieving spatial variation in belowground microbial properties across North America.

3.2 Methods

3.2.1 Study location & the NEON network

In-situ field measurements and remote sensing data were sourced from the National Ecological Observatory Network (NEON). NEON is a continental-scale network designed to collect standardised, reproducible ecological datasets across the United States over a period of 30 years, with the first datasets available from 2012 and becoming fully operational in 2019 (Keller et al., 2008). Thirteen sites were sampled from the network for this study (out of 87 sites in total); sites were selected that had coincident soil microbial, plant trait and airborne remote sensing data and were characterised by grassland or shrubland. Sites represent ten different ecoclimatic domains, a geographic range of around 4500km and climate gradients of 26 degrees Celsius and 1167mm rainfall. Figure 1 shows the location of the 13 study sites, a description of each sites' environmental conditions is presented in Table 1. Previous work at these sites has established that airborne imaging spectroscopy is able to retrieve pre-selected plant traits known to be associated with soil microbe communities, such as SLA and phenolics, with some success, but also that the high levels of within-pixel species diversity in grassland systems presents a challenge (Pau et al., 2022; Z. Wang et al., 2020). In both these studies, multivariate statistical approaches utilising the full range of spectral information were found to be the most successful.

Field sampling plots at NEON sites measure 40x40m and are distributed across each site as to capture landscape-scale variation in environmental conditions such as elevation, aspect and vegetation type (for a full justification of the NEON spatial sampling design see (Barnett et al., 2019a; Thorpe et al., 2016)). Many sites contain a variety of different vegetation types; only plots with land cover classified as grassland/herbaceous, shrub/scrub or pasture/hay according to the National Land Cover Definition (NLCD) were taken forward, resulting in between one and ten plots per site, and 59 plots in total. Soil microbial, plant trait and airborne spectroscopy data for the period 2017-2020 was downloaded from the NEON data repository. A full list of the NEON data products used, and variables contained therein, is presented in Table 2. All data in this study were aggregated to the scale of a single sampling plot (40 x 40 m), and analyses carried out at the plot level.

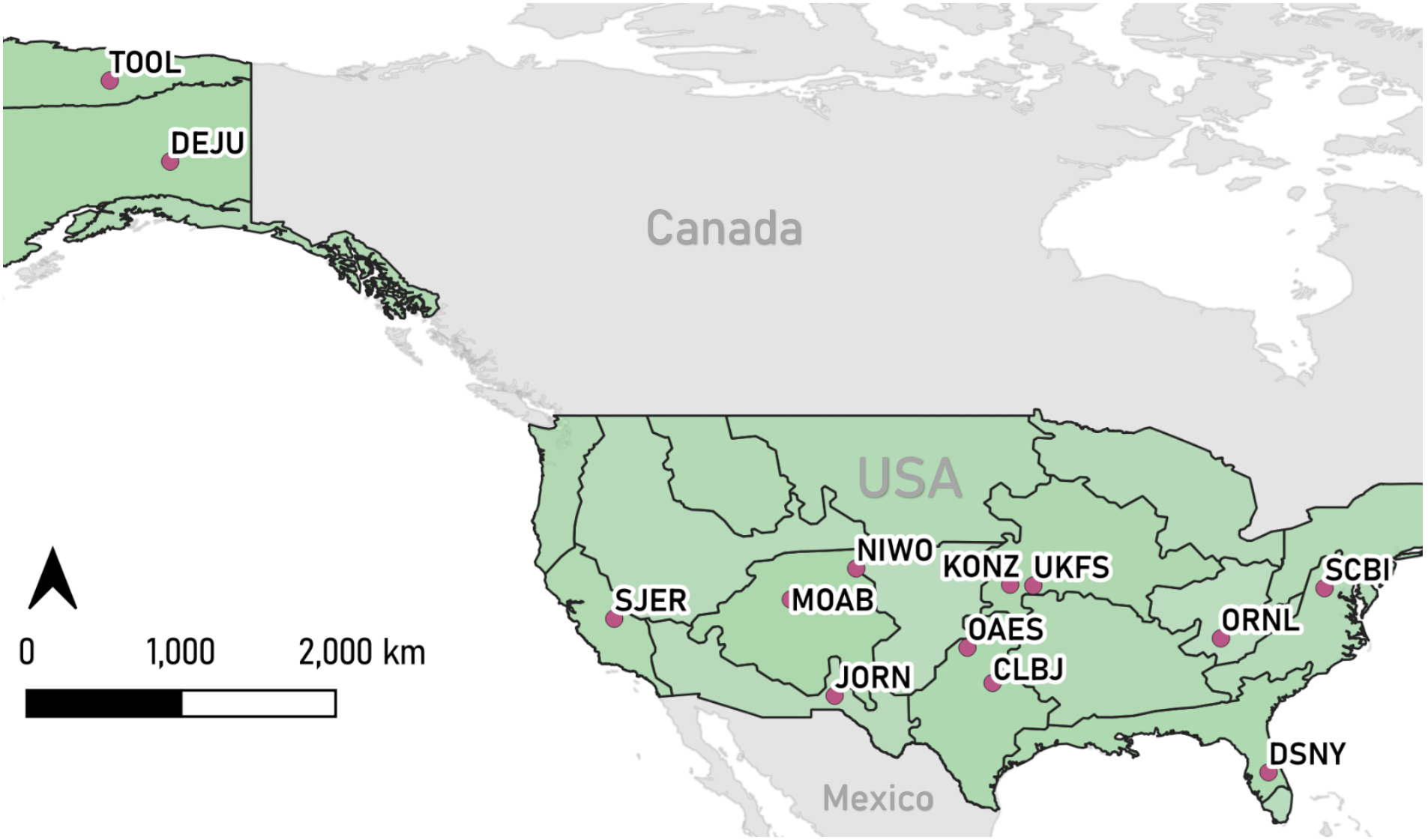

Figure 1 Location of the 13 grassland and shrubland sites from the NEON network, and their ecoclimatic domains.

Table 1. Climate and location background information about the 13 NEON sites in this study. Only plots with grassland/herbaceous, shrub/scrub or pasture/hay NLCD definitions were sampled from each site, with the number of sampled plots per site shown.

Site Name	Site ID	Domain	Mean Annual Temp (°C)	Mean Annual Precipitation (mm)	Dominant NLCD Classes	Elevation	*n* plots
LBJ National Grassland	CLBJ	Southern Plains	18	840	Deciduous Forest, Grassland/Herbaceous	259 m	2
Delta Junction	DEJU	Taiga	-3	305	Evergreen Forest, Shrub/Scrub, Woody Wetlands	517 m	3
Disney Wilderness Preserve	DSNY	Southeast	22	1150	Pasture/Hay, Woody Wetlands	15 m	5
Jornada LTER	JORN	Desert Southwest	17	173	Shrub/Scrub	1329 m	10
Konza Prairie Biological Station	KONZ	Prairie Peninsula	12	860	Deciduous Forest, Grassland/Herbaceous	381 m	9
Moab	MOAB	Southern Rockies & Colorado Plateau	11	200	Evergreen Forest, Shrub/Scrub	1767 m	9
Niwot Ridge Mountain Research Station	NIWO	Southern Rockies & Colorado Plateau	0	758	Evergreen Forest, Grassland/Herbaceous	3513 m	2
Klemme Range Research Station	OAES	Southern Plains	15	670	Grassland/Herbaceous, Shrub/Scrub	516 m	10
Oak Ridge	ORNL	Appalachians & Cumberland Plateau	14	1340	Deciduous Forest, Evergreen Forest, Pasture/Hay	344 m	1
Smithsonian Conservation Biology Institute	SCBI	Mid-Atlantic	13	1054	Deciduous Forest, Evergreen Forest, Pasture/Hay	361 m	1
San Joaquin Experimental Range	SJER	Pacific Southwest	17	270	Evergreen Forest, Grassland/Herbaceous, Shrub/Scrub	368 m	5
Toolik	TOOL	Tundra	-4	331	Dwarf Scrub, Shrub/Scrub	843 m	1
The University of Kansas Field Station	UKFS	Prairie Peninsula	12	870	Deciduous Forest, Pasture/Hay	335 m	1

3.2.2 Field data: soil microbial properties

Three soil cores (sampled to a depth of 30cm) are collected per sampling plot to capture fine-scale spatial heterogeneity (Parnell & Blevins, 2022). The three repeats were averaged to give a single mean value of soil properties per plot. All soil measures were transformed from a concentration to a per-area or stock basis (per m^2 soil to 10cm depth), which is more relevant for plant communities and from the spatial perspective used in remote sensing. To do this, the bulk density of the soils at third bar pressure was used, from the *Soil physical and chemical properties, megapit* data product (DP1.00096.001, https://data.neonscience.org). Missing bulk density data for sites TEAK, HEAL, SRER and TOOL was substituted from nearby sites of the same land cover or from other published work at the site (Mack & Schurr, 2013).

Soil microbial community size and structure were determined from concentrations of microbially-synthesised phospholipid fatty acids (PLFAs) in the soil, contained within the *Soil Microbial Biomass* NEON data product (for NEON data product codes see Table 2). We attributed the different PLFAs to bacterial or fungal communities following summaries by (Quideau et al., 2016; Willers et al., 2015). Soil fungi were represented by the PLFAs *18:2ω6,9*, the most commonly used fungal marker, and *18:1ω9*, which has been attributed to saprophytic fungi in grasslands (De Deyn et al., 2011). The total concentrations of the relevant PLFAs are used to describe total microbial biomass, bacterial biomass, and fungal biomass. The ratio of fungal to bacterial biomass, F:B ratio, was used as a common measure of soil microbial community structure (Bardgett et al., 1996; de Vries, Bloem, et al., 2012; de Vries, Manning, et al., 2012; Orwin et al., 2010).

Rates of nitrogen transformations were used to indicate the activity of the microbial community, as the transformation of nitrogen from organic to mineral forms is a key function that microbial communities perform in the ecosystem (Bengtsson et al., 2003; Risch et al., 2019). N mineralisation is the transformation of organic nitrogen structures into NH_4^+, the preferred form of nitrogen for plant metabolism (C. Wang et al., 2018). Nitrification is the immobilisation of NH_4^+ into nitrate, a major sink of N in biogeochemical cycling (Butterbach-Bahl et al., 2013). Respectively, rates of these processes represent soil microbial contributions to the maintenance of soil fertility and the reduction of nitrogen leaching from soils; two key ecosystem service functions (Pommier et al., 2018). These two variables were calculated from the *Soil inorganic N pools & transformations* data product, using the *neonNTrans* package in R (Weintraub, 2021).

3.2.3 Field data: aboveground plant traits

Vegetation data were acquired from the NEON data product *Foliar physical and chemical properties*. Nine foliar traits were included in this study, including photosynthetic pigments (chlorophyll a & b, combined to give total chlorophyll; carotenoids), secondary metabolites (lignin, cellulose), structural properties (specific leaf area, leaf dry matter content), carbon and nitrogen from which we derived C:N ratio, an indicator of litter quality. This selection of traits is characteristic of the LES and has been used to predict soil microbial communities in previous studies (de Vries, Manning, et al., 2012; Leff et al., 2018; Orwin et al., 2010). Foliar traits are measured by NEON from unsorted clip strips of herbaceous vegetation, giving a community-level mean value. Where woody plants are also present within a plot, trait measurements are taken from woody individuals if they are one of the dominant three species at plot level (2016-2018 field seasons), or according to site-level target taxa lists (2019 field season onwards). Data giving the percentage by biomass of herbaceous and woody vegetation in the plot-level community was not available. Therefore, analyses in this chapter were carried out using the mean trait value of all herbaceous clip strips and woody individual samples collected within a plot. For a detailed explanation of the NEON methodology for sampling and measuring foliar traits, see Weintraub (2022).

3.2.4 Imaging spectroscopy data

The spectrometer on board the NEON Airborne Observation Platform measures reflectance of light in the range 380 – 2500nm, in bands of 5 nm width and with a spatial resolution of 1 m^2 (Kampe et al., 2010). The product is delivered calibrated to scaled reflectance (0-1), orthorectified to account for variations in elevation and atmospherically corrected to ground-level reflectance. Most sites have a single flight each year, which is timed to coincide with the historical peak biomass. Collection of spectral imagery and plant trait data on the ground are coordinated so that they take place within two weeks of each other. Reflectance of pixels within the bounds of each 40x40m plot (1600 pixels) represented in the field data were extracted and averaged to give a mean spectral reflectance signature per plot. Atmospheric absorption regions 1350-1460 nm and 1790-1960nm were excluded, leaving 344 spectral bands for analysis.

3.2.5 Statistical approach

To identify patterns of plant and soil attribute covariation across the plots we performed an exploratory Principal Components Analysis (PCA). It was expected that plant traits which facilitate rapid growth (e.g. high SLA and leaf N) and soil traits which facilitate rapid nutrient cycling (high total and bacterial microbial biomass and rates of N transformations) would be associated along the most significant latent axes of variation (Bardgett, 2017; Pérez-Ramos et al., 2012; Saetre & Bååth, 2000; I. J. Wright et al., 2004).

Random forest regression modelling (Breiman, 2001) was used to determine the explanatory power of aboveground community-level plant traits for predicting belowground soil microbial properties. A separate model was created for each of the six soil microbial properties of interest, with the nine plant traits as predictors. Prior to modelling, foliar trait predictors were checked for collinearity (Pearson's correlation coefficient >0.8) and *z*-standardized. Standardization does not impact the overall performance of random forest models, but it ensures that the variable importance scores (%increase MSE) are comparable between predictor variables measured in differing units. Forests had 1000 trees and used the optimum number of variables tested at each node, as identified by the tuneRF() function in *rfUtilities* (Evans & Murphy, 2017). Irrelevant predictors were identified and removed using a two-step process; first using the Boruta algorithm, permuted 100 times (Kursa & Rudnicki, 2010; Räsänen et al., 2021), and second by inspecting the variable importance scores of each predictor in the resulting random forest models, and selecting only those with a % increase MSE >= 5. Error was based on the out-of-box error. Because random forest is a stochastic algorithm, producing a slightly different result each time, models were run 100 times, from which the mean explained variance (random forest pseudo R^2) and NRMSE (RMSE/observed range), as well as mean variable importance for each predictor, were taken as the final model outputs. Outputs of the models were overall percentage variance explained, normalised root mean square error of prediction, and variable importance of each predictor variable. Variable importance is measured using the percentage increase mean square error (MSE); the average increase in the MSE that is observed when the variable in question is excluded as a predictor when building individual trees in the ensemble forest model.

To explore the potential of airborne imaging spectroscopy to predict belowground microbial attributes, partial least squares regression (PLSR) modelling was used (Wold et al., 2001). This type of multivariate model is able handle a large number of predictor variables, and therefore effectively utilise the fine detail and resulting large number of spectral bands that characterise spectroscopy data, often giving stronger results than other methods such as using spectral indices (Van Cleemput et al., 2018). PLSR has recently been used to map

aboveground plant traits over the NEON sites from the airborne observation platform (AOP) dataset (Z. Wang et al., 2020). Individual PLSR models were created to predict each of the six microbial attributes in turn, using all 344 spectral reflectance bands as predictors. Models were created using leave-one-out-cross-validation, with the overall predictive power of the model reported as validation R^2, based on the optimum number of model components as identified by the PRESS statistic (Garson, 2016; Wakeling & Morris, 1993).

All statistical analyses were carried out in R using the packages *vegan* (Oksanen *et al.*, 2020), *randomForest* (Liaw & Wiener, 2002), and *plsdepot* (Sanchez, 2013).

3.3 Results

3.3.1 Field measured community-level plant traits and soil properties

Table 2 shows the field-measured ranges of plant and soil properties in plots across the 13 grassland and shrubland sites. These ranges are large compared to others presented in studies of aboveground-belowground linkages and retrieval of plant traits from remote sensing, at a range of scales (De Long et al., 2019; de Vries, Manning, et al., 2012; Delgado-Baquerizo et al., 2018; Orwin et al., 2010; Rossi et al., 2020; Z. Wang et al., 2020).

Table 2. Plant and soil properties investigated in this study. Values given are the plot-level averages, calculated by averaging the mean trait value of herbaceous and woody samples. Soil properties are the average of three repeat soil cores.

NEON data product	Variable	Min	Max	Mean	St. Dev.
Soil microbial biomass, (DP1.10104.001)	Total microbial biomass (µmol m^{-2})	3,826.51	196,740.90	42,998.12	55,290.97
	F:B ratio	0.072	0.605	0.244	0.147
	Fungal biomass (µmol m^{-2})	247.31	26,921.08	4,523.72	5,508.24
	Bacterial biomass (µmol m^{-2})	1,962.40	141,698.40	26,239.05	37,775.83
Soil inorganic N pools & transformations (DP1.10080.001)	N mineralisation (mgN m^{-2} day^{-1})	-21.067	109.234	13.999	19.728
	Nitrification (mgN m^{-2} day^{-1})	-15.322	104.321	10.632	18.368
Plant foliar physical and chemical properties, (DP1.10026.001)	SLA (mm^2 mg^{-1})	3.345	23.31	12.088	4.678
	LDMC (g g^{-1})	0.164	0.99	0.561	0.222
	C (mg g^{-1})	358.300	518.800	447.750	32.810
	N (mg g^{-1})	6.000	28.600	15.340	5.890
	C:N ratio	15.9	81.6	34.574	13.999
	Total chlorophyll (µmol m^{-2})	30.884	451.754	194.592	92.46
	Carotenoids (µmol m^{-2})	13.393	234.25	87.906	49.877
	Lignin (mg g^{-1})	26.900	194.770	79.510	41.420
	Cellulose (mg g^{-1})	124.500	412.700	284.810	77.280

3.3.2 Co-variation of measured plant traits and soil microbial properties

Principal components analysis was used to determine whether the associations between fast-growing plant traits and fast-cycling soil microbes, and slow-growing plant traits and slow-cycling microbes, were evident at the community level across the plots. These

associations are predicted by the leaf economics spectrum (Pérez-Ramos et al., 2012; Reich, 2014), and form the basis of aboveground-belowground linkages in soil ecology (Bardgett, 2017). The first two principal components (PC1, PC2) combined explained 53.4% of variation in the plant and soil properties across all plots (Figure 2). PC1 broadly described a trade-off in the plant traits between acquisitive traits (high SLA and leaf N) and conservative traits (high C:N ratio, cellulose and LDMC) (Figure 3). This was matched by the soil microbial properties, where high F:B ratio, characteristic of slow-cycling microbial communities suited to breaking down tough, low-quality litter, was aligned with conservative plant traits, and all other microbial properties including rates of N cycling were aligned with acquisitive plant traits along PC1. Sites with these traits included prairie ecosystems such as KONZ and SJER, and also high-latitude tundra sites DEJU and TOOL. Photosynthetic pigments chlorophyll and carotene were not aligned with other plant traits facilitating rapid plant growth along PC1 and PC2, for example aligning in the opposite quarter of the biplot to SLA, but were instead associated with resource-conservative trait LDMC. Pigments were however negatively correlated with lignin, a tough leaf structural property. This result was replicated when pigments were incorporated using both mass-based and area-based units (Westoby et al., 2013). Observations in the quarter of the biplot representing high levels of photosynthetic pigments (bottom-right) but low levels of other acquisitive traits came from only two sites, JORN and MOAB, both of which are desert sites (Table 1).

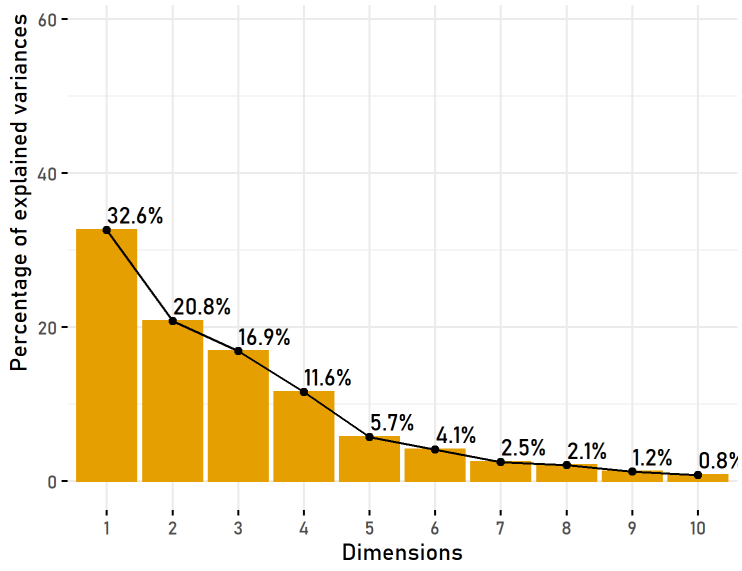

Figure 2 Scree plot showing the percentage of explained variance in the combined plant and soil dataset which is attributable to each of the first 10 principal components.

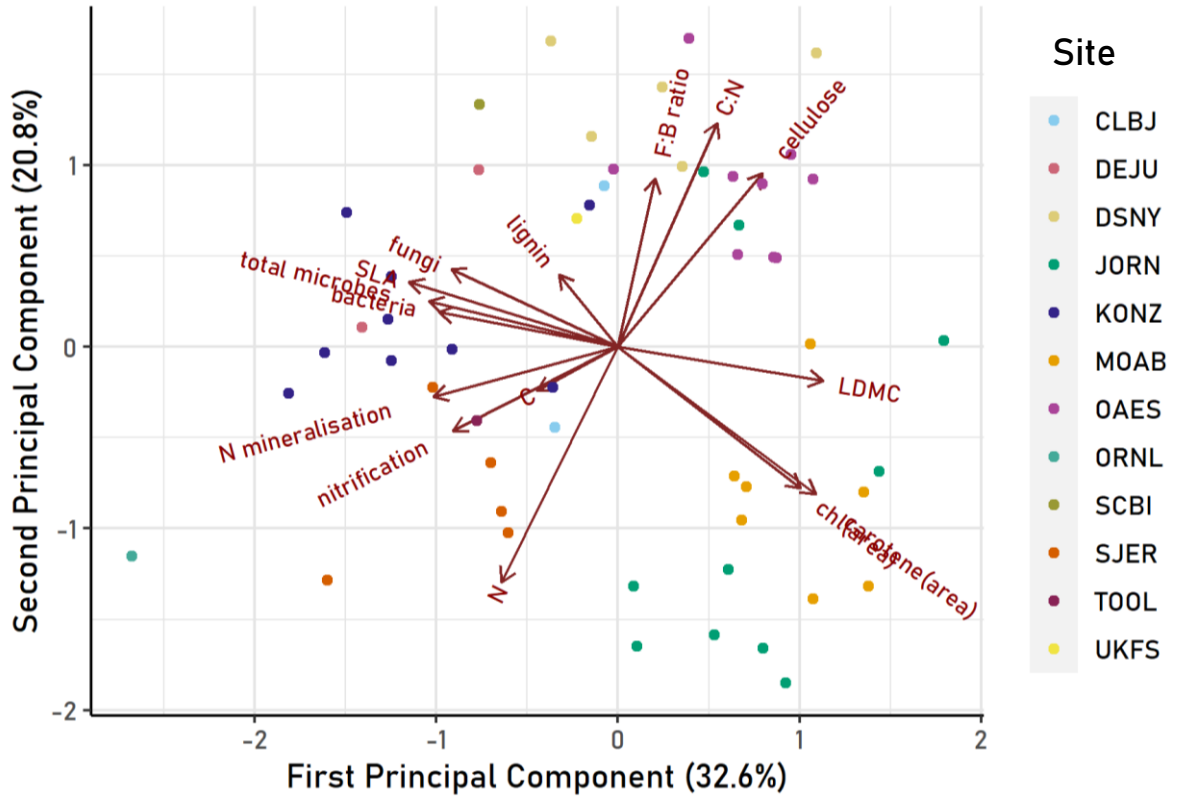

Figure 3. PCA of plant traits (SLA, C, N, C:N ratio, chl (area), carotene (area), cellulose, lignin) and soil microbial properties (total microbes, fungi, bacteria, F:B ratio, nitrification, N mineralisation). Each point represents a sampling plot, colours represent the field site.

3.3.3 Prediction of soil microbial community size, structure and functions from community-level aboveground plant traits

Random forest was used to model variation in each of the six microbial community properties in turn, using the nine plant traits measured in the field as predictor variables (Table 2). Table 3 shows the average results from 100 model runs for each of the six microbial properties. Plant traits explained between 31% and 59% of variation in soil microbial properties, with fungal biomass being the best-modelled (variation explained 58.7%, NRMSE 13%). For all other soil microbial properties, variation explained was around 30-35%, and NRMSE varied from 12 – 23% the measured range of the response variables.

Variable importance scores of the nine plant traits, for each of the individual soil attribute models, are shown in Figure 4, and used to infer which plant traits best represent which soil microbial properties. The most important plant traits differed for each microbial property, and were consistent with associations found during principal components analysis (Figure 3) and expected from theory (Bardgett, 2017; Pérez-Ramos et al., 2012). The most important predictor traits for fungal biomass, the best-explained soil microbial property, were

foliar lignin and carbon content, both traits which are indicative of tough leaves which are preferentially decomposed by soil fungi. Soil F:B ratio was best predicted by foliar C, N and the ratio between them. C:N ratio is a typical indicator of the position of a vegetation community on the LES, and F:B ratio the equivalent indicator for the microbial community. Similar soil properties were predicted by similar plant traits; for example total and bacterial microbial biomass, or the two measures of nitrogen transformations. SLA was the most important trait for predicting soil bacteria and rates of N transformations. Finally, community-level carotene concentrations emerged as an important plant trait for predicting soil microbial properties overall, being in the top three predictor variables in all six models.

Table 3. Results of random forest modelling of the six soil microbial properties from nine aboveground plant traits. RMSE is normalised by dividing by the range of the response variable. % variation explained and NRMSE are the averages of 100 model runs.

Soil property	**variation explained (%)**	**NRMSE**
Total microbial biomass	35.4	0.23
Bacterial biomass	31.5	0.22
Fungal biomass	58.7	0.13
F:B ratio	35.4	0.19
Nitrification	31.6	0.12
N mineralisation	27.5	0.13

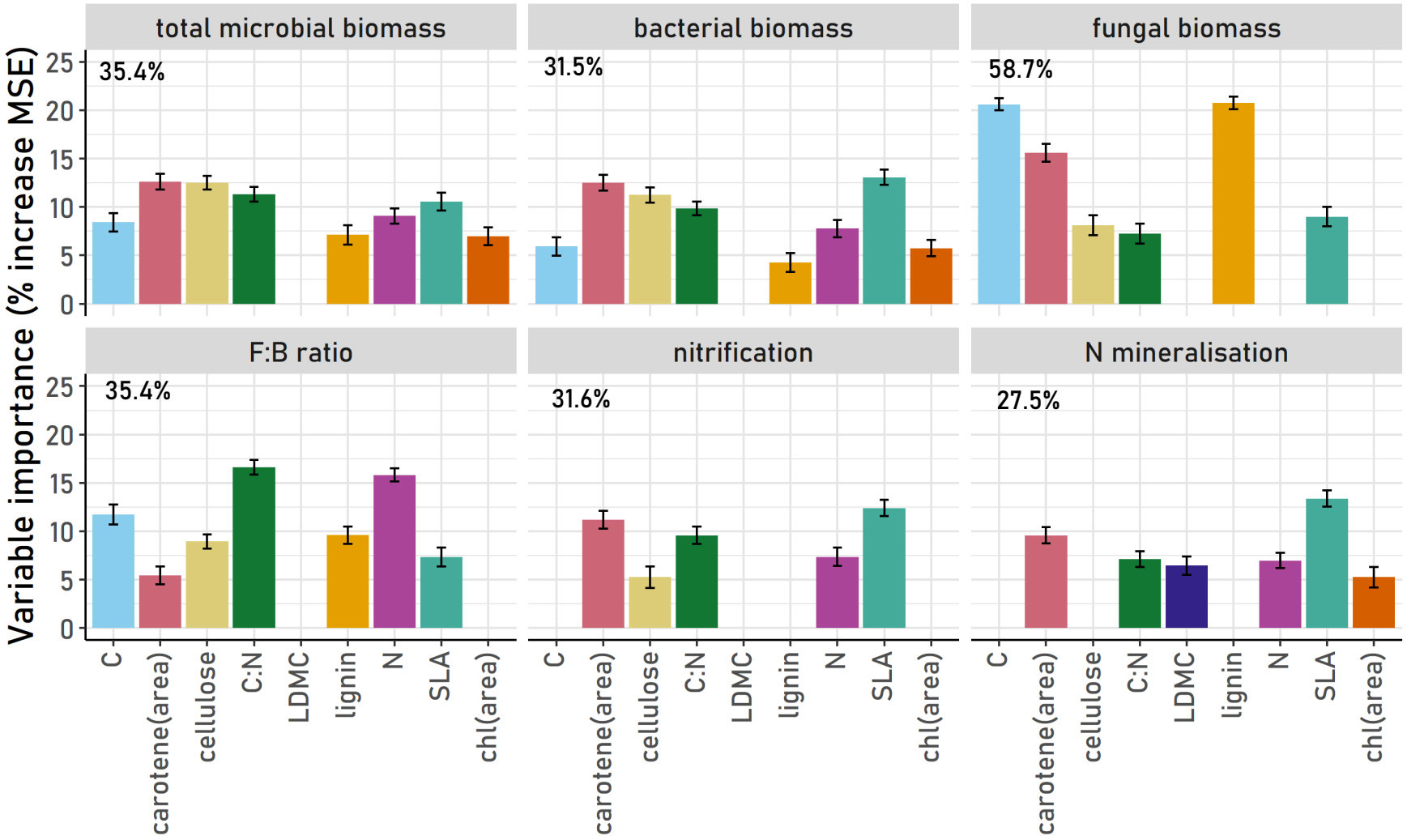

Figure 4. Variable importance scores (% increase MSE) of the plant trait predictor variables in random forest modelling of soil microbial properties. Variable importance scores are the mean of 100 model runs; error bars show standard deviation. Labels show the % variation explained in each soil property by plant functional traits

3.3.4 Prediction of soil microbial community size, structure and functions from imaging spectroscopy

Figure 5 shows two example spectral reflectance profiles from sites KONZ and MOAB, a prairie and a desert site in Kansas and Utah respectively (Table 1). These spectral profiles demonstrate the contrasting reflectance of densely and sparsely vegetated plots. The KONZ spectral profile is typical of a dense photosynthetic vegetation surface; a peak in green wavelengths at around 500nm, caused by reflectance of green light by chlorophyll, low reflectance in red wavelengths (around 650nm) caused by absorption of red light during photosynthesis, a steep 'red-edge' between red and near-infrared (NIR) wavelengths (680 to 800nm) caused by leaf structures reflecting NIR light, and absorption in SWIR wavelengths above 1500nm caused by leaf moisture. The MOAB spectral profile is much more characteristic of bare soil, indicated particularly by higher reflectance in red and SWIR wavelengths. This demonstrates the contrast in reflectance profiles caused by contrasts in vegetation density, bare soil visibility and plant functional traits such as leaf moisture which are key to revealing patterns in belowground communities.

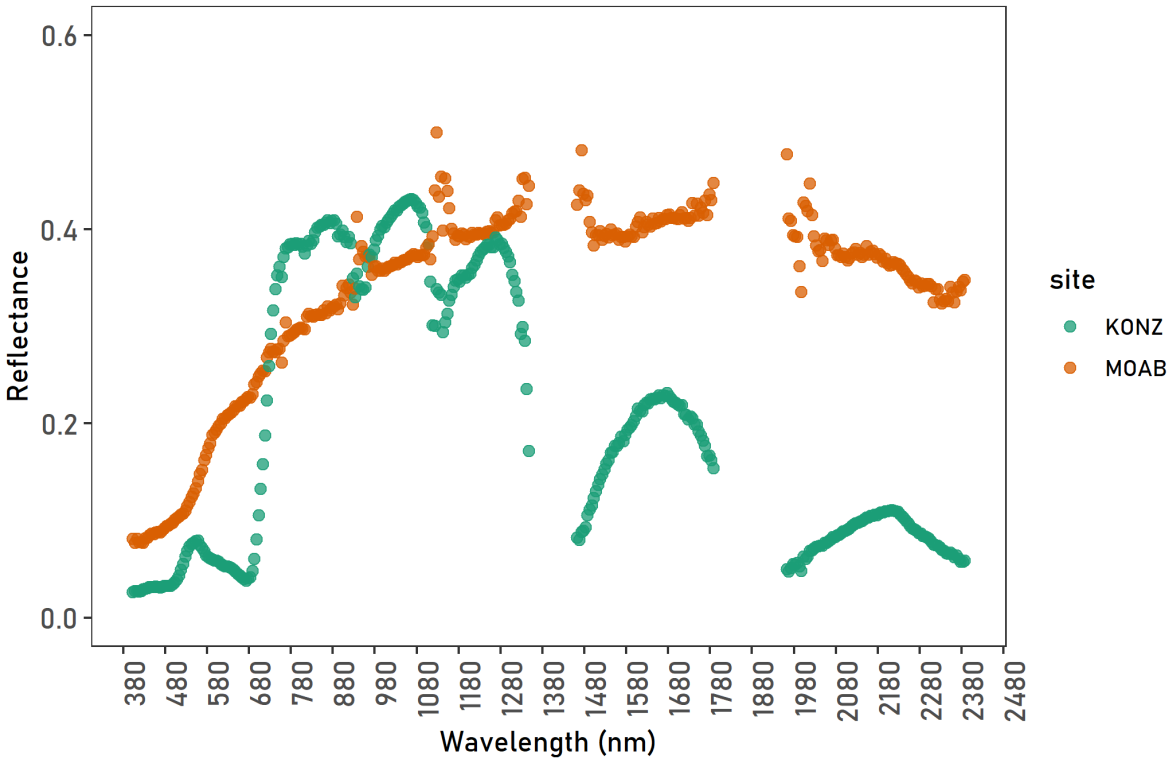

Figure 5. Hyperspectral reflectance profiles for sites KONZ, a productive prairie site, and MOAB, a sparse desert site.

PLSR was used to model variation in the six soil microbial properties representing the size (total microbial biomass, bacterial biomass, fungal biomass), structure (soil microbial F:B ratio) and functions (rates of nitrification and N mineralisation) of soil microbial communities. The results of the PLSR models are shown in Figure 6(a-f). Soil microbial properties were predicted from spectroscopy with R^2 ranging from 0.09 to 0.61, and NRMSE ranging from 8% to 14%. Spectral PLSR models were able to explain the most variation in soil F:B ratio (R^3 = 0.68, NRMSE = 9%) and fungal biomass (R^2 = 0.61, NRMSE = 8%). Rates of N transformations had lower overall variation explained (R^2 = 0.09 and 0.23) but also low errors of prediction (NRMSE = 0.13 and 0.14); it can be seen from the plots that rates of N transformations are well-predicted in the middle of the range of variation, giving low overall errors, but that extremely high or low rates of N cycling are not captured from spectroscopy (Figure 6 e, f).

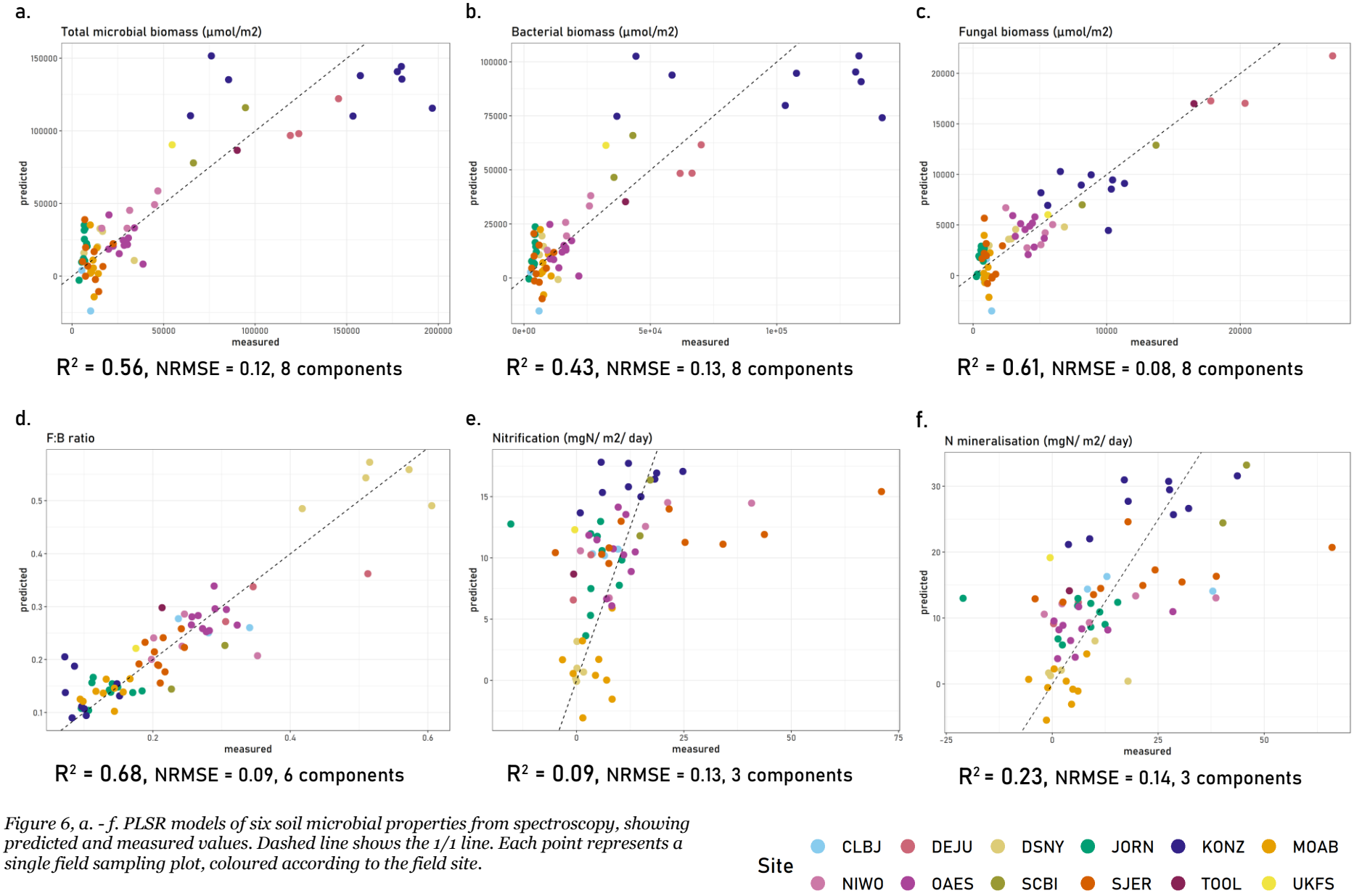

Figure 6, a. - f. PLSR models of six soil microbial properties from spectroscopy, showing predicted and measured values. Dashed line shows the 1/1 line. Each point represents a single field sampling plot, coloured according to the field site.

The contributions of individual spectral bands to the PLSR models are represented in Figure 7 (a-f), which show the coefficients between each of the 344 spectral bands used as predictors, and all PLSR components. Wavelengths and wavelength ranges which were important for each soil microbial property, identified from the plots, are shown in Table 4, along with the interpretation of the wavelength range from the literature (Z. Wang et al., 2020). The coefficient plots of total microbial biomass and bacterial biomass were very similar, with key peaks between 700-750nm (red-edge), 1050-1120nm, 1300-1350nm 1700-1750nm and 1950-2000nm. Fungal biomass had slightly different wavelength peaks to total and bacterial biomass models, with overall greater amplitude. Peaks in visible and NIR portions of the spectrum were similar, but the fungal PLSR model also had key peaks at 1500-1550nm, 1700-1750nm, and 2350-2400nm, which are absent for bacterial and total biomass. These wavelengths are related to starch and cellulose (1500-1550), cellulose and protein (1700-1750) and protein (2350-2400), and were important in recent modelling of foliar carbon from spectroscopy across the NEON sites (Z. Wang et al., 2020). The PLSR model of F:B ratio had much smaller correlation coefficients across the wavelength range, likely due to the smaller number of components used to build this model, with key peaks at 675nm, 760nm, 940nm, 1130nm and 2000nm. Peaks were in similar wavelength ranges to measures of microbial biomass, but in the opposite direction, for example a positive coefficient with red visible wavelengths (around 675nm), indicating inverse relationships between F:B ratio and the wavelengths, relative to microbial biomass. PLSR models of nitrification and N mineralisation had virtually no coefficient peaks across the wavelength range, with some in the visible and red-edge regions (400nm – 750nm) and again at 940nm and 1130nm. Peaks at 940 and 1140nm in PLSR coefficient graphs have been interpreted by others as artefacts of atmospheric correction (Z. Wang et al., 2019).

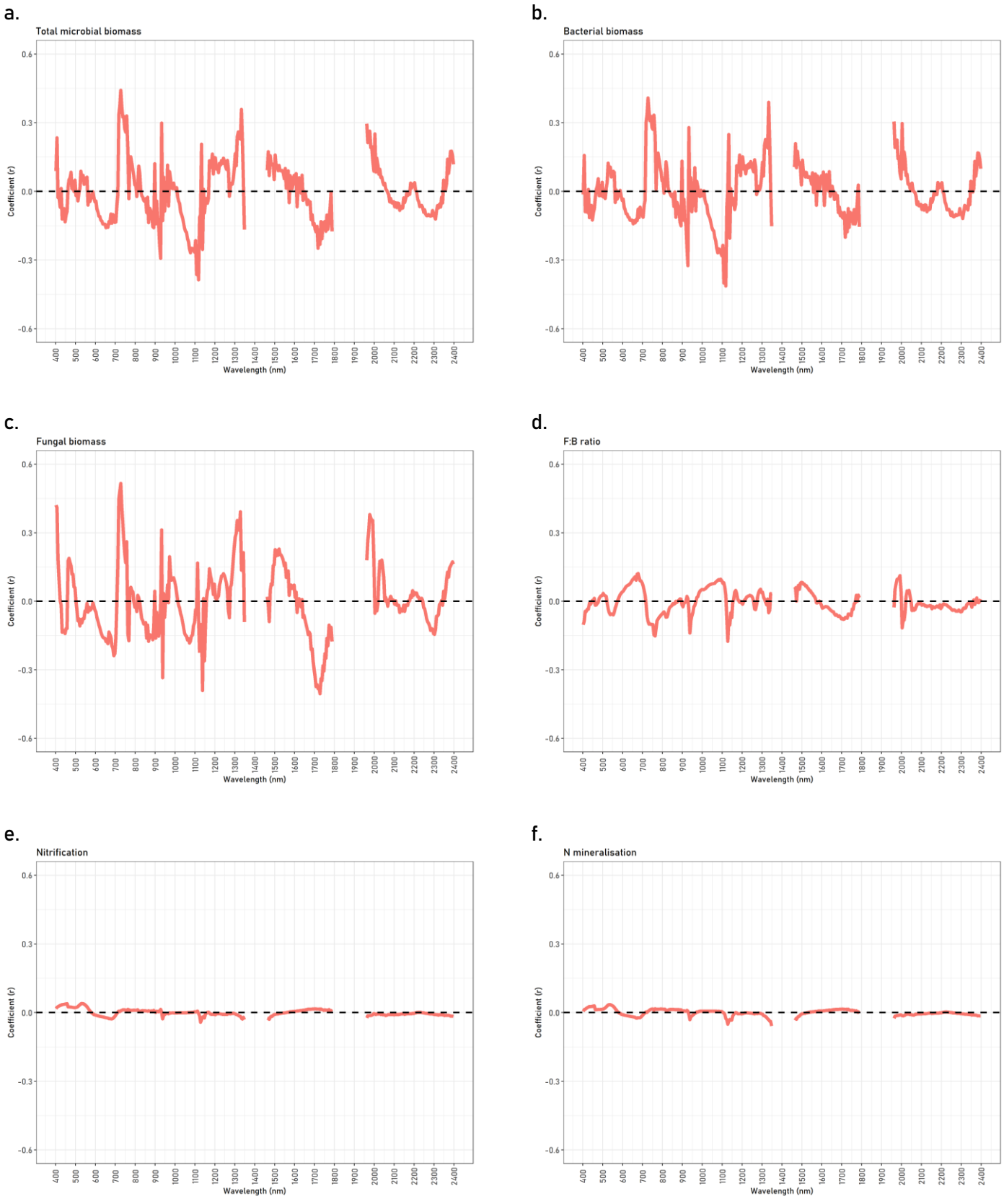

Figure 7 (a. - f.). Coefficient plots showing the coefficient of each individual wavelength in the PLSR models of soil microbial properties, based on all components used to build the final model.

Table 4. Important wavelengths and wavelength ranges during PLSR modelling of the six soil microbial properties, identified from the coefficient plots. Wavelengths identified as being important for modelling aboveground foliar traits from spectroscopy across NEON sites are indicated.

Soil microbial property	Important wavelengths	Known absorption features	
Total microbial biomass & bacterial biomass	700-750	Red-edge	
	1050 - 1120		
	1300-1350	Important for modelling leaf mass per area, water and carotene	
	1700-1750	Important for modelling a variety of foliar traits, ascribed to cellulose and protein	
	1950-2000	Important for modelling a variety of foliar traits, ascribed to protein	
Fungal biomass	*(as above for total and bacterial biomass)*		
	475		
	1500-1550	Starch, cellulose	Wavelengths above 1500nm are also influenced by soil
	1700-1750	Cellulose, protein	
	2350-2400	Protein	
F:B ratio	675	Red visible wavelengths; soils and photosynthesis	
	760		
	940	Important for modelling leaf mass per area	
	1130	Important for modelling foliar carbon, cellulose, carotene, chlorophyll, starch and water	
	2000	Water	
Nitrification & N mineralisation	400-750	Visible and red-edge	
	940	Identified as an artefact of atmospheric correction by (Z. Wang et al., 2019)	
	1130	Important for modelling foliar carbon, cellulose, carotene, chlorophyll, starch and water	

3.4 Discussion

The aim of this study was to establish the extent to which imaging spectroscopy of the vegetation canopy can be used to predict variation in soil microbial community size, structure and functions across grasslands and shrublands distributed at the continental scale. The results demonstrate that continental-scale spatial variation in belowground microbial communities is evident in the spectral reflectance patterns of the aboveground vegetation surface, and that this link can be used to predict the soil microbial component of grassland and shrubland ecosystems, over large spatial extents, from imaging spectroscopy. Furthermore, imaging spectroscopy was able to retrieve more variation in soil microbial community size and structure than were plant traits measured *in-situ*. This study adds to the growing body of evidence that the potential of imaging spectroscopy to offer new perspectives on the biosphere at unprecedented detail and scale is not limited to the aboveground biosphere but extends belowground as well (Madritch et al., 2014; Sousa et al., 2021).

3.4.1 Associations between in-situ measured aboveground plant traits and belowground microbial properties

One of the objectives of the study was to establish the extent to which aboveground plant traits measured *in-situ* represented the soil microbial communities below, with a view to providing a link between soils and spectroscopy. This was assessed using principal components analysis (Figure 3) and random forest (Table 3, Figure 4). PCA showed that aboveground and belowground ecosystem properties broadly aligned across the plots in groups predicted by the LES; with properties indicative of fast-cycling ecosystems grouped together and opposing those indicative of slow-cycling ecosystems. Random forest showed that these associations can be used to predict variation in soil communities from aboveground traits (variation explained 29% - 57%, Table 3), and that the traits which were important for predicting different microbial properties were often those which were aligned with the microbial property across the plots, as shown by PCA (Figure 3).

Relationships between field-measured community-level plant traits and soil microbial communities at the 13 NEON sites studied broadly described the LES continuum: from acquisitive to conservative plant growth strategies aboveground, matched belowground with large, rapid-cycling to small, slow-cycling microbial communities. In particular, SLA was closely associated with soil microbial community biomass (Figure 3), which is consistent with previous studies finding SLA to be a key trait for predicting soils (de Vries, Manning, et al., 2012; Grigulis et al., 2013). This finding adds this large-scale grass and shrubland dataset to

the existing evidence base for these relationships across a plethora of ecosystems worldwide (Cornwell et al., 2008; Freschet et al., 2010; Pérez-Ramos et al., 2012). This is an important finding, given that several previous studies have reported that leaf economics relationships are less evident among herbaceous relative to woody plants, due to smaller variation in leaf lifespan (undermining the fundamental trade-off of the LES) or differing contributions of leaf, stem and root traits to overall plant functioning (Freschet et al., 2010; Funk & Cornwell, 2013; Pierce et al., 2007).

Our results suggest that above ground plant traits can be used to predict soil microbial communities at the continental scale (variation explained 27% - 59%) (Table 3). The proportions of variation explained in microbial properties were comparable to others' results at national and global scales (de Vries, Manning, et al., 2012; Delgado-Baquerizo et al., 2018). Soil fungal biomass was the most predictable soil attribute (variation explained 59%; NRMSE 13%). It has been suggested that soil fungal communities are particularly sensitive to the trait syndrome of the aboveground plant community because they tend to be abundant in ecosystems with relatively low rates of aboveground biomass production, rendering the *quality* of those inputs more crucial (Grigulis et al., 2013). However, other authors report the opposite effect, whereby the quality of inputs is unimportant relative to their quantity in unproductive systems (Cavender-Bares et al., 2022). In our study, plant traits indicating litter quality were used successfully to distinguish between sites spanning a large gradient from high to low productivity. The quantity and quality of litter inputs belowground is not independent, as high-quality litter is inherently associated with rapid biomass production (Reich, 2014), therefore although only the quality (plant traits) of inputs was explicitly investigated during random forest modelling, it is likely that both quantity and quality of inputs contribute to the explanation of soil microbial properties across these sites.

Traits which were most important for predicting belowground microbial properties tended to be those which covaried with them according to LES relationships. For example, foliar C:N ratio is the key indicator of litter quality, and was an important predictor of soil F:B ratio, a key indicator of soil microbial community preference for high or low quality litter. SLA was an important predictor trait across for all microbial properties, which was expected from previous studies (de Vries, Manning, et al., 2012). However, the other most important predictor trait overall was carotene, which was unexpected as this foliar pigment is rarely included in field-based studies of aboveground-belowground linkages, and is not clearly associated with the LES across these sites (Figure 3). Although the majority of foliar traits covaried consistent with LES relationships in this study, the role of photosynthetic pigment concentration in ecosystem economics was not clear from our analyses. Chlorophyll indicates photosynthetic capacity and would therefore be expected to covary with fast-growth traits such

as leaf N and SLA (Croft et al., 2017); however our results showed that the opposite was true (Figure 3). This finding suggests that concentrations of foliar pigments are not clearly associated with any particular type of soil microbial community, and therefore may not be able to contribute to predictive models of soils from aboveground. Random forest models partially supported this suggestion in that chlorophyll was not an important predictor for any soil microbial properties (Figure 4); carotene however was one of the top three most important predictors for five out of six microbial properties.

Reasons for the unexpected foliar pigment relationships in this study could be the interaction of site-specific relationships with the broad-scale, general LES relationships evident across the sites at the continental scale. Specifically, the two desert sites MOAB and JORN had extremely high levels of foliar pigments despite otherwise conservative aboveground and belowground traits, such as low microbial community biomass and SLA (Figure 3). Desert plants produce large amounts of carotene to protect leaves against the high levels of harmful UV rays experienced in deserts (Mibei et al., 2017). This indicates that although there are some associations and trends which are common across diverse grasslands, there are other site-specific factors which influence ecosystem processes and community traits. Across the continental-scale selection of sites, there were other instances where seemingly contrasting ecosystems had similar plant trait and microbial communities. For example, plots from the two high-latitude Alaskan sites with sub-zero mean annual temperatures, TOOL and DEJU, had acquisitive plant trait syndromes and large microbial communities similar to those found in productive, temperate prairie sites such as KONZ (Figure 3). A local reason for this rapid-growth plant trait strategy, seemingly at odds with the overall patterns of productivity and leaf economics, could be the highly seasonal nature of the herbaceous community at the high-latitude sites, characterised by short-lived plants which exhibit an acquisitive trait syndrome for their limited seasonal lifespan. This points to suggestions made by previous authors (Bardgett et al., 2005) that relationships between above- and belowground communities may have an element of seasonal variation; multi-seasonal monitoring could be an important avenue for further research in efforts to understand and monitor the belowground biosphere. From a remote sensing perspective, satellite systems produce imagery at regular time intervals and therefore could be valuable for such seasonal investigations. However, field sampling efforts would also need to take place across seasons to produce coincident *in-situ* and remote data.

3.4.2 Predicting soils from spectral reflectance by remote sensing

Spectral reflectance of the land surface was able to predict large portions of the variation in belowground soil microbial communities, evidencing that strong links between imaging spectroscopy and soil communities found by other authors in forests are also evident in mixed grasslands and shrublands at the continental scale (Madritch et al., 2014; Sousa et al., 2021). PLSR models predicted between 43 and 68% of the variation in soil microbial community size and structure, with small errors between 8 and 13% the measured variable range. Further to this, for soil total microbial biomass, bacterial biomass, fungal biomass, and F:B ratio imaging spectroscopy bands were able to predict more variation than were the set of plant traits measured in the field, indicating that a spectral perspective of the vegetation community may be able to offer more important information than can be given by the limited number of pre-determined plant traits which it is practically feasible to measure in the field.

Of the six microbial properties studied, canopy spectral reflectance was able to predict microbial community structure (F:B ratio) the best using PLSR (R^2 0.68; NRMSE 9%). F:B ratio is an important, broad measure of soil microbial structure that is widely used in ecology as an indicator of soil microbial communities and associated functions, for example the carbon storage capacity of the soil biome (Bardgett et al., 1996; de Vries, Bloem, et al., 2012; de Vries, Manning, et al., 2012; Orwin et al., 2010). Being able to characterise this soil F:B ratio rapidly and over large spatial scales would be valuable for monitoring change in carbon storage capacity of ecosystems (Malik et al., 2016). For soil microbial functions, here indicated by rates of nitrification and N mineralisation, spectroscopy was able to predict less variation than were field-measured plant traits. Nitrogen transformations were modelled well from spectroscopy in the middle of their measured range, but that for plots with unusually fast or slow rates of N transformations the link to aboveground reflectance was lost. In a contrast to the other trends shown, the outlying nitrogen transformation observations were caused by isolated plots rather than a whole site. This suggests that localised environmental variables, for example unusual topography or a historic soil event which are not evident in the spectral reflectance, are influencing the unusual rates of nitrogen transformations in these plots.

Identifying the links and mechanisms that connect imaging spectroscopy to environmental properties on the ground is a challenge for remote sensing (Cavender-Bares et al., 2020b). Often, mechanism-led approaches whereby the spectral regions associated with known aboveground traits are first isolated, for example through the use of spectral indices, are less effective than multivariate approaches, where all spectral bands are used as predictors in statistical models and the important spectral regions and potential mechanisms must be inferred afterwards (Pau et al., 2022; Van Cleemput et al., 2018). This study supports these

conclusions; multivariate PLSR models of soil properties from imaging spectroscopy were able to predict more variation than were models of soils from field-measured plant traits, similar to previous findings in forests (Madritch et al., 2014). Relationships between remote sensing imagery and belowground properties presented here are also stronger than those in a recent similar experiment in two contrasting US grasslands, in which remote sensing data was first used to derive aboveground vegetation properties, which were then linked to soils (Cavender-Bares et al., 2022). For a trait to provide a link between imaging spectroscopy and soil communities, it must be both important for predicting soils and well-retrieved from imagery. SLA and carotene are the two identified traits which link spectra to soils in this dataset. SLA is well-known as a key trait indicator of belowground communities in ecology (de Vries, Manning, et al., 2012; Delgado-Baquerizo et al., 2018; Leff et al., 2018), but has historically been overlooked in remote sensing, though recent studies are addressing this (Van Cleemput et al., 2018). Carotene however is not routinely included in field-based trait assessments, perhaps due to the expensive gas chromatography needed to measure it. A spectral perspective of vegetation surfaces is relatively successful in retrieving carotene (Gitelson et al., 2002; Kozhoridze et al., 2016; Ustin, Asner, et al., 2009; Van Cleemput et al., 2018), which could be a valuable contribution to plant-trait-based approaches for predicting belowground conditions.

Imaging spectroscopy was overall able to explain more variation in soil microbial properties than were the set of field-measured plant traits, indicating that there is some other environmental variable or variables represented in the reflectance signal that convey patterns of soil microbial communities aboveground. These could be other 'traits' not explicitly measured in the field survey. For example, pigments and water content, phylogenetic variation, species variation, and functional variation (Lausch et al., 2018; Schweiger et al., 2018). Many of these traits vary together via constellation effects, even if they do not have a specific absorption feature. The PLSR coefficient plots show that the red-edge region (700-800nm) is important for prediction of all three types of soil microbial biomass (Figure 7). This region is associated with vegetation greenness or density, therefore describing aboveground productivity of the vegetation community which translates into the quantity of plant inputs to the soil via litter and root exudates. Quantity of inputs is a key control on soil microbial populations, determining the amount of carbon and nutrient resources available (Cavender-Bares et al., 2022). This was not directly captured through field-measured community-level traits, and could therefore be a key reason for the additional explained variation from spectra.

Besides other sources of biological variation in the vegetation community, there are many other environmental and physical variables which canopy-level imagery is influenced by. These include an element of random parameters like leaf angles, sun angles, topographic

variation, hydrologic variation. In this dataset, a key signal likely contributing to explained variation is influence of soils in the canopy reflectance. Total vegetation coverage across the plots ranges from 15 to 270%, and low-vegetation pixels were not masked out via NDVI threshold before making the plot-level mean spectra, because it was envisaged that the coverage of vegetation could be an important environmental variable in itself and therefore contribute valuable information to the plot-level spectra (Cavender-Bares et al., 2022; Hauser et al., 2021). It can be seen in Figure 5 that an example plot from the MOAB site, a desert site in Utah with low vegetation coverage, has a spectral profile characteristic of bare soil. Spectral wavelengths in the SWIR region, above 1500nm, respond to soil properties and therefore represent a combination of the amount of bare soil visible over the plot (i.e. vegetation coverage) and the properties of the soil itself such as soil moisture or biological soil crusts (Gaitán et al., 2013; Ustin, Valko, et al., 2009). These wavelengths were important for predicting soil fungal biomass much more than total microbial or bacterial biomass, which is consistent with expectations that the former would be more dominant in less productive plots where the soil surface is more influential on canopy reflectance. This result indicates that bare soil areas in sparsely vegetated plots may not necessarily weaken links between spectra and belowground communities, and therefore it may be valuable not to mask out bare pixels when modelling belowground communities.

3.4.3 Limitations of PLFA

The use of phospholipid fatty acid (PLFA) analysis is well-established in the ecological literature and is common in studies that use aboveground plant traits to predict properties of belowground microbial communities (e.g. De Long et al., 2019; de Vries et al., 2012; Fry et al., 2017; Grigulis et al., 2013; Lange et al., 2015; Orwin et al., 2010; Waldrop et al., 2017). PLFA gives a measure of the biomass of broad microbial groups, such as fungi vs bacteria, or saprophytic vs mycorrhizal fungi. However, PLFA is in general an imprecise measure of microbial communities, and has some important limitations.

It is challenging to attribute PLFAs to specific microbial groups, and criticisms of PLFA analyses are often related to over-confident attribution of PLFAs to specific groups (Frostegård et al., 2011). PLFAs are present in fungi, bacteria and plants in varying quantities and even the most commonly used marker PLFAs are not truly exclusive to any one group. For example, the PLFAs used in this chapter to indicate fungal biomass (*18:2ω6,9*; *18:1ω9*) are common in fungi and two of the most commonly used fungal marker PLFAs in the literature (Quideau et al., 2016). However, these PLFAs are also present in plants and bacteria to some extent, and therefore some authors have recommended that in the presence of plant material, these PLFAs should not be used to indicate fungi (Joergensen, 2022). However, others argue

that the proportion of root material remaining in soils after sieving is small enough that variations in *18:2ω6,9* are still overwhelmingly derived from fungi and therefore these PLFAs should continue to be used (Frostegård et al., 2011; Kaiser et al., 2010). Because of the uncertainty inherent in attributing PLFAs to specific groups, PLFA markers may be more confidently attributed to a specific group in some ecosystems than in others. For example, the small amount of fungal marker *18:1ω9* which is present in bacteria has a greater effect on the PLFA concentration in bacteria-rich agricultural soils than bacteria-poor coniferous forests (Frostegård et al., 2011). It may consequently be particularly challenging to use PLFAs to indicate microbial groups across a range of contrasting ecosystems, compared to using PLFAs to compare a single ecosystem over time. Therefore, in this chapter a cautious approach was taken and only the PLFAs most widely used to indicate either fungi or bacteria across different ecosystems were attributed to the group. As a result, estimated biomass of the fungi or bacteria group may be conservative at some sites.

In order to enhance the PLFA analysis presented in this chapter, more detailed attribution of PLFAs to different groups could be carried out on a site-by-site basis, taking into consideration the wider environmental conditions at each site. In particular, the PLFA *16:1ω5* is associated with arbuscular mycorrhizal fungi and has recently been recommended for use as an indicator for this group (Joergensen, 2022). In this chapter, *16:1ω5* was not included in the fungal biomass estimate due to the conservative approach to attributing PLFAs to specific groups. *16:1ω5* has also been observed in bacteria and therefore is sometimes recommended for use as a fungal marker only in ecosystems with low bacterial abundance (Willers et al., 2015). In addition, mycorrhizal fungi are considered to be less directly related to ecosystem-level decomposition rates than saprotrophic fungi, being more closely associated with root traits and specific plant species, which are not the focus of this thesis. However, mycorrhizal fungi are becoming more of a research focus, and have been found to have significant indirect effects on ecosystem carbon and nutrient cycling, for example influencing saprotrophic fungi populations by competing with them for nutrients (Orwin et al., 2011). Therefore, the PLFA analysis in this chapter could be enhanced by the inclusion of *16:1ω5* to indicate arbuscular mycorrhizal fungi.

Alternative measures of soil microbial communities include measuring the activity of specific enzymes in the soil which are associated with different microbial groups and functions (e.g. Madritch et al., 2014), and analysis of marker genes which can be attributed with high precision to microbial taxa. The NEON data product *Soil microbial group abundances* (DP1.10081.001) was tested for relationships with other aboveground and belowground properties in the initial stages of this research chapter, but no relationships were found and the data product has since been discontinued due to issues widely reported from the

community. Comparison of multiple independent measures for soil microbial communities increases confidence in results, and could be used to enhance the research presented in this chapter should data become available in the future.

3.5 Conclusions and further work

These results demonstrate the powerful potential of imaging spectroscopy to retrieve important information about spatial variation in the belowground biosphere, which is an important component of biogeochemical cycles and under significant interacting pressures worldwide from climate and land use changes. This potential is not limited only to forest ecosystems, where promising results have previously been demonstrated (Madritch et al., 2014; Sousa et al., 2021), but as shown here also applies to mixed grassland and shrubland communities which are traditionally more challenging to interpret with remote sensing due to communities being heterogenous at the sub-pixel scale (Van Cleemput et al., 2018). Grasslands and shrublands are extensive across the Earth's surface and dynamics within and between them are especially relevant to human activities including agriculture, making these ecosystems, including their soil component, especially crucial to study. The contribution of imaging spectroscopy lies both in offering a different perspective of the vegetation community, which simultaneously accounts for multiple axes of biological variation including traits, species and genetics which it is impractical or even impossible to fully account for in the field, and in scaling-up studies to unprecedented spatial extents and detail. The plot size used in this study, 40x40m, is comparable to the pixel resolution of forthcoming hyperspectral satellite missions such as EnMAP and HyspIRI (Anderson, 2018; Pettorelli et al., 2018a), which could be invaluable for scaling up relationships. Conversely, this work demonstrated the ability of imaging spectroscopy to distinguish between soil communities at highly contrasting grassland and shrubland sites; it would also be valuable to attempt to resolve more subtle differences in soil microbial communities from airborne imaging spectroscopy, for example over a single site. This would be a step towards being able to resolve temporal differences in soil communities – i.e. change over time – which are likely to be smaller than broad scale spatial differences. Airborne data across single NEON sites over multiple years will continue to become available in the coming decades, and will enable future studies to be carried out across smaller spatial extents which are more relevant for monitoring, land management and identifying mechanisms than the continental set of sites presented here. Multivariate statistical methods were found in this study, in agreement with previous work (Van Cleemput et al., 2018), to be highly effective at utilising the spectral detail of imaging spectroscopy in grasslands, but they can also obscure mechanistic links. Further work is needed to disentangle

the physical and biological properties of the vegetation community that translates patterns of soil microbial communities into aboveground reflectance. As the NEON network progresses through its projected lifespan and more data becomes available from the sites, this will provide a valuable resource for such studies, improving our understanding of the belowground biosphere at a range of spatial scales.

4. Retrieving aboveground plant functional traits from Sentinel-2 across North American grasslands

Abstract

Foliar traits are important ecosystem parameters which control ecosystem functioning, indicate ecosystem response to changing environmental conditions and can be used as proxies for biological diversity (Funk et al., 2017; Hauser et al., 2021). There have been significant recent efforts to document and characterise plant trait variation across the worlds biomes, using databases of networked field sampling campaigns and recently using remote sensing data. Spectral properties of the vegetation community surface, captured remotely by sensors aboard aircraft and satellites, can reflect a number of important foliar traits relating to plant growth strategies and carbon capture, including chlorophyll content, carbon and nitrogen and morphological properties such as specific leaf area (SLA). However, there has thus far been a significant bias towards forests in trait retrieval from remote sensing, with grassland systems remaining relatively understudied at large scales, and complex systems incorporating mixed areas of grassland and woodland even less frequently investigated despite being of significant conservation importance. Recent work characterising grassland traits from detailed hyperspectral remote sensing has shown promising results, but it remains unknown to what extent satellite data, which has greater global coverage but at coarser spectral and spatial resolution, may also be able to retrieve grassland plant traits. Here, we determine the potential of the Sentinel-2 satellite for estimating 20 grassland foliar traits at the continental scale, using field sites from the National Ecological Observatory Network (NEON). Morphological and biochemical traits were modelled successfully by random forest, using Sentinel-2 satellite data along with climate variables, with variation explained comparable to that found in hyperspectral studies (23.1% - 75.8%). The most successfully-modelled traits were Specific Leaf Area (SLA) (66.5%, NRMSE 13%), a morphological trait relatively under-studied in grasslands but central to plant growth strategies, along with biochemical traits carbon (58.7%, NRMSE 13%), and cellulose (variation explained 44.9%, NRMSE 12%), and leaf macronutrients phosphorus (variation explained 75.8%, NRMSE 11%), and potassium (variation explained 63.4%, NRMSE 11%). The results also suggest that knowledge of vegetation composition, specifically the proportion of woody vegetation present in the community, are important for effective trait retrieval. These results indicate that satellite remote sensing, and Sentinel-2 in particular, has the potential to retrieve grassland foliar traits across large, continental geographic extents, expanding the reach of trait-based approaches to an extensive and globally important ecosystem.

4.1 Introduction

Foliar traits are the physical and chemical properties of leaves such as leaf area, water content, concentrations of nutrients and elements and proportions of complex carbohydrates such as lignin and cellulose. The traits of a leaf control the rate at which important plant processes and interactions with the environment take place; for example greater leaf area and chlorophyll content in leaves facilitates faster rates of photosynthesis, or larger proportions of dry matter in the form of tough, complex carbon structures such as lignin promote leaf longevity and slow decomposition of leaves when they are transferred to the soil as litter. When traits are considered together as a trait 'syndrome' there are consistent associations between traits which facilitate acquisitive or conservative plant growth strategies, which have been found across a range of plant life forms all over the globe (Díaz et al., 2016; Reich, 2014; I. J. Wright et al., 2004). When plant traits and associated growth strategies are scaled up to the community, landscape or even regional level, they are important drivers of global biogeochemical cycles (Funk et al., 2017; Lavorel & Grigulis, 2012). Trait composition can be used to infer the rates of important plant-driven ecosystem processes such as carbon storage at the ecosystem scale, to predict ecosystem-level responses to environmental disturbance (Grigulis et al., 2013; Gross et al., 2008, 2009), and to infer other closely linked aspects of the system, such as the abundance and structure of microbial communities belowground (Bardgett, 2017; de Vries, Manning, et al., 2012; Legay et al., 2014; Orwin et al., 2010; Wardle David A. et al., 2004). The diversity of plant functional traits is also emerging as an important axis of biodiversity (Hauser et al., 2021; Jetz et al., 2016; Rossi et al., 2020, 2021). Therefore, understanding the variation of plant traits in space and time across large geographical extents is an emerging field of research effort in ecology.

Plant trait variation occurs both between and within species, termed interspecific and intraspecific variation. Variation in traits between species contributes the largest proportion of trait variation, and species mean trait values can be aggregated to the community level using species composition data to create community-weighted mean (CWM trait values), which have been linked to ecological functioning across a wide range of environments (de Vries, Manning, et al., 2012; Grigulis et al., 2013; Manning et al., 2015; Rossi et al., 2020). CWM approaches to ecosystem-level trait assessment can be used in conjunction with trait values sourced from worldwide trait databases such as TRY, which constitute an important resource for trait-based research (Gallagher et al., 2020; Kattge et al., 2011). However, CWM and database approaches that use species means are not able to effectively capture the portion of trait variation that occurs within a species, or intraspecific variation, which contribute around 30% of total trait variation (Albert et al., 2010; Siefert et al., 2015; Violle et al., 2012). As well as varying between individuals of the same species, traits can vary plastically over time in response to change, for

example root length among individuals increasing as a response to lowering of water tables (Mao et al., 2018). Community-level trait change from species-based approaches occurs through succession, as species' relative competitiveness leads to an increase or decrease in abundance in the changed environment, and with it a change in CWM traits (Suding et al., 2003). For many ecosystems, succession takes place over long timescales and so accounting for the plastic, intraspecific component of trait variability in large scale models is crucial (Funk et al., 2017).

Being able to effectively capture intraspecific variation and trait plasticity are important steps towards realising the potential of plant trait-based approaches, which despite advances are still regularly out-performed by species based approaches in efforts to model environmental properties (Hauser et al., 2021; Leff et al., 2018). Many authors recommend more extensive and thorough field measurement of plant traits, especially in regions of the globe which are under-sampled, and while this is a fundamentally important research effort, it is challenging and possibly unfeasible to be able to capture the variation of plant traits worldwide at sufficient spatial and temporal detail using ground-based methods alone (Asner, 2013; Jetz et al., 2016; Schimel et al., 2015). Remote sensing offers a new perspective for assessing plant trait variation, by retrieving spectral properties of the vegetation community that are known to be closely linked to functional traits, rapidly and across large spatial extents. Remote sensing is increasingly recognised as a valuable and promising tool to augment fundamental field-based data collections and expand our understanding of plant trait variation across the worlds biomes (Asner, 2013; Asner & Martin, 2016; Dana Chadwick & Asner, 2016; Jetz et al., 2016).

Remote sensing of plant traits is fundamentally based on the relationships between foliar traits and the reflectance and absorption of electromagnetic radiation which is detected by the sensor (Asner et al., 2015; Cavender-Bares et al., 2017; Kokaly et al., 2009; Ustin, Asner, et al., 2009). Some traits which directly interact with radiation have characteristic absorption features in reflectance spectra; for example chlorophyll is a trait commonly retrieved using remote sensing because it directly absorbs blue and red wavelengths for photosynthesis (Clevers & Gitelson, 2013; Revill et al., 2019; Ustin, Asner, et al., 2009). Other traits are detected through constellation effects, where the trait itself does not have a particular absorption feature but covaries with other traits which do (Dana Chadwick & Asner, 2016; Nunes et al., 2017). The traits most commonly retrieved from remote sensing are not always those for which ecological understanding is the most developed – for example, there is a remote sensing bias towards chlorophyll and other pigments, and an ecological bias towards structural properties such as vegetation height and SLA which are relatively easy to assess in the field. Previous reviews have recommended that future remote sensing studies include

morphological traits SLA and LDMC in order to be able to link spectral trait retrieval with ecological understanding at large scales (Van Cleemput et al., 2018). The current body of research retrieving foliar traits from remote sensing includes studies carried out at the local (A. M. Ali, Darvishzadeh, & Skidmore, 2017; Pau et al., 2022; Rossi et al., 2020; Schneider et al., 2017), regional (Asner et al., 2015; Ma et al., 2019; Z. Wang et al., 2020) and global (Aguirre-Gutiérrez et al., 2021; Butler et al., 2017; Moreno-Martínez et al., 2018) scale.

Despite a growing body of evidence linking remote sensing data to plant traits across forests, and imaging spectroscopy to traits in grasslands (Van Cleemput et al., 2018), grassland ecosystems remain under-studied, and rarely studied using satellite data (Pau et al., 2022; Rossi et al., 2020; Veldman et al., 2015). One challenge of using satellite data to retrieve field-measured traits is acquiring satellite imagery which is temporally matched to field data. In hyperspectral studies, the sensor is often deployed specifically to gather data equivalent to the field campaign; for example NEON coordinates airborne observation platform (AOP) flights with plant trait sampling on the ground. Satellite systems have regular return periods, which makes it possible to temporally coordinate satellite overpasses with field data collection, as some authors have begun to do recently (Hauser et al., 2021). However, accounting for satellite schedules is not common when planning field campaigns, where many other factors impact the logistics of data collection (Cavender-Bares et al., 2020a). Temporal offset between field and remote measurements is important, because some plant traits such as pigments and water content are variable over short timescales (Croft et al., 2017). However, it has yet to be explicitly tested the effect of increasing temporal offset on the link between satellite-derived reflectance and various plant functional traits.

Another challenge for satellite remote sensing particular to grasslands is the size of individual organisms relative to the size of image pixels; where in a forest individual tree crowns can often be delineated in remote sensing imagery, in grasslands there are likely to be mixtures of species and also higher-order plant lifeforms such as graminoids, shrubs and trees within a single image pixel. This mixing becomes more likely with increasing size of the image pixel, so is particularly pertinent to satellite remote sensing which typically has pixel sizes of over 10x10m. While trait-based approaches which characterise the surface as a continuous grid of trait values, rather than a mix of categorical species or functional types, could be particularly relevant to the biological assessment of such mixed pixels, spectral mixing of multiple species and lifeforms is known to reduce the strength of relationships between spectra and foliar traits, relative to homogenous single-species reflectance signals (Hacker et al., 2022). Mixing of grassland and woodland occurs at sub-pixel scales in ecosystems which are widespread and of particular importance for conservation and human livelihoods, including in savannah ecosystems, at grassland-woodland boundaries and in places where

land cover change from grassland to woodland or vice-vera is taking place (House et al., 2003; Ratajczak et al., 2012; Sexton et al., 2015; Soliveres et al., 2014; Veldman et al., 2015). It is therefore important to include these mixed grassland-woodland areas in empirical models of plant traits from remote sensing, despite the challenges. Trait mapping over mixed grassland-woodland landscapes has only been attempted by a handful of studies using hyperspectral imaging spectroscopy, from which results have been mixed and the diversity of the grassland community at small spatial scales identified as a reason for model errors (Dahlin et al., 2013; Hacker et al., 2022; Hacker & Coops, 2022; Z. Wang et al., 2020).

This study will address these research gaps by modelling variation in 20 foliar traits across diverse grassland ecosystems at the continental scale, using multispectral satellite data from Sentinel-2 in combination with climate information to answer the overall research objective; establishing to what extent aboveground plant functional traits can be retrieved in grasslands across large spatial extents from Sentinel-2. Further to this overall aim are two specific objectives. First, to establish the extent to which heterogeneity of land cover and vegetation composition at grassland sites impacts the ability of spectral data to retrieve foliar traits, and whether the herbaceous and woody portions of vegetation at these grasslands can be modelled together. Finally, we will test the impact on model performance of varying the maximum temporal offset between satellite imagery and field sampling that is permitted when matching *in-situ* observations to spectral data. This is an important methodological consideration when carrying out investigation of surface properties from satellite data, as it simultaneously affects the quality and the quantity of matched field and spectral observations.

4.2 Methods

4.2.1 Study sites and sampling strategy

Study sites and *in-situ* data for this study were sampled from the National Ecological Observatory Network (NEON). NEON is a network of sites distributed across North America, which collect ecological and climate data with the purpose of understanding the impacts of climate and land use change on continental-scale ecology (Kampe et al., 2010). The sampling design of NEON has been created with a view to linking ecological data on the ground with remote sensing data, both the network airborne spectroscopy platform and satellite data such as Sentinel-2. The 81 sites in the network span many different ecosystem and land cover types, and many sites are characterised by more than one type of ecosystem. Plant traits are measured every five years at NEON sites as part of the broad suite of terrestrial and aquatic environmental data collection which is standardised and reproducible across the network (Barnett et al., 2019b; Kampe et al., 2010). For this study, 11 sites were sampled from the network. These were sites at which grassland is a dominant land cover type, according to a site-wide classification based on the National Land Cover Definition (NLCD), and which had plant trait data available between 2017 and 2020. The eleven grassland sites chosen for this study from the NEON network span a latitudinal gradient of 18 -47° (Figure 8) and climate gradients of 0.7 - 26°C mean annual temperature and 367 – 1081mm mean annual precipitation (Table 5). Values of the Global Aridity Index (GAI) for sites range from 2142 (semiarid) to 5901 (dry subhumid) (Zomer et al., 2022).

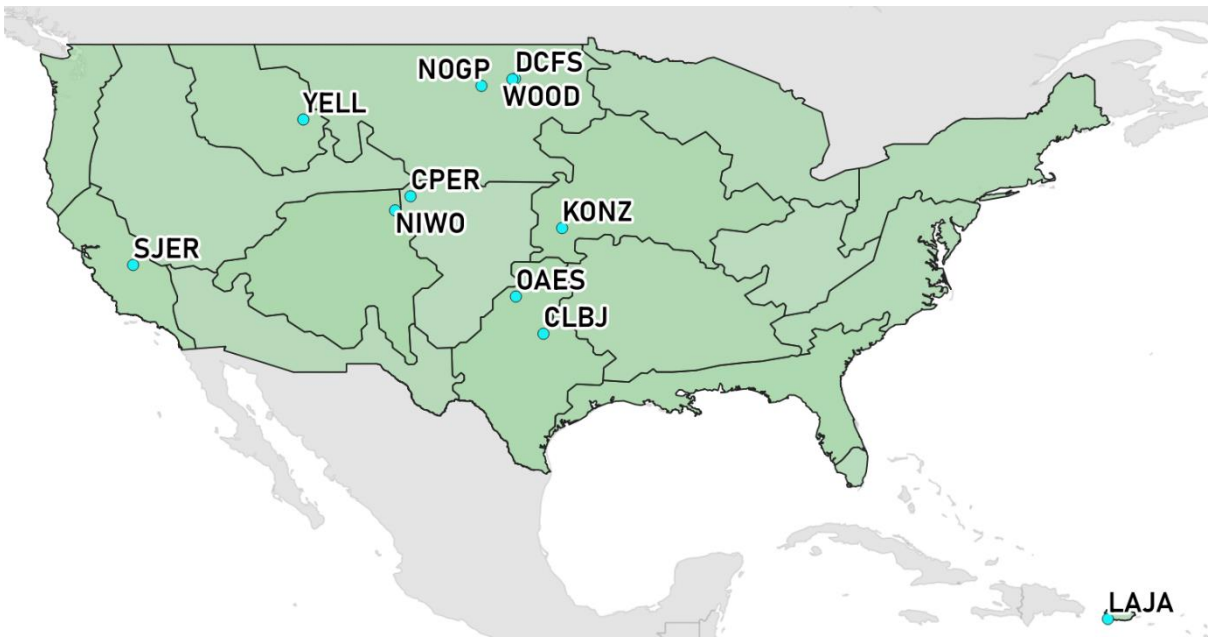

Figure 8 Location map of the eleven NEON grassland sites, distributed across the North American continent

Table 5. Details of the eleven grassland sites in this study, including location and site level averages of the five climate variables used in modelling. Temperature seasonality is given by the annual standard deviation of temperature x 100, precipitation seasonality is the coefficient of variation (C.V.) of annual precipitation. Global Aridity Index (GAI) is unitless, and has been multiplied by a factor of 1000; lower GAI indicates more arid sites.

Site ID	Dominant landcover classes	Lat °	Long °	Elevation (m)	MAT (°C)	MAP (mm)	Temperature Seasonality (°C)	Precipitation seasonality (mm)	GAI
DCFS	Grassland/Herbaceous	47.179	-99.125	575	4.4	437	1259	71	3830
WOOD	Emergent Herbaceous Wetlands, Grassland/Herbaceous	47.138	-99.247	591	4.3	421	1262	74	3695
NOGP	Grassland/Herbaceous	46.785	-100.915	589	5.7	427	1219	65	3454
YELL	Evergreen Forest, Grassland/Herbaceous, Shrub/Scrub	44.947	-110.511	2133	2.3	543	908	17	4681
CPER	Grassland/Herbaceous	40.826	-104.727	1654	9	367	886	60	2142
NIWO	Evergreen Forest, Grassland/Herbaceous	40.045	-105.57	3490	0.7	626	715	18	5207
KONZ	Deciduous Forest, Grassland/Herbaceous	39.097	-96.568	414	12.3	890	1028	51	5901
SJER	Evergreen Forest, Grassland/Herbaceous, Shrub/Scrub	37.104	-119.734	400	16.6	545	721	85	2573
OAES	Grassland/Herbaceous, Shrub/Scrub	35.41	-99.062	519	15.5	701	932	50	3598
CLBJ	Deciduous Forest, Grassland/Herbaceous	33.394	-97.588	272	17.4	869	829	36	4669
LAJA	Cultivated Crops, Grassland/Herbaceous, Pasture/Hay	18.026	-67.076	16	26	1081	134	53	5471

Foliar traits at NEON grassland sites are sampled from 20 sampling plots, measuring 20x20m, distributed across field sites so as to capture the full variation of environmental conditions such as elevation, and also the full range of land cover types across the site. Herbaceous vegetation is sampled from plots using a clip strip, measuring 0.1 x 2m, from which all aboveground biomass is harvested and homogenised before foliar trait assessment in the laboratory. The average foliar trait value from all individual leaves harvested from the clip strip is given as the community-level trait value. Many of the grassland-dominated sites in NEON have significant portions of woody vegetation present across the landscape, both as large woody areas and as isolated individuals in the herbaceous-dominated land cover (Figure 9). Although this study is focused on grassland ecosystems, the distinction between grassland and forest at many of the sites is ambiguous (Figure 9, c.), and one of the study objectives is to determine to what extent empirical models are able to capture trait variation from spectral reflection across as well as within vegetation types. Therefore trait measurements from woody plants across the sites were included in some of the trait modelling from Sentinel-2 in this study. Prior to 2019, woody plants present in grassland sites in NEON were sampled according to their abundance at the sampling plot level, with species constituting >25% aerial coverage of the plot sampled for traits. However, after 2019 the sampling protocol for woody individuals changes to reflect a site-based rather than a plot-based approach, with particular taxa targeted for sampling according to species richness at the site level (Weintraub, 2022). Target-based sampling at the site level means that woody plant trait samples in the NEON plant trait data product (DP1.10026.001) are not necessarily representative of community-level traits at the scale of the 20x20m field plot. Therefore, rather than aggregating plant trait values to the plot level, field samples (clip strips and woody individuals) were precisely geo-located to within 1.25m using the NEON data product *Woody vegetation structure* (NEON.DP1.10098). The precise location of *in-situ* plant trait observations was used to identify the single corresponding Sentinel-2 pixel from which to source spectral data, making the assumption that the clip strip or woody individual sample was the dominant influence on reflectance of the land surface for the surrounding 10x10m area covered by the Sentinel-2 pixel. Any plant trait samples which were spatially located within the boundaries of the same Sentinel-2 pixel were excluded from further analysis.

Between 13 and 33 field-measured plant trait observations were available for analysis from each site (n=11), including both herbaceous clip strip and woody individual samples (Figure 9a). Herbaceous samples across the sites originated from areas of seven different land cover classes across the grasslands, the proportions of which are shown in Figure 9b. There is considerable variation in species composition and landscape heterogeneity across the sites, and only three of the eleven grassland sites in the NEON network, comprised of 81 sites in

total, were characterised purely by herbaceous vegetation and land cover classed as grassland (DCFS, CPER, NOGP). Samples of herbaceous vegetation from all land cover types found across the predominantly grassland sites were included in trait models, for example samples of herbaceous vegetation originating from a wooded area of the grassland, because it is important to capture the full variation of land cover types and heterogeneity present across a range of natural and managed grasslands, in order to build models which are representative of a range of landscapes found at the continental scale. The extent to which foliar trait-spectra relationships in herbaceous plants are consistent across different land cover classes is not well understood and is a key part of this investigation. Figure 9, c. shows two aerial photographs of sites with various vegetation types spatially arranged both in distinct areas of woodland and grassland, and as a mixed matrix which is heterogenous at finer scales than Sentinel-2 (10x10m).

a.

b.

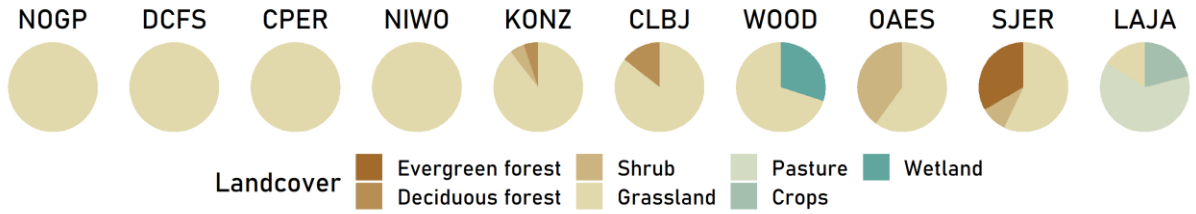

c.

Figure 9 a. Bars show the number of matched field and satellite observations from each of the eleven grassland sites, coloured by vegetation type. b. Pie charts showing the breakdown of land cover classes represented by herbaceous vegetation samples at each site. Land covers are assessed using the National Land Cover Database, and sites are ordered left-right from the highest to the lowest proportion of land cover class grassland. Site YELL is not shown as there were no herbaceous samples collected from this site. c. Aerial photographs showing the distribution across the landscape of mixed herbaceous and woody vegetation types at NEON sites SJER (left) and CLBJ (right), taken from the NEON flight survey (Credit: NEON Science).

4.2.2 Foliar functional traits

Twenty foliar traits from the NEON *Plant physical and chemical traits* data product (DP1.10026.001) were modelled from Sentinel-2 MSI imagery. Traits included specific leaf area (SLA), leaf dry matter content (LDMC), carbon content and C:N ratio, all of which are important traits for determining plant growth strategies and associated ecosystem economics and have been identified as priority traits for retrieval with remote sensing (Van Cleemput et al., 2018). Plant biochemical traits lignin and cellulose are indicative of leaf longevity and slow decomposition in the ecosystem, but are also relatively under-studied and authors often report large errors in models (Z. Wang et al., 2020). Nitrogen, phosphorus and potassium are key nutrients for plant growth and therefore elements which are strongly associated with photosynthesis and biomass production at the vegetation community level. Three photosynthetic pigments were modelled; chlorophyll-a (chl-a), chlorophyll-b (chl-b) and carotene. These pigments are some of the most commonly retrieved traits in remote sensing studies and have direct influence on the reflectance properties of vegetated surfaces (Gitelson et al., 2002; Homolová et al., 2013b; Revill et al., 2019; Ustin, Asner, et al., 2009). Finally, eight major and minor trace foliar elements were modelled; calcium, magnesium, sulphur, manganese, copper, iron, boron and zinc. Units of the 20 foliar traits, their range and distribution can be found in Figure 10. Photosynthetic pigments were converted to units of concentration per area of leaf (Poorter et al., 2014). Per-area pigment concentration is relevant for a spatial remote sensing perspective, and previous trait mapping across NEON sites from hyperspectral data found that pigments were retrieved more accurately on a per-area basis than a per-mass basis (Z. Wang et al., 2020). Foliar trait records were downloaded from the NEON data repository, and geo-located and pre-processed in R using the packages neonUtilities and geoNEON (Lunch *et al.*, 2022).

4.2.3 Satellite data acquisition and pre-processing

Multispectral satellite data from Sentinel-2 was sourced, pre-processed and downloaded using Google Earth Engine (Gorelick et al., 2017a). Sentinel-2 bands representing the visible, red-edge (RE), near infra-red (NIR) and short wave infra-red (SWIR) regions of the spectrum were selected, details of which can be found in Table 6. RE and SWIR bands were resampled to 10 x 10 m spatial resolution, in order to match the resolution of the visible bands. In addition to the individual spectral bands, five spectral indices were calculated and included as predictors in the foliar trait models (Table 6). These indices have been used by previous authors for retrieving foliar traits from satellite and hyperspectral data, in forest and grassland ecosystems. The normalised difference vegetation index (NDVI) is the most well-known vegetation index, and is strongly associated with vegetation productivity and associated

properties such as density, coverage and biomass (Pettorelli et al., 2005; Ren & Feng, 2015). The enhanced vegetation index (EVI) is an alternative to the NDVI, also capturing productivity but unlike the NDVI does not saturate in scenarios of high vegetation density, and has therefore been used to capture traits over forests (A. M. Ali, Darvishzadeh, & Skidmore, 2017; A. M. Ali, Darvishzadeh, Skidmore, et al., 2017; Wallis et al., 2019); however, Pau and colleagues found that NDVI also showed signs of saturating at the NEON grassland site KONZ, which is one of the sites in this study (Pau et al., 2022). Therefore, EVI was also included in our selection of indices. By contrast, in areas of low vegetation coverage where surface soil may have an influence on reflectance, the modified soil adjusted vegetation index (MSAVI) is used to reduce the effect of background soils on apparent vegetation. MSAVI has been used for trait retrieval in forests (Aguirre-Gutiérrez et al., 2021; A. M. Ali, Darvishzadeh, & Skidmore, 2017), although some have reported that it does not improve spectral retrieval of grassland properties relative to NDVI, even in sparsely vegetated areas (Ren & Feng, 2015). The chlorophyll red-edge index (Cl_{re}) was developed specifically to take advantage of the relatively high spectral resolution red-edge bands on Sentinel-2, and has been found to retrieve canopy chlorophyll in grass and croplands (Clevers & Gitelson, 2013). The normalised difference moisture index (NDMI, also termed normalised difference water index) utilises the short-wave infrared portion of the spectrum to retrieve the water content of the canopy (A. M. Ali, Darvishzadeh, & Skidmore, 2017; I. Ali et al., 2016; Obermeier et al., 2019).

We selected the nearest suitable (i.e. cloud and shadow -free) satellite image pixel to the date of field sampling for each sampling location, up to a maximum of fourteen days either side of the field sampling date. Where two satellite images were available and equidistant in time, the earlier image was chosen. The resulting dataset consisted of 237 plant trait observations, matched with the nearest high-quality Sentinel-2 image pixel within a fourteen-day window. To determine the influence of temporal offsets between field sampling and image acquisition on subsequent trait models, the temporal offset between field and spectral sample collection was calculated and categorised into one of four time categories: one-day (offset <= 1); five-day (offset 2 - 5); seven-day (offset 6 - 7) and fourteen-day (offset 8 - 14). The proportion of sampling plots in each time category are shown in Figure 13, a.

Table 6. Details of the predictor variables used to model the foliar traits

Category	Index	Description	References
Visible	B2	Blue visible light	
	B3	Green visible light	
	B4	Red visible light	
Red-edge	B5	Narrow Sentienl-2 red edge bands	
	B6		
	B7		
Near Infra Red	B8	Near infra red	
Short Wave Infra Red	B11	Associated with vegetation moisture content and phenolic compounds	(Couture et al., 2016)
	B12		
Spectral index	NDVI	(NIR – Red)/(NIR + Red)	(A. M. Ali, Darvishzadeh, & Skidmore, 2017; A. M. Ali, Darvishzadeh, Skidmore, et al., 2017; Ren & Feng, 2015)
	EVI	2.5(NIR-Red)/ NIR + 6Red - 7.5Blue + 1	(A. M. Ali, Darvishzadeh, Skidmore, et al., 2017; Vermote et al., 2016; Wallis et al., 2019)
	Cl_{re}	(B7/B5)-1	(Clevers & Gitelson, 2013)
	NDMI	(NIR-SWIR1)/(NIR+SWIR1)	(A. M. Ali, Darvishzadeh, Skidmore, et al., 2017)
	$MSAVI_2$	(2 * Band 5 + 1 – sqrt ((2 * Band 5 + 1)^2 – 8 * (Band 5 – Band 4))) / 2	(Aguirre-Gutiérrez et al., 2021; A. M. Ali, Darvishzadeh, Skidmore, et al., 2017; Qi et al., 1994; Ren & Feng, 2015)
Climate	MAT	Control the resources available for plant growth and therefore plant traits	
	MAP		
	Temperature seasonality		
	Precipitation seasonality		
	GAI	The ratio of precipitation to potential evapotranspiration	(Zomer et al., 2022)

4.2.4 Climate data

Climate is a key driver of aboveground plant traits across large geographic extents, therefore variation in traits due to climate was accounted for in the models of foliar traits by including climate variables as predictors (Table 6). Climate data was sourced from Worldclim, as 30-year averages delivered in 1 km grid squares (Fick & Hijmans, 2017; Hijmans et al., 2005). Five climate variables were retrieved: mean annual temperature (MAT), mean annual precipitation (MAP), and their annual variability, termed temperature seasonality (annual standard deviation of temperature) and precipitation seasonality (annual coefficient of variation of precipitation). The global aridity index (GAI) was also used, which gives the ratio of precipitation to potential evapotranspiration, and is commonly used as a predictor of plant traits and associated ecosystem properties at large scales (Delgado-Baquerizo et al., 2018; Zomer et al., 2022).

4.2.5 Statistical analysis

Random Forest (RF) modelling was used for foliar trait estimation (Breiman, 2001). Random forest is a machine learning algorithm which is often used in large-scale remote sensing studies, and has been used to retrieve foliar traits (Aguirre-Gutiérrez et al., 2021; Moreno-Martínez et al., 2018; Thomson et al., 2021) as well as other ecosystem properties such as diversity (Fauvel et al., 2020; Harris & Baird, 2019; Y. Zhao, Yin, et al., 2022). Benefits of random forest include the algorithm's ability to account for multiple types of predictor variable and the output of variable importance scores.

We developed individual RF models to predict each of the 20 traits from a combination of spectral reflectance, spectral indices and climate variables. We repeated this analysis using different combinations of satellite and field data, to determine the influence of grassland vegetation composition on trait retrieval. The first set of RF models used only herbaceous vegetation samples collected across the sites (n=167), and the second set of models included all vegetation samples together, i.e. both herbaceous clip strip samples and woody individuals found across the sites (n= 237). For both model runs, the feature selection algorithm Boruta was used to select only the most relevant predictor variables for each trait model (Degenhardt et al., 2019; Kursa & Rudnicki, 2010). Each trait model was constructed with 1000 trees and a model optimised mtry using the package RFUtilities (Evans & Murphy, 2017). Due to the relatively low sample numbers, model accuracy was assessed using out-of-box (OOB) validation. For each trait model, we obtained the variation explained (%) and the MSE, which was subsequently transformed and reported as the RMSE. We used the variable importance

RF output metric (% increase MSE) to identify which predictor variables were the most useful for explaining variation in each foliar trait.

Because random forest is a stochastic algorithm, each trait was modelled 100 times and the mean variation explained, RMSE and importance of each predictor variable were calculated and are presented as the final model performance statistics for each trait (Aguirre-Gutiérrez et al., 2021). Standard deviation of variation explained across the 100 model runs was <0.01 for all foliar traits, indicating that the models were stable (results not shown). RMSE was normalised by the range of the measured trait value in order to be able to compare model results directly to those recently achieved over the same sites using hyperspectral data (Z. Wang et al., 2020). To investigate the effect of temporal offsets between *in-situ* data collection and satellite data retrieval on model performance, the RF modelling was repeated a further three times but this time restricting the dataset to those observations categorised as having (i) a seven-day, (ii) five-day or (iii) one-day temporal offset between the image and field data collection dates.

Finally, variation partitioning, based on redundancy analysis, was carried out in order to show the proportion of variation in each foliar trait that was attributable to the spectral and the climate predictor variable groups uniquely and in combination (Borcard et al., 1992; Löfgren et al., 2018; Weber et al., 2018). In a similar manner to the variable importance outputs from RF, the redundancy analysis was undertaken to contrast the explanatory power of climate and spectral predictor variables.

All statistical analyses were carried out in R using the packages randomForest, RFUtilities, and vegan.

4.3 Results

4.3.1 Distribution of foliar traits across NEON grasslands

The distribution of *in-situ* measured trait values among herbaceous vegetation across the sites is shown in Figure 10. Woody samples are not included in these distributions, because the main random forest trait models are based on herbaceous samples only. LAJA has particularly variable trait values, particularly for SLA, N, phosphorus and sulphur content. Sites KONZ, SJER, CLBJ and OAES have intermediate trait variability across all traits. Sites DCFS, NOGP, CPER and NIWO have relatively small ranges of traits. Site WOOD has high values and large inter-quartile ranges of chl-a and chl-b. The single herbaceous clip strip sample from site NIWO had unusually large values of C, lignin and manganese. Some sites show trait syndromes characteristic of the rapid or conservative ends of the leaf economics spectrum; for example OAES has low foliar nutrients nitrogen, phosphorus and potassium, matched with a high proportion of dry matter in leaves indicative of conservative growth, and site SJER has high foliar nutrients, high SLA and low LDMC indicative of acquisitive growth. For most traits, there was overlap in the inter-quartile ranges of trait values between sites.

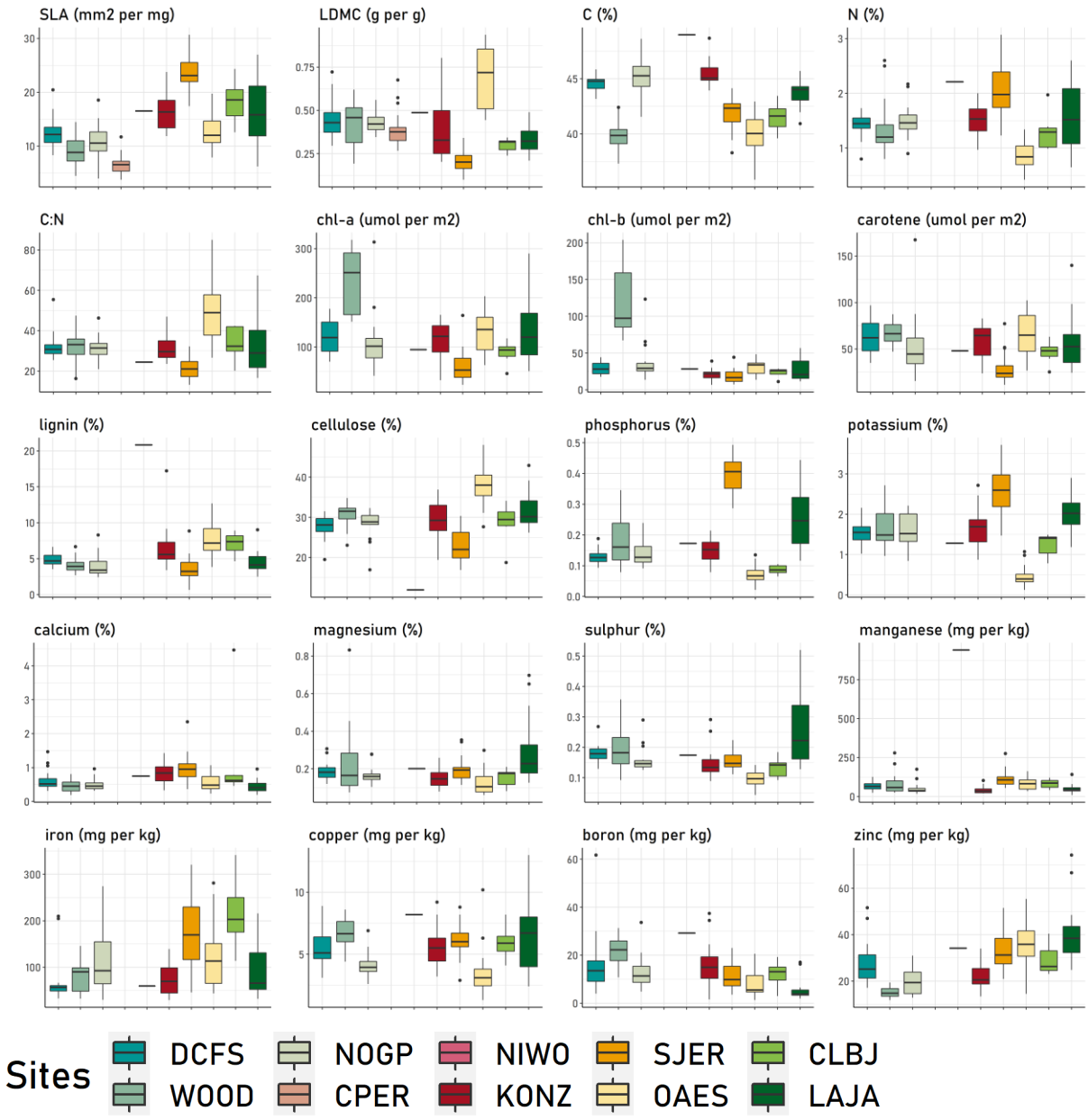

Figure 10. Comparison between sites of the field-measured distributions of 20 foliar traits in this study. These are based on herbaceous samples only. The centre line of each box represents the median trait value, the box shows inter-quartile range, and whiskers extend to the largest and smallest trait values. Observations that are greater or less than 1.5 times the inter-quartile range of the trait are shown as individual dots. Sites are ordered in descending latitude, left-right. Site YELL is not shown as there were no herbaceous samples collected from this site.

4.3.2 Foliar trait model performance

Table 7 shows the results of all random forest modelling of the 20 foliar traits from climate and spectral variables undertaken in this study. These include the model repeats using herbaceous samples only vs herbaceous and woody samples together, and the models based on differing time windows for matching *in-situ* and spectral data. The main models of this analysis are herbaceous-only, fourteen-day models. These main models are also shown in Figure 11, where predicted vs measured trait values are plotted along with the variable importance scores.

4.3.3 Foliar trait retrieval from herbaceous vegetation samples using a 14-day temporal window

The results for the foliar trait modelling of herbaceous vegetation across the sites were variable, indicating that some, but not all foliar traits were predictable. The models explained between 0% (calcium) to 75.8% (phosphorus) of trait variation, with errors (RMSE), which ranged from 9 to 20% of the measured range, within the range (< 25%) considered acceptable for foliar trait estimation (Z. Wang et al., 2020). Over half of the models (11/20) were able to explain more than 30% of the variation in the target trait. The best-retrieved foliar traits were macronutrients phosphorus and potassium (variation explained 78% and 63% respectively). Structural properties SLA, LDMC and C:N were also retrieved successfully from Sentinel-2 data (variation explained 43 – 66%, NRMSE 13 – 14%). Biochemical properties (carbon, lignin, cellulose and pigments chl-a, chl-b, carotene) were retrieved with varying success. Foliar carbon and cellulose were the best-retrieved biochemical properties (variation explained 59% and 43%, NRMSE 13% and 11%). Lignin was mostly well-retrieved, except two high values of lignin from sites KONZ and NIWO which were not accurately predicted (Figure 11). Chl-a and chl-b were also predicted better among lower values, with the high chlorophyll content of samples at WOOD not predicted accurately, and thus contributing large errors to the models. Carotene was not accurately retrieved from Sentinel-2. Among the foliar trace elements modelled, sulphur, copper and zinc were modelled with more than 20% variation explained.

For almost all traits, climate variables were the most important predictors, making up at least three of the top five predictors (Figure 11, right-hand panels). Although different for different traits, variables that characterised the seasonality of climate, i.e. the variation in temperature and precipitation throughout the year, were more important predictors than absolute mean temperature and precipitation. Precipitation seasonality was overall the most important climate variable among foliar trait models. Among spectral variables, spectral indices, comprising two or more spectral bands were, in general, more important model

predictors than individual spectral bands. The chlorophyll red-edge index, based on the narrow Sentinel 2 red-edge bands, in particular scored highly across most foliar trait models, including that of Chl-a. The Chl_{re} and NDMI indices were the most important spectral predictors for leaf structural traits SLA, LDMC, and C:N, cellulose, and macronutrients foliar nitrogen and potassium. For models of phosphorus, the trait with highest explained variance, individual red-edge and SWIR bands were the most important spectral predictors, after climate. SWIR bands (B11, B12) were also the most important for explaining variation in foliar copper content (Figure 11).

Table 7. Results of the random forest modelling of each plant trait using satellite data from the one, five, seven and fourteen-day time windows, along with climate data. The number of plots with suitable satellite data returned in each time window is reported. NRMSE is RMSE/measured trait value range. Models with var explained < 0% are not shown

Trait	Herbaceous vegetation only *n* = 167								Mixed vegetation *n* = 237							
	Fourteen-day window *n* = 167		Seven-day window *n* = 137		Five-day window *n* = 120		One-day window *n* = 70		Fourteen-day window *n* = 237		Seven-day window *n* = 204		Five-day window *n* = 186		One-day window *n* = 106	
	% var explained	NRMSE	% var explained	NRMSE	% var explained	NRMSE	% var explained	NRMSE	% var explained	NRMSE	% var explained	NRMSE	% var explained	NRMSE	% var explained	NRMSE
SLA	66.47	0.129	68.04	0.131	68.45	0.134	78.46	0.118	29.06	0.185	28.05	0.190	28.14	0.195	44.97	0.168
LDMC	54.74	0.135	62.56	0.125	68.08	0.118	73.56	0.117	37.31	0.140	43.82	0.132	46.70	0.129	53.72	0.131
C	58.68	0.128	50.42	0.134	47.04	0.138	46.65	0.151	58.72	0.129	56.31	0.136	52.47	0.142	66.20	0.132
N	38.77	0.153	43.06	0.158	44.77	0.154	40.56	0.181	32.94	0.132	32.53	0.138	30.49	0.143	34.15	0.142
C:N	43.67	0.135	46.08	0.143	50.05	0.143	28.43	0.176	46.15	0.134	46.46	0.142	48.33	0.143	51.81	0.144
Chl-a	26.41	0.163	24.25	0.154	16.53	0.155	32.15	0.167	-	-	-	-	-	-	3.21	0.145
Chl-b	48.10	0.091	15.46	0.123	20.54	0.113	29.34	0.130	16.19	0.143	-	-	4.66	0.152	5.27	0.146
Carotene	10.58	0.153	18.54	0.152	13.70	0.155	26.77	0.170	-	-	-	-	-	-	-	-
Lignin	23.15	0.115	25.98	0.112	26.56	0.118	34.06	0.193	62.77	0.111	66.57	0.110	63.65	0.116	75.49	0.110
Cellulose	44.91	0.121	53.22	0.118	53.61	0.126	44.80	0.164	63.11	0.126	65.33	0.127	61.19	0.137	60.07	0.154
Phosphorus	75.81	0.117	79.03	0.120	83.02	0.110	81.40	0.118	45.51	0.164	47.07	0.172	46.52	0.175	56.05	0.169
Potassium	63.36	0.119	69.17	0.117	69.99	0.118	70.88	0.128	25.58	0.178	25.83	0.185	20.75	0.192	47.14	0.159
Calcium	-	-	3.92	0.111	0.96	0.118	40.82	0.130	9.49	0.116	3.10	0.126	2.28	0.129	19.02	0.135
Magnesium	9.56	0.138	15.19	0.145	1.68	0.153	-	-	9.11	0.129	15.69	0.135	7.42	0.138	12.39	0.171
Sulphur	41.12	0.115	50.06	0.105	44.26	0.101	23.26	0.164	36.31	0.112	40.50	0.107	30.09	0.106	21.72	0.169
Manganese	8.76	0.087	8.23	0.094	6.01	0.100	21.86	0.158	47.04	0.127	45.45	0.137	41.64	0.143	58.82	0.124
Iron	10.54	0.196	11.89	0.210	12.97	0.219	-	-	10.01	0.172	10.18	0.182	12.62	0.184	24.65	0.202
Copper	29.36	0.145	35.30	0.144	24.19	0.150	16.78	0.172	12.96	0.173	11.81	0.181	9.57	0.186	24.12	0.191
Boron	11.24	0.140	6.81	0.134	1.12	0.137	-	-	28.53	0.149	31.82	0.148	29.93	0.155	40.45	0.160
Zinc	42.28	0.141	32.73	0.155	29.95	0.160	32.65	0.156	24.35	0.150	16.86	0.162	14.72	0.167	10.61	0.192

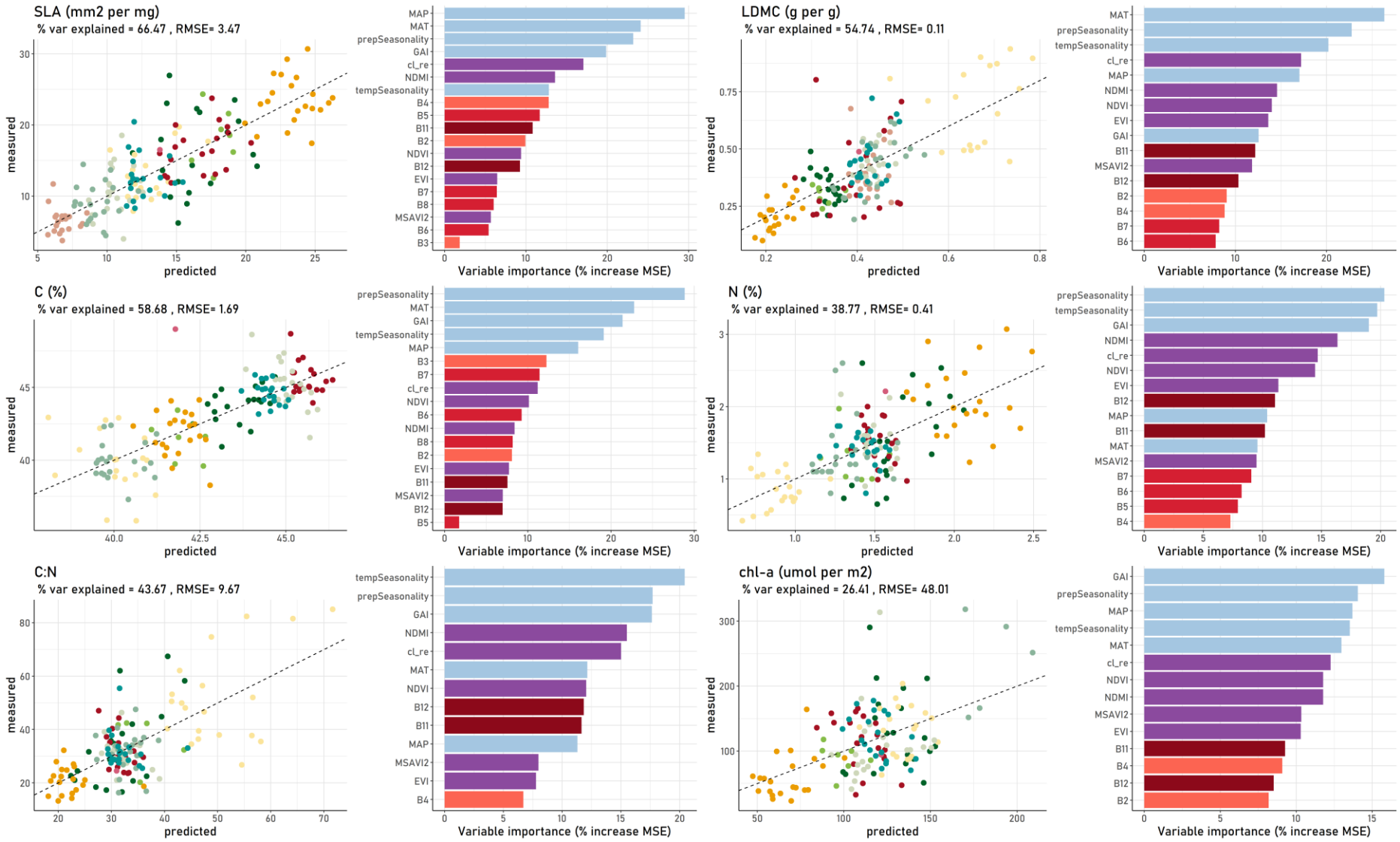
SLA (mm2 per mg)
% var explained = 66.47 , RMSE= 3.47
measured
predicted
MAP
MAT
prepSeasonality
GAI
cl_re
NDMI
tempSeasonality
B4
B5
B11
B2
NDVI
B12
EVI
B7
B8
MSAVI2
B6
B3
Variable importance (% increase MSE)
LDMC (g per g)
% var explained = 54.74 , RMSE= 0.11
MAT
prepSeasonality
tempSeasonality
cl_re
MAP
NDMI
NDVI
EVI
GAI
B11
MSAVI2
B12
B2
B4
B7
B6
C (%)
% var explained = 58.68 , RMSE= 1.69
B3
B7
B6
B8
B5
N (%)
% var explained = 38.77 , RMSE= 0.41
B4
C:N
% var explained = 43.67 , RMSE= 9.67
chl-a (umol per m2)
% var explained = 26.41 , RMSE= 48.01
Sites
DCFS
NOGP
NIWO
SJER
CLBJ
WOOD
CPER
KONZ
OAES
LAJA
category
Climate
Index
SWIR
RE
Visible

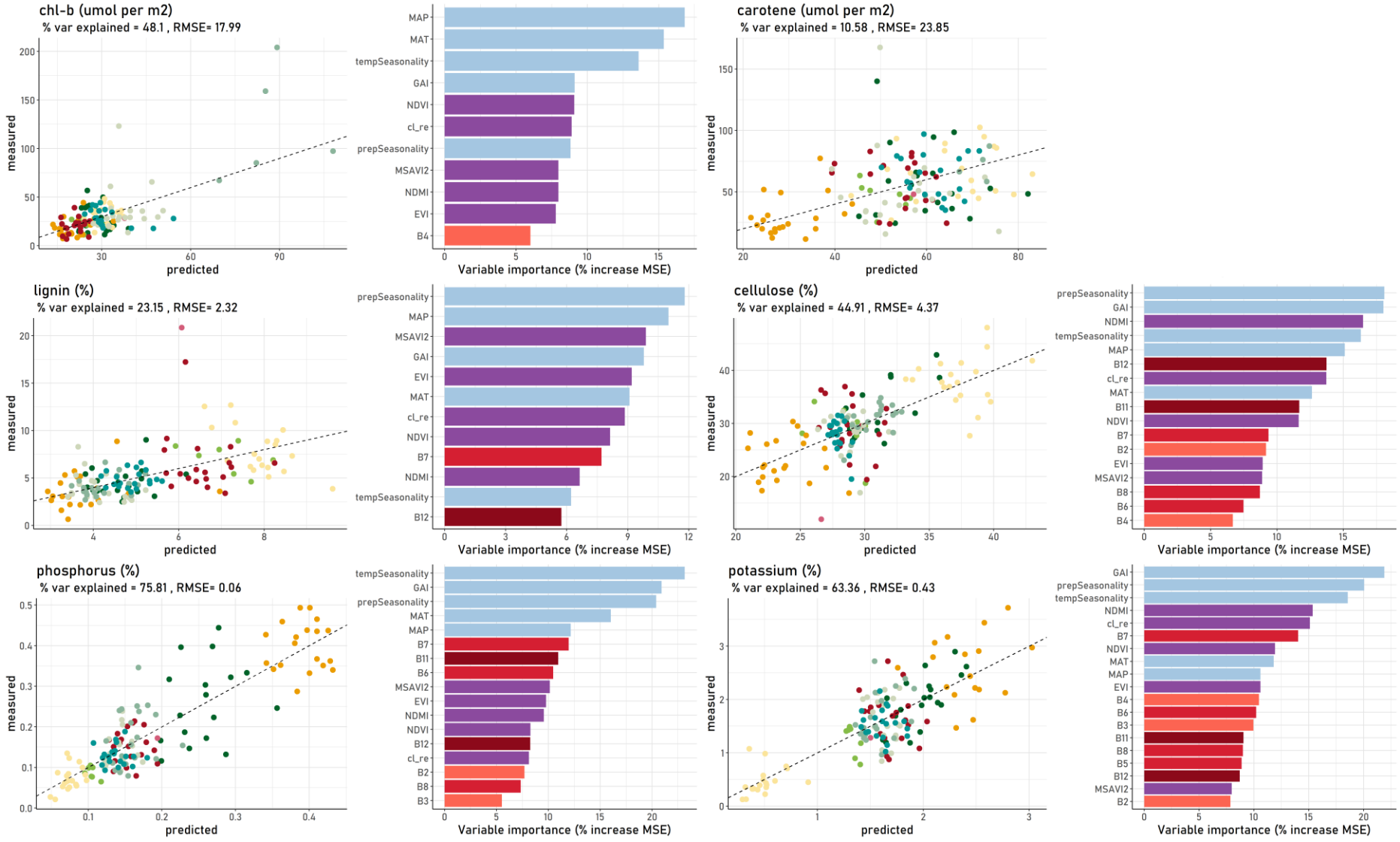

Sites: DCFS, NOGP, NIWO, SJER, CLBJ, WOOD, CPER, KONZ, OAES, LAJA

category: Climate, Index, SWIR, RE, Visible

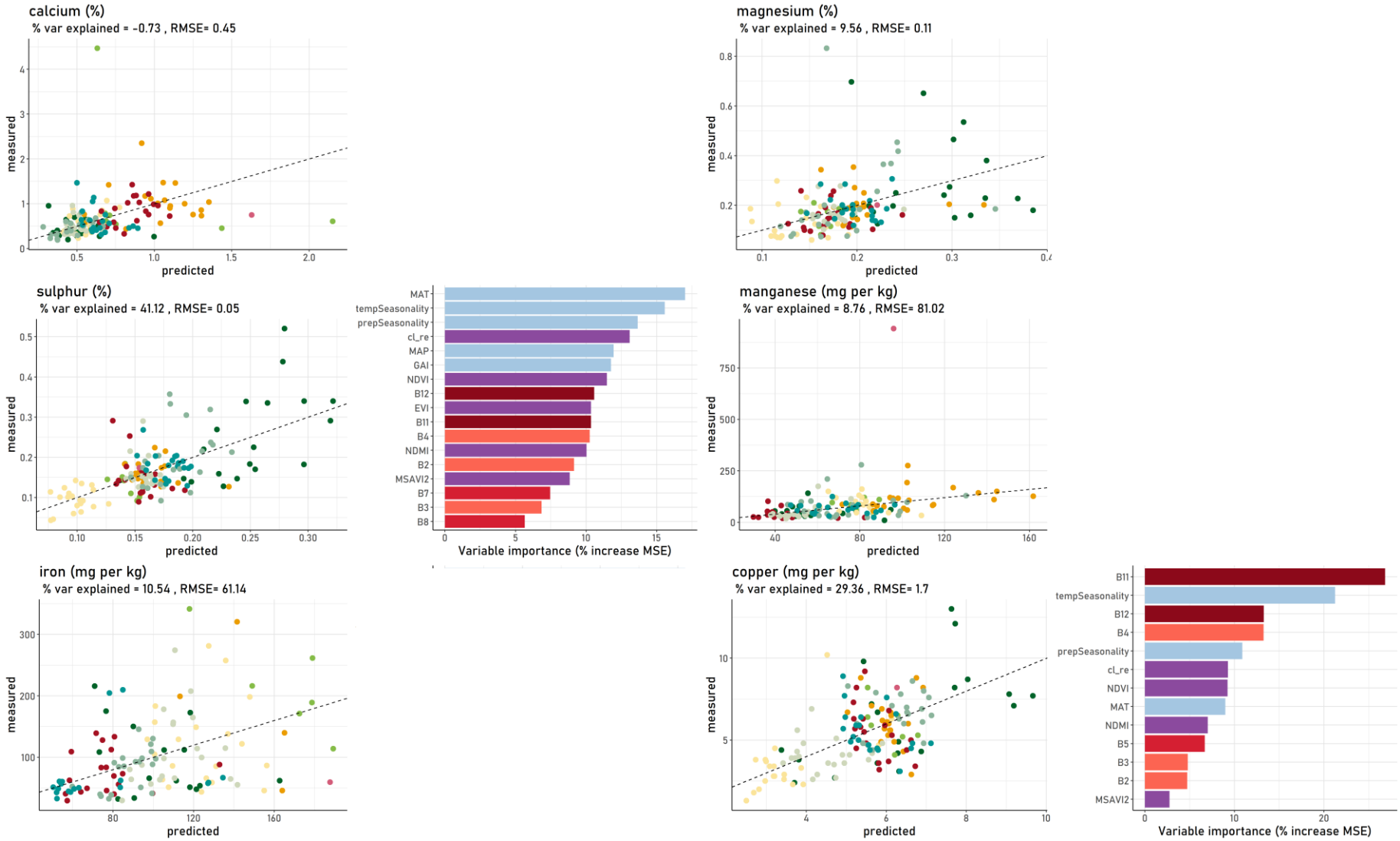
calcium (%)
% var explained = -0.73 , RMSE= 0.45
magnesium (%)
% var explained = 9.56 , RMSE= 0.11
sulphur (%)
% var explained = 41.12 , RMSE= 0.05
MAT
tempSeasonality
prepSeasonality
cl_re
MAP
GAI
NDVI
B12
EVI
B11
B4
NDMI
B2
MSAVI2
B7
B3
B8
Variable importance (% increase MSE)
manganese (mg per kg)
% var explained = 8.76 , RMSE= 81.02
iron (mg per kg)
% var explained = 10.54 , RMSE= 61.14
copper (mg per kg)
% var explained = 29.36 , RMSE= 1.7
B11
tempSeasonality
B12
B4
prepSeasonality
cl_re
NDVI
MAT
NDMI
B5
B3
B2
MSAVI2
Variable importance (% increase MSE)
measured
predicted
Sites
DCFS
NOGP
NIWO
SJER
CLBJ
WOOD
CPER
KONZ
OAES
LAJA
category
Climate
Index
SWIR
RE
Visible

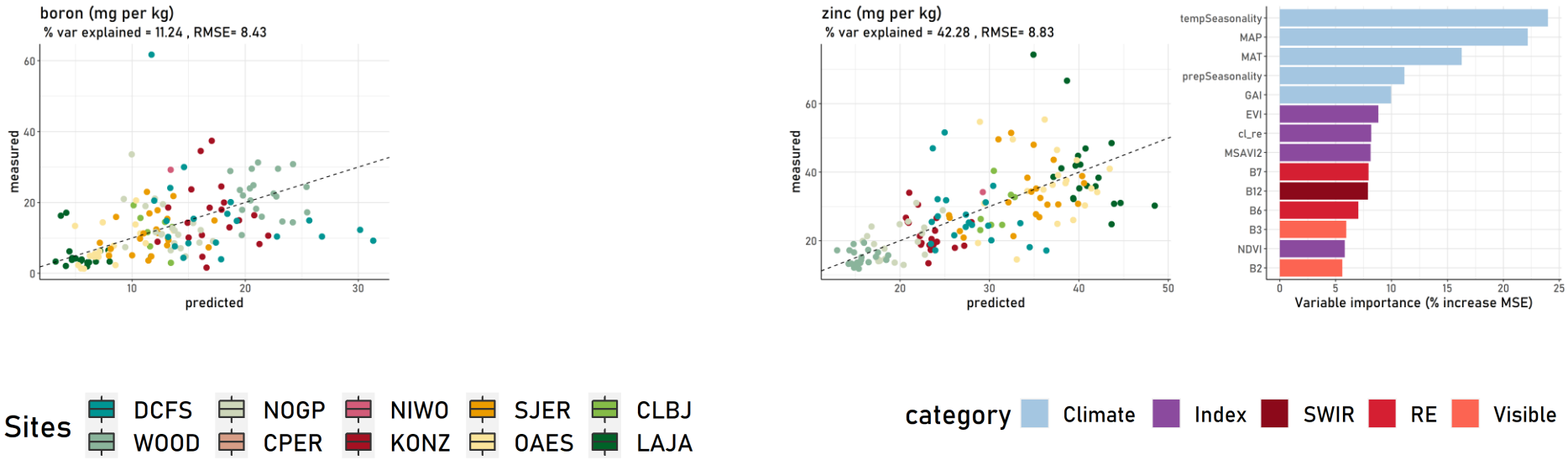

Figure 11. Models of 20 foliar functional traits, estimated from Sentinel-2 satellite data along with climate data, using random forest. Models are created from herbaceous vegetation samples only across 10 grassland sites (n = 167), using satellite data sourced from within a fourteen-day time window of field sampling. Scatter plots show measured trait values against those predicted from random forest models, coloured by site. The dashed line represents the 1:1 line. Variation explained (%) and RMSE of the models, and the units of measurement for each trait are shown in the scatter plot headings. The corresponding variable importance scores are plotted alongside each trait model, showing which variables were of greatest utility when modelling traits. Predictor variables are coloured according to category. Variable importance scores are not displayed for models which explained <20% of the variation in the target trait.

4.3.4 Variation partitioning

Variation partitioning based on redundancy analysis was carried out in order to ascertain whether spectral predictor variables were able to explain a unique portion of variation in foliar traits, beyond what was explained by climate. Note that this method does not remove redundant variables as was done using the variable selection algorithm (Boruta) for random forest modelling, therefore all climate and spectral variables contribute to the explained variance of their predictor group. Table 8 shows the result of variation partitioning.

Table 8. Variation partitioning of foliar traits to determine the portion of variation explained by climate and spectral variables, individually and in combination. Shaded cells indicate the largest partition of variance between climate, spectral or shared predictor variables. Negative values for variation explained should be interpreted as zero.

Trait	Climate	Shared	Spectral	Residual
SLA	0.26	-0.13	0.33	0.54
LDMC	0.03	0.22	0.15	0.59
C	0.19	0.32	0.07	0.42
N	0.08	0.17	0.04	0.72
C:N	0.06	0.16	0.20	0.58
Chl-a	0.08	-0.11	0.21	0.81
Chl-b	0.07	-0.01	0.19	0.75
Carotene	0.04	-0.07	0.13	0.90
Lignin	0.39	0.09	0.02	0.50
Cellulose	0.13	0.23	0.16	0.48
Phosphorus	0.34	0.17	0.11	0.38
Potassium	0.15	0.35	0.10	0.41
Calcium	0.02	0.23	0.05	0.70
Magnesium	-0.01	0.11	0.12	0.78
Sulphur	0.03	0.32	0.06	0.60
Manganese	0.65	0.15	0.02	0.18
Iron	0.08	0.07	-0.02	0.87
Copper	-0.02	0.16	0.16	0.70
Boron	0.08	0.15	0.01	0.76
Zinc	0.08	0.20	0.09	0.63

For 9/20 traits, the largest portion of explained variation was not able to be attributed uniquely to either climate or spectral variables, but was shared between the two predictor groups. However, for all traits other than foliar iron, there was a portion of variation uniquely explained by spectral variables and not explained by climate variables. Traits for which the set of spectral variables explained more unique variation than climate included foliar pigments Chl-a, Chl-b and carotene, along with leaf litter quality traits SLA and C:N ratio. Climate

explained a small amount of variation in foliar pigments relative to other traits and there was no explanatory power shared between climate and spectral properties. This result is not consistent with the random forest variable importance plots, which showed climate variables to be more important than spectra for photosynthetic pigments. The reason for this discrepancy could be that variation partitioning does not exclude any predictors which were eliminated during variable selection for random forest, but partitions the variation based on all variables in the group. Foliar phosphorus, the best-modelled foliar trait in terms of variation explained, was overwhelmingly explained by climate.

4.3.5 Foliar trait retrieval from mixed herbaceous and woody vegetation samples using a 14-day temporal window

To explore how applicable climate and spectral data are to the retrieval of foliar traits across a range of different plant lifeforms found in grasslands, a second set of random forest models were developed, this time incorporating both herbaceous clip strip and woody individual samples from the eleven grassland sites (n = 237). 70 woody individual samples from five sites were added to the dataset, including samples from site YELL which was represented only by woody samples in the field data despite having large areas of grassland land cover (Figure 9 b). A comparison of the overall variation explained in the 20 foliar traits of mixed vegetation and herbaceous only vegetation is shown in Figure 12.

When herbaceous and woody vegetation samples were included together in mixed RF models, the majority (13/20) of foliar traits were modelled with lower variation explained and higher NRMSE. This effect is particularly strong for SLA (37.4% lower), phosphorus (30.3% lower) and potassium (37.8% lower), and among photosynthetic pigments, which were modelled very poorly using the mixed samples dataset. For carbon, nitrogen, C:N ratio and sulphur, the inclusion of woody samples did not affect the amount of variance explained by much (<6%), indicating that these traits can be modelled successfully using a universal model across grasslands composed of different plant lifeforms. Lignin, cellulose, manganese and boron were better-modelled using a mixed dataset, with improvements in variation explained from 17.3 – 39.6%.

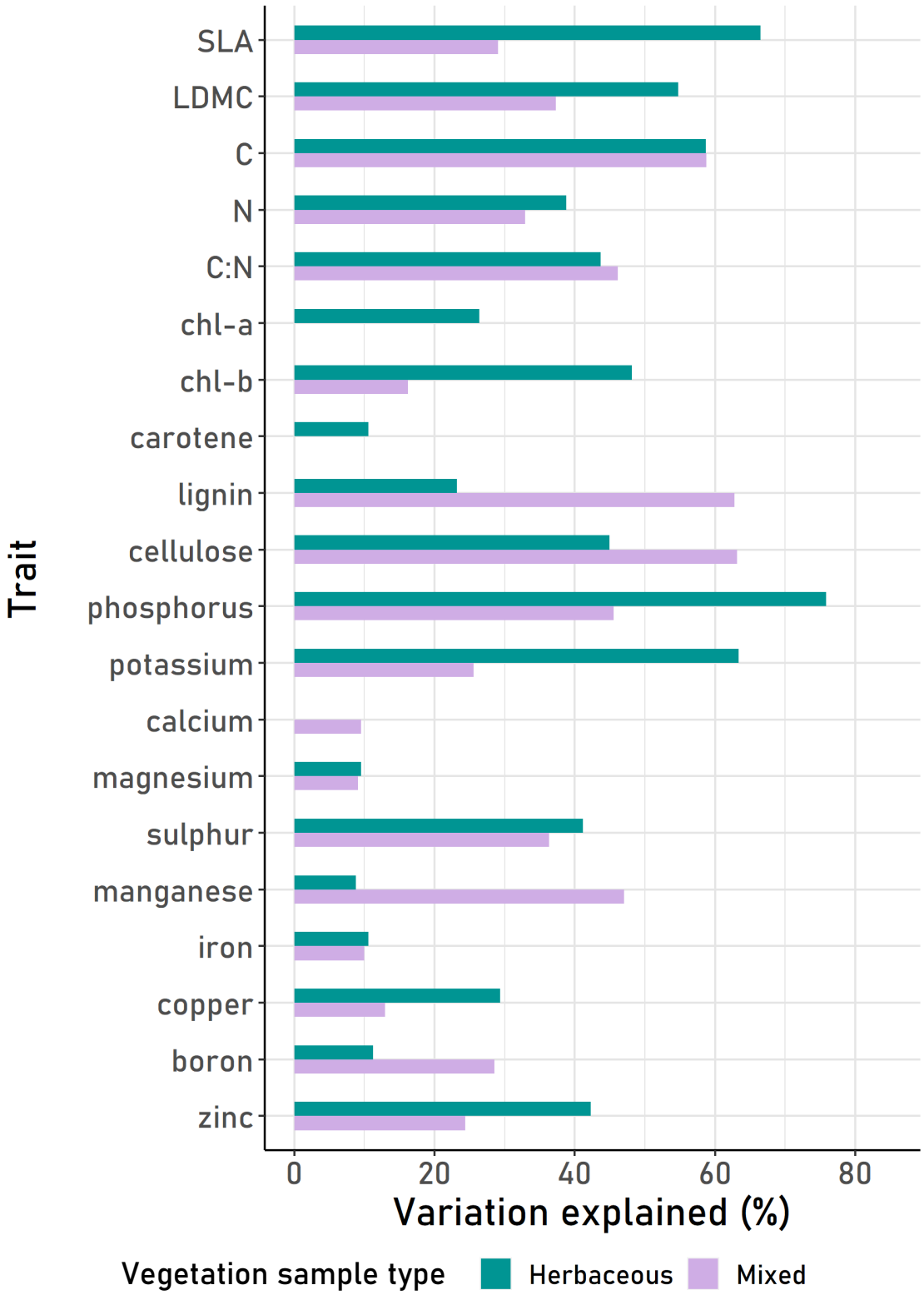

Figure 12. Variation explained in foliar traits of herbaceous vegetation only (n = 167) and mixed herbaceous and woody vegetation (n = 237), by climate and satellite-derived variables using random forest. Results of modelling where satellite data is taken from within fourteen days of field sampling.

4.3.6 Effect of restricting the time window for matching satellite and field data

Figure 13 shows the proportion of herbaceous field samples which were able to be matched with a suitable cloud-free Sentinel 2 image within one, five, seven and fourteen days of field sample collection. Reducing the time window from which to source satellite data from fourteen days to one day results in a loss of 97 observations from the dataset, or 58% of the total number of herbaceous field observations. This includes all observations from sites WOOD and KONZ, for which suitable, spatially-matched, cloud-free Sentinel-2 data was only available within seven to fourteen days.

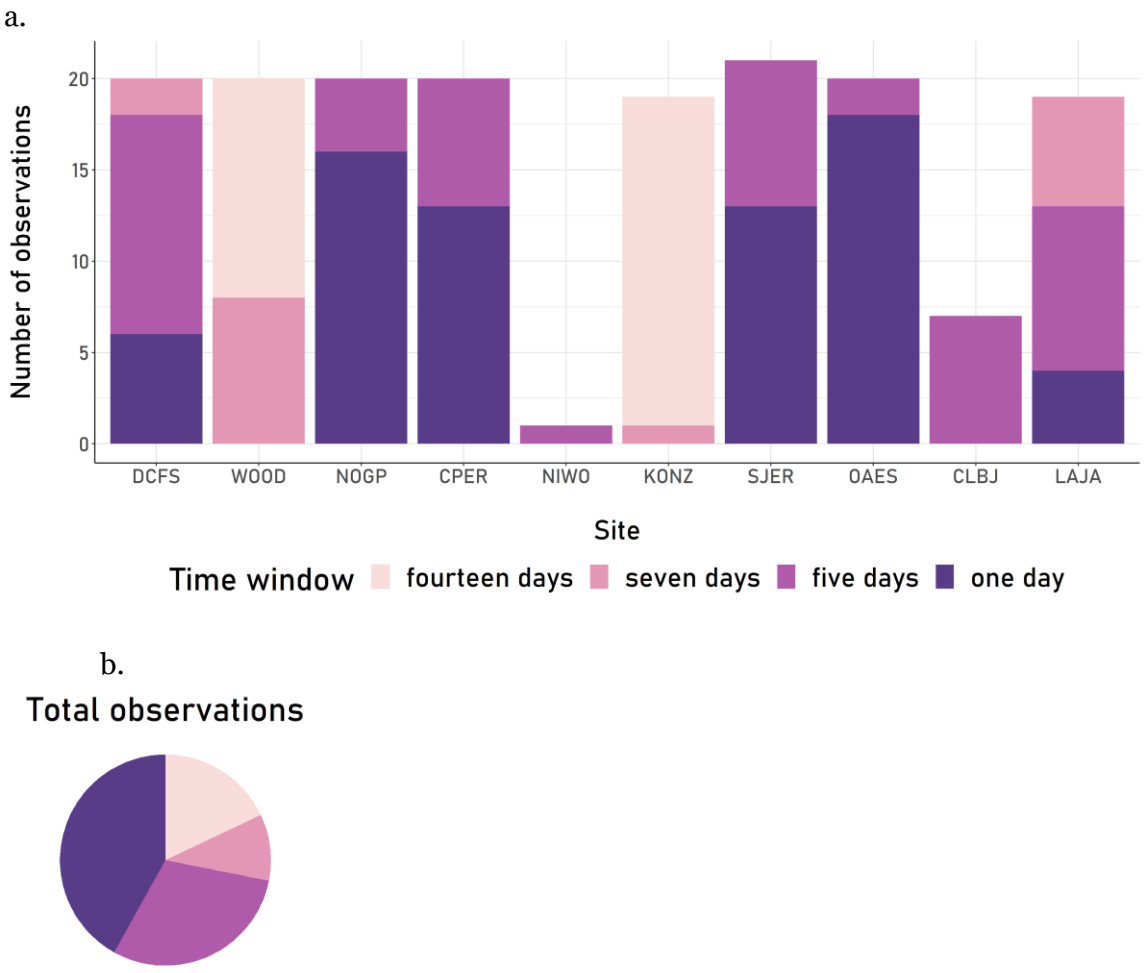

Figure 13. a. the number of in-situ *foliar trait measurements at each site which were able to be matched with a Sentinel-2 image within one day (temporal offset <=1), five days (temporal offset 2-5 days), seven days (temporal offset 6-7 days) and fourteen days (temporal offset 8-14 days) of field sample collection. b. the number of* in-situ *foliar trait measurements in total which were able to be matched with a Sentinel-2 image taken within each time window. These graphs indicate herbaceous samples only.*

Figure 14 shows the results of the RF trait models for herbaceous only samples, using climate data and satellite imagery from within one, five, seven and fourteen days of field sampling. For SLA, LDMC and potassium, and to a lesser extent lignin, there was a clear stepwise reduction in the amount of variation that could be explained by the RF models from one-day to fourteen-days. The largest decrease in model performance was for predicting LDMC; where 18.8% less variation was explained using a fourteen-day model compared to a one-day model. The opposite trend was true for carbon which was best-modelled from the wider fourteen-day time window. Other traits including cellulose, nitrogen and C:N ratio were best-modelled using intermediate five and seven-day windows. The time window of satellite data collection also had a large effect on the model of foliar calcium, which was only modelled with success using the one-day dataset, which explained variation of 40.8% with a NRMSE of 13%.

Differences in the NRMSE between models constructed using different time windows (Table 9) were lower than 8% for all foliar traits. Despite the larger variation explained in most traits from one-day data, prediction errors were slightly larger for all traits except for SLA and LDMC when traits were modelled from one-day data compared with 14-day data.

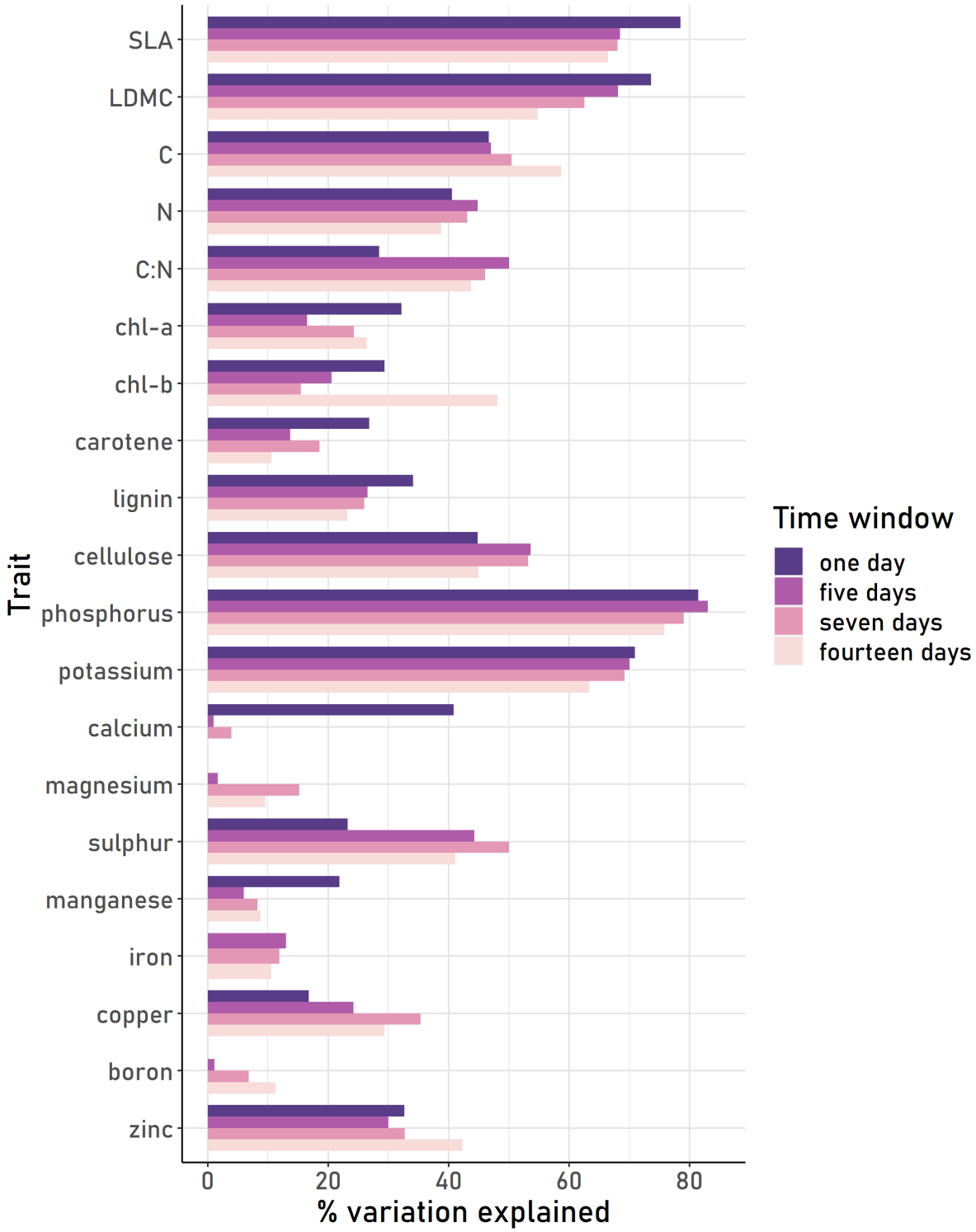

Figure 14. Variation explained in 20 foliar traits of herbaceous vegetation types by climate data and satellite imagery sourced from within one day (n = 106), five days (n = 186), seven days (n = 204) and fourteen days (n = 237) of field sample collection.

Table 9. Difference in variation explained (%) and NRMSE between the fourteen-day and one-day models of foliar traits from satellite and climate variables. Positive values indicate a larger value for the one-day model and vice versa.

Trait	Change in % variation explained between fourteen-day and one-day window	Change in NRMSE between fourteen-day and one-day window
SLA	+ 12.0	- 0.011
LDMC	+ 18.8	- 0.018
C	- 12.0	+ 0.023
N	+ 1.8	+ 0.028
C:N	- 15.2	+ 0.041
Chl-a	+ 5.7	+ 0.004
Chl-b	- 18.8	+ 0.039
Carotene	+ 16.2	+ 0.017
Lignin	+ 10.9	+ 0.078
Cellulose	- 0.1	+ 0.043
Phosphorus	+ 5.6	+ 0.001
Potassium	+ 7.5	+ 0.009
Calcium	+ 41.5	+ 0.024
Magnesium	-	-
Sulphur	- 17.9	+ 0.049
Manganese	+ 13.1	+ 0.071
Iron	-	-
Copper	- 12.6	+ 0.027
Boron	-	-
Zinc	- 9.6	+ 0.015

4.4 Discussion

The objectives of this study were to establish the potential of Sentinel-2 satellite imagery to model grassland foliar traits, and to explore the extent to which the composition of vegetation and temporal offset between field and spectral data impacts on the strength of empirical trait models. The results suggest that data from Sentinel-2 in conjunction with climate variables can explain variation in leaf structural traits and macronutrients (variation explained 39 – 76%), and to a lesser degree biochemical traits including pigments (variation explained 10 – 59%). Using RF models in conjunction with redundancy analysis, the results indicate that even though climate variables were the most important predictors of traits at this geographic scale, spectral data contributes a unique portion of explained variation for 19 out of 20 foliar traits tested (all traits except foliar iron), with spectral indices capturing photosynthetic capacity and moisture content the most useful spectral properties in the models. Inclusion of woody vegetation samples in the models generally decreased the accuracy of trait retrieval, indicating that prior knowledge of vegetation composition may be important when estimating foliar traits across grasslands. Temporal offset between field and satellite data of up to fourteen days decreased the strength of models by up to 20%, relative to the same-day models. This represents a trade-off between maximising the number of observations and ensuring that spectral data is representative of values measured in the field when building empirical models using satellite data. Overall, the results show that there is potential to map traits of herbaceous plants across diverse natural grassland ecosystems and covering large geographic extents using multispectral satellite data, building on previous work retrieving foliar traits from remote sensing which has thus far focused on high resolution imaging spectroscopy, or forest ecosystems (Aguirre-Gutiérrez et al., 2021; Homolová et al., 2013b; Van Cleemput et al., 2018; Z. Wang et al., 2020).

4.4.1 Links between foliar traits and satellite reflectance spectra

Traits which were modelled well were those which have strong associations to plant growth strategies, for example SLA, LDMC, C:N ratio and leaf N, and nutrients phosphorus and potassium, all of which were retrieved with comparable accuracy to recent hyperspectral mapping (Z. Wang et al., 2020). These traits typically covary as an overall trait syndrome facilitating rapid or conservative growth (Díaz et al., 2016; Reich, 2014; I. J. Wright et al., 2004). These traits are most likely related to spectral reflectance via their association with vegetation community productivity and biomass, for which Sentinel-2's narrow spectral bands along the red-edge are important predictors (Clevers & Gitelson, 2013; Delegido et al., 2011;

Pau et al., 2022). The spatial estimation of community-level growth strategies from their associated plant traits is valuable because growth strategies can indicate the environmental functions and services of grassland landscapes, including those which take place belowground (Baxendale et al., 2014; Grigulis et al., 2013; Orwin et al., 2010).

Foliar pigments were unexpectedly poorly modelled across the selected grassland sites (variation explained 10 – 48%), given their strong links to photosynthesis and therefore the interaction of vegetation surfaces with light. They were particularly poorly modelled compared to hyperspectral mapping efforts in grasslands, which report high accuracy for pigment retrieval; for example recent hyperspectral mapping over the same sites as this study retrieved chlorophyll and carotenoids with R2 of 0.68 and 0.69 respectively (Z. Wang et al., 2020), and in a review of hyperspectral trait studies the average strength of pigment retrieval was over 0.75 (Van Cleemput et al., 2018). This indicates that high levels of spectral detail are important for retrieving foliar pigments. Future work incorporating remotely-sensed pigments into ecosystem models, for example predictions of belowground communities as suggested by the results of Chapter 3, is likely to be more successful using hyperspectral data. Future hyperspectral satellite missions may be valuable for this task, combining the high spectral detail required with the temporal and spatial benefits of satellite systems (Pettorelli et al., 2018b). Foliar pigment models were also shown to be highly sensitive to the inclusion of mixed vegetation types, being modelled with limited to no explanatory power across mixed herbaceous and woody observations (Figure 12), and were also highly sensitive to temporal offset; for example the variation explained in carotene increased by 16% when the data was reduced to same-day observations. Another possible reason for the low overall explained variance in pigments from the models could be the relatively low explanatory power of climate for pigments compared to other foliar traits; although the random forest variable importance scores indicated that individual climate predictors were more important than individual spectral predictors, redundancy analysis showed that as a group, spectral predictors were able to explain more unique variation in pigments than climate. Variable importance scores (Figure 11) showed that the most important spectral predictor for chl-a and chl-b was the Cl_{re} index, which was specifically developed to retrieve canopy chlorophyll in grassland and cropland sites from Sentinel-2 (Clevers & Gitelson, 2013), and the most important spectral predictor for carotene was NDMI. Though not explicitly related to SWIR wavelengths, foliar carotenoid content has been associated with water stress in trees and crops (Baccari et al., 2020; Mibei et al., 2017). These results suggest that spectral information from Sentinel-2 is related to foliar pigments across grasslands, but that the relationships are sensitive to mixed ecosystems and temporal offsets and may not be applicable across diverse grassland landscape types, but better resolved among smaller sets of more similar sites.

Among the eight foliar trace elements modelled sulphur, copper and zinc were retrieved with success using Sentinel-2 and climate variables (variation explained 41.12%, 29.36%, 42.28% respectively and all RMSE <25% measured variable range, Figure 11). Though plant growth is most commonly limited by nitrogen and phosphorus in terrestrial ecosystems, micronutrients can also limit plant growth and therefore have implications for ecosystem-level productivity and functioning (Fay et al., 2015; Hayes et al., 2014). After N, P and K, sulphur is the most abundant trace element in leaves, and plays an important role in plant growth and catalysis. Copper is an essential micronutrient for plant growth, for example being involved in the action of enzymes (Shabbir et al., 2020), and zinc is a vital component of many plant proteins (Broadley et al., 2007). The mechanisms by which plants uptake and accumulate nutrients can be affected by stress conditions such as drought, nutrient deficiencies, pathogens, and grazing (J. Liu et al., 2022). For example, higher foliar sulphur concentration has been associated with environmental stress across ecosystems distributed across China (W. Zhao et al., 2022). Changes in ecosystem nitrogen levels and pH can also impact the mechanisms by which plants uptake nutrients and therefore their foliar concentration (Cai et al., 2017). Therefore, changes in the concentration of foliar trace elements across grasslands could indicate important changes in environmental conditions. Foliar trace elements are less commonly incorporated into models of ecosystem functioning than other traits such as structural properties, and though there have been attempts to retrieve trace elements from leaf-level spectroscopy (e.g. Nunes et al., 2017), there have been few previous studies retrieving foliar micronutrients from remote sensing at large spatial scales (though see Wang et al., 2020). The results presented in this chapter indicate that foliar sulphur, copper and zinc can be retrieved accurately from Sentinel-2 with comparable accuracy to more commonly-investigated structural and chemical traits (Figure 11). These results suggest that foliar trace elements could be valuable foliar traits to study further using large-scale remote sensing methods, as they may provide a link between spectral data and ecosystem functioning.

Despite some key exceptions, grassland foliar traits were overall predicted with lower accuracies than those reported by previous authors using hyperspectral data, but there was overlap in the ranges of model strength indicating that some traits were retrieved with comparable accuracy (R^2 range presented here 0.00 – 0.81; (Z. Wang et al., 2019) 0.57 – 0.87; (Z. Wang et al., 2020) 0.28 – 0.82; (Van Cleemput et al., 2018) 0.64 – 0.80; (Obermeier et al., 2019) 0.51 – 0.94). Less accurate retrieval of foliar traits by satellite data is likely related to the reduced spectral detail, as traits are retrieved indirectly via their association with plant growth strategies and vegetation density, rather than through their specific narrow absorption features. The other major difference between Sentinel-2 imagery and hyperspectral airborne imagery used by previous authors is the size of image pixels, or spatial resolution. Research

suggests that coarser spatial resolution is not necessarily detrimental to the remote retrieval of plant traits, because fine-scale topographical variation is smoothed out and geolocation errors are less influential (Pau et al., 2022; Van Cleemput et al., 2018). However, the inevitable effect of reducing spatial resolution in all but the most homogenous plant communities is an increase in the sub-pixel heterogeneity and mixing of plant species and life forms, which has the potential to weaken the relationship between traits and spectra (Hacker et al., 2022). Mixing of herbaceous and woody plant observations in empirical models was shown to reduce retrieval accuracy of most traits (Figure 12), so it would be expected that sub-pixel mixing of spectra might have the same effect.

Compared to previous trait retrieval efforts from satellite data over forests (Aguirre-Gutiérrez et al., 2021), grasslands (Li et al., 2018) and mixed ecosystems (Moreno-Martínez et al., 2018), the accuracy of the models presented in this study are similar or better. Some foliar traits, for example SLA, have been retrieved successfully in grasslands using radiative transfer models (Rossi et al., 2020). However, the selection of traits currently included in radiative transfer models is limited. In this study, all 20 foliar traits were retrieved with a NRMSE below 25%, the threshold deemed an acceptable level of precision (Asner et al., 2015).

Climate variables were identified as the most important predictors by the RF models, for almost all of the traits under investigation. This finding was expected given that climate is the main driver of ecosystem resources and vegetation communities at continental scales (Aguirre-Gutiérrez et al., 2021; Delgado-Baquerizo et al., 2018). Accounting for environmental drivers which cause spatial autocorrelations at continental scales, such as climate and geology, is important in order not to overestimate the explanatory power of imagery. If spectral data does not capture any variation beyond what could be retrieved from climate data then the usefulness of remote sensing for monitoring traits at these scales is negated (Ploton et al., 2020). A spatially-explicit modelling technique such as geographic random forest is one way of addressing this issue (Aguirre-Gutiérrez et al., 2021; Georganos et al., 2019), but was not undertaken in this study due to a relatively small number of samples at each site. Inclusion of key climate variables and variation partitioning in this study confirmed that spectral variables explained a unique portion of variation in plant traits beyond that accounted for by climate.

Variation partitioning (Table 8) indicated that for many traits, there was a large portion of residual variation unaccounted for by climate and spectral data. Factors affecting this residual portion of variation likely include soil chemical and physical properties, including pH, topography and interactions which take place between species in the vegetation assemblage to influence traits. The present study as an assessment of the potential of Sentinel-2 satellite imagery for retrieving plant traits did not include such additional datasets, but they

will be important for future studies working to resolve large-scale models of environmental processes and fluxes of which plant traits are a component. Alternative methods of integrating remote sensing and *in-situ* data include methods such as FLUXCOM ensemble, whereby satellite data is matched with measurements from global flux towers (Jung et al., 2019). This method gives global estimates of gross primary productivity (GPP) at a spatial resolution of approximately 10km^2, which are likely to be closely related to plant traits and phenology and therefore could be a valuable additional dataset for estimating plant traits across large spatial extents in the future.

4.4.2 Modelling over heterogenous grassland landscapes

The results of this study indicated that for most traits (13/20), estimating trait values across the herbaceous and woody fraction of grassland landscapes together resulted in lower prediction accuracies, compared to when herbaceous areas were isolated. This suggests that prior knowledge and quantification of grassland vegetation composition may be important for estimating traits from satellite data in grasslands. Grassland ecosystems are rarely homogenous. They often include a mix of herbaceous plants, trees and shrubs at multiple scales of heterogeneity, from isolated individuals observed in park landscapes to the gradient of tree density that is observed in savannahs or at grassland-woodland boundaries (Ratnam et al., 2011; Sexton et al., 2015). For example, only four out of the 81 sites in the NEON network are characterised exclusively by herbaceous vegetation (Figure 9). For this reason, grasslands and shrublands have sometimes been grouped together in large-scale studies (Van Cleemput et al., 2018). Image pixels of heterogenous grassland landscapes commonly represent not only multiple plant species but multiple plant lifeforms or functional groups; a challenge specific to remote sensing of grasslands that is not experienced in forests, where the graminoid and shrub fraction of the vegetation community does not impact the canopy reflectance. Mixing vegetation types at the sub-pixel scale has been found to weaken the relationships between spectral properties and foliar traits, because of differences in growth strategies and leaf structures between herbaceous and woody plant life forms (Hacker et al., 2022; Hacker & Coops, 2022). For example, stem and root traits as well as foliar traits play a large role in the functioning of herbaceous plant communities (Funk et al., 2017; Funk & Cornwell, 2013; Poorter et al., 2014), environmental drivers such as water table depth can alter LES relationships in wetland communities (J. P. Wright & Sutton-Grier, 2012), and some key foliar compounds (tannins) which have been found to link canopy spectroscopy to ecosystem functioning in forests are not significantly present in graminoid leaves (Madritch et al., 2014). Despite these challenges, a few studies have successfully retrieved foliar traits across mixed grassland, shrubland and woodland ecosystems using hyperspectral data (Dahlin et al., 2013; Z. Wang et al., 2020).

The evidence presented in this study indicates that the retrieval of foliar traits from satellite imagery is less successful in mixed vegetation grassland ecosystems. Empirical models of foliar traits using only herbaceous samples were more accurate than those including a mixture of herbaceous and woody vegetation, for most traits (Figure 12). However, the magnitude of this effect differed among traits, suggesting that some traits are more likely to be able to be retrieved over mixed vegetation landscapes than others. Foliar carbon, nitrogen and C:N ratio which were all modelled relatively successfully (variation explained around 40% and NRMSE around 15%) were equally well-modelled over the herbaceous and mixed vegetation samples. Lignin and cellulose were better-modelled by a mixed dataset, possibly because these two structural traits are typically higher in woody and herbaceous plants respectively, so the inclusion of both observations gave a wider range of trait values across which the model could distinguish. However, the most successfully modelled traits across all models, SLA, LDMC, phosphorus and potassium, were significantly better-retrieved using a herbaceous only model. Future work explicitly investigating the effect of increasing shrub or woody plant density on spectral retrieval of foliar traits among grassland woodland boundaries would be valuable, particularly given the conservation importance of these ecosystems (Sexton et al., 2015).

4.4.3 The impact of temporal offset between in-situ and satellite data collection

To the best of our knowledge this is the first attempt to explicitly test the influence of temporal offset between satellite and field data collection when constructing empirical trait models. The results indicate that a temporal offset of up to fourteen days decreases the variation explained in traits by satellite data by up to 20% with retrieval of leaf dry matter content, SLA and carotene the most impacted. Some traits, including foliar carbon and C:N ratio, were better-modelled from the fourteen-day dataset, suggesting that these traits do not significantly vary in grassland canopies over the time period and therefore that the larger dataset available for the fourteen-day time window was more important for estimating these traits. The available time window for matching remote and *in-situ* data is a relevant question for building empirical models of plant traits from optical satellite data, because revisit periods of the most commonly used, publicly-available satellite sensors are often a period of days to weeks, and the frequency of usable imagery further reduced in many environments by frequent cloud cover. The trade-off between gathering spectral data of the highest quality, i.e. the smallest temporal offset, and collecting enough observations is demonstrated clearly in this study, where the optimum time window of one day between field and satellite data collection yielded useable, cloud-free satellite data for only 42% of field observations.

Similar satellite-based trait investigations use data with a range of temporal offsets, up to several months or years, with success (Aguirre-Gutiérrez et al., 2021; Hauser et al., 2021; Ma et al., 2019). These long windows can be justified using detailed knowledge of site history such as disturbances and weather conditions. For example, short-term disturbance events such as insect outbreaks, fire, and extreme climatic events such as heatwaves or drought can rapidly alter the functional traits and spectral reflectance of the vegetation community, and if such events take place between field and spectral data collection then the relationship between the two is likely to be lost. Therefore, knowledge of site-level disturbance regimes and conditions should be used where possible to ascertain the appropriate temporal window for spectral data collection, or to further investigate anomalous observations in models. The seasonality of studies is important too – for example, temporal offset may have a greater effect at crucial stages of phenology such as the start or the end of the growing season. Therefore, though the results of this study indicate that across a broad set of grasslands, more temporally variable traits such as pigments and water content (LDMC) are likely to be best retrieved using empirical models from spectral data with a small temporal offset, it is acknowledged that this may not always be possible, and maximising the number of observations is more important than minimising the temporal offset between field and satellite data collection when empirically modelling foliar traits from remote sensing data across large geographic extents. Furthermore, due to the reduction in observations associated with restricting the temporal sampling window, the one-day results in this study are based on a small number of observations (n = 70); a larger dataset is needed to confirm these findings, possibly available from NEON as more data is collected throughout the lifespan of the network. Designing future field-based data collection to coincide with the overpass of publicly-available satellite missions such as Sentinel-2 (Hauser et al., 2021) would be a valuable step towards aligning field-based and remote sensing data collection in the future.

4.5 Conclusions and avenues for future work

This study presents the retrieval of multiple foliar traits from satellite and climate data in heterogenous grasslands across North America using RF modelling. The study builds upon previous work modelling traits from satellite data in forests, and hyperspectral data in grasslands. Plant structural traits and macronutrients were particularly well-modelled, including SLA which is an important trait in terms of leaf economics and linking plant traits to above- and belowground ecosystem functioning. Though climate variables were important for the retrieval of traits, multispectral satellite data made a valuable contribution to all models, and the Sentinel-2 narrow red-edge bands and indices derived thereof were

particularly useful. This study also adds to the small body of literature linking remote sensing data to traits across different grassland plant lifeforms, which will be essential to interrogate and realise the potential of the species-independent perspective of plant trait-based approaches.

5. Phenology derived from satellite NDVI explains variation in ecosystem multifunctionality in grasslands at the global scale

Abstract

Multifunctionality is an important concept in ecology for evaluating the provision of multiple ecosystem functions and services simultaneously. Multifunctionality has been shown to be closely related to the diversity, productivity and stability of aboveground plant communities in a variety of ecosystems worldwide, but methods for assessing multifunctionality *in-situ* are limited at large scales by practical constraints of field sampling. Here, we apply remote-sensing methods for retrieving phenological information about aboveground plant dynamics, including the annual peak biomass, the length of growing season, rates of green-up and senescence and the multi-year variability of these properties to the retrieval of multifunctionality across a global network of 90 grasslands. Seven satellite metrics based on the Normalised Difference Vegetation Index (NDVI) were positively associated with and able to explain statistically significant, though small, portions of variation in multifunctionality (R^2 0.10 – 0.37, $p < 0.01$), and one measure of phenological stability was significantly, though weakly associated with multifunctionality ($R^2 = 0.07$, $p = 0.007$). The most strongly-associated NDVI metrics varied depending on the overall stability of ecosystems, with sites experiencing significant change better represented by annual maximum NDVI and those with stable productivity overall more closely linked to the more sensitive metric time-integrated NDVI. The length of satellite timeseries used to extract NDVI metrics affected the amount of variation in multifunctionality retrieved from NDVI metrics, along with climate and location variables, using random forest, with decadal timeseries (18-30 years) able to retrieve more variation than short (3-year) timeseries (variation explained 50.2% and 61.4% respectively). These results indicate that ecosystem multifunctionality of grasslands at global scales is evident in the phenology of the aboveground plant community, and that satellite-derived NDVI timeseries have the potential to retrieve multifunctionality at large spatial scales by providing valuable information on current and past plant phenology.

5.1 Introduction

The impacts of ongoing and predicted environmental changes including climate change, land use change and biodiversity loss on the functioning of ecosystems is a major research concern in ecology. It is increasingly recognised that in order to fully understand the effect of environmental pressures, multiple functions which have synergies and trade-offs in the real world cannot be considered completely in isolation but should be assessed simultaneously; termed ecosystem multifunctionality. Ecosystem multifunctionality generally refers to an assessment of ecosystem status and health which incorporates more than one ecosystem function. There are different interpretations and definitions of multifunctionality, which have been extensively discussed by previous authors (Byrnes et al., 2014; Garland et al., 2021; Jing et al., 2020; Manning et al., 2018). Here, we refer to ecosystem function multifunctionality, aiming to understand how biotic attributes of ecological communities shape ecosystem functioning in general or across a variety of ecosystems, as opposed to a land-management perspective, ecosystem service multifunctionality, where functions are assessed relative to local management goals at specific locations (Manning et al., 2018). The most relevant functions may not be universal among all sites and contexts, but in general, production of biomass and maintenance of soil carbon and nutrients are considered the most important ecosystem functions for human societies (Delgado-Baquerizo et al., 2016). Being able to monitor these functions simultaneously and across large scales is important to be able to ascertain how they respond to large-scale drivers and how whole landscapes can be managed for multifunctionality.

Fundamental drivers of ecosystem functioning at global scales are climate and geology, which drive functions both directly through controlling energy and water balances of the system, and indirectly through their influence on the plant and soil communities. For example, aridity has been shown to alter the respective influence of above- and belowground communities on overall ecosystem functioning, with soil communities more influential in arid conditions (Berdugo et al., 2017; Delgado-Baquerizo et al., 2013; W. Hu et al., 2021; Jing et al., 2015). Underlying landscape geology is a key driver of soil functions, for example shaping pH conditions in soil which, while not considered an ecosystem function, is an important soil property which determines the conditions in which other functions take place (Allan et al., 2015; Garland et al., 2021). A large proportion of the research into fundamental drivers of ecosystem multifunctionality has focused on biological diversity as a driver (Byrnes et al., 2014; Dooley et al., 2015; Hautier et al., 2018; Hector & Bagchi, 2007; Isbell et al., 2011; Maestre et al., 2012). A greater diversity of species, genetic histories (phylogeny) and functional traits better equips the community to fill niche space and maintain functioning over time, throughout environmental perturbations (Hautier et al., 2015; Hector et al., 2010;

Oliveira et al., 2022). Both the plant and the soil microbe components the biological community are important, respectively performing functions relating to aboveground acquisition and belowground transformation and storage of resources and energy (Delgado-Baquerizo et al., 2016; Fry et al., 2018; Guo et al., 2021; Wagg et al., 2014). Multiple spatial scales of biodiversity influence multifunctionality and interact with one another; species richness (alpha diversity) establishes the total available pool of species in the landscape, and spatial turnover (beta diversity) gives the heterogeneity of community composition across the landscape (Hautier et al., 2018; Jing et al., 2021; Pasari et al., 2013; Y. Yan et al., 2020). Temporal turnover in plant and soil communities is also relevant to multifunctionality; contemporary multifunctionality in a landscape is determined by a combination of historic as well as current climatic and biological conditions, because feedbacks between plant and soil communities propagate the influence of past conditions through time (Garland et al., 2021; Löfgren et al., 2018; Wilson et al., 2017). Efforts to retrieve plant biodiversity from remote sensing also often incorporate temporal variation, as different species dominate and subside over time to fill temporary niches created by short term dynamics (Rossi et al., 2020, 2021). Therefore, the multifunctionality of an ecosystem can best be understood using a spatial and multi-temporal perspective. However, collecting multi-temporal data in the field which also thoroughly captures multiple scales of spatial variation is challenging. Satellite remote sensing data can rapidly capture spatially explicit information over global extents, at regular intervals, and so is well-placed to fill temporal and spatial gaps between field observations. The close links between multifunctionality, plant diversity and productivity may provide a mechanism by which the multifunctionality of an ecosystem can be retrieved from spectral properties of the aboveground vegetation community and their variation over time.

Aboveground productivity, or the density and activity of the vegetation community, is one of the most extensively researched and successfully retrieved environmental properties from remote sensing. Vegetation indices highlight parts of the electromagnetic spectrum which are particularly sensitive to vegetation structure and chemistry, the most widely-used being the Normalised Difference Vegetation Index (NDVI) (Pettorelli et al., 2005). The NDVI has been linked to a wide variety of ecological properties and processes in grasslands, including species diversity, species composition, habitat quality, and soil properties (Gaitán et al., 2013; García-Gómez & Maestre, 2011; Gholizadeh et al., 2019; K. S. He et al., 2009; Löfgren et al., 2018; Mapfumo et al., 2016; Paruelo et al., 2016; Pettorelli et al., 2005; Tan et al., 2022; R. Wang, Gamon, Montgomery, et al., 2016; Weber et al., 2018). Fundamentally responding to vegetation productivity, the NDVI is useful for the retrieval of such a wide variety of related ecosystem properties because plant primary productivity introduces carbon and resources into the system and thereby drives almost all other ecosystem functions (Zaret et al., 2022).

There is also a well-documented and much-researched, though not necessarily straightforward or linear, association between plant productivity and species diversity. Similar to ecosystem multifunctionality, productivity is maximised and maintained to a greater degree by more diverse communities which are better able to fill ecological niches, including those which appear temporarily with environmental fluctuations (Hector et al., 2010; Tilman et al., 2006). Greater species diversity has been shown to increase ecosystem productivity by prolonging the growing season, as different species in the community are active at different points throughout the year (Dronova and Taddeo, 2022). Therefore, by capturing the dynamics of aboveground productivity over time satellite NDVI may be able to retrieve the associated properties of ecosystem biodiversity and multifunctionality.

Temporal variation in productivity which occurs in regular seasonal cycles is termed phenology, and can be retrieved from satellite timeseries of NDVI captured at regular intervals, showing the rise and fall of NDVI with plant growth and senescence throughout the year. From the seasonal NDVI curve can be derived phenological metrics or phenometrics, describing plant community dynamics including the rate, duration and magnitude of plant growth and senescence throughout a season (Dronova & Taddeo, 2022; Weber et al., 2018). For example, the start and the end of the growing season can be determined by points of inflection indicating the rise and fall of NDVI, and the time difference between these two points represents the length of the growing season (Eklundh & Jönsson, 2015; R. Singh et al., 2022). Figure 15 shows a simulated single-year NDVI curve labelled with important phenometics, and a description of their ecological significance can be found in Table 10. It is not only the absolute value or magnitude of a phenometric, for example maximum NDVI ($NDVI_{max}$), that is relevant to ecology, but also the year-on-year variability of phenometrics which indicate the stability of an ecosystem and ecosystem productivity across years. *In-situ* measures of ecosystem stability have been shown to be associated with higher plant biodiversity and multifunctionality in grasslands (Hector et al., 2010; Isbell et al., 2015; Liang et al., 2022; Oehri et al., 2017; Tilman et al., 2006). Using satellite phenometrics, Dronova, Taddeo and Harris (2022) found that lower inter-annual variability of NDVI phenometrics across wetland ecosystems ($NDVI_{max}$ and $NDVI_{mean}$) was indicative of more species-rich systems, because asynchrony in growth among different species promoted not only longer but also more consistent growing seasons year-on-year. Phenometrics and phenological variability have been used to estimate multiple ecosystem services in grasslands at the individual landscape scale, with the purpose of directing management strategies (Paruelo et al., 2016; Weber et al., 2018). There have also been a few studies retrieving indicators of multifunctionality from satellite datasets in dryland ecosystems, based on simple measures of NDVI and albedo (García-Gómez and Maestre, 2011; Zhao *et al.*, 2018). However, the extent

to which links between multifunctionality and plant community phenology may enable multifunctionality to be estimated at large scales from satellite data has yet to be explored. The long-term data archives available from satellite missions enable the stability of plant phenology to be estimated across timescales relevant for variation in belowground properties, which may be valuable for this purpose.

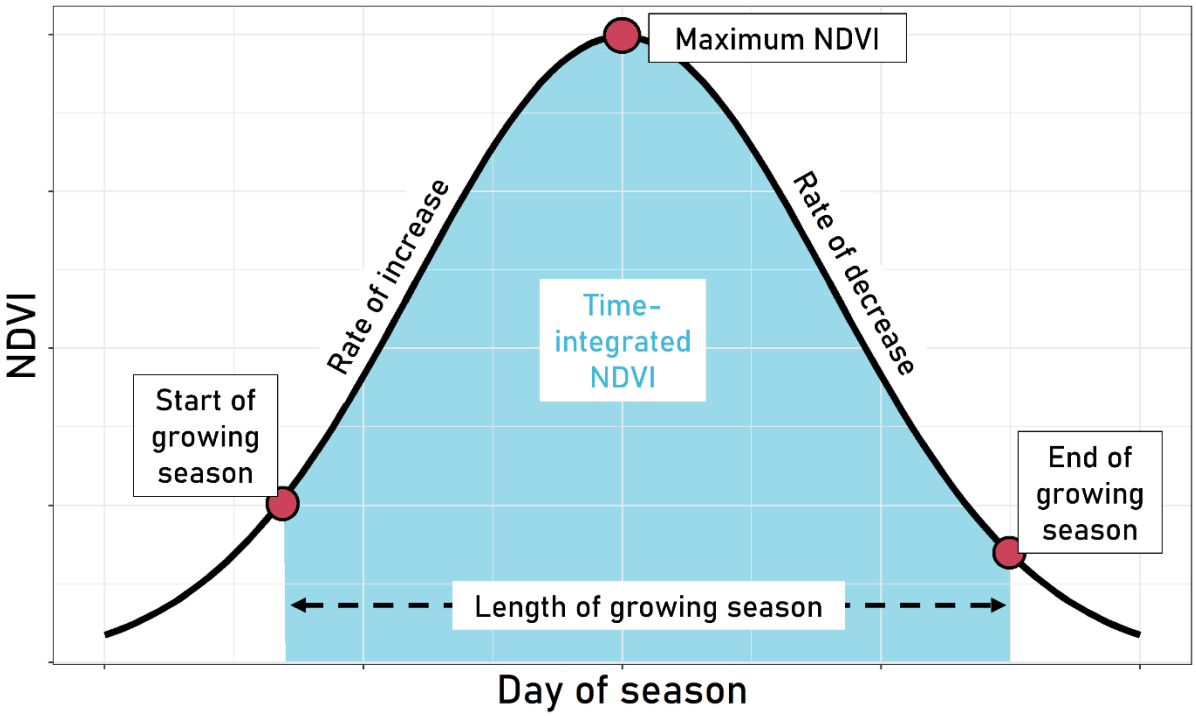

Figure 15. Example of a seasonal NDVI curve, labelled with phenological properties.

Phenometrics describe the temporal variation in productivity throughout a season, but multifunctionality of the ecosystem, particularly the belowground components, is shaped across multiple growing seasons, up to decadal scales (Garland *et al.*, 2021). Therefore, more than one season of phenology is likely required to retrieve ecosystem multifunctionality. Multi-year satellite timeseries are often used to determine phenology and are necessary for the estimation of phenological stability; in a selection of studies reviewed here, satellite NDVI timeseries were retrieved for between 3 and 27 years (García-Gómez & Maestre, 2011; Paruelo et al., 2016; Paruelo & Lauenroth, 1995; Weber et al., 2018; J. Yan et al., 2022; Y. Zhao et al., 2018). The longest timeseries of 27 years was found to significantly contribute to explained variation in soil carbon across a prairie site, where a shorter satellite timeseries of two years did not (Wilson *et al.*, 2017). With some of the longest satellite records now spanning multi-decadal timescales at many locations across the world, it is possible to account for past as well as present phenology. It remains untested how a longer-term perspective on vegetation

dynamics could contribute to assessments of multifunctionality, which incorporate functions which are dynamic over a range of timescales, up to decadal (Garland et al., 2021).

This study links field-measured ecosystem multifunctionality to satellite-derived metrics of aboveground productivity, phenology and phenological stability across a global dataset of diverse natural grasslands obtained from the Nutrient Network, in order to test the following hypotheses. **H1.** Landscape-scale multifunctionality is positively associated with species richness, aboveground productivity and phenological stability in global grasslands; sites with higher plant species richness are more productive and phenologically stable, and have higher multifunctionality. **H2.** Ecosystem multifunctionality is more closely associated with the long-term (decadal) average of aboveground productivity and phenology than short-term, recent (under 10 years) productivity and phenology, because historic site conditions shape contemporary multifunctionality through feedbacks, and important constituent ecosystem properties such as soil carbon are variable on decadal timescales. **H3.** Satellite phenometrics capturing the magnitude and variability of productivity and the length of the growing season, and the long-term stability of these properties, will contribute valuable explanatory power to models of multifunctionality at the global scale, beyond what is explained by fundamental climate and location drivers. The third hypothesis is a step towards assessing the potential of satellite datasets to contribute to measuring and monitoring multifunctionality across large scales, by filling temporal and spatial gaps in field-measured data.

5.2 Methods

5.2.1 Grassland sites and soil multifunctionality

The Nutrient Network (NutNet) comprises 156 grassland sites across 27 countries and 6 continents. The aims of the network are to investigate productivity-diversity relationships in diverse herbaceous-dominated communities worldwide, and the effects of nutrient limitation and management including grazing and fertilisation on these properties (Borer et al., 2014, 2017). Each site hosts a replicated experimental setup, in which field plots are distributed across the landscape and subject to combinations of nutrient additions, with some plots left untreated as controls. Properties of the plant communities are measured every year, and soil properties are measured every three years at NutNet sites. The first sites were added to the Nutrient Network in 2007, and the most recent sites were established in 2022. Previous work on multifunctionality at NutNet sites has shown that plant species diversity promotes multifunctionality and stabilises productivity, and that these effects are apparent at both community (alpha) and landscape (beta) scales (Hautier et al., 2014, 2018; Jing et al., 2021).

Figure 16. Location map showing the global distribution of the 90 nutrient Network sites used in this study.

For this study, data on five plant and nine soil properties were retrieved from 90 NutNet sites worldwide (Figure 16). Sites were only included in the selection if they had both plant and soil measurements available, although not every property was measured at every site; Appendix A lists the individual functions measured at each site. The most recent data from each site was taken, which ranged from 2007, for some early NutNet sites at which the

experiment was observational-only, to 2021. Only measurements from untreated plots were used; either those designated as controls, taken from the baseline pre-treatment year of the experiment, or from some sites which are observational-only so no nutrient additions are applied. Plots at NutNet sites measure 5x5m, and are arranged in blocks of 10, within which each plot is given a different nutrient treatment or designated as a control. There are 3-5 replicated blocks at each site, distributed across the landscape to capture environmental and floristic gradients; therefore, the properties of the untreated control plots from spatially distributed blocks are assumed to be representative of the wider landscape at each site. Details of the individual properties measured at each site can be found in Table 10, along with justification for their inclusion in multifunctionality. Litter turnover is based on the proportion of live plant biomass and litter aboveground, after Hautier *et al.* (2018). Invasion resistance is the proportion of native to introduced species. Plant and soil property values were averaged across all untreated plots at the site, to give a single site-level mean value of each ecosystem property. To investigate the role of aboveground plant diversity in linking multifunctionality to aboveground productivity and phenology, plant species richness across the sites was also acquired from NutNet. The total site-wide species count for the sampling year was used to represent site level species richness, because species richness is highly scale-dependent so the average richness among 5x5m blocks would underestimate richness at the whole site level. Relationships between the individual functions are presented in Figure 17. Strong correlations (> 0.8) were found between soil carbon, nitrogen and organic matter; however all three variables were retained because they are indicative of different ecosystem functions, in line with previous authors (Hautier et al., 2018; W. Hu et al., 2021).

Table 10 Individual ecosystem functions measured at NutNet sites which were combined into ecosystem multifunctionality

Variable name	Units	Max	Min	Mean	Description
Belowground properties					
Soil Carbon	%	20.51	0.11	4.31	Indicator of soil carbon storage, a key ecosystem function
Soil Nitrogen	%	1.17	0.01	0.29	Macronutrients indicative of soil fertility. Can be inverted to indicate nutrient use efficiency or resistance to leaching.
Soil Phosphorus	ppm	237.33	1.00	41.84	
Soil Potassium	ppm	1276.07	24.98	222.13	
Soil Zinc	ppm	435.20	0.44	31.67	Micronutrients linked to aboveground productivity in previous work at these sites (Radujković et al., 2021).
Soil Iron	ppm	897.67	23.42	331.75	
Soil C:N ratio		48.26	5.26	15.19	Indicators of soil nutrient availability.
Soil N:P ratio		1983.33	1.55	189.48	
Soil organic matter	%	35.17	0.32	6.15	Indicator of soil carbon storage and soil structure.
Aboveground properties					
Aboveground biomass	gm^{-2}	1609.00	9.50	362.03	Indicator of aboveground productivity.
Proportion of Photosynthetically Absorbed Radiation aboveground	%	1.00	0.00	0.54	Indicator of aboveground productivity.
Invasion resistance	-	1.00	0.00	0.73	Ratio of native to introduced species.
Litter turnover	-	4.72	0.25	1.68	Indicator of decomposition.
Species richness	count	83.00	1.00	37.20	Indicator of plant species biodiversity

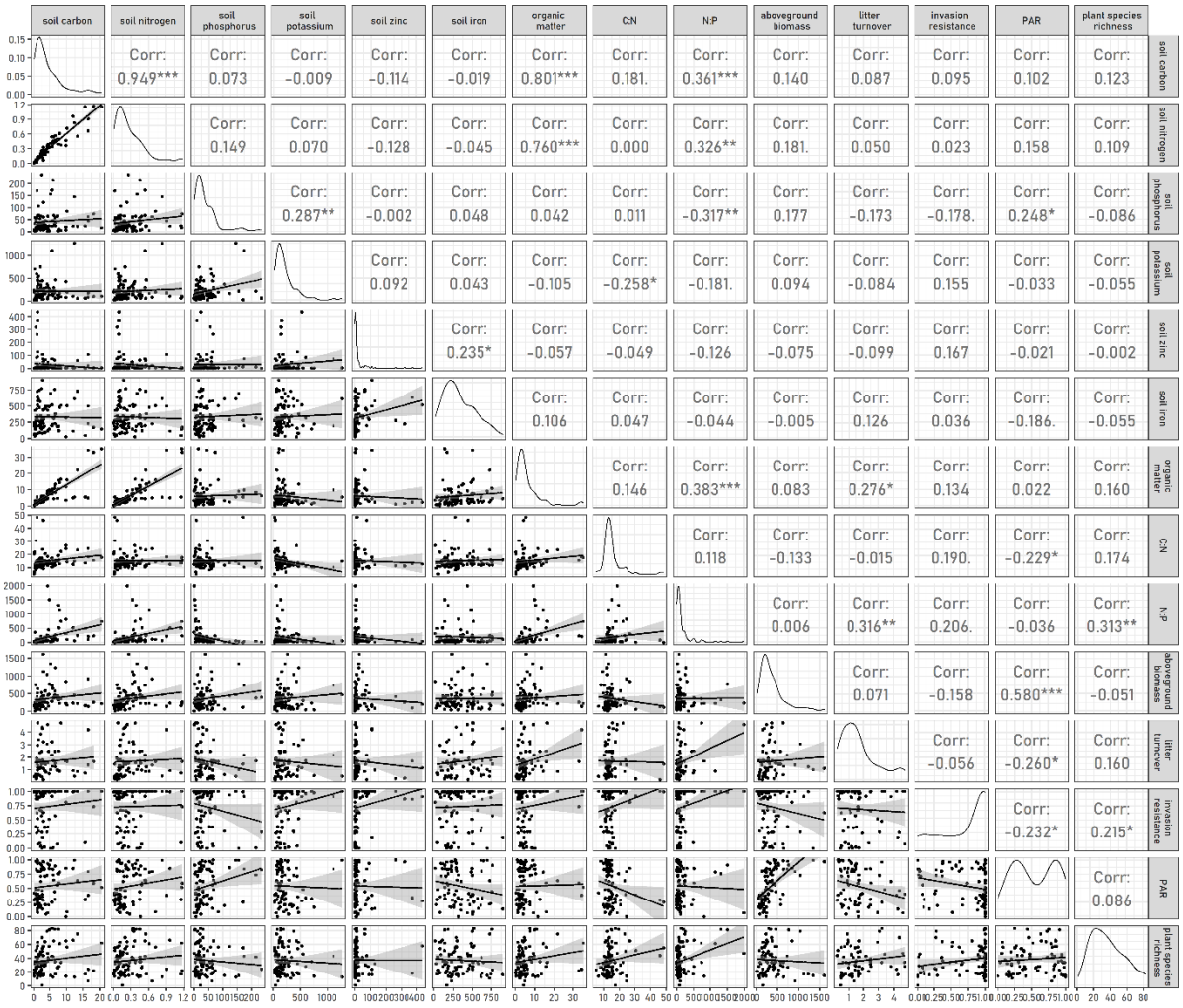

Figure 17. Correlation matrix showing relationships between the individual ecosystem properties

There is no single best way to calculate multifunctionality, especially across a broad range of grassland sites which are likely to incorporate a variety of habitats and ecosystem types (Byrnes et al., 2014; Manning et al., 2018). Therefore, eight different multifunctionality measures were initially calculated from plant and soil data at NutNet sites. Previous authors have similarly tested different multifunctionality measures; the most thorough approach being to test all combinations of all available properties (Delgado-Baquerizo et al., 2016; Jing et al., 2020). In this study, the alternative measures have been chosen following multifunctionality calculation approaches from the literature for which the same or similar plant and soil properties were available in the NutNet data. The ecosystem properties included in each measure along with the source publication are shown in Table 11. Two multifunctionality measures include inverting the values of N, P and K, by subtracting the value from the dataset maximum. This is recommended in ecosystems which are not nutrient-limited and where a higher concentration of soil macronutrients therefore indicates that

nutrients are not being taken up efficiently by the plant community and could be causing leaching, negatively contributing to desirable ecosystem functioning (Hautier et al., 2018; Manning et al., 2018; Y. Xu et al., 2022). However, inverting macronutrients is not always appropriate especially in more nutrient-poor systems such as arid sites, where higher soil concentrations of N, P and K instead indicate a build-up of soil fertility and therefore a positive contribution to multifunctionality (Delgado-Baquerizo et al., 2016; Y. Hu et al., 2022; Jing et al., 2015; Y. Zhao et al., 2018). Because the NutNet dataset presented here incorporates a wide range of sites at the global scale, multifunctionality measures using both standard and inverted N, P and K were tested. Micronutrients iron and zinc were included in some multifunctionality measures; though micronutrients are not often incorporated into multifunctionality, there is evidence that they are important components of soil and responsive to plant community and environmental change (Dias et al., 2020; Fay et al., 2015; J. G. White & Zasoski, 1999), and recent work (Radujković et al., 2021) indicated that zinc and iron were positively associated with productivity across sites in the Nutrient Network; therefore these micronutrients were included in this study.

To combine ecosystem properties into a single value of multifunctionality, the selected plant and soil properties were tested for normality (Shapiro-Wilk) and log-transformed if necessary, z-standardised in order to give equivalent scales across all variables, and then the mean taken across the standardised variables. The scale of means-based multifunctionality does not have units, and centres around 0. Three threshold-based multifunctionality measures were also calculated, to account for possible trade-offs between important ecosystem functions at the sites (Byrnes et al., 2014). The threshold-based measures are calculated by counting the proportion of plant and soil properties at each site which exceed a given threshold of the total range of that property across all sites; thresholds chosen here were 25%, 50% and 75%, giving three different threshold-based values of multifunctionality for each site. Distributions of the different multifunctionality measures are shown in Figure 19, relationships between the different multifunctionality measures are presented in Figure 20. All eight multifunctionality measures were tested for associations with satellite-derived NDVI phenometrics; some comparison between relationships found using different multifunctionality measures is presented, however as the relationships to satellite-derived phenology were broadly consistent, the majority of analysis is based on the multifunctionality measure which showed the strongest associations.

Table 11. The alternative multifunctionality measures calculated and tested across the sites.

Name	Properties included	Calculation	References
MF1	Soil Carbon (%) Soil Nitrogen (%) Soil Phosphorus (ppm) Soil Potassium (ppm) Aboveground biomass (gm-2) Proportion of Photosynthetically Absorbed Radiation aboveground (%) Invasion resistance (%) Litter turnover	Mean, NPK inverted	The measure of multifunctionality previously linked to multiple spatial scales of plant species diversity at these sites (Hautier et al., 2018)
MF2	Soil Carbon (%) Soil Nitrogen (%) Soil Phosphorus (ppm) Soil C:N ratio Soil N:P ratio Soil organic matter (%) Aboveground biomass (gm-2)	Mean	The measure of multifunctionality shown to be linked to plant species diversity and aridity in grasslands at a regional scale. Does not include soil micronutrients (Y. Yan et al., 2020)
MF3	Soil Carbon (%) Soil Nitrogen (%) Soil Phosphorus (ppm) Soil Potassium (ppm) Soil Zinc (ppm) Soil Iron (ppm) Soil C:N ratio Soil N:P ratio Soil organic matter (%) Aboveground biomass (gm-2) Proportion of Photosynthetically Absorbed Radiation aboveground (%) Invasion resistance (%) Litter turnover	Mean	Using all the available measured ecosystem properties. There is evidence that the more functions included the stronger the relationship of multifunctionality to diversity (Delgado-Baquerizo et al., 2016, 2018; Jing et al., 2020; Maestre et al., 2012) (Jing et al., 2020) although this has been shown in some cases to be a statistical artefact (Gamfeldt & Roger, 2017).
MF4	*All ecosystem properties, as MF3*	Mean, NPK inverted	Inverting macronutrients is done in some cases, to represent nutrient retention and less likelihood of leaching (Byrnes et al., 2014; Hautier et al., 2018; Manning et al., 2018; C. Xu et al., 2022)

MF5	Soil Carbon (%) Soil Nitrogen (%) Soil Phosphorus (ppm) Soil Potassium (ppm) Soil Zinc (ppm) Soil Iron (ppm) Soil C:N ratio Soil N:P ratio Soil organic matter (%) Aboveground biomass (gm-2)	Mean	A measure of soil multifunctionality, using all available soil properties plus aboveground biomass, as the approach of previous authors (Fry et al., 2018; Guo et al., 2021; W. Hu et al., 2021; Lavorel, 2013; Q. Liu et al., 2021; Schittko et al., 2022; Vazquez et al., 2021; Y. Xu et al., 2022; Y. Yan et al., 2020; Zwetsloot et al., 2021)
MF25	*All ecosystem properties, as MF3*	Threshold	Multiple threshold-based measures of multifunctionality, which can account for potential trade-offs between ecosystem functions. Threshold-based multifunctionality measures are often included in studies but are not the main measure reported, due to being more complicated to interpret than means-based multifunctionality (Byrnes et al., 2014; Pasari et al., 2013)
MF50	*All ecosystem properties, as MF3*	Threshold	
MF75	*All ecosystem properties, as MF3*	Threshold	

5.2.2 Satellite-derived phenology

Satellite timeseries for this study were derived from Landsat, a multispectral satellite mission with nine bands at a spatial resolution (pixel size) of 30x30m, which is an appropriate spatial scale for pairing with field data from the NutNet sites at which plant and soil data is collected within spatial blocks measuring 10x25m. Some of the NutNet sites comprise small areas of grassland within a larger matrix of mixed land cover types, which is another reason for choosing the relatively small pixel size of Landsat over other satellite products which are commonly used for time series analysis, such as MODIS at a spatial resolution of 500m (Araya et al., 2016; Dronova et al., 2022). The location of a single 30x30m Landsat pixel was chosen to represent each site, in an area adjacent to the field plots but not directly over them so as not to be impacted by any nutrient addition treatments in plots neighbouring the sampled control plots. The spatial location of the representative Landsat pixel was chosen for each site based on visual inspection of the site, including the surrounding landscape and specific locations of the treatment plots, in Google Earth. Satellite data for each site-representative pixel was acquired from Landsat 5 (1984 – 2011), Landsat 7 (1999 – 2021) and Landsat 8 (2013 – 2021), from the year of field sampling backwards for as many years as data were available, up to 30 years. Data was acquired from the Landsat Collection 2, Level-2 data product archive, which has had pre-processing including correction to surface reflectance and cloud masking applied.

The revisit period of Landsat is 16 days, shortening to 8 for periods which are covered by more than one of the three sensors, which orbit asynchronously. The sampling approach yielded between 281 and 5449 images, giving satellite timeseries of 1 – 30 years, per site. Data was downloaded through Google Earth Engine (Gorelick et al., 2017b).

NDVI was selected as the appropriate vegetation index to capture seasonal cycles of vegetation growth and senescence across a global set of contrasting grasslands. NDVI has known limitations at particularly high or low levels of vegetation density. At low levels, background soil properties can influence the red and NIR portions of the spectrum and cause artificially high NDVI values. Therefore, an alternative soil-adjusted vegetation index (SAVI) can be used in cases of low vegetation density (Qi et al., 1994). At high levels of vegetation density, the NDVI maxes out and fails to distinguish variation in vegetation density above the threshold. The enhanced vegetation index (EVI) is an alternative to NDVI in such cases (Huete & Jackson, 1988). All three indices, amongst others, have previously been used to predict multiple ecosystem functions in different types of grasslands, including arid grasslands, with NDVI and EVI most commonly reported to yield successful results (García-Gómez & Maestre, 2011; Pettorelli et al., 2005; Ren & Feng, 2015; Wilson et al., 2017; Y. Zhao et al., 2018). In this study, both NDVI and EVI were initially calculated and analyses run using each index. NDVI was found to have greater variability among sites and stronger relationships with multifunctionality and species richness, therefore NDVI was chosen as the final index and only the results based on NDVI are presented.

Phenological metrics were extracted for each year, per site using Timesat software (Eklundh & Jönsson, 2017; Jönsson & Eklundh, 2004). Timesat applies gap-filling and smoothing to the seasonal NDVI curves. Specific tuning was applied by visually inspecting the timeseries for each site in the Timesat graphical user interface (GUI); the fitting method was double logistic, and start and end of the growing season were defined relative to the overall seasonal amplitude (start = 0.25 and end = 0.15). Any years for which there was insufficient data to fit a curve, likely due to prevalence of cloud cover, were removed from timeseries. Phenometrics indicating the maximum NDVI, length of the growing season, within-year variability, rates of green-up and senescence and overall average NDVI were outputted from the Timesat software. The phenometrics used in this study were selected from those outputted by Timesat for their ecological relevance, interpretability and uniqueness; description of the seven phenometrics along with their ecological significance is shown in Table 12. To investigate whether a longer history of phenology is more relevant to ecosystem multifunctionality than shorter timeseries, the mean of each phenometric was calculated across different lengths of timeseries, from 3 years to 30 years, increasing in three-year increments. These multi-year means of phenometrics are used in the statistical analyses

described below. To investigate the relationship between ecosystem stability and multifunctionality, the inter-annual variation (coefficient of variation, c.v., calculated as standard deviation/mean) of each phenometric was also calculated over the different lengths of timeseries. This method of ascertaining phenological variability has been used by previous authors (Dronova et al., 2022; Paruelo et al., 2016).

Table 12. NDVI phenometrics retrieved from timeseries in this study. All phenometrics are used as both magnitude (average over the timeseries) and variability (cv over the timeseries)

Phenometric	Abbreviation	Min	Max	Ecological interpretation & hypothesised relationship to multifunctionality
Annual maximum NDVI	NDVImax	0.15	0.98	Represents maximum vegetation greenness at the peak of the growing season, often used to represent peak biomass (J. Yan et al., 2022)
Mean NDVI	NDVImean	0.11	0.80	The overall average NDVI throughout the season, commonly used to represent productivity (Paruelo et al., 2016; Wilson et al., 2018)
Time-integrated NDVI or area-under-curve	NDVIauc	30.0	1.9	Cumulative productivity throughout the growing season. Affected by both magnitude of NDVI and the length of the growing season. Has been found to be a sensitive measure of aboveground ecosystem properties in managed and natural grasslands (Weber et al., 2018; J. Yan et al., 2022)
Length of growing season (days)	NDVIlen	278	98	The time difference between the start and end of the growing season. Longer growing seasons are associated with more diverse plant communities (Dronova & Taddeo, 2022)
Rate of NDVI increase or green-up	NDVIinc	0.13	0.01	There is evidence that more diverse grassland communities are associated with faster rates of green-up and senescence (Zaret et al., 2022)
Rate of NDVI decrease or senescence	NDVIdec	0.13	0.00	
Seasonal variation in NDVI, given by the annual coefficient of variation	NDVIcv	0.97	0.02	Measure of the seasonality of vegetation growth. Has been used to retrieve species diversity (Gholizadeh et al., 2019; Tan et al., 2022) and multivariate ecosystem services (Paruelo et al., 2016) in grasslands

5.2.3 Statistical analyses

Pearson's correlations were used to explore relationships between satellite-derived phenometrics, phenological variability, plant species richness and ecosystem multifunctionality. The effect of using historic average values of the phenometrics was assessed by comparing the strength of associations between multifunctionality and phenometrics averaged across increasing lengths of timeseries, 3 – 30 years. Bivariate linear models were also created between individual phenometrics and multifunctionality, using the optimum length of timeseries identified by Pearson's correlations, to ascertain the amount of variation in multifunctionality that could be accounted for by variation in each phenometric.

Overall variability of satellite-derived productivity (NDVI curves) at each site was assessed using Mann-Kendall tests, which indicate whether a data series with regular fluctuation has a significant trend overall (J. Yan et al., 2022). Pearson's correlations were found among sites with and without significant overall trends in NDVI. It was hypothesised that for sites with significant overall trends, a historical perspective of phenometrics i.e. averaged over a longer timeseries, would be more important than for sites with no overall trend, where phenometrics are likely to be similar throughout the years and therefore incorporating more years into the average has little effect.

Random forest regression was used to ascertain the utility of NDVI phenometrics for retrieving variation in multifunctionality in the presence of large scale climate and location drivers. Random forest was chosen to look for general associations across the large range of sites, rather than creating complex linear models of ecological functioning, which are likely to be different at different sites given the large geographic gradients and diverse climate and ecosystem types included in this set of 90 global grasslands. The climate parameters included were mean annual temperature (MAT), mean annual precipitation (MAP) and global aridity index (GAI) (Zomer et al., 2022), and location information latitude, longitude and elevation to account for spatial autocorrelation. Climate data was sourced from Worldclim, as 30-year averages (Fick & Hijmans, 2017; Hijmans et al., 2005). These covariates have been used previously to model multifunctionality in grasslands distributed in contrasting regions of the globe (Delgado-Baquerizo et al., 2018). The ranges of the climate and location variables are shown in Table 13. The Boruta algorithm, an extension to random forest, was used to test for and eliminate non-significant predictor variables from the final models (Degenhardt et al., 2019; Kursa & Rudnicki, 2010). Random forest models were constructed with 1000 trees, and the optimal value of mtry as determined using the RFtune() function of package rfUtilities (Evans & Murphy, 2017). Models were run 100 times and the average of the 100 model runs taken as the final model output. The model outputs include % variation explained, RMSE

(based on out-of-bag samples) and a variable importance score, based on the reduction in mean square error (MSE), indicating the contribution of individual predictor variables to the final model.

All analyses were run in R, using packages *rfUtilities, randomForest, Boruta, Kendall*.

Table 13. The ranges of the climate and location predictor variables incorporated into random forest models of multifunctionality

Variable	Mean	Min	Max
Mean annual temperature (MAT) (°C)	11.0	-7.6	24.1
Mean annual precipitation (MAP) (mm)	820.3	192.0	2224.0
Elevation (m)	535.6	0.0	3500.0
Latitude (°)	28.6	-51.9	78.7
Longitude (°)	-40.6	-124.0	152.9

5.3 Results

5.3.1 Distribution of above- and belowground functions and multifunctionality

Figure 18 shows the distribution of the ecosystem properties measured in the field at the 90 NutNet sites, coloured according to their aridity following published thresholds of the GAI (Zomer et al., 2022). There were 62 humid, 7 dry subhumid, 17 semiarid and 4 arid sites in the data. Arid and semiarid sites have the lowest values of most ecosystem properties, with the exception of soil iron, invasion resistance and plant species richness. A correlation matrix of individual ecosystem properties (Figure 17) shows that there are no strong, significant negative correlations indicating trade-offs between functions (Manning et al., 2018). Soil carbon was collinear with soil nitrogen (R = 0.949) and soil organic matter (R = 0.801). However, all three properties were retained as they represent different important functions of soils, and previous authors have found the inclusion of collinear soil carbon and nitrogen variables not to change the outcome of analyses (Hautier et al., 2018; W. Hu et al., 2021).

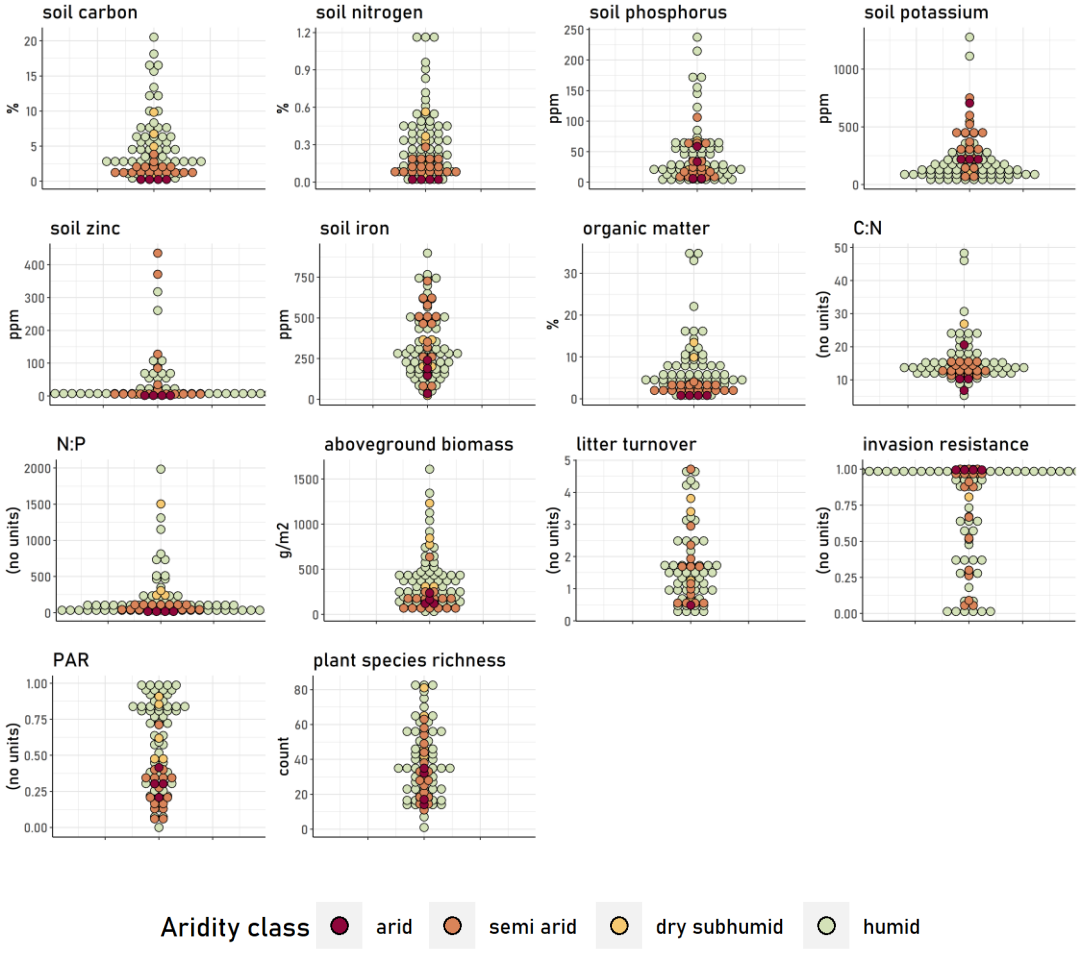

Figure 18. Distribution of the field-measured ecosystem properties, including the 9 belowground (soil) properties and 4 aboveground (plant) properties used to calculate ecosystem multifunctionality. The distribution of site-level plant species richness is also shown.

Figure 19 shows the distribution of the eight different multifunctionality measures calculated from various combinations of above- and belowground properties at each site (Table 11), coloured by aridity. Sites which are arid or semiarid have lower values of most multifunctionality measures. This effect is less apparent for *MF1*, the multifunctionality measure with inverted macronutrients and a greater proportion of aboveground relative to belowground properties. Two sites, Hog Island and Metompkin, have unusually low multifunctionality values for most multifunctionality measures, and are outliers in some of the relationships between different multifunctionality measures (Figure 20). These sites are the only coastal grassland sites in the dataset, and only belowground properties were incorporated into multifunctionality at these sites (Appendix A).

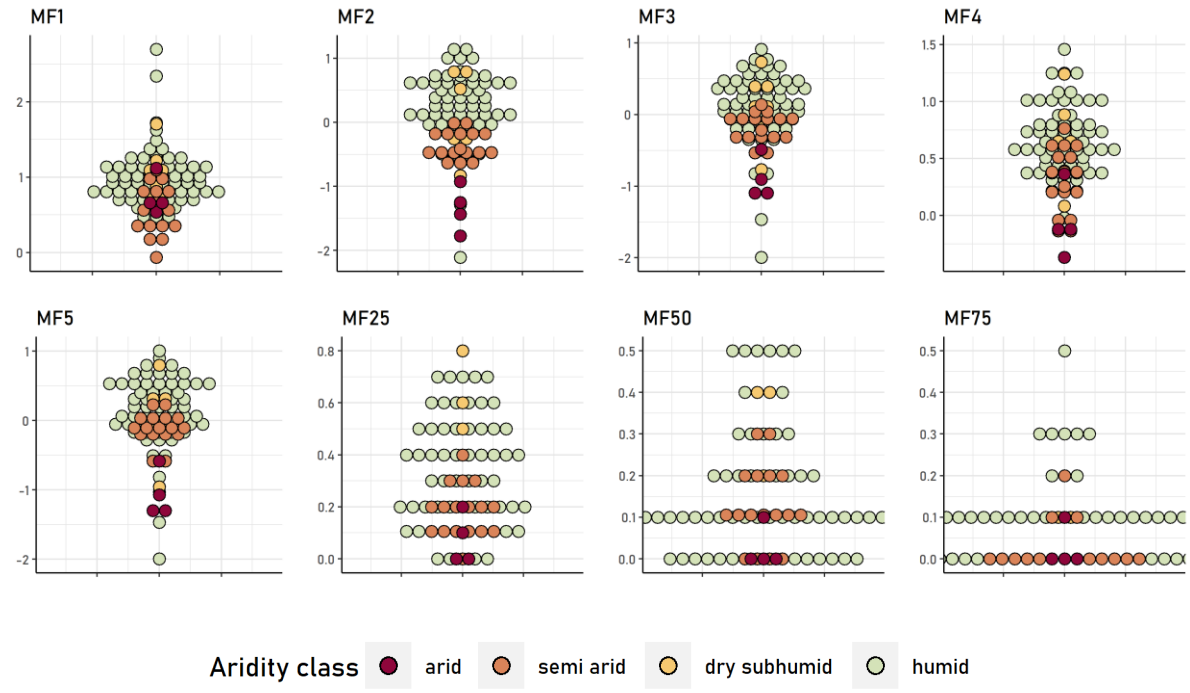

Figure 19. The distribution of values of eight different multifunctionality measures, following calculation approaches in the literature. Five measures are means-based, and the remaining three are threshold-based (Table 11). Colours indicate the aridity class of the site, based on the GAI.

5.3.2 Associations between above- and belowground functions

Figure 20 shows relationships between the eight different multifunctionality measures. There are significant positive correlations between all of the measures except *MF1,* the measure which incorporates fewer soil properties than the others, includes some aboveground properties, litter turnover and invasion resistance, which are not commonly incorporated into multifunctionality measures, and involves inversion of soil N, P and K.

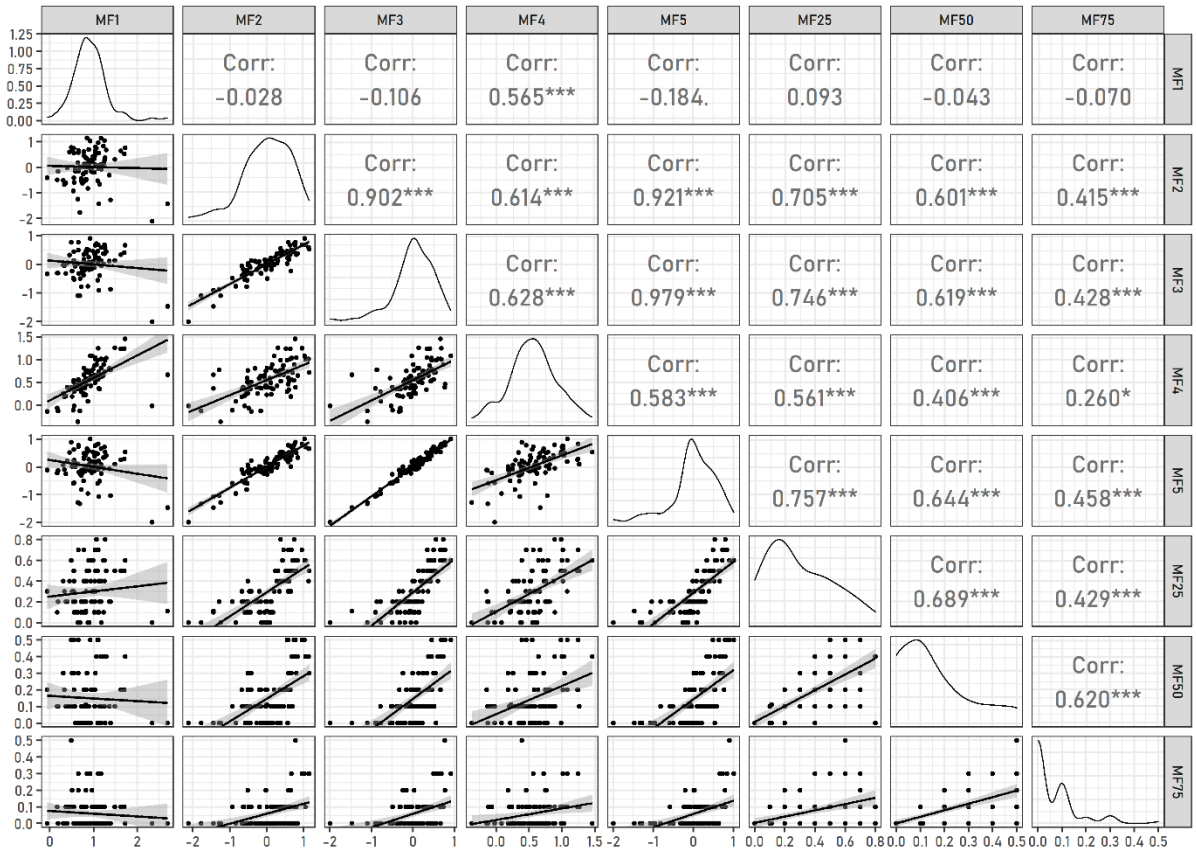

Figure 20. Scatter plots (lower) and Pearson's R values (upper) showing relationships between the eight different multifunctionality measures.

*. = p < 0.1, * = p < 0.05, ** = p < 0.01, *** = p < 0.001.*

Figure 21 shows the relationship between multifunctionality measures and plant species richness across the NutNet sites. There are no strong correlations between site-level species richness and multifunctionality. However, four multifunctionality measures (*MF2, MF3, MF4, MF5*) have weak but significant positive correlations with plant species richness, at the 0.05 level (Pearson's R 0.21 – 0.29), with the most significant relationship for *MF4*, including all measured properties and inverted N, P and K. None of the threshold-based measures have significant correlations with plant species richness. Arid and semi arid sites tend to have low multifunctionality relative to their species diversity, in comparison to the sites as a whole, shown by the line of best fit.

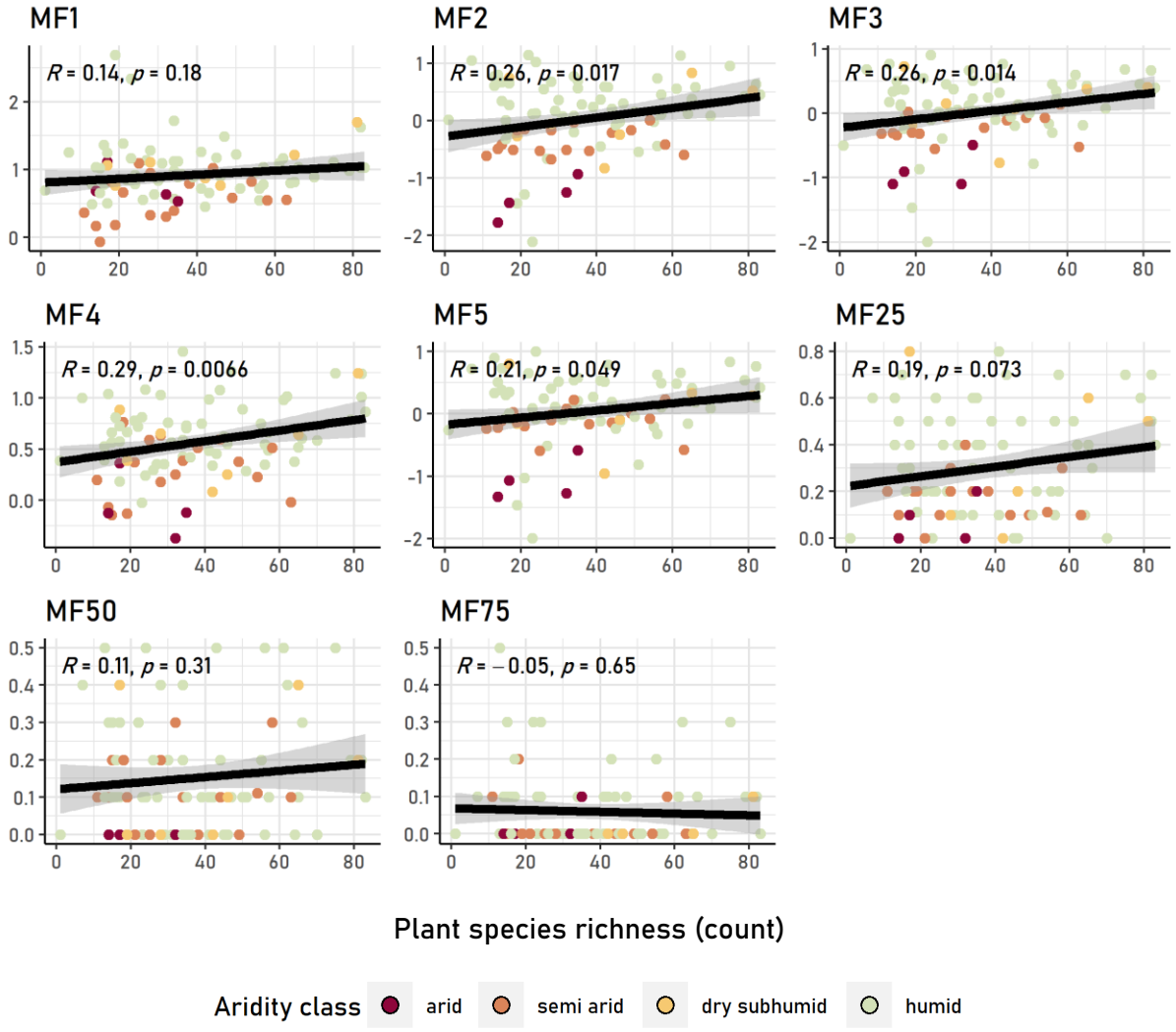

Figure 21. Scatter plots showing the association between eight multifunctionality measures and plant species richness, counted at the site level. Colours show the aridity class of the sites. Line shows the linear line of best fit, and the surrounding grey area represents the 95% confidence level.

5.3.3 Associations between NDVI-derived phenometrics and ecosystem functions

The variability of phenometrics across the whole 30-year timeseries at sites are shown in Figure 22. Annual maximum NDVI has the lowest year-on-year variability, and also the smallest range of variability among sites, indicated by the narrow box. The most variable phenometrics year-on-year, were the rates of increase and decrease in NDVI.

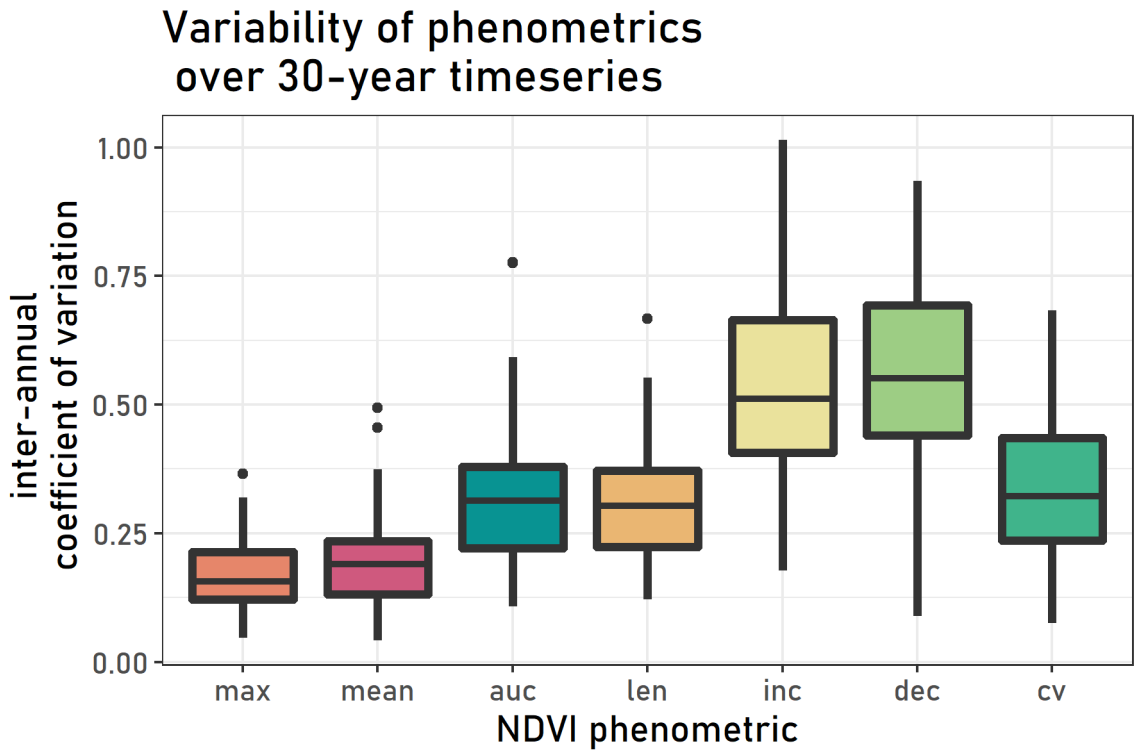

Figure 22. Distribution of phenometric variability across the whole 30-year timeseries of all sites. Colours indicate the phenometric: auc = area under curve, or time-integrated NDVI; cv = intra-annual coefficient of variation, dec = rate of decrease (senescence); inc = rate of increase (green-up); len = length of growing season; max = NDVI max; mean = NDVI mean. Phenometric variability is given by the coefficient of variation of each phenometric, standard deviation / mean. Boxes show the inter-quartile range of values, the centre line shows the median, and whiskers extend to the largest, or 1.5 times the interquartile range. Values which are greater than 1.5 times the interquartile range are represented by a dot.

Pearson's correlations were found between the individual ecosystem properties and the seven NDVI phenometrics, averaged over 3 – 30 years of seasonal NDVI curves. The key relationships are summarised in Table 14 (correlations for individual properties shown in Appendix B). Aboveground biomass is most strongly associated with shorter NDVI timeseries, i.e. the phenology of the plant community in the 3 years preceding field measurement. Soil properties carbon and organic matter content were more strongly associated with phenometrics averaged over longer timeseries of up to 30 years. There are no associations between phenometrics and site-level species richness across the sites, for any length of

timeseries. Invasion resistance and litter turnover were not strongly associated with phenometrics overall, and nor were soil micronutrients zinc and iron.

Table 14. Key information about the associations between NDVI phenometrics and the individual ecosystem functions which are incorporated into measures of multifunctionality. The correlations are shown in Appendix B.

Ecosystem property	Key associations with phenometrics
Soil Carbon (%)	Significant positive correlations (R = 0.2 – 0.4) with most phenometrics. Generally stronger relationships for longer timeseries. No significant correlations with phenologic variability.
Soil Nitrogen (%)	Significant positive correlations (R = 0.2 – 0.4) with most phenometrics. Variable effect of increased length of timeseries for different phenometrics. No significant correlations with phenologic variability.
Soil Phosphorus (ppm)	Significant positive correlations with $NDVI_{mean}$ and $NDVI_{auc}$ (R = 0.2 – 0.35). Generally stronger relationships for shorter timeseries. No significant correlations with phenologic variability.
Soil Potassium (ppm)	No significant correlations with NDVI phenometrics. Few significant correlations with phenologic variability.
Soil Zinc (ppm)	No significant correlations
Soil Iron (ppm)	No significant correlations
Soil C:N ratio	Few significant correlations
Soil N:P ratio	Significant positive correlation (R ~= 0.25) with $NDVI_{auc}$, for 15-30 year timeseries. Significant positive correlation with phenometric variability measured by $NDVI_{mean}$, strongest for a 3-year timeseries.
Soil organic matter (%)	Significant positive correlations with most phenometrics (R = 0.2 – 0.4). Generally stronger relationships for longer timeseries. No significant correlations with phenologic variability.
Aboveground biomass (gm-2)	Significant positive correlations with most phenometrics (R = 0.4 – 0.5). Generally the strongest relationships for shorter timeseries, decreasing from 3-30 years. Significant negative correlation with phenologic variability measured by $NDVI_{max}$, around R = -0.3.
Proportion of Photosynthetically Absorbed Radiation aboveground (%)	Significant positive correlations with most phenometrics (R = 0.2 – 0.6). Generally consistent correlation strengths for timeseries from 3 – 30 years. Significant negative correlations with phenologic variability, based on most phenometrics, for timeseries from 6 – 30 years.
Invasion resistance (%)	Significant negative correlation (R = -0.2 – -0.3) with $NDVI_{mean}$
Litter turnover	No significant correlations
Species richness	No significant correlations

Associations between multifunctionality and plant community phenology, measured using satellite NDVI, were found for all eight multifunctionality measures. Overall relationships and conclusions drawn from the analysis were consistent across all of the means-based multifunctionality measures. Threshold-based multifunctionality measures had some correlations with phenometrics, up to R = 0.4, however the best-correlated phenometrics fluctuated with timeseries length and were not consistent among the three different thresholds. The multifunctionality measure most strongly correlated with phenometrics overall was *MF2*, therefore the results based on this multifunctionality measure are presented from this point forward.

All phenometrics had significant, positive associations with multifunctionality. $NDVI_{max}$ was the phenometric with the strongest correlations to multifunctionality, and the second-strongest was $NDVI_{inc}$, representing the rate of green-up. Length of growing season ($NDVI_{len}$) had the weakest correlations to multifunctionality (Figure 23 a.). Between 12 and 18 years is the timeseries length for which positive correlations between NDVI phenometrics and multifunctionality are strongest for the majority of phenometrics. However, the variation in the R and *p* values were less than 0.1 and 0.01 respectively, indicating that increasing the length of timeseries used to calculate the average phenometric value did not significantly improve models. Only one indicator of phenological variability, inter-annual variation in $NDVI_{max}$, was significantly negatively correlated with multifunctionality. Again, timeseries of between 12 and 18 years gave the strongest correlations; however, this time there was a larger effect of increasing the length of timeseries (R = -0.068 to -0.300, p = 0.551 to 0.005).

NDVI phenometrics averaged over a timeseries of 18 years had the strongest correlations with multifunctionality for most phenometrics. Figure 24 shows scatter plots of phenometrics (18-year) and multifunctionality. The four arid sites have lower multifunctionality in relation to their phenometrics than the sites as a whole.

a.

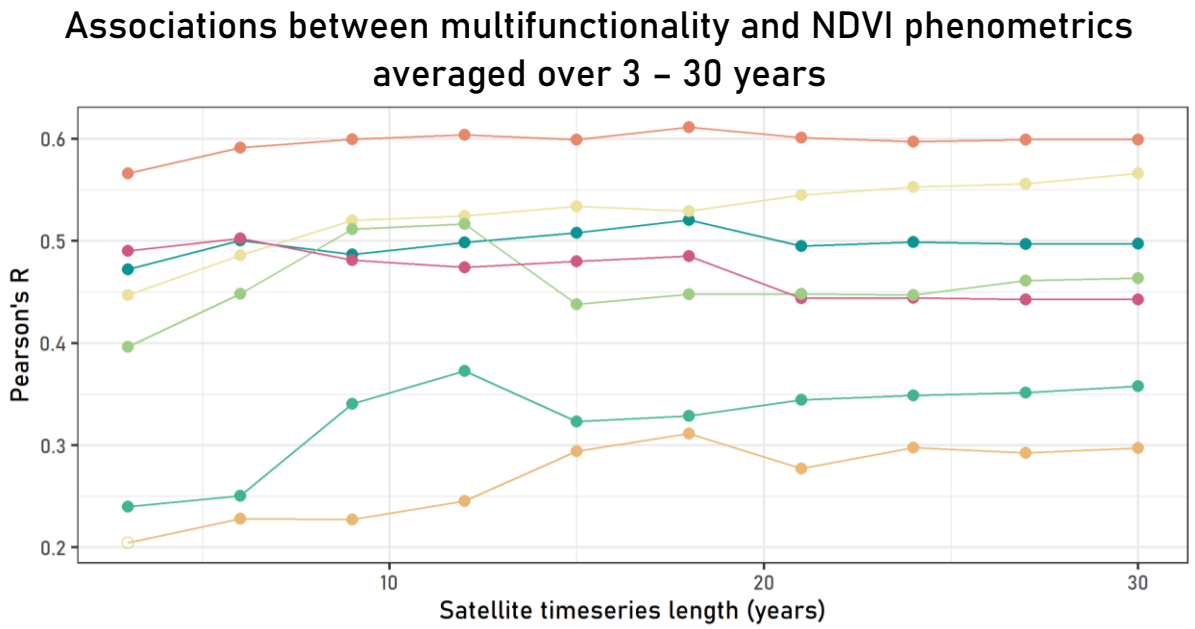

b.

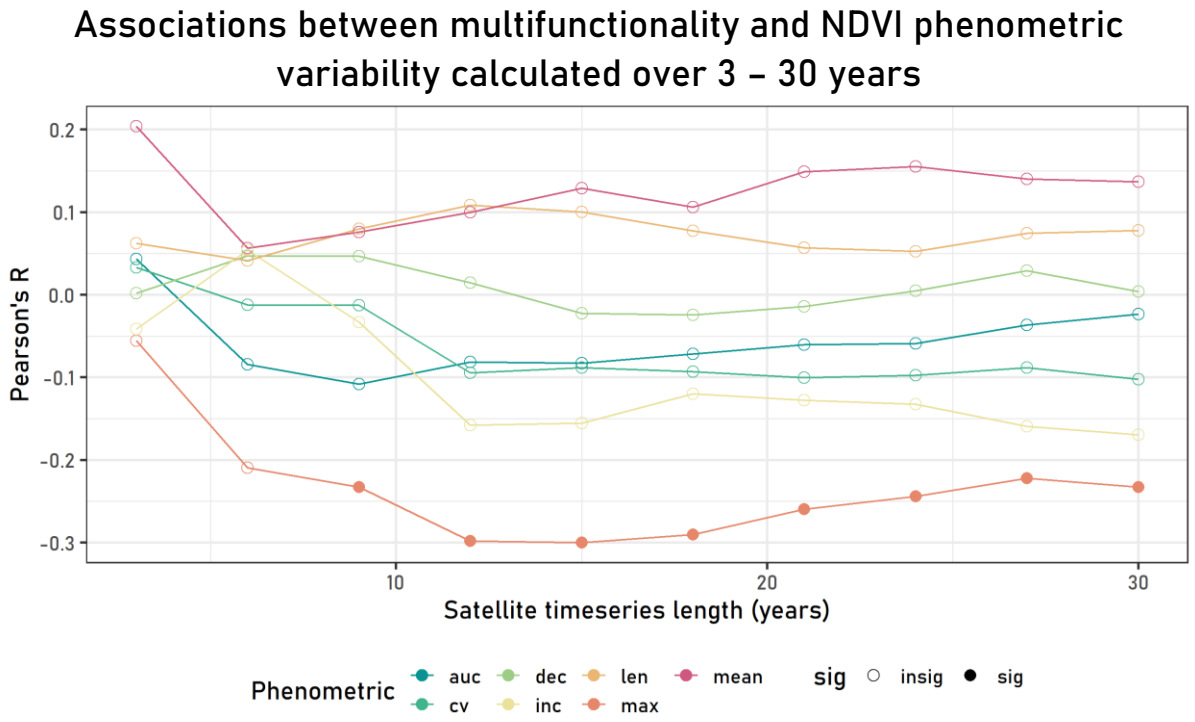

Figure 23. Pearson's correlations between ***a.*** *NDVI phenometrics (average over 3 – 30 years) and* ***b.*** *NDVI phenometric variability (inter-annual coefficient of variation over 3 – 30 years) and multifunctionality. Colours indicate the phenometric: auc = area under curve, or time-integrated NDVI; cv = intra-annual coefficient of variation, dec = rate of decrease (senescence); inc = rate of increase (green-up); len = length of growing season; max = NDVI max; mean = NDVI mean. Significant correlations ($p < 0.05$) are shown by filled-in points, insignificant correlations are shown by empty points.*

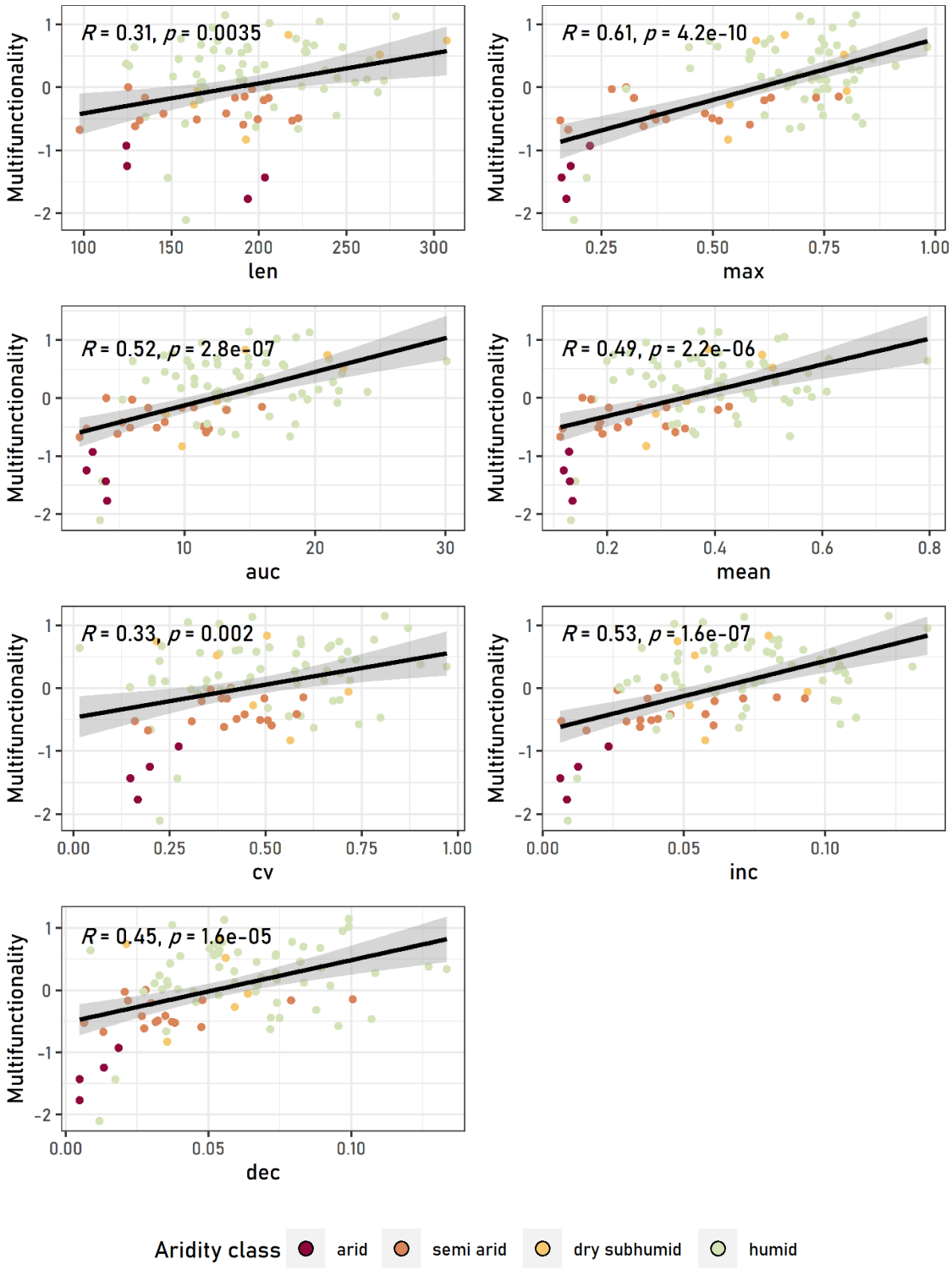

Figure 24. Scatter plots and Pearson's correlations between the individual phenometrics, averaged over 18 years. Black lines show the linear model line of best fit, grey area shows 95% confidence interval. Colours show the aridity class of the sites.

Mann-Kendall tests were used to identify which sites had stable NDVI across the whole 30-year timeseries, and which sites experienced a significant change in NDVI. 58 sites had significant changes in NDVI across the 30-year timeseries (p <= 0.01), and 29 sites did not

have significant NDVI trends. These two subsets of sites were tested separately for relationships between multifunctionality and phenometrics, to investigate whether the overall long-term stability of vegetation at the site influences the timescales over which phenology most closely represents multifunctionality. Figure 25 shows Pearson's correlations between multifunctionality and NDVI phenometrics averaged over increasing lengths of timeseries, from 3-30 years.

a.

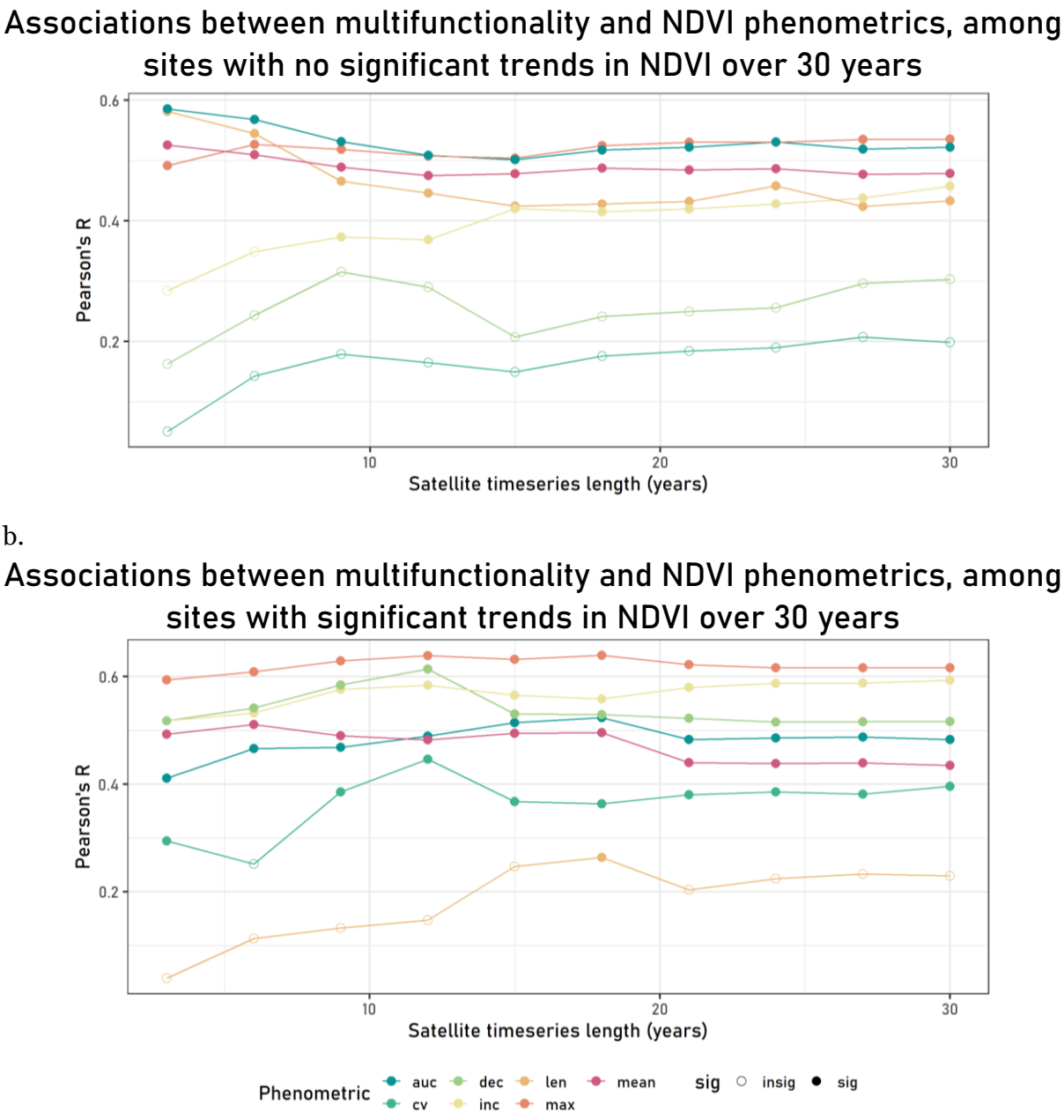

Figure 25. Pearson's correlations between multifunctionality and NDVI phenometrics among ***a.*** *sites without (n = 29) and* ***b.*** *sites with (n = 58) significant trends in NDVI over the 30 year timeseries, determined by Mann-Kendall tests. Colours indicate the phenometric: auc = area under curve, or time-integrated NDVI; cv = intra-annual coefficient of variation, dec = rate of decrease (senescence); inc = rate of increase (green-up); len = length of growing season; max = NDVI max; mean = NDVI mean.*

Separate analysis of sites with and without significant trends in NDVI over 30 years showed different relationships between then individual phenometrics and multifunctionality within each group. Time-integrated NDVI and growing season length were more strongly associated with multifunctionality among sites which were overall phenologically stable (Figure 25). The relationship of growing season length to multifunctionality was particularly affected by site stability, being one of the most strongly correlated phenometrics among stable sites, and not significantly correlated to multifunctionality among sites with significant trends in NDVI. Rates of green-up and senescence were oppositely affected, not being associated with multifunctionality among stable sites but being some of the most strongly correlated phenometrics among unstable sites. Long-term site stability also impacted the effect of longer versus shorter timeseries for retrieving phenometrics; among sites with no overall trends in NDVI, the shortest timeseries of 3 years gave stronger relationships between phenometrics and multifunctionality (Figure 25).

Bivariate linear models were created to explain variation in multifunctionality from each of the NDVI phenometrics and measures of phenologic variability (inter-annual phenometric variation). Phenometrics retrieved from timeseries of 18 years were used for linear modelling, because this length of timeseries had the strongest Pearson's correlations between phenometrics and multifunctionality (Figure 23). Phenometrics which explained significant portions of multifunctionality (p <= 0.05) were the same as those which had significant Pearson's correlations (Figure 23). Results of linear models are presented in Table 15.

Table 15. bivariate linear models predicting multifunctionality from average and variability of NDVI phenometrics, calculated over an 18-year timeseries

predictor	adjusted R^2	intercept	slope	*p*	RMSE
Mean average					
max	0.366	-1.167	1.938	0.000	0.506
mean	0.226	-0.754	2.218	0.000	0.559
auc	0.262	-0.704	0.058	0.000	0.546
len	0.086	-0.888	0.005	0.004	0.608
inc	0.271	-0.682	11.143	0.000	0.543
dec	0.191	-0.522	10.062	0.000	0.572
cv	0.097	-0.469	1.052	0.002	0.604
Variability (inter-annual coefficient of variation)					
max	0.073	0.418	-2.364	0.007	0.612

5.3.4 Predicting variation in multifunctionality

Random forest regression was carried out to explain variation in multifunctionality from NDVI phenometrics, climate and location variables. NDVI phenometrics averaged over 3, 18 and 30 years were used in three separate models, and compared in Table 16. An additional 11.21% of variation in multifunctionality was explained using 18-year average phenometrics compared to 3-year averages, though there was little difference in explained variation between 18-year and 30-year averages. All models including both phenometrics and climate & location variables explained more variation than those using just one of the two predictor groups. The most successful random forest model is presented along with the importance scores of individual predictor variables in Figure 26 (a., b.). The most important predictor variable by a large margin is aridity, given by Global Aridity Index. Six phenometrics were retained as important predictor variables in model construction, the most important being $NDVI_{mean}$. Climate and location variables were also retained as important predictors, though less important than four of the phenometrics. Phenological variability (c.v. of $NDVI_{max}$) was not retained during variable selection as an important predictor of multifunctionality. For all models, the standard deviation of variation explained among the 100 model runs was 0.006 or less, indicating that the models were stable.

Table 16. Results of random forest regression of multifunctionality. Average of 100 model runs.

Length of timeseries	**% variation explained**	**Standard deviation**	**RMSE**	**NRMSE (RMSE/ range)**
3-year	50.19	0.006	0.440	0.135
18-year	61.40	0.005	0.397	0.122
30-year	61.17	0.005	0.398	0.122
Results of random forest regression of multifunctionality, using only the NDVI phenometrics or the climate and location variables as predictors.				
NDVI phenometrics only (18-year)	47.13	0.005	0.465	0.142
Climate & location variables only	46.82	0.006	0.473	0.145

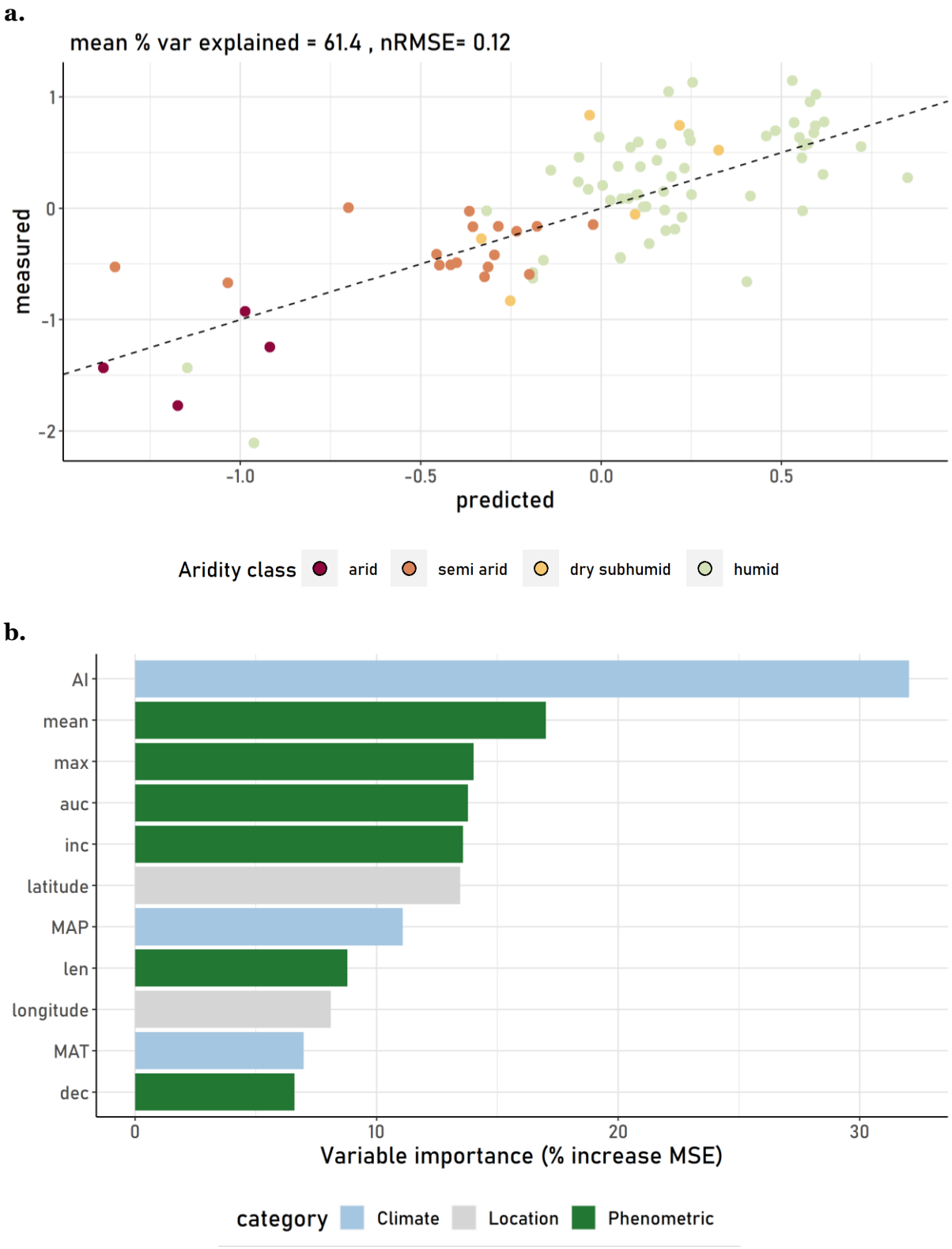

Figure 26. ***a.*** *Random forest model of multifunctionality from phenometrics, climate and location variables. Points are coloured according to aridity class.* ***b.*** *The importance of predictor variables in modelling multifunctionality. auc = area under curve, or time-integrated NDVI; cv = intra-annual coefficient of variation, dec = rate of decrease (senescence); inc = rate of increase (green-up); len = length of growing season; max = NDVI max; mean = NDVI mean; AI = aridity index; MAP = mean annual precipitation; MAT = mean annual temperature*

5.4 Discussion

These results indicate that variation in the multifunctionality of grassland systems at a global scale can be detected from satellite NDVI phenometrics representing the magnitude, temporal variation and stability of aboveground productivity across multiple growing seasons. Higher and more stable aboveground productivity, i.e. an increase in the magnitude of phenometrics and a decrease in their inter-annual variability, were both indicative of higher-multifunctionality systems (Pearson's R of up to 0.61 and -0.30 respectively). These findings build on existing landscape-scale studies which have found that multiple ecosystem services, or multivariate indicators of grassland health and status, can be retrieved using satellite NDVI across individual grassland landscapes, for the purpose of managing the landscape for multiple services (Gaitán et al., 2013; García-Gómez & Maestre, 2011; Paruelo et al., 2016; Weber et al., 2018; Y. Zhao et al., 2018). The contribution of the present work is to demonstrate that the links between satellite phenology and ecosystem multifunctionality which exist at small scales can be found at the global scale, generalised across diverse natural grassland ecosystems, and have the potential to be used to enhance field-based assessments of multifunctionality by filling temporal and spatial gaps.

5.4.1 Links between satellite NDVI phenometrics and ecosystem functioning

Multifunctionality was expected to be linked to NDVI phenometrics via two main mechanisms. First, and primarily by phenometrics capturing the magnitude of aboveground productivity, the main process by which carbon and energy enter the system and therefore control on the amount of resources available to drive other ecosystem functions (Pettorelli et al., 2005). The multifunctionality measures all incorporated at least one direct measure of aboveground productivity, and some two (aboveground biomass and proportion PAR), which were significantly correlated to phenometrics themselves, thereby providing a mechanism for at least part of the link. The most strongly correlated phenometric to multifunctionality was the annual maximum NDVI, which represents the quantity of vegetation at the height of the growing season, and has been widely used in remote sensing as an indicator of productivity (Dronova et al., 2022; Weber et al., 2018; J. Yan et al., 2022). However, multifunctionality had similar or slightly stronger correlations with NDVI measures overall than did individual measures of productivity, and was significantly associated with more different aspects of plant phenology, suggesting that the overall relationship between multifunctionality and phenometrics was not only driven by aboveground productivity.

The second mechanism hypothesised to link multifunctionality and phenometrics was via links to aboveground plant diversity. Plant diversity has been shown to enhance multifunctionality across a wide range of ecosystems including the NutNet sites (Hautier et al., 2018), as well as affecting phenology by prolonging the growing season and promoting phenological stability, evidence for which has been found using both *in-situ* (Liang et al., 2022; Oehri et al., 2017; Tilman et al., 2006) and remote sensing datasets (Dronova et al., 2022; Dronova & Taddeo, 2022). Across these sites there were significant relationships between species richness and multifunctionality, but not between species richness and *in-situ* measured productivity (aboveground biomass or PAR) (Table 14). The link between plant species richness and productivity has been widely researched and is one of the key questions of the Nutrient Network overall. Generally, the Nutrient Network has found a complex relationship between diversity and productivity across the global network of grassland sites, with other environmental factors such as climate gradients and soil fertility levels tending to have greater influence on diversity than productivity alone; it is noted in the review by Borer *et al.* (2017) that bivariate productivity : diversity relationships are often not in evidence (Adler et al., 2011; Borer et al., 2017; Grace et al., 2016). However, there were also no relationships between plant species diversity and any of the phenometrics, including growing season length, or phenometric stability, which was surprising because these associations have been frequently demonstrated in grasslands at a variety of spatial scales, including large scales (Hector et al., 2010; Isbell et al., 2015, 2018). Reasons for the lack of relationship could be the use of species count as a measure of plant diversity, where species evenness, functional or phylogenetic diversity could be more relevant (Rossi et al., 2021; Tan et al., 2022; C. Xu et al., 2022). Alternatively, it could be that at these large spatial scales and among these contrasting sites climate and geological properties exert more influence over plant community phenology than do the effects of plant diversity. Overall it is concluded that though plant species richness does promote multifunctionality across these sites, there are other drivers which obscure the potential effect of species richness on satellite-derived phenology at such large geographic scales, and species richness therefore does not provide a direct link.

Multiple different aspects of annual phenology curves, representing different ecological stages of vegetation growth and senescence, were positively correlated with ecosystem multifunctionality at the global scale. Of the seven phenometrics investigated, annual maximum NDVI was the phenometric most strongly associated with multifunctionality during Pearson's and bivariate linear modelling. Annual maximum NDVI represents the quantity of vegetation at the height of the growing season, at peak biomass, and has been widely used as an indicator of productivity dynamics (Dronova et al., 2022; Paruelo et al., 2016; Weber et al., 2018; J. Yan et al., 2022). Annual maximum NDVI is a single-time measure

which was relatively stable year-on-year across the whole dataset, having the lowest inter-annual coefficient of variation of the phenometrics (Figure 22). The inter-annual variation in annual maximum NDVI was also the only measure of phenological stability which was able to explain significant variation in multifunctionality (Table 15). Given the low overall variation in $NDVI_{max}$, this suggests a large signal-to-noise ratio; i.e. variation in $NDVI_{max}$ is caused by significant variations in the plant community, and such significant variations are negatively correlated with multifunctionality. Variation in the other phenometrics year-on-year are larger do not contribute to distinguishing multifunctionality between sites, suggesting that these phenometrics are influenced by other factors which are less important for determining multifunctionality. This is further evidenced by the consistent relationships between $NDVI_{max}$ and multifunctionality among different lengths of satellite timeseries (Figure 23). These results suggest that annual maximum NDVI is less sensitive to variation in the plant community, but that for resolving differences in multifunctionality across contrasting and geographically disparate sites this insensitivity is beneficial, making the metric insensitive to noise and therefore a more stable indicator of ecosystem conditions.

Annual maximum NDVI is a commonly used metric of productivity in remote sensing, but more recent studies have also found time-integrated NDVI (the area under curve of annual NDVI, $NDVI_{auc}$) to be a more sensitive measure of cumulative productivity and associated ecosystem dynamics in grasslands. For example, time-integrated NDVI outperformed annual maximum NDVI for the retrieval of temporally dynamic aboveground processes in grasslands across China (J. Yan et al., 2022). Time-integrated and annual maximum NDVI were compared for their utility in retrieving various habitat quality measures in managed dry grasslands; in this case, maximum NDVI was found to be more consistently useful overall, but time-integrated NDVI was sensitive to different management scenarios (Weber et al., 2018). Similar results are found in this study, when comparing phenometric-multifunctionality relationships between sites with stable or variable NDVI overall. Time-integrated NDVI and growing season length were the most strongly associated phenometrics to NDVI among stable sites, though only the short-term averages of 3 years were especially strongly correlated, declining over time. These results suggest that the best choice of phenometric for retrieving multifunctionality, and the most suitable time period over which to average phenometrics, may depend on the overall variability of the site. For more variable sites, the relatively stable and insensitive maximum NDVI, averaged over decadal timescales, may be more appropriate, whereas for stable sites the more sensitive time-integrated NDVI and growing season length from recent seasons is more suitable.

5.4.2 Long-term versus short-term satellite timeseries for retrieving ecosystem multifunctionality

The effects of including historic NDVI dynamics over a varying timescale from 3 to 30 years were mixed. It was expected that different ecosystem functions would correlate to surface NDVI over different time periods, for example temporally dynamic aboveground functions such as proportion PAR and biomass are related to productivity at timescales of a single day and a single growing season respectively. However, belowground functions are variable over longer timescales, as they represent the cumulation of aboveground inputs over time combined with transformations and feedbacks of these inputs (Garland et al., 2021; Kaisermann et al., 2017). These hypotheses were supported by Pearson's correlations between NDVI phenometrics and individual ecosystem properties; more dynamic aboveground properties were more strongly associated with recent phenology, and belowground properties were more strongly associated with long-term (decadal) average phenology (Table 14).

When individual functions were considered simultaneously as multifunctionality, there were overall only small changes in the strength of correlations from 3-30 year timeseries, but for most phenometrics relationships were strongest for 12 to 18-year averages (Figure 23). When multifunctionality was retrieved from satellite phenometrics along with climate and location data, there was an increase of 11.21% variation explained using 18 years of phenometric data compared to only 3, but then little change between 18 and 30 years (Table 16). Phenological variability, calculated as the inter-annual variation in maximum NDVI, was only associated with multifunctionality when calculated across timeseries of 9 years or more. These results suggest that the length of timeseries used for the retrieval of phenology and phenological variability can have a significant impact on their relationship to ecosystem functions. This is important because the length of timeseries used across studies is generally not consistent (García-Gómez & Maestre, 2011; Paruelo et al., 2016; Weber et al., 2018; J. Yan et al., 2022; Y. Zhao et al., 2018). A previous comparative study of different lengths of satellite timeseries on the retrieval of soil carbon in a prairie grassland found that associations between a satellite vegetation index (EVI) and soil carbon were highly variable depending on the year of satellite data used (Wilson et al., 2017). This work also found that a multi-decadal average EVI was more powerful for the retrieval of soil carbon than a short (2-year) average and reported a stronger effect than in this study which may be due to the spatial extent of the study across a single field (landscape-scale). It could be that at the global scale presented here, the contrast between NDVI patterns from site to site overwhelms the influence of year-on-year variability at a single site, so when resolving differences between sites the impact of temporal variation is less than it would be on a landscape scale.

There are many other ways in which current and historical ecosystem processes may influence phenology-multifunctionality relationships on an individual site level, which are obscured using a global-scale dataset. For example, coupling between NDVI and soils may happen at different rates in different ecosystems, depending on whether they are exploitative or conservative in terms of nutrient cycling; as this dataset encompasses broad gradients of grassland systems there may not be a single temporal trend throughout the data. In arid sites, the activity of the aboveground plant community has been shown to be less influential on multifunctionality than that of the belowground microbial community (Delgado-Baquerizo et al., 2013; W. Hu et al., 2021; Y. Yan et al., 2020), which could explain why the arid sites in this dataset were outliers from the overall trend between multifunctionality and satellite-derived productivity (Figure 24). The long-term stability of an ecosystem influences the timescales over which historic productivity is most related to present-day functioning. For example, at sites with very stable phenology, which have not experienced a change in patterns of vegetation growth and senescence for 30 years, the inclusion of additional years' phenological metrics has little effect on the multi-year average of phenometrics, and therefore on their relationship to multifunctionality (Figure 23). Among sites which have experienced significant trends in productivity, the number of years' timeseries required to capture relevant historic conditions may depend on whether the change occurred as a rapid state change, in which case the timeseries should cover the year of the change to capture preceding conditions, or as a gradual trend in which case the relevant number of years may be less clear (Dronova & Taddeo, 2022). Weighting of historic years' phenology could also be appropriate; though the productivity of the plant community at a site 10 years ago may still have some influence on present-day soil conditions, it is likely to be less influential than current phenology.

While this global-scale analysis has suggested that the length of satellite timeseries used to retrieve phenology can have a significant effect on its relationships to other ecosystem properties, further research is needed at landscape scales to establish the relative influence of past and present ecological conditions on contemporary functioning of different ecosystems. Based on these results it is recommended that where possible, decadal timeseries of satellite data should be acquired for efforts to retrieve multifunctionality, or to retrieve individual belowground functions such as carbon storage and nutrient cycling which are also more strongly related to longer term averages of phenology. Analysis of historic phenology through NDVI timeseries could identify whether the site has experienced significant change, and when this occurred, in order to decide how many years phenological data to include in models. The Landsat archive is a valuable resource for this purpose, being freely available and extending back for decades across many locations worldwide (Wulder et al., 2022). Preliminary assessment of phenological stability using Landsat would complement analyses requiring

higher spatial and spectral resolution data that can be acquired from more recent, less temporally extensive satellite missions such as Sentinel.

Across this global set of contrasting grasslands, NDVI was chosen as the most appropriate vegetation index for detecting phenological patterns, but across smaller spatial extents, other indices may be valuable. For example, soil-adjusted vegetation indices may be more sensitive to biomass changes during particularly early or late phenological stages in sparse grassland sites (Ren & Feng, 2015). Other important phenological stages in grassland plants, such as flowering seasons, may have other impacts on the spectral reflectance of the land surface and therefore be captured by alternative spectral indices. Indices detecting flowering stages of phenology are in the early stages of development and often use high-resolution UAV and/or hyperspectral data, and focus on clearly identifiable crop flowering, such as yellow flowering of rape crops (Gallmann et al., 2022; Shao et al., 2023). The use of NDVI is a broad measure which is suitable for distinguishing patterns across large geographic extents, but other means of remotely detecting phenological patterns should be explored at smaller landscape scales.

5.5 Conclusions

The results presented here demonstrate that long-term satellite NDVI timeseries have potential to retrieve multifunctionality of varied grassland ecosystems at the global scale, by capturing plant community productivity, phenology and stability. Phenological metrics of plant community growth including maximum greenness, rate of green-up and annual average greenness are associated with multifunctionality and are important predictor variables in global models of multifunctionality also incorporating climate and location information. Among the range of phenometrics, annual maximum NDVI was the most closely associated with multifunctionality overall, though there was evidence that time-integrated NDVI was a more sensitive measure of productivity among sites with more stable plant communities. There were small differences in the relationships between multifunctionality and phenometrics retrieved over long-term (up to 30 years) and short-term (3-9 years) NDVI timeseries, but generally timeseries of 12 or more years gave stronger results. It is recommended that future efforts to retrieve ecosystem multifunctionality from satellite data make use of long-term archives such as Landsat to establish a history of vegetation conditions which may have continuing legacy effects on ecosystem functions. The global-scale dataset was effective for distinguishing between multifunctionality of highly contrasting grasslands, giving evidence that there are general, broad-scale associations between multifunctionality and satellite NDVI metrics in natural grasslands. However, across such large spatial extents and including grasslands with diverse site histories it was not possible to investigate the individual

mechanisms acting at each site to link surface reflectance over time with ecosystem functions; future work should explore these further using paired satellite and *in-situ* data at a range of spatial scales. Overall, the contribution of this study is to show that phenometrics derived from long-term satellite timeseries can reveal information about aboveground and belowground grassland functions at the global scale.

6. Discussion

This chapter aims to provide an overarching discussion of the three individual research chapters (Chapters 3, 4, 5). The thesis is structured around three main research objectives; 1) to predict soil microbial community properties from canopy imaging spectroscopy 2) to retrieve important plant functional traits from multispectral satellite data and 3) to use plant community phenology retrieved from multispectral satellite timeseries to predict ecosystem multifunctionality. All objectives are in the context of diverse grassland ecosystems at continental to global spatial scales. The research objectives were addressed through three distinct, yet interlinked, pieces of research presented in chapters 3 – 5. Chapter 3 demonstrated that soil microbial community properties, in particular microbial community structure (F:B ratio) could be predicted with success from canopy level imaging spectroscopy in grasslands and shrublands spanning large productivity and aridity gradients across North America (validation R^2 for six microbial properties between 0.09 and 0.68). Chapter 3 further identified that field-measured plant traits, in particular SLA, C:N ratio and carotene, were also able to represent soil communities at the surface, though predictions from spectra had greater accuracy than those made from traits measured *in-situ* highlighting the value of imaging spectroscopy in this context. These results were explored further in Chapter 4, addressing the second objective to show that some plant traits identified as being important for representing soil communities at the surface (SLA, C:N ratio) were able to be retrieved from multispectral satellite data (variation explained 67%, 44%, NRMSE 13%, 14%). The use of satellite data for retrieval of grassland functions was also addressed in Chapter 5 for objective 3, this time utilizing the multitemporal capabilities of satellite missions to retrieve long-term (up to 30 years) and contemporary phenology at 90 grassland sites distributed globally. Chapter 5 demonstrated that different aspects of satellite-derived phenology are able to contribute valuable explained variation to large-scale models of grassland functioning.

Within the individual research chapters is already presented the specific research gaps, methodologies, findings and discussion; the purpose of this chapter is to provide a wider discussion of the key themes that emerged across the three chapters and place their key findings in the context of the overarching thesis aims and objectives. Key themes which emerged across the research chapters included the relative value of hyperspectral, multispectral and multitemporal perspectives of landscape surfaces for retrieving information about grassland ecosystems; the impact of diverse grassland ecosystems and large environmental gradients on the ability of remote sensing datasets to retrieve ecosystem functions; and interacting effects of plant material quality (functional traits) and quantity (biomass and productivity) for linking soils, plants and reflectance. These themes are used to

organize this chapter. Finally, this discussion also acknowledges some of the limitations of the work, including the inherent limitations of empirical modelling approaches and challenges relating to the use of secondary datasets, and makes recommendations for future research.

6.1 To what extent are multispectral satellite data able to retrieve aboveground grassland functions?

Satellite missions have great potential for retrieving information about the biosphere at global spatial scales (Pettorelli et al., 2018a). New satellite missions have been launched for this purpose in recent years including the European Space Agency's Sentinel-2 missions, which have spectral specifications specifically to enhance vegetation monitoring (Revill et al., 2019), and the recent launch of Landsat 9, continuing the Landsat missions to provide consistent data spanning multiple decades (Wulder et al., 2022). Upcoming hyperspectral satellite missions such as EnMAP and HyspIRI are also anticipated to facilitate new perspectives on the world's ecosystems (Anderson, 2018; Pettorelli et al., 2018a). It is therefore an important time to establish the potential and the limitations of the application of satellite data to grassland ecology. Recent work has explored the use of satellite data to retrieve diversity in a range of ecosystems (Ma et al., 2019; Rocchini et al., 2021b), and to study productivity patterns in managed grasslands (I. Ali et al., 2016; Punalekar et al., 2018). The ease with which satellite systems can generate multi-temporal data has been shown to be valuable both for quantifying the temporal portion of biological variation (Fauvel et al., 2020; Rossi et al., 2021; Stumpf et al., 2020), though not always (Lopes et al., 2017), and for retrieving phenology (Dronova et al., 2022; Oehri et al., 2017; Weber et al., 2018). Some methods for estimating diversity from satellites incorporate plant functional traits; for example variation in SLA has been increasingly studied using satellites (A. M. Ali, Darvishzadeh, & Skidmore, 2017; Li et al., 2018) and used to estimate grassland diversity (Rossi et al., 2020). However, there has been a lack of research into the retrieval of a comprehensive set of grassland functional traits from satellite systems, despite promising results from forests (Aguirre-Gutiérrez et al., 2021), and satellite-derived aboveground properties have rarely been linked to soil functions, with some exceptions (García-Gómez & Maestre, 2011; Günal et al., 2021; Wilson et al., 2017). Chapters 4 and 5 in this thesis explored two different applications of multispectral satellite data to the retrieval of grassland functions. First, using Sentinel-2 data explicitly to retrieve a wide set of important plant functional traits in North American grasslands, and second by using multi-decadal Landsat timeseries to link phenology and ecosystem multifunctionality across global grasslands.

Plant functional foliar traits represent an important component of the ecosystem which drives many crucial ecosystem functions (Bardgett, 2017; Funk et al., 2017; Grigulis et al., 2013; Lavorel, 2013). Retrieval of foliar traits across large spatial extents is important for assessment and monitoring of functional diversity and associated ecosystem functions and services, and remote sensing technologies offer an opportunity for this at unprecedented scales (Jetz et al., 2016; Ma et al., 2019). In grasslands, however, functional trait modelling has been heavily biased toward hyperspectral data, with high spectral resolution but a restricted geographic coverage (Van Cleemput et al., 2018).

Chapter 4 tested, for the first time, whether a wide selection of 20 important grassland foliar traits were retrievable from Sentinel-2 satellite imagery. The results suggested that multispectral reflectance data acquired from satellite platforms is able to retrieve variation in key foliar functional traits across grasslands at the continental scale. All 20 foliar traits were retrieved with a RMSE below 25%, the threshold deemed an acceptable level of precision (Asner et al., 2015; Moreno-Martínez et al., 2018; Z. Wang et al., 2020). The best-modelled traits from Sentinel 2 were SLA and leaf nutrients phosphorus and potassium, all of which have strong associations with plant productivity and growth strategy (Reich, 2014), indicating that a satellite-based method for retrieving functional traits could be particularly useful for modelling ecosystem economics and trait relationships to belowground function (see Chapter 3). The most important spectral variables for retrieving plant traits tended to be vegetation indices incorporating multiple spectral regions, with indicators in the red edge and short-wave infrared regions particularly valuable, as has been found previously in forests (Ma et al., 2019). The value of the narrow red-edge spectral bands specific to Sentinel-2 particularly highlights the potential of this satellite for trait mapping (Rossi et al., 2020).

Comparison to previous studies show that functional traits can be retrieved from multispectral satellite data in grasslands with comparable accuracy to those achieved in tropical forest ecosystems (Aguirre-Gutiérrez et al., 2021), and across mixed ecosystems globally (Moreno-Martínez et al., 2018). This suggests that the small size of herbaceous plants relative to pixels and mixed nature of grassland systems at pixel scales, expected to pose a challenge in grasslands (Van Cleemput et al., 2018), do not cause the link to be lost between traits and spectra. This is in agreement with the results reported in a review of hyperspectral retrieval of grassland traits – that coarser spatial resolution of data can serve to smooth out noise rather than diminish the influence of traits on the reflectance signal (Van Cleemput et al., 2018). Though grassland foliar traits were generally predicted with lower accuracies from multispectral satellite data used here (Chapter 4) than those reported using hyperspectral data, significant overlap in the ranges of R^2 and RMSE values indicate that there were some traits retrieved with comparable accuracy. In particular, SLA, potassium and phosphorus were

retrieved well from Sentinel-2, with comparable accuracy to the most similar precedent study, also using data from NEON and modelling traits with hyperspectral data (Z. Wang et al., 2020). These comparisons suggest that while the enhanced spectral detail of hyperspectral sensors does improve accuracy of trait retrieval, the resolution of Sentinel-2 is sufficient to model broad-scale variation in a large number of important foliar traits. However, there are some caveats and practical considerations.

Retrieval of foliar pigments carotene and chlorophyll was relatively unsuccessful using Sentinel-2, despite the calculation of a specific chlorophyll-sensitive spectral index (Clevers & Gitelson, 2013). Pigments were sensitive to the temporal offset between satellite and field data collection, being retrieved with highly variable accuracy across the different time windows (Figure 14, Chapter 4). Carotene in particular was not well-retrieved from satellite data compared to previous work using hyperspectral data (Z. Wang et al., 2020), suggesting that despite field-measured carotene representing soil communities well (Figure 4, Chapter 3), there may be limited potential to use this trait as a link between spectra and soils using multispectral satellite data. This should however be a research priority for forthcoming hyperspectral satellite missions, combining high spectral detail with increased spatial coverage. Grassland-woodland mixing will continue to pose a practical challenge for trait retrieval across heterogenous natural grasslands, especially at the spatial scale of satellite pixels (usually at least 10m). Detailed mapping of the canopy size and location of woody individuals, as has begun to be incorporated into the sampling strategy of NEON (Weintraub, 2022), and other field design methods such as spatially matching field plots to pixel boundaries (Hauser et al., 2021) will be valuable for aggregating community-level trait values of mixed vegetation grasslands and grassland-woodland boundaries. The limitations inherent in aggregation methods such as community-weighted means, for example that they cannot account for intraspecific variation, can potentially be overcome by remote sensing approaches in the future (Funk et al., 2017). However, the limitations of field-based aggregation will continue to affect trait retrieval when finding empirical relationships between community-level functional traits and reflectance, therefore detailed spatial sampling methods are important at this stage of research.

An avenue of recent remote sensing research which is likely to be advanced by the ability to retrieve a large selection of different functional traits from satellite data is the retrieval of plant diversity from spectral data, an important current research topic in remote sensing in which plant functional traits play a key role (Rocchini et al., 2021a; Rossi et al., 2020, 2021, 2022; Schweiger et al., 2018). For example, multiple individually-modelled traits have been used to calculate functional richness and divergence in forests from remote sensing, using both hyperspectral (Schneider et al., 2017) and satellite (Helfenstein et al., 2022) data.

Satellite-derived spatial and temporal variation in a single trait, SLA, has also been used to infer functional diversity across grassland landscapes (Rossi et al., 2020). Therefore, though direct spectra-diversity modelling was beyond the scope of this thesis, the retrieval of grassland foliar functional traits from satellite data demonstrated in Chapter 4 is an important contribution towards this topic.

Apart from the estimation of foliar traits, the other important aspect of satellite data researched in this thesis was the use of multitemporal timeseries for retrieving grassland functions. In Chapter 5, it was shown that Landsat timeseries data spanning 30 years was an important contributor to prediction of ecosystem multifunctionality at the global scale (Figure 26, Chapter 5). First, by capturing different aspects of vegetation community phenology which were associated with different individual ecosystem functions. The best models of ecosystem multifunctionality used six different phenometrics as predictors, capturing peak biomass, average biomass, rate of green-up and senescence, growing season length and time-integrated productivity. This result builds on previous work at the landscape scale (Weber et al., 2018), by demonstrating that the relationships are not unique to a single site but can be found across a wide set of varied sites, and therefore may be applicable to other grasslands around the world. However, though the phenometrics with a temporal aspect, such as rate of green-up and time-integrated NDVI, were useful predictors, the single-time metric capturing peak biomass, annual maximum NDVI, was the most valuable at the global scale, a contrast to recent results at landscape scales (Weber et al., 2018; J. Yan et al., 2022). The importance of annual maximum NDVI suggests that the overall productivity of the grassland communities was a more important link between soils and reflectance than links driven by diversity, which were not evident in this data despite being found previously in grasslands and wetlands at national scales (Dronova et al., 2022; Oehri et al., 2017).

The long timeseries of satellite data also contributed to the retrieval of multifunctionality by accounting for historic productivity which continues to have a legacy effect on soils in particular (Garland et al., 2021; Millard & Singh, 2010). Using phenometrics averaged across an 18-year timeseries increased the prediction accuracy of multifunctionality by 11% relative to phenometrics averaged across three years (Table 16), which builds on previous research finding similar results when predicting soil carbon at the landscape scale (Wilson et al., 2017). Finally, the multi-year satellite timeseries were able to contribute by quantifying ecosystem stability remotely, both by finding the inter-annual variation in individual phenometrics and by identifying which sites experienced significant changes in productivity over the 30 years. Ecosystem stability has been incorporated into remote sensing studies of vegetation communities for example being linked to diversity, ecosystem services and land use change (Dronova et al., 2022; Paruelo et al., 2016). In Chapter 5, inter-annual

variability of phenometrics contributed little to predictions of multifunctionality, however the overall stability of the ecosystem over the previous 30 years changed which aspects of phenology were most closely linked to ecosystem functioning, with the more sensitive time-integrated metrics being more useful across relatively stable ecosystems. Therefore, a recommendation of this study was that future efforts to model slow-changing soil properties from spectral reflectance should take advantage of long-term satellite legacy datasets to assess historic ecosystem conditions and changes, as a preliminary analysis to inform which aspects of phenology may be most valuable and across what timescales.

Overall, the results from Chapters 4 and 5 demonstrate that satellite data has great potential to contribute to understanding of grassland systems. The spectral detail of Sentinel-2 is able to resolve spatial differences in important plant functional traits, and the ability to extract long timeseries from Landsat enhances retrieval of ecosystem multifunctionality at large scales.

6.2 Is spectral reflectance able to predict belowground communities and functions?

A key objective of this thesis was to use remote sensing to retrieve information about belowground as well as aboveground functions in grasslands. This was achieved by bringing together bodies of research from ecology, demonstrating that belowground communities and functions can be predicted from properties of the plant community evident at the surface, and from remote sensing demonstrating that plant community properties can be retrieved from spectral reflectance. The results presented in this thesis (Chapter 3, Chapter 5) show that spectral reflectance of grassland surfaces can reveal variation in both the structure of soil microbial communities and the ecosystem functions that take place belowground, and show that remote sensing methodologies can make a unique contribution to the study of aboveground-belowground linkages by retrieving aspects of the vegetation community which do not have equivalent field-based methods for assessing, and by expanding the spatial and temporal scope of investigations.

In Chapter 3, airborne hyperspectral data were used to retrieve soil community properties by directly linking canopy spectra to soil properties of interest using multivariate statistical techniques, with high accuracy for all four microbial properties tested (prediction R^2 0.43 – 0.68) (Chapter 3). The best-retrieved property was soil microbial community structure (F:B ratio: R^2 0.68, NRMSE 0.09) and to our knowledge this thesis presents the first attempt to retrieve this important soil microbial property from remote sensing. Soil F:B ratio

is frequently used in ecology to represent soil ecosystem economics and infer rates of carbon and nutrient turnover (de Vries, Bloem, et al., 2012; de Vries, Manning, et al., 2012; Malik et al., 2016). Therefore, the ability to predict soil F:B ratio rapidly and across large spatial extents from remote sensing data would be valuable for modelling and monitoring ecosystem service provision (Grigulis et al., 2013).

The evidence for strong links between spectroscopy and soil microbial communities in grasslands demonstrated in Chapter 4 adds to the small, but promising body of studies in forest ecosystems where researchers have reported R^2 up to 0.92 (Madritch et al., 2014; Sousa et al., 2021). Canopy spectra were shown to have greater explanatory power when modelling soil communities than what could be achieved using field-measured plant traits, both in this thesis (Table 3, Figure 6, Chapter 3) and in previous work (Madritch et al., 2014). The reason posed for the enhanced predictive power of spectra over field-measured traits is that using spectra directly to predict soil properties enables multiple axes of biological variation to be accounted for simultaneously, for example variation in species composition as well as functional traits, because all these axes of variation influence the interactions of the vegetation surface with light (Kothari & Schweiger, 2022; Lausch et al., 2016; Schweiger et al., 2018; Van Cleemput et al., 2018). In previous field-based research, it was found that plant taxonomy, phylogeny and traits all contribute to predictions of soil communities but that the use of traits was limited by only being able to account for traits of which researchers have prior knowledge and the capacity to measure in the field (Leff et al., 2018). Spectral approaches are not constrained to a pre-determined and limited set of traits but can potentially respond to other, unknown traits of the plant community. The combination of high-dimensionality hyperspectral data and multivariate statistical techniques such as PLSR (Sousa et al., 2021) and canonical correlation analysis (Madritch et al., 2014) facilitates the inclusion of these unknown traits.

To further explore the use of spectral bands directly to predict soils, the results presented in Chapter 3 can be compared to those of a similar recent study, also predicting soil communities from spectra in grassland but this time by retrieving a pre-determined selection of individual plant functional traits from spectra, and then using the modelled traits as predictors of soil communities (Cavender-Bares et al., 2022). The prediction accuracies achieved using this two-step method were generally lower than those presented in Chapter 3 using direct, multivariate statistical approaches and accounting for all hyperspectral bands (of the directly equivalent soil properties, (Cavender-Bares et al., 2022) reported R^2 of 0.12 – 0.40 for models of soil microbial biomass, compared to 0.56 in Chapter 3, and 0.05 – 0.15 for N mineralisation rate, compared to 0.23). The comparison supports the suggestion that using spectral reflectance bands directly accounts for important plant community variation that is

not captured by traits which can be measured in the field. From an operational perspective this is useful as it removes the need for extensive plant trait sampling in the field, or prior knowledge of the important functional traits in a particular ecosystem. However, a powerful advantage of the two-step approach used by (Cavender-Bares et al., 2022) is increased mechanistic understanding; identifying and quantifying specifically which functional traits provide how strong a link between soils and reflectance. For example, the authors identified that vegetation coverage was more important than functional traits for predicting soils in a relatively unproductive grassland. Similar inferences were made in Chapter 3 of this thesis, but could only be inferred through inspection of the wavelength correlations (Figure 7, Chapter 3) rather than statistically interrogated.

The ability of remote sensing data to contribute unique perspectives on aboveground-belowground linkages was further demonstrated in Chapter 5. This chapter demonstrated that satellite-derived phenometrics, including those which do not have a field-based equivalent such as time-integrated NDVI, were significantly correlated to belowground functions and contributed important explained variation to global models of grassland ecosystem functioning. This contributes to recent work suggesting that the temporal aspect of remote sensing systems, including archive length and return frequency, enable rapid retrieval of under-studied phenological aspects of vegetation communities which may be important for understanding ecological functions and resilience (Dronova & Taddeo, 2022).

Therefore, Chapters 3 and 5 of this thesis add evidence from grasslands across the world that hyperspectral and multispectral properties of vegetation canopies and land surfaces can be considered important ecological parameters in their own right, rather than just as proxies for properties that can be measured *in-situ* (Cavender-Bares et al., 2017; Kothari & Schweiger, 2022; Schweiger et al., 2018). Furthermore, the spectral properties of grassland surfaces can aid retrieval of information on soil communities and functions across diverse and contrasting grassland environments.

6.3 How do large geographic and environmental gradients affect the ability of remote sensing to retrieve ecosystem functions?

Further to retrieving unique properties of vegetation, one of the most important ways in which remote sensing can advance understanding of above- and belowground properties of grasslands is by expanding the spatial and temporal extents at which ecosystems can be studied. The value of multitemporal data stretching across long temporal extents for retrieving ecosystem functions, in particular soil functions, has already been discussed above. A key contribution of this thesis is to investigate spectra-plant-soil

relationships over large spatial extents and across different types of grasslands, where the majority of previous work has been focused at the landscape scale. The results of the research chapters in this thesis taken together suggest that there is a trade-off when resolving relationships between reflectance and ecosystem properties across large scales using a universal model. On one hand, the large scales give large gradients in ecological properties which may be easier to distinguish using remote sensing (Aguirre-Gutiérrez et al., 2021; Sousa et al., 2021; Wallis et al., 2019). On the other hand, relationships between environmental properties and reflectance may be different among sites with contrasting conditions, weakening models.

Chapters 3 and 5 presented evidence that the large gradients inherent in continental to global datasets were important for the ability of remote sensing to resolve differences in grassland functions between sites. Chapter 3 presented results from one of the first studies to investigate the use of canopy spectra for retrieving soil communities in grasslands. Previous similar modelling in forests acknowledged that the broad spatial distribution of observations and wide range of tree species included in the models was useful for resolving differences in canopies and soils from spectra (Sousa et al., 2021). The sites included in Chapter 3 spanned a geographic range of 4500km and spanned a large productivity gradient, from lush grassy prairies to more barren desert-like sites. The results of this investigation suggested that the large gradients were important in the ability of spectra to identify spatial differences in soil communities, because strongly contrasting surface reflectance at different sites was matched with strongly contrasting soil communities. For example the range of F:B ratio was 0.07 – 0.6 (Table 2), compared to 0.04 – 0.1 reported by previous authors across the UK (de Vries, Manning, et al., 2012). Across the wide range of sites, wavelengths representing both the quantity and the quality of vegetation were useful predictors in the PLSR models (Table 4, Chapter 3), which is consistent with and builds upon previous work which found that quantity was more important in a less productive site, and quality more important in a more productive site (Cavender-Bares et al., 2022).

Chapter 5 used multispectral, multitemporal data to retrieve above and belowground grassland functions and multifunctionality across 90 grasslands distributed at the global scale, across five continents. Models presented in Chapter 5 achieved similar or slightly stronger results (R^2 0.61) as those which have been found in similar previous studies using multitemporal indices of vegetation to predict ecosystem functions at landscape scales ((García-Gómez & Maestre, 2011), R^2 0.44 – 0.65; (Paruelo et al., 2016), R^2 0.48 – 0.66); (Weber et al., 2018), R^2 0.34 – 0.57). This result is another piece of evidence to suggest that large contrasts improve the capabilities of remote sensing to detect variation in ecosystems. However, there were some relationships found in Chapter 5 between above- and belowground

ecosystem functions and remote sensing data that were stronger among smaller subsets of more similar sites. When sites were subset according to their stability, correlations between functions and some phenometrics such as time-integrated NDVI were stronger than when stable and unstable sites were modelled together. This result suggests that though there are some relationships between multifunctionality and spectral reflectance patterns that are general across global grasslands, in particular the overall positive correlation between annual maximum NDVI and multifunctionality, retrieval of grassland functions may be more successful when empirical models are created using smaller sets of more similar sites. Another piece of evidence from Chapter 5 suggesting that contrasting grassland types may be better modelled separately was that the small number of arid sites did not have relationships between surface properties and functioning that were consistent with the overall set of observations (Figure 24, Chapter 5). Aridity is well-known to impact relationships between aboveground vegetation and ecosystem multifunctionality by altering the influence of soil and plant communities (W. Hu et al., 2021).

Results from Chapter 4 also indicated that the inclusion of mixed landscape types can decrease the strength of empirical models. Plant traits were estimated with most success when only the herbaceous fraction of vegetation was included in the models; when observations of both herbaceous and woody plants from across the sites were included together in empirical models, the overall prediction accuracy was lower for most traits (Figure 12, Chapter 4). The reason for the lower prediction accuracies is likely because different plant life forms, i.e. herbaceous and woody plants, have different typical functional trait syndromes and different relationships between traits and reflectance, due to many factors including plant structure and the ecological role of leaves, stems and roots (Funk & Cornwell, 2013; Poorter et al., 2014). Therefore when herbs and shrubs are modelled together, either in a mixed empirical model or at the sub-pixel scale in more heterogenous sites, relationships between traits and spectra are weakened. This effect has been identified previously in mixed models at the leaf level (Hacker et al., 2022).

However, when building empirical models of grassland functions and if applying them to new sites in order to comprehensively model the world's ecosystems, it is important to be able to account for the woody and shrubby fraction of grassland systems. If models were created only from the most homogenous herbaceous grassland surfaces then it is unlikely that they would be applicable to the more heterogenous landscapes found in nature, as demonstrated in Chapter 4. Mixed grassland and woodland landscapes, such as savannas, are extremely important conservation priorities, as this kind of vegetation matrix occurs at marginal grasslands and where climate and land use changes are taking place, resulting in grassland-woodland transition zones (Ratajczak et al., 2012; Ratnam et al., 2011; Sexton et al.,

2015). Though they are challenging to model due to the mixed nature of their vegetation assemblage, these types of landscape should not be excluded from remote sensing studies. The inclusion of mixed landscapes must take place during field campaign design, where there are competing priorities. For example the field protocol of NEON was updated recently to give higher sampling priority of rare woody plants at the site-level, following feedback from the ecological community (Weintraub, 2022). However from the remote sensing perspective, the relative abundance of species in terms of aerial extent is more important for linking vegetation surfaces to pixel-level reflectance, and the sampling of rare plants which may account for a small fraction of the canopy coverage is not a priority. A new approach to delineate the size and location of woody individual crowns in field sampling is an important development in the NEON sampling protocol which will facilitate easier matching of field and spectral data in future. However, challenges will remain; for example the functional influence of a plant belowground may not be proportional to its visibility in spectra (Soliveres et al., 2016).

Overall, results from the three research chapters in this thesis suggest that remote sensing data is able to model grassland ecosystem functions with success across large gradients and across different types of grassland. This is important and valuable given the global scale of climate pressures and land cover changes which are affecting grassland ecosystems (Obermeier et al., 2019). There are some relationships between above- and belowground functions and reflectance which are generalizable across disparate grasslands, such as the association between annual maximum NDVI and multifunctionality (Chapter 5), or soil F:B ratio and hyperspectral wavelengths relating to vegetation biomass, coverage and secondary metabolites (Figure 7, Table 4, Chapter 3). However, in some cases such as arid sites or those with mixed woodland and grassland the global model is less applicable; it is important to collect observations from a variety of sites representing large environmental gradients, in order to build models of ecosystem functioning which are applicable across the diversity of ecosystems found in nature.

6.4 How does vegetation link soils to reflectance?

The final theme that emerged across the three research chapters was the potential mechanisms linking soils to surface reflectance. The aboveground vegetation properties known to represent belowground conditions in the field are vegetation quantity, functional traits or quality, and diversity. These three aspects of the vegetation community are not independent; for example functional traits drive aboveground productivity and therefore vegetation quantity. Quantitative comparison of the mechanisms linking soils, plant and spectra was beyond the scope of this thesis, however the relative influence of the vegetation community properties were inferred in Chapter 3 by inspecting the spectral wavelengths

important for creating PLSR models of soil communities and comparing these to known absorption features, and in Chapter 5 by comparing the importance of different phenological metrics representing temporal dynamics of aboveground productivity for predicting ecosystem multifunctionality. Evidence from Chapters 3 and 5 suggest that both the quality and the quantity of vegetation aboveground provide links between surface reflectance and belowground soil communities and functions.

Plant traits covaried across both the global and continental sites according to growth strategy and as predicted by the leaf economics spectrum (Figure 3, Chapter 3; Chapter 4). Covariation of traits at the community level and among herbaceous vegetation is less well-evidenced than among tree leaves (Funk & Cornwell, 2013; Mason & Donovan, 2015; Pierce et al., 2007) and is valuable for the purpose of modelling ecosystem properties from spectra because it gives a strong whole-community signal which is closely related to aboveground productivity (Kothari & Schweiger, 2022). The parallel belowground variation in soil communities, as whole-ecosystem economics, also provides a mechanism for aboveground-belowground relationships which can be utilised to predict soil properties from above (Bardgett, 2017). The successful retrieval of soil F:B ratio, one of the most typical indicators of soil fast-slow functioning, is evidence that these ecosystem-economics links are a key mechanism linking aboveground and belowground properties across these grasslands, and therefore facilitating prediction of the belowground system from aboveground reflectance. Although satellite-retrieved traits were not directly linked to soils in Chapter 4, the most successfully retrieved aboveground plant traits were all those which were indicative of high quality, fast-growing vegetation (SLA, phosphorus, potassium). SLA, one of the best-modelled properties, is known to be a key indicator trait for the leaf economics spectrum (Shipley et al., 2006; I. J. Wright et al., 2004), and was also identified as an important plant trait predictor of belowground properties in Chapter 3. Evidence presented here that traits which can be successfully retrieved from satellite data are also those which are important for revealing patterns of soils (Chapters 3 & 4) suggests that there is potential to retrieve belowground microbial community properties such as F:B ratio from satellite multispectral data.

Results of this thesis suggested that across large spatial scales and wide environmental gradients the coverage and quantity of vegetation aboveground is key to revealing belowground properties. The gradient of productivity was a key axis of variation in all three research chapters, driving foliar trait composition, belowground microbial communities and ecosystem functioning at continental to global spatial scales. When predicting soil microbial community properties from hyperspectral reflectance, wavelengths relating to vegetation quantity on the red edge (700-750nm) and to soils in the SWIR (>1500nm) consistently emerged as important for the prediction of soil microbial communities. Previous authors have

also found that vegetation coverage has a large influence on spectra and is useful for predicting belowground properties in ecosystems with significant areas of bare soil visible in the vegetation canopy (Cavender-Bares et al., 2022; Hauser et al., 2021). The importance of vegetation quantity at large scales offers an opportunity for multispectral sensing in this context, which has a much better-established ability to retrieve aboveground vegetation quantity than aboveground vegetation quality or traits (Pettorelli et al., 2005, 2018a). This thesis (Chapter 5) demonstrated that although sensitive multitemporal spectral phenometrics were valuable predictors of ecosystem functioning in grasslands, across global scales the most important aspects of aboveground vegetation growth patterns were maximum annual NDVI, and mean annual NDVI; relatively simple metrics of productivity which are less complicated to retrieve and less sensitive than the other multitemporal measures tested. This finding was a contrast to other recent work at landscape scales, which found more sensitive, multi-temporal phenometrics to be more powerful indicators of grassland conditions (Weber et al., 2018; J. Yan et al., 2022). Results from Chapters 3 and 5 together suggest that at large continental and global scales, and across highly contrasting grassland sites, relatively simple remote sensing measures of aboveground productivity and coverage explain a large amount of variation in the belowground ecosystem.

6.5 Methodological considerations

The investigations presented in the research chapters of this thesis are all large-scale empirical studies, which are vital for evidencing relationships between interacting properties of ecosystems in nature, but have inherent limitations. Empirical models are limited by the representativeness of the samples on which they are based and can therefore be site-specific. They are known to perform poorly when transferred to different times or places, especially if attempting to extrapolate beyond the range of training data (Homolova et al., 2014; Kothari et al., 2023). In this thesis, the large geographic scale of observations in all three research chapters (Chapters 3-5) aimed to create generalisable models relevant and representative of the diversity of grassland ecosystems, as previous authors have done in forests (Aguirre-Gutiérrez et al., 2021; Sousa et al., 2021). However, observations still have geographical bias towards North America and Europe, as is the case for many large-scale networked datasets (Borer et al., 2014; Kattge et al., 2011). Sites were also not evenly distributed across all environmental gradients and therefore more unusual sites, or those situated at extreme ends of gradients, may be poorly captured; for example the NutNet dataset used in Chapter 5 contained a small number of arid sites (4) compared to non-arid sites (86), and as such the arid sites were outliers for some of the empirical relationships (Y. Zhao, Guirado, et al., 2022).

Empirical models of environmental parameters often incorporate a degree of spatial autocorrelation, which can cause over-optimistic interpretations of the explanatory power of remote sensing variables at large scales (Ploton et al., 2020). This is particularly likely where observations are spatially clustered, as in Chapters 3 and 4 in this thesis where observations originate from plots organised within NEON sites. There is debate in the literature as to the best way to address spatial autocorrelation (Meyer & Pebesma, 2022), but many options for example Geographic Random Forests (Aguirre-Gutiérrez et al., 2021; Georganos et al., 2019) require larger datasets than were available for this thesis. The approach used in this thesis was to incorporate climate and location variables, which are a large part of the source of spatial autocorrelation, into models following the approach of others (Delgado-Baquerizo et al., 2013). As more data becomes available from a larger number of sites in the NEON network, other more sophisticated approaches to accounting for spatial autocorrelation could be applied.

Temporal mismatch between field measurements and remote sensing data is a necessary feature and practical consideration of remote sensing approaches, but can affect empirical models (Homolova et al., 2014). Results of Chapter 4 demonstrate both the reduction in model strength that is associated with an increase in temporal offset from one to fourteen days, but also the limitation of available data (a loss of 42% of field observations) when limited to same-day satellite observations. Given that the return frequency of Sentinel satellites is five days, it may be possible to time field data collection with satellite overpasses in many ecosystems, which would be a valuable consideration for future, remote-sensing-compatible field campaigns.

The main alternative to empirical studies in remote sensing are radiative transfer models, where relationships between physical parameters and leaf and canopy-level reflectance are established and then used to simulate spectra which can be compared to those retrieved from remote sensing instruments (Jacquemoud et al., 2009). Physical-based models can overcome some of the inherent limitations of empirical studies, such as the necessary use of field-based trait aggregation methods such as community-weighted means (Grime, 1998). Radiative transfer models are effective at retrieving some plant traits including SLA at the leaf and canopy levels, and have been incorporated into landscape-scale models of biomass (Punalekar et al., 2018), structure (A. M. Ali et al., 2016) and functional diversity (Hauser et al., 2021; Rossi et al., 2020). However, the number of plant traits which can currently be retrieved from radiative transfer models is limited, so this approach may not be able to sufficiently capture all the axes of biological variation present in vegetation canopy spectra and relevant for belowground processes. Radiative transfer models have largely been developed for forest ecosystems, and though the use of forest-designed models for retrieving grassland

properties has been shown to be effective in some cases, it can also to result in large errors (Pau et al., 2022). Radiative transfer models require parameterisation which includes large amounts of ancillary environmental data which may not be included in the standard data collection of large-scale ecological networks. Therefore, empirical models are a good approach for expanding current knowledge and evidence to new traits and new ecosystems.

A combination of theoretical and empirical evidence is required to develop novel understanding of the world's environments. In ecology, lots of research takes place in controlled laboratory and experimental conditions at small scales, developing strong theoretical frameworks which then are supported to various degrees using empirical data from real-world ecosystems. For example, the ecological literature linking aboveground and belowground ecosystem, or linking multifunctionality to various axes of biological diversity, have well-established theoretical frameworks but until recently have been lacking in extensive empirical evidence to support them (Bardgett, 2017; Delgado-Baquerizo et al., 2018). There is a growing body of evidence from increasingly diverse ecosystems around the world to support (for example) leaf and whole-ecosystem economics relationships (Funk et al., 2017), but empirical evidence is often mixed and highlights the complexity of theoretical systems in the real world (Leff et al., 2018). Remote sensing is fundamentally interested in relationships which take place and can be measured across large spatial scales and in natural environments. It is therefore relatively common to retrieve empirical relationships between reflectance spectra and a range of environmental variables, but these can obscure mechanistic understanding, especially for example using high-dimensionality hyperspectral data and powerful but complex multivariate statistical approaches, as in Chapter 3 in this thesis. The solution to this is to incorporate remote sensing compatibility into the spatial design of ecological experiments, so that remote sensing methodologies are not precluded from future application to field data archives.

Some of these limitations stem from the use of secondary data sources which may not have been collected with remote sensing research objectives in mind. The lack of primary field data collection was a limitation of this thesis. Field work was limited by the COVID-19 pandemic in the summers of 2020 and 2021, and a pilot study (2019) using field spectroscopy at the leaf and the canopy level to detect species and trait composition and belowground communities along a gradient of management (fertilizer application) was not able to be completed or incorporated into the thesis. As a result, there were challenges spatially and temporally matching field data from secondary sources with spectral data, which influenced the research questions which could and could not be answered. For example, data from many Nutrient Network sites (Chapter 5) was collected before 2014, so continuing the exploration of Sentinel-2 satellite data which showed promising potential in Chapter 4 was not possible,

as Sentinel-2 launched in 2014. Recent remote sensing studies have incorporated extremely thorough field campaigns tailored to the matching of field and satellite data, for example by GPS-locating sampling plot boundaries in the field to match the boundaries of satellite pixels (Hauser et al., 2021). This approach enabled the researchers to quantify which components of the vegetation community contributed to satellite spectral diversity in more detail than the community-level inferences presented in this thesis (Chapters 3-5), but the spatial extent and number of observations in the study was necessarily limited. Arguably, when investigating relationships at the global scale there may be no option but to use secondary datasets, because of the unfeasible spatial scales and time-consuming nature of field campaigns which are often cited as a key reason for using remote sensing technology in the first place.

Going forward, large-scale, networked field campaigns will be extremely important for realizing the potential of remote sensing systems to monitor the biosphere at global scales, and designing field campaigns with a spatial arrangement suitable for remote sensing studies is an important consideration for future networked data collection (Pettorelli et al., 2014). The secondary data used in this thesis was sourced from two large-scale networks, one established recently with remote sensing explicitly included (NEON), and one designed without specific reference to remote sensing (NutNet). The spatial sampling design of NEON is tailored to remote sensing approaches, in particular to gather field data compatible with its airborne hyperspectral surveys, but also using a nested design for multiple spatial scales. For example, NEON sampling plots measure 20x20m and are distributed widely across the landscape, making them broadly compatible with the most widely available satellite missions Sentinel and Landsat. However, there are trade-offs to be made when accounting for different research priorities; for example sampling to capture incidence of rare plants or those which are important at a site level, versus sampling those which will have the most influence on spectral reflectance at a plot level. Sampling for rare species posed challenges when linking field-measured traits to Sentinel-2 pixels in Chapter 4, because it was challenging to aggregate functional trait measures to a representative community-level value at the plot level. Going forward, NEON have committed to spatially locating all sampled woody individuals and creating spatial polygon files delineating their size, which will be valuable for weighting individual plant traits when aggregating (this data was not available at the time of this thesis). The relative scarcity of coincident plant trait and soil community data across NEON sites will also be addressed through the planned continuing data collection campaigns.

Matching satellite data to field data across the Nutrient Network sites was challenging; despite being a prolific global network of ecological research there has been very little remote sensing work carried out across NutNet sites. The spatial arrangement of nutrient treatments, in contiguous plots measuring 5x5m, is prohibitive for remote sensing approaches with pixel

sizes more often 10m or more, as treated and untreated vegetation will combine into a single spectral signature. Therefore remote sensing at NutNet is limited to testing untreated control plots and assuming that these are representative of the broader landscape, matching control plot data with a satellite pixel adjacent to but not covering the treated plots. This approach was applied successfully in Chapter 5 in this thesis, but there was potential error introduced by the spatial mismatch of field and satellite observations. It would be valuable to spatially distribute sampling plots at scales suitable for retrieval using satellite remote sensing in the future. However, one of the benefits of the NutNet field sampling design is its simplicity and versatility, so proscribing spatial requirements in order to be able to match plots directly with satellite pixels may exclude potential new sites from being able to join the network; for example if the total area of available grassland is small and surrounded by other land cover types such as cropland or forest, as was the case for some sites. Therefore it is acknowledged that it may not always be straightforward to incorporate remote sensing compatibility into the spatial and temporal design of ecological field surveys. However, given the increasing availability of remote sensing datasets and the evidence for their potential to fill gaps in data and understanding between disparate field studies, consideration of remote sensing systems should be a priority for future large-scale environmental data collection efforts.

6.5.1 Statistical approach and limitations

Random forest was the key regression algorithm used across the chapters of this thesis. Random forest is a powerful machine learning algorithm which is popular for use in remote sensing modelling due to its ability to handle large numbers of predictor variables, such as spectral bands, robustness in comparison to simple decision-tree algorithms, ability to handle relatively sparse field samples, and the output of the variable importance scores which are valuable for comparing the influence of predictor variables (Breiman, 2001; Moreno-Martínez et al., 2018; Thomson et al., 2021; Zhao et al., 2022). Random forest often compares favourably to other algorithms in remote sensing studies (Aguirre-Gutiérrez et al., 2021; Fauvel et al., 2020). However, there are some limitations to random forest which are important to acknowledge.

First, although random forest is generally robust to overfitting, it is known to overfit to training data particularly when sample sizes are small, meaning that the relationships identified between predictor and response variables may not be applicable beyond the observations included in the training data set. Out-of-box samples from each individual decision tree are used to derive the variable importance scores (e.g. Aguirre-Gutiérrez et al., 2021; Delgado-Baquerizo et al., 2018) and can be used to give an overall score of model accuracy, but models can be interpreted with greater confidence where an independent

validation dataset has been used. In the research chapters presented in this thesis, it was not feasible to reserve a portion of observations for independent validation, because of the relatively small number of observations available in each of the secondary datasets sourced. The datasets cover wide environmental gradients and therefore are assumed to be representative of the varied grassland habitats which are found across continental and global scales. The models and relationships presented here demonstrate the potential for remote sensing and spectral datasets to be used to predict variation in above and belowground grassland ecosystem properties; however, before being used for prediction these early models need to be developed further using more comprehensive datasets and independent validation.

Second, Random Forest is known to be sensitive to the quality and characteristics of input data. Although the variable importance measure in theory filters out irrelevant predictor variables, predictor variables should be chosen as inputs based on theoretical mechanisms linking them to the response variable of interest. Importance as a predictor variable, in this case indicted by a high mean increase in mean square error (MSE) when the variable is permuted in individual trees, does not necessarily indicate a causal relationship to the response variable. Similarly, if two predictor variables are collinear or closely related, one may be retained by the random forest algorithm over the other, at random in the various decision trees. Noisy, irrelevant or missing predictor variables can impact the performance of random forest models. In the chapters presented in this thesis, predictor variables for models were selected based on a combination of their theoretical linkages to grassland ecosystem properties, successful use in previous studies, and availability in the secondary datasets sourced for this project. Some variables which may have been valuable, such as soil physical characteristics like pH, were not available for all sites and as such their inclusion would have incurred a reduction in the already small number of samples.

Random forest is known to be sensitive to tuning parameters and the input predictor variables. The Boruta algorithm (Kursa & Rudnicki, 2010) along with functions from the *RFUtilities* package (Evans & Murphy, 2017) were used for model tuning. These were chosen because they are commonly used to tune random forest models in similar remote sensing studies in the literature, and Boruta has performed favourably in comparison to other feature selection algorithms (Degenhardt et al., 2019). Boruta is known to be sensitive to tuning parameters, including number of trees and tree depth. These parameters were selected using the *tuneRF* function from *RFUtilities*, which runs the model multiple times and selects the parameters which give the lowest RMSE. In addition, manual testing using different combinations of predictor variables was carried out, for example running the models using only variables with importance scores over a certain threshold, or using subsets of the most important variables from initial modelling. This was carried out both to explore the data and

to increase confidence in the final selection of predictor variables. The models presented in each chapter are the highest-performing among these tests.

In all cases, Random Forest models were run 100 times and the average of these model runs taken. The standard deviation of this average is reported and was in all cases very low, increasing confidence in the models. In addition, the models presented are the final choice of a range of multivariate statistical approaches which were tested. PLSR was used to model relationships in Chapter 5, with similar results. Linear modelling was also tested for relationships in Chapter 6, but was not chosen finally because of the greater importance of researcher input and understanding of the specific ecosystem in question when choosing in which order to fit predictor variables, which is challenging when looking for generalisable relationships across a dataset that spans a variety of ecosystems in which operate different environmental mechanisms. Variation partitioning based on redundancy analysis is used in Chapter 5 as a complimentary statistical test to random forest, as has been used by others (Delgado-Baquerizo et al., 2018). Where multiple statistical tests give the same or similar outcomes, i.e. where the interpretation does not change, this affords extra confidence in the results. In cases where the outcomes of multiple tests do not align, for example in Chapter 5 the relation between spectral predictors and leaf pigments, this indicates that the variables or observations need to be further explored before conclusions can be confidently drawn. Creating models of ecosystem parameters at the global scale almost always relies upon clustered observations in which some regions are sparsely represented, and therefore such models should be presented and interpreted with caution even when thorough statistical approaches have been applied with the aim of minimising spatial bias (Meyer & Pebesma, 2022). In the chapters presented in this thesis, such validation approaches were not used due to the small number of observations. Therefore, it is important to reiterate that the models presented here are intended to demonstrate the potential of spectral data for the novel application of retrieving information about the belowground functions of grasslands. More thorough training data at multiple spatial scales is required to realise this potential in the future.

Finally, the models presented in this thesis are limited by uncertainty and variability in the input datasets, which is carried through to the final model results. For example, the use of WorldClim 30-year climate averages rather than contemporary weather and climate records from each field site may have resulted in weakened apparent relationships between ecological response variables and climate drivers. This effect may have been particularly strong for predicting plant traits (Chapter 5) which are likely to adapt to climate and weather changes on timescales shorter than 30 years. Recent antecedent conditions, for example an unusually dry preceding summer, are likely to impact many of the ecosystem properties under investigation

in this thesis and may therefore have weakened links between predictor and response variables. For soil properties which are dynamic across longer decadal timescales, the use of 30-year climate averages rather than current weather conditions may be more appropriate (Garland et al., 2021; Millard & Singh, 2010).

Similarly, many of the models presented are based on variable means, at the plot (Chapter 4, Chapter 5) and site (Chapter 6) level. For example, soil measures used are the average of three soil cores taken across a 40x40m plot at NEON sites. This averaging approach was taken in this case to be able to match soil, plant and spectral data. Models can only be built at the spatial resolution of the most coarse dataset. This was most apparent in Chapter 6, where the uncertainty in spatial location of the field plots lead to spectral data being collected at the site level, at which all subsequent analyses were then required to take place. This approach has inherent limitations. Soil microbial communities and properties are highly heterogenous across short distances, for instance due to species-specific mycorrhizal associations (Leff et al., 2018; Sousa et al., 2021). Therefore an approach which uses plot-level or site-level means loses information on small scale; local variability which may be an important source of uncertainty when extrapolated to the regional or global scale. In order to best take advantage of new remote sensing datasets, matching between remote and *in-situ* data must take place at a range of spatial scales (Rossi et al., 2020), and compatibility with remote sensing datasets should become a key consideration when designing field campaigns for the future (Hauser et al., 2021; Thorpe et al., 2016).

7. Conclusions

This thesis set out to investigate how remote sensing can be used to characterise aboveground and belowground functions of grasslands across large spatial scales. The thesis aim was addressed through three distinct but linked research chapters, which used empirical models to predict variation in plant and soil communities and functions from remote sensing data in grasslands distributed across the globe.

The first key contribution of this thesis is to demonstrate that variation in soil microbial communities can be predicted with high levels of accuracy from imaging spectroscopy of grassland canopies (Chapter 3). This result contributes important new evidence to the small but growing body of research using spectroscopy to directly retrieve variation in soil communities, by showing that links previously detected in forests and within individual grassland sites are also evident across grassland systems spanning large ecoclimatic gradients. This thesis also presents the first retrieval of broad-scale soil microbial community structure (F:B ratio) from remote sensing (R^2 0.68, NRMSE 9%), which is important because F:B ratio is a key indicator of soil microbial community structure and associated carbon storage and nutrient cycling functions, which are vital for grassland ecosystem services globally. The implications of these findings are that hyperspectral data have the potential to estimate continental-scale differences in soil bacterial and fungal populations, expanding the practical benefits of remote sensing technologies to the relatively understudied belowground portion of the biosphere.

The second key contribution of this thesis is the finding that multispectral satellite data can accurately retrieve community-level plant functional traits in grasslands, including structural and biochemical traits which have implications for aboveground and belowground ecosystem functioning. Previously, functional trait retrieval in grasslands has focused on the use of hyperspectral systems, which are significantly more limited in coverage and accessibility than multispectral satellites. Chapter 5 showed that some traits, including SLA and leaf nutrients phosphorus and potassium, were able to be retrieved from Sentinel-2 with comparable accuracy to hyperspectral data. This finding presents the possibility to monitor changes in functional traits of grassland vegetation at unprecedented spatial extents and temporal detail; for example trait estimations can be updated at the rate of the satellite return period which for Sentinel-2 is five days. If the empirical models developed in this thesis were to hold true across grasslands more widely, satellite trait estimations could be incorporated into large-scale models of biogeochemical cycles which are driven by the functional traits of

vegetation and can be used to monitor and predict the effects of large-scale climate and land use changes. Beyond the retrieval of plant functional traits, the thesis also showed that satellite data are able to estimate a measure of ecosystem functionality which combines above- and belowground grassland functions (Chapter 6). Historic vegetation productivity and variability over decadal timescales were important contributions to predictions of multifunctionality, demonstrating the unique contributions that satellite systems can make.

A third important contribution of this thesis was to demonstrate that links between soils, plant traits and spectra in grasslands are not only found at landscape scales or within individual grassland landscapes, but can be found across a broad spectrum of different grasslands found worldwide. Grasslands are a diverse biome, spanning large gradients of productivity, vegetation coverage, nutrient status and vegetation composition including the fraction of herbaceous and woody vegetation at marginal grasslands, those undergoing change and those at grassland-woodland boundaries. The research chapters of this thesis presented relationships that are general across grasslands, which is important for being able to apply the findings to other sites and systems in the future. Large-scale ecology is vital at a time when pressures affecting ecosystems take place across global scales.

Several opportunities and priorities for further research arose from this thesis. The ability to retrieve plant community functional traits from multispectral satellite data in grasslands has the potential to contribute to estimations of functional diversity across large spatial scales, by enabling spatial and temporal variation in multiple functional traits to be included. Multitemporal retrieval of plant functional traits, across and between seasons, facilitated by the regular revisit of multispectral satellites could also represent a valuable avenue of research. Seasonal patterns of NDVI have been shown to be valuable predictors of ecosystem properties including diversity, carbon storage and multifunctionality (e.g. Chapter 5), suggesting that seasonal patterns of other important functional traits could also have important implications for above and belowground functions. In order to realise this potential there is a need for *in-situ* data collection across seasons, to match with multitemporal remote sensing data and find empirical relationships. In general, the findings of this thesis should be confirmed in future using more spatially intensive (as opposed to extensive) field datasets to build empirical models *within* as well as *across* sites and regions, bridging the gap between the continental-scale relationships presented here and previous work at the landscape scale. The data forecast to be provided from NEON over its 30-year lifespan will be valuable for building upon the work presented in this thesis. Future field campaigns, particularly large-scale networks, should be designed with a view to accommodating the application of remote sensing imagery. Spatially arranging sampling plots to be discriminated in satellite imagery,

i.e. at the scale of tens of metres, is vital and timing field data collection to coincide with satellite overpasses, where possible, would be an advantage.

Overall, this thesis showed that remote sensing can contribute to our understanding of aboveground and belowground grassland functioning by capturing aspects of the ecosystem beyond what can be measured in the field, such as multitemporal vegetation attributes and integrated axes of biological variation. Remote sensing can also contribute by increasing the frequency with which information can be gathered, enabling the incorporation of temporal dynamics and long-term (decadal) variability into models of contemporary functioning, which is particularly important for belowground functions which vary across long timescales. Finally, remote sensing can contribute by expanding the spatial extent across which ecosystems can be studied, finding relationships which are common to grasslands across the world, which is important for monitoring global-scale pressures. To build on these results, future work should seek to confirm the relationships presented here within as well as between grassland types, for example in dry grassland or woodland-grassland boundaries, at a range of spatial scales, and across seasons. Coincident soil and plant data from collaborative ecological monitoring networks will be instrumental for such research, along with continuing multispectral and forthcoming hyperspectral satellite missions. This future work is needed to realise the potential, demonstrated in this thesis, for remote sensing technologies to enable us to understand, monitor and predict changes in the vital ecosystem functions which take place in grasslands worldwide, and to ensure the continuing ability of human societies to depend on grassland ecosystems through the changes to come in the 21st century.

References

Adler, P. B., Seabloom, E. W., Borer, E. T., Hillebrand, H., Hautier, Y., Hector, A., Stanley Harpole, W., O'Halloran, L. R., Grace, J. B., Michael Anderson, T., Bakker, J. D., Biederman, L. A., Brown, C. S., Buckley, Y. M., Calabrese, L. B., Chu, C. J., Cleland, E. E., Collins, S. L., Cottingham, K. L., … Yang, L. H. (2011). Productivity is a poor predictor of plant species richness. *Science*, *333*(6050), 1750–1753. https://doi.org/10.1126/SCIENCE.1204498/SUPPL_FILE/1204498TABLES3.ZIP

Aguirre-Gutiérrez, J., Rifai, S., Shenkin, A., Oliveras, I., Bentley, L. P., Svátek, M., Girardin, C. A. J., Both, S., Riutta, T., Berenguer, E., Kissling, W. D., Bauman, D., Raab, N., Moore, S., Farfan-Rios, W., Figueiredo, A. E. S., Reis, S. M., Ndong, J. E., Ondo, F. E., … Malhi, Y. (2021). Pantropical modelling of canopy functional traits using Sentinel-2 remote sensing data. *Remote Sensing of Environment*, *252*(September 2020), 112122. https://doi.org/10.1016/j.rse.2020.112122

Albert, C. H., Thuiller, W., Yoccoz, N. G., Soudant, A., Boucher, F., Saccone, P., & Lavorel, S. (2010). Intraspecific functional variability: Extent, structure and sources of variation. *Journal of Ecology*, *98*(3), 604–613. https://doi.org/10.1111/j.1365-2745.2010.01651.x

Albrecht, J., Peters, M. K., Becker, J. N., Behler, C., Classen, A., Ensslin, A., Ferger, S. W., Gebert, F., Gerschlauer, F., Helbig-Bonitz, M., Kindeketa, W. J., Kühnel, A., Mayr, A. V, Njovu, H. K., Pabst, H., Pommer, U., Röder, J., Rutten, G., Schellenberger Costa, D., … Schleuning, M. (2021). Species richness is more important for ecosystem functioning than species turnover along an elevational gradient. *Nature Ecology and Evolution*, *5*(12), 1582–1593. https://doi.org/10.1038/s41559-021-01550-9

Ali, A. M., Darvishzadeh, R., & Skidmore, A. K. (2017). Retrieval of Specific Leaf Area from Landsat-8 Surface Reflectance Data Using Statistical and Physical Models. *IEEE Journal of Selected Topics in Applied Earth Observations and Remote Sensing*, *10*(8), 3529–3536. https://doi.org/10.1109/JSTARS.2017.2690623

Ali, A. M., Darvishzadeh, R., Skidmore, A. K., & Duren, I. Van. (2016). Effects of Canopy Structural Variables on Retrieval of Leaf Dry Matter Content and Specific Leaf Area from Remotely Sensed Data. *IEEE Journal of Selected Topics in Applied Earth Observations and Remote Sensing*, *9*(2), 898–909. https://doi.org/10.1109/JSTARS.2015.2450762

Ali, A. M., Darvishzadeh, R., Skidmore, A. K., & van Duren, I. (2017). Specific leaf area estimation from leaf and canopy reflectance through optimization and validation of vegetation indices. *Agricultural and Forest Meteorology*, *236*, 162–174. https://doi.org/10.1016/j.agrformet.2017.01.015

Ali, I., Cawkwell, F., Dwyer, E., Barrett, B., & Green, S. (2016). Satellite remote sensing of grasslands: From observation to management. *Journal of Plant Ecology*, *9*(6), 649–671. https://doi.org/10.1093/jpe/rtw005

Allan, E., Manning, P., Alt, F., Binkenstein, J., Blaser, S., Blüthgen, N., Böhm, S., Grassein, F., Hölzel, N., Klaus, V. H., Kleinebecker, T., Morris, E. K., Oelmann, Y., Prati, D., Renner, S. C., Rillig, M. C., Schaefer, M., Schloter, M., Schmitt, B., … Fischer, M. (2015). Land use intensification alters ecosystem multifunctionality via loss of biodiversity and changes to functional composition. *Ecology Letters*, *18*(8), 834–843. https://doi.org/10.1111/ele.12469

Anderson, C. B. (2018). Biodiversity monitoring, earth observations and the ecology of scale. *Ecology Letters*, *21*(10), 1572–1585. https://doi.org/10.1111/ele.13106

Aneece, I., & Epstein, H. (2015). Distinguishing early successional plant communities using ground-level hyperspectral data. *Remote Sensing*, *7*(12), 16588–16606. https://doi.org/10.3390/rs71215850

Aneece, I. P., Epstein, H., & Lerdau, M. (2017). Correlating species and spectral diversities using hyperspectral remote sensing in early-successional fields. *Ecology and Evolution*, *7*(10), 3475–3488. https://doi.org/10.1002/ece3.2876

Araya, S., Lyle, G., Lewis, M., & Ostendorf, B. (2016). Phenologic metrics derived from MODIS NDVI as indicators for Plant Available Water-holding Capacity. *Ecological Indicators*, *60*, 1263–1272. https://doi.org/10.1016/j.ecolind.2015.09.012

Asner, G. P. (2013). Biological diversity mapping comes of age. *Remote Sensing*, *5*(1), 374–376. https://doi.org/10.3390/rs5010374

Asner, G. P., & Martin, R. E. (2016). Spectranomics: Emerging science and conservation opportunities at the interface of biodiversity and remote sensing. *Global Ecology and Conservation*, *8*, 212–219. https://doi.org/10.1016/j.gecco.2016.09.010

Asner, G. P., Martin, R. E., Anderson, C. B., & Knapp, D. E. (2015). Quantifying forest canopy traits: Imaging spectroscopy versus field survey. *Remote Sensing of Environment*, *158*, 15–27. https://doi.org/10.1016/j.rse.2014.11.011

Baccari, S., Elloumi, O., Chaari-Rkhis, A., Fenollosa, E., Morales, M., Drira, N., Ben Abdallah, F., Fki, L., & Munné-Bosch, S. (2020). Linking Leaf Water Potential, Photosynthesis and Chlorophyll Loss With Mechanisms of Photo- and Antioxidant Protection in Juvenile Olive Trees Subjected to Severe Drought. *Frontiers in Plant Science*, *11*. https://doi.org/10.3389/fpls.2020.614144

Bardgett, R. D. (2017). Plant trait-based approaches for interrogating belowground function. *Biology and Environment*, *117B*(1), 1–13. https://doi.org/10.3318/bioe.2017.03

Bardgett, R. D. (2018). *Linking Aboveground–Belowground Ecology: A Short Historical Perspective*. 1–17. https://doi.org/10.1007/978-3-319-91614-9_1

Bardgett, R. D., Bowman, W. D., Kaufmann, R., & Schmidt, S. K. (2005). A temporal approach to linking aboveground and belowground ecology. *Trends in Ecology and Evolution*, *20*(11), 634–641. https://doi.org/10.1016/j.tree.2005.08.005

Bardgett, R. D., Hobbs, P. J., & Frostegård, Å. (1996). Changes in soil fungal:bacterial biomass ratios following reductions in the intensity of management of an upland grassland. *Biology and Fertility of Soils*, *22*(3), 261–264. https://doi.org/10.1007/BF00382522

Bardgett, R. D., & Van Der Putten, W. H. (2014). Belowground biodiversity and ecosystem functioning. *Nature*, *515*(7528), 505–511. https://doi.org/10.1038/nature13855

Barnett, D. T., Duffy, P. A., Schimel, D. S., Krauss, R. E., Irvine, K. M., Davis, F. W., Gross, J. E., Azuaje, E. I., Thorpe, A. S., Gudex-Cross, D., Patterson, M., McKay, J. M., McCorkel, J. T., & Meier, C. L. (2019a). The terrestrial organism and biogeochemistry spatial sampling design for the National Ecological Observatory Network. *Ecosphere*, *10*(2). https://doi.org/10.1002/ECS2.2540

Barnett, D. T., Duffy, P. A., Schimel, D. S., Krauss, R. E., Irvine, K. M., Davis, F. W., Gross, J. E., Azuaje, E. I., Thorpe, A. S., Gudex-Cross, D., Patterson, M., McKay, J. M., McCorkel,

J. T., & Meier, C. L. (2019b). The terrestrial organism and biogeochemistry spatial sampling design for the National Ecological Observatory Network. *Ecosphere*, *10*(2). https://doi.org/10.1002/ECS2.2540

Bartholomeus, H., Kooistra, L., Stevens, A., van Leeuwen, M., van Wesemael, B., Ben-Dor, E., & Tychon, B. (2011). Soil Organic Carbon mapping of partially vegetated agricultural fields with imaging spectroscopy. *International Journal of Applied Earth Observation and Geoinformation*, *13*(1), 81–88. https://doi.org/10.1016/j.jag.2010.06.009

Baxendale, C., Orwin, K. H., Poly, F., Pommier, T., & Bardgett, R. D. (2014). Are plant-soil feedback responses explained by plant traits? *Journal of Physiology*, *204*(2), 408–423. https://doi.org/10.1111/nph.12915

Bengtsson, G., Bengtson, P., & Månsson, K. F. (2003). Gross nitrogen mineralization-, immobilization-, and nitrification rates as a function of soil C/N ratio and microbial activity. *Soil Biology and Biochemistry*, *35*(1), 143–154. https://doi.org/10.1016/S0038-0717(02)00248-1

Berdugo, M., Kéfi, S., Soliveres, S., & Maestre, F. T. (2017). Plant spatial patterns identify alternative ecosystem multifunctionality states in global drylands. *Nature Ecology & Evolution 2017 1:2*, *1*(2), 1–10. https://doi.org/10.1038/s41559-016-0003

Bernays, E. A., Driver, G. C., & Bilgener, M. (1989). Herbivores and Plant Tannins. *Advances in Ecological Research*, *19*(C), 263–302. https://doi.org/10.1016/S0065-2504(08)60160-9

Borcard, D., Legendre, P., & Drapeau, P. (1992). Partialling out the spatial component of ecological variation. *Ecology*, *73*(3), 1045–1055. https://doi.org/10.2307/1940179

Borer, E. T., Grace, J. B., Harpole, W. S., MacDougall, A. S., & Seabloom, E. W. (2017). A decade of insights into grassland ecosystem responses to global environmental change. *Nature Ecology and Evolution*, *1*(5), 1–7. https://doi.org/10.1038/s41559-017-0118

Borer, E. T., Harpole, W. S., Adler, P. B., Lind, E. M., Orrock, J. L., Seabloom, E. W., & Smith, M. D. (2014). Finding generality in ecology: A model for globally distributed experiments. *Methods in Ecology and Evolution*, *5*(1), 65–73. https://doi.org/10.1111/2041-210X.12125

Bradford, M. A., Jones, T. H., Bardgett, R. D., Black, H. I. J., Boag, B., Bonkowski, M., Cook, R., Eggers, T., Gange, A. C., Grayston, S. J., Kandeler, E., McCaig, A. E., Newington, J. E., Prosser, J. I., Setälä, H., Staddon, P. L., Tordoff, G. M., Tscherko, D., & Lawton, J. H. (2002). Impacts of soil faunal community composition on model grassland ecosystems. *Science*, *298*(5593), 615–618. https://doi.org/10.1126/science.1075805

Breiman, L. (2001). *Random Forests*. *45*, 5–32.

Broadley, M. R., White, P. J., Hammond, J. P., Zelko, I., & Lux, A. (2007). Zinc in plants: Tansley review. In *New Phytologist* (Vol. 173, Issue 4, pp. 677–702). https://doi.org/10.1111/j.1469-8137.2007.01996.x

Brooks, T. M., Mittermeier, R. A., Da Fonseca, G. A. B., Gerlach, J., Hoffmann, M., Lamoreux, J. F., Mittermeier, C. G., Pilgrim, J. D., & Rodrigues, A. S. L. (2006). Global biodiversity conservation priorities. In *Science* (Vol. 313, Issue 5783, pp. 58–61). https://doi.org/10.1126/science.1127609

Butler, E. E., Datta, A., Flores-Moreno, H., Chen, M., Wythers, K. R., Fazayeli, F., Banerjee, A., Atkin, O. K., Kattge, J., Amiaud, B., Blonder, B., Boenisch, G., Bond-Lamberty, B.,

Brown, K. A., Byun, C., Campetella, G., Cerabolini, B. E. L., Cornelissen, J. H. C., Craine, J. M., … Schlesinger, W. H. (2017). Mapping local and global variability in plant trait distributions. *Proceedings of the National Academy of Sciences of the United States of America*, *114*(51), E10937–E10946. https://doi.org/10.1073/pnas.1708984114

Butterbach-Bahl, K., Baggs, E. M., Dannenmann, M., Kiese, R., & Zechmeister-Boltenstern, S. (2013). Nitrous oxide emissions from soils: How well do we understand the processes and their controls? *Philosophical Transactions of the Royal Society B: Biological Sciences*, *368*(1621). https://doi.org/10.1098/RSTB.2013.0122

Byrnes, J. E. K., Gamfeldt, L., Isbell, F., Lefcheck, J. S., Griffin, J. N., Hector, A., Cardinale, B. J., Hooper, D. U., Dee, L. E., & Emmett Duffy, J. (2014). Investigating the relationship between biodiversity and ecosystem multifunctionality: Challenges and solutions. *Methods in Ecology and Evolution*, *5*(2), 111–124. https://doi.org/10.1111/2041-210X.12143

Cai, J., Weiner, J., Wang, R., Luo, W., Zhang, Y., Liu, H., Xu, Z., Li, H., Zhang, Y., & Jiang, Y. (2017). Effects of nitrogen and water addition on trace element stoichiometry in five grassland species. *Journal of Plant Research*, *130*(4), 659–668. https://doi.org/10.1007/s10265-017-0928-2

Cantarel, A. A. M., Pommier, T., Desclos-theveniau, M., Dumont, M., Grassein, F., Kastl, E., Grigulis, K., Laîné, P., Cantarel, A. A. M., Pommier, T., Desclos-theveniau, M., Diquélou, S., Dumont, M., Grassein, F., Kastl, E., Grigulis, K., Laîné, P., Lavorel, S., Lemauviel-lavenant, S., … Schloter, M. (2019). *Using plant traits to explain plant — microbe relationships involved in nitrogen acquisition Franck Poly Published by : Wiley on behalf of the Ecological Society of America Stable URL : https://www.jstor.org/stable/43494694 Using plant traits to explain p*.

Cardinale, B. J., Wright, J. P., Cadotte, M. W., Carroll, I. T., Hector, A., Srivastava, D. S., Loreau, M., & Weis, J. J. (2007). Impacts of plant diversity on biomass production increase through time because of species complementarity. *Proceedings of the National Academy of Sciences of the United States of America*, *104*(46), 18123–18128. https://doi.org/10.1073/PNAS.0709069104

Cavender-Bares, J., Gamon, J. A., Hobbie, S. E., Madritch, M. D., Meireles, J. E., Schweiger, A. K., & Townsend, P. A. (2017). Harnessing plant spectra to integrate the biodiversity sciences across biological and spatial scales. *American Journal of Botany*, *104*(7), 966–969. https://doi.org/10.3732/ajb.1700061

Cavender-Bares, J., Gamon, J. A., & Townsend, P. A. (2020a). Remote sensing of plant biodiversity. In *Remote Sensing of Plant Biodiversity*. https://doi.org/10.1007/978-3-030-33157-3

Cavender-Bares, J., Gamon, J. A., & Townsend, P. A. (2020b). Remote sensing of plant biodiversity. In *Remote Sensing of Plant Biodiversity*. https://doi.org/10.1007/978-3-030-33157-3

Cavender-Bares, J., Meireles, J. E., Couture, J. J., Kaproth, M. A., Kingdon, C. C., Singh, A., Serbin, S. P., Center, A., Zuniga, E., Pilz, G., & Townsend, P. A. (2016). Associations of leaf spectra with genetic and phylogenetic variation in oaks: Prospects for remote detection of biodiversity. *Remote Sensing*, *8*(3). https://doi.org/10.3390/rs8030221

Cavender-Bares, J., Schweiger, A. K., Gamon, J. A., Gholizadeh, H., Helzer, K., Lapadat, C., Madritch, M. D., Townsend, P. A., Wang, Z., & Hobbie, S. E. (2022). Remotely detected

aboveground plant function predicts belowground processes in two prairie diversity experiments. *Ecological Monographs*, *92*(1). https://doi.org/10.1002/ecm.1488

Clevers, J. G. P. W., & Gitelson, A. A. (2013). Remote estimation of crop and grass chlorophyll and nitrogen content using red-edge bands on sentinel-2 and-3. *International Journal of Applied Earth Observation and Geoinformation*, *23*(1), 344–351. https://doi.org/10.1016/j.jag.2012.10.008

Cline, L. C., Hobbie, S. E., Madritch, M. D., Buyarski, C. R., Tilman, D., & Cavender-Bares, J. M. (2018). Resource availability underlies the plant-fungal diversity relationship in a grassland ecosystem. *Ecology*, *99*(1), 204–216. https://doi.org/10.1002/ecy.2075

Cornwell, W. K., Cornelissen, J. H. C., Amatangelo, K., Dorrepaal, E., Eviner, V. T., Godoy, O., Hobbie, S. E., Hoorens, B., Kurokawa, H., Pé Rez-Harguindeguy, N., Quested, H. M., Santiago, L. S., Wardle, D. A., Wright, I. J., Aerts, R., Allison, S. D., Van Bodegom, P., Brovkin, V., Chatain, A., … Westoby, M. (2008). Plant species traits are the predominant control on litter decomposition rates within biomes worldwide. *Ecology Letters*, *11*, 1065–1071. https://doi.org/10.1111/j.1461-0248.2008.01219.x

Couture, J. J., Singh, A., Rubert-Nason, K. F., Serbin, S. P., Lindroth, R. L., & Townsend, P. A. (2016). Spectroscopic determination of ecologically relevant plant secondary metabolites. *Methods in Ecology and Evolution*, *7*(11), 1402–1412. https://doi.org/10.1111/2041-210X.12596

Croft, H., Chen, J. M., Luo, X., Bartlett, P., Chen, B., & Staebler, R. M. (2017). Leaf chlorophyll content as a proxy for leaf photosynthetic capacity. *Global Change Biology*, *23*(9), 3513–3524. https://doi.org/10.1111/gcb.13599

Dahlin, K. M., Asner, G. P., & Field, C. B. (2013). Environmental and community controls on plant canopy chemistry in a Mediterranean-type ecosystem. *Proceedings of the National Academy of Sciences*, *110*(17), 6895–6900. https://doi.org/10.1073/pnas.1215513110

Dana Chadwick, K., & Asner, G. P. (2016). Organismic-scale remote sensing of canopy foliar traits in lowland tropical forests. *Remote Sensing*, *8*(2), 1–16. https://doi.org/10.3390/rs8020087

Davidson, A., & Csillag, F. (2001). The influence of vegetation index and spatial resolution on a two-date remote sensing-derived relation to C4 species coverage. *Remote Sensing of Environment*, *75*(1), 138–151. https://doi.org/10.1016/S0034-4257(00)00162-0

De Deyn, G. B., Quirk, H., & Bardgett, R. D. (2011). Plant species richness, identity and productivity differentially influence key groups of microbes in grassland soils of contrasting fertility. *Biology Letters*, *7*(1), 75–78. https://doi.org/10.1098/rsbl.2010.0575

De Long, J. R., Jackson, B. G., Wilkinson, A., Pritchard, W. J., Oakley, S., Mason, K. E., Stephan, J. G., Ostle, N. J., Johnson, D., Baggs, E. M., & Bardgett, R. D. (2019). Relationships between plant traits, soil properties and carbon fluxes differ between monocultures and mixed communities in temperate grassland. *Journal of Ecology*, *107*(4), 1704–1719. https://doi.org/10.1111/1365-2745.13160

de Vries, F. T., Bloem, J., Quirk, H., Stevens, C. J., Bol, R., & Bardgett, R. D. (2012). Extensive Management Promotes Plant and Microbial Nitrogen Retention in Temperate Grassland. *PLoS ONE*, *7*(12), 1–12. https://doi.org/10.1371/journal.pone.0051201

de Vries, F. T., Manning, P., Tallowin, J. R. B., Mortimer, S. R., Pilgrim, E. S., Harrison, K. A., Hobbs, P. J., Quirk, H., Shipley, B., Cornelissen, J. H. C., Kattge, J., & Bardgett, R. D. (2012). Abiotic drivers and plant traits explain landscape-scale patterns in soil microbial communities. *Ecology Letters*, *15*(11), 1230–1239. https://doi.org/10.1111/j.1461-0248.2012.01844.x

Degenhardt, F., Seifert, S., & Szymczak, S. (2019). Evaluation of variable selection methods for random forests and omics data sets. *Briefings in Bioinformatics*, *20*(2), 492–503. https://doi.org/10.1093/bib/bbx124

Delegido, J., Verrelst, J., Alonso, L., & Moreno, J. (2011). Evaluation of Sentinel-2 Red-Edge Bands for Empirical Estimation of Green LAI and Chlorophyll Content. *Sensors*, *11*, 7063–7081. https://doi.org/10.3390/s110707063

Delgado-Baquerizo, M., Eldridge, D. J., Ochoa, V., Gozalo, B., Singh, B. K., & Maestre, F. T. (2017). Soil microbial communities drive the resistance of ecosystem multifunctionality to global change in drylands across the globe. *Ecology Letters*, *20*(10), 1295–1305. https://doi.org/10.1111/ELE.12826

Delgado-Baquerizo, M., Fry, E. L., Eldridge, D. J., de Vries, F. T., Manning, P., Hamonts, K., Kattge, J., Boenisch, G., Singh, B. K., & Bardgett, R. D. (2018). Plant attributes explain the distribution of soil microbial communities in two contrasting regions of the globe. *New Phytologist*, *219*(2), 574–587. https://doi.org/10.1111/nph.15161

Delgado-Baquerizo, M., Maestre, F. T., Gallardo, A., Bowker, M. A., Wallenstein, M. D., Quero, J. L., Ochoa, V., Gozalo, B., García-Gómez, M., Soliveres, S., García-Palacios, P., Berdugo, M., Valencia, E., Escolar, C., Arredondo, T., Barraza-Zepeda, C., Bran, D., Carreira, J. A., Chaieb, M., … Zaady, E. (2013). Decoupling of soil nutrient cycles as a function of aridity in global drylands. *Nature 2013 502:7473*, *502*(7473), 672–676. https://doi.org/10.1038/nature12670

Delgado-Baquerizo, M., Maestre, F. T., Reich, P. B., Jeffries, T. C., Gaitan, J. J., Encinar, D., Berdugo, M., Campbell, C. D., & Singh, B. K. (2016). Microbial diversity drives multifunctionality in terrestrial ecosystems. *Nature Communications 2015 7:1*, *7*(1), 1–8. https://doi.org/10.1038/ncomms10541

Dias, T., Crous, C. J., Ochoa-Hueso, R., Manrique, E., Martins-Loução, M. A., & Cruz, C. (2020). Nitrogen inputs may improve soil biocrusts multifunctionality in dryland ecosystems. *Soil Biology and Biochemistry*, *149*, 107947. https://doi.org/10.1016/J.SOILBIO.2020.107947

Díaz, S., Kattge, J., Cornelissen, J. H. C., Wright, I. J., Lavorel, S., Dray, S., Reu, B., Kleyer, M., Wirth, C., Colin Prentice, I., Garnier, E., Bönisch, G., Westoby, M., Poorter, H., Reich, P. B., Moles, A. T., Dickie, J., Gillison, A. N., Zanne, A. E., … Gorné, L. D. (2016). The global spectrum of plant form and function. *Nature*, *529*(7585), 167–171. https://doi.org/10.1038/nature16489

Dooley, A., Isbell, F., Kirwan, L., Connolly, J., Finn, J. A., & Brophy, C. (2015). *Testing the effects of diversity on ecosystem multifunctionality using a multivariate model*. https://doi.org/10.1111/ele.12504

Dronova, I., & Taddeo, S. (2022). Remote sensing of phenology: Towards the comprehensive indicators of plant community dynamics from species to regional scales. *Journal of Ecology*, *110*(7), 1460–1484. https://doi.org/10.1111/1365-2745.13897

Dronova, I., Taddeo, S., & Harris, K. (2022). Plant diversity reduces satellite-observed phenological variability in wetlands at a national scale. *Science Advances*, *8*(29), 8214. https://doi.org/10.1126/SCIADV.ABL8214/SUPPL_FILE/SCIADV.ABL8214_SM.PDF

Eisenhauer, N., Beßler, H., Engels, C., Gleixner, G., Habekost, M., Milcu, A., Partsch, S., Sabais, A. C. W., Scherber, C., Steinbeiss, S., Weigelt, A., Weisser, W. W., & Scheu, S. (2010). Plant diversity effects on soil microorganisms support the singular hypothesis. *Ecology*, *91*(2), 485–496. https://doi.org/10.1890/08-2338.1

Eisenhauer, N., & Scheu, S. (2008). Invasibility of experimental grassland communities: The role of earthworms, plant functional group identity and seed size. *Oikos*, *117*(7), 1026–1036. https://doi.org/10.1111/j.0030-1299.2008.16812.x

Eklundh, L., & Jönsson, P. (2015). TIMESAT: A software package for time-series processing and assessment of vegetation dynamics. *Remote Sensing and Digital Image Processing*, *22*, 141–158. https://doi.org/10.1007/978-3-319-15967-6_7/FIGURES/4

Eklundh, L., & Jönsson, P. (2017). *TIMESAT 3.3 with seasonal trend decomposition and parallel processing Software Manual*.

Ellis, E. C., & Ramankutty, N. (2008). Putting people in the map: Anthropogenic biomes of the world. In *Frontiers in Ecology and the Environment* (Vol. 6, Issue 8, pp. 439–447). https://doi.org/10.1890/070062

Eswaran, H., Van Der Berg, E., & Reich, P. (1993). Organic Carbon in Soils of the World. *Soil Science Society of America*, *57*, 192–194.

Evans, J., & Murphy, M. (2017). *Package "rfUtilities" Title Random Forests Model Selection and Performance Evaluation*.

Faucon, M. P., Houben, D., & Lambers, H. (2017). Plant Functional Traits: Soil and Ecosystem Services. In *Trends in Plant Science*. https://doi.org/10.1016/j.tplants.2017.01.005

Fauvel, M., Lopes, M., Dubo, T., Rivers-Moore, J., Frison, P. L., Gross, N., & Ouin, A. (2020). Prediction of plant diversity in grasslands using Sentinel-1 and -2 satellite image time series. *Remote Sensing of Environment*, *237*(November 2019), 111536. https://doi.org/10.1016/j.rse.2019.111536

Fay, P. A., Prober, S. M., Harpole, W. S., Knops, J. M. H., Bakker, J. D., Borer, E. T., Lind, E. M., MacDougall, A. S., Seabloom, E. W., Wragg, P. D., Adler, P. B., Blumenthal, D. M., Buckley, Y. M., Chu, C., Cleland, E. E., Collins, S. L., Davies, K. F., Du, G., Feng, X., … Yang, L. H. (2015). Grassland productivity limited by multiple nutrients. *Nature Plants 2015 1:7*, *1*(7), 1–5. https://doi.org/10.1038/nplants.2015.80

Fick, S. E., & Hijmans, R. J. (2017). WorldClim 2: new 1-km spatial resolution climate surfaces for global land areas. *International Journal of Climatology*, *37*(12), 4302–4315. https://doi.org/10.1002/joc.5086

Foley, J. A., Defries, R., Asner, G. P., Barford, C., Bonan, G., Carpenter, S. R., Chapin, F. S., Coe, M. T., Daily, G. C., Gibbs, H. K., Helkowski, J. H., Holloway, T., Howard, E. A., Kucharik, C. J., Monfreda, C., Patz, J. A., Prentice, I. C., Ramankutty, N., & Snyder, P. K. (2005). *Global Consequences of Land Use*. *July*, 1–5.

Fraser, L. H., Pither, J., Jentsch, A., Sternberg, M., Zobel, M., Askarizadeh, D., Bartha, S., Beierkuhnlein, C., Bennett, J. A., Bittel, A., Boldgiv, B., Boldrini, I. I., Bork, E., Brown, L., Cabido, M., Cahill, J., Carlyle, C. N., Campetella, G., Chelli, S., … Zupo, T. (2015). Worldwide evidence of a unimodal relationship between productivity and plant species

richness. *Science*, *349*(6245), 302–305. https://doi.org/10.1126/SCIENCE.AAB3916/SUPPL_FILE/FRASER-SM.PDF

Freschet, G. T., Cornelissen, J. H. C., van Logtestijn, R. S. P., & Aerts, R. (2010). Evidence of the "plant economics spectrum" in a subarctic flora. *Journal of Ecology*, *98*(2), 362–373. https://doi.org/10.1111/j.1365-2745.2009.01615.x

Fry, E. L., Pilgrim, E. S., Tallowin, J. R. B., Smith, R. S., Mortimer, S. R., Beaumont, D. A., Simkin, J., Harris, S. J., Shiel, R. S., Quirk, H., Harrison, K. A., Lawson, C. S., Hobbs, P. J., & Bardgett, R. D. (2017). Plant, soil and microbial controls on grassland diversity restoration: a long-term, multi-site mesocosm experiment. *Journal of Applied Ecology*, *54*(5), 1320–1330. https://doi.org/10.1111/1365-2664.12869

Fry, E. L., Savage, J., Hall, A. L., Oakley, S., Pritchard, W. J., Ostle, N. J., Pywell, R. F., Bullock, J. M., & Bardgett, R. D. (2018). Soil multifunctionality and drought resistance are determined by plant structural traits in restoring grassland. *Ecology*, *99*(10), 2260–2271. https://doi.org/10.1002/ecy.2437

Funk, J. L., & Cornwell, W. K. (2013). Leaf traits within communities: Context may affect the mapping of traits to function. *Ecology*, *94*(9), 1893–1897. https://doi.org/10.1890/12-1602.1

Funk, J. L., Laughlin, D. C., Larson, J. E., Firn, J., Ames, G. M., Funk, J. L., Sutton-Grier, A. E., Cavender-Bares, J., Wright, J., Williams, L., & Butterfield, B. J. (2017). Revisiting the Holy Grail: using plant functional traits to understand ecological processes. *Biological Reviews*, *92*(2), 1156–1173. https://doi.org/10.1111/brv.12275

Gaitán, J. J., Bran, D., Oliva, G., Ciari, G., Nakamatsu, V., Salomone, J., Ferrante, D., Buono, G., Massara, V., Humano, G., Celdrán, D., Opazo, W., & Maestre, F. T. (2013). Evaluating the performance of multiple remote sensing indices to predict the spatial variability of ecosystem structure and functioning in Patagonian steppes. *Ecological Indicators*, *34*, 181–191. https://doi.org/10.1016/J.ECOLIND.2013.05.007

Gallagher, R. V., Falster, D. S., Maitner, B. S., Salguero-Gómez, R., Vandvik, V., Pearse, W. D., Schneider, F. D., Kattge, J., Poelen, J. H., Madin, J. S., Ankenbrand, M. J., Penone, C., Feng, X., Adams, V. M., Alroy, J., Andrew, S. C., Balk, M. A., Bland, L. M., Boyle, B. L., … Enquist, B. J. (2020). Open Science principles for accelerating trait-based science across the Tree of Life. *Nature Ecology and Evolution*, *4*(3), 294–303. https://doi.org/10.1038/s41559-020-1109-6

Gallmann, J., Schüpbach, B., Jacot, K., Albrecht, M., Winizki, J., Kirchgessner, N., & Aasen, H. (2022). Flower Mapping in Grasslands With Drones and Deep Learning. *Frontiers in Plant Science*, *12*, 774965. https://doi.org/10.3389/FPLS.2021.774965/BIBTEX

Gamfeldt, L., & Roger, F. (2017). Revisiting the biodiversity-ecosystem multifunctionality relationship. In *Nature Ecology and Evolution* (Vol. 1, Issue 7, p. 168). https://doi.org/10.1038/s41559-017-0168

Gao, B.-C. (1996). NDWI - A Normalized Difference Water Index for Remote Sensing of Vegetation Liquid Water From Space. In *REMOTE SENS. ENVIRON* (Vol. 7212). ©Elsevier Science Inc.

García-Gómez, M., & Maestre, F. T. (2011). Remote sensing data predict indicators of soil functioning in semi-arid steppes, central Spain. *Ecological Indicators*, *11*(5), 1476–1481. https://doi.org/10.1016/J.ECOLIND.2011.02.015

Garland, G., Banerjee, S., Edlinger, A., Miranda Oliveira, E., Herzog, C., Wittwer, R., Philippot, L., Maestre, F. T., & van der Heijden, M. G. A. (2021). A closer look at the functions behind ecosystem multifunctionality: A review. *Journal of Ecology*, *109*(2), 600–613. https://doi.org/10.1111/1365-2745.13511

Garson, G. D. (2016). *PARTIAL LEAST SQUARES (PLS-SEM) 2016 Edition*.

Georganos, S., Grippa, T., Niang Gadiaga, A., Linard, C., Lennert, M., Vanhuysse, S., Mboga, N., Wolff, E., & Kalogirou, S. (2019). Geographical random forests: a spatial extension of the random forest algorithm to address spatial heterogeneity in remote sensing and population modelling. *Https://Doi.Org/10.1080/10106049.2019.1595177*, *36*(2), 121–136. https://doi.org/10.1080/10106049.2019.1595177

Gholizadeh, H., Gamon, J. A., Townsend, P. A., Zygielbaum, A. I., Helzer, C. J., Hmimina, G. Y., Yu, R., Moore, R. M., Schweiger, A. K., & Cavender-Bares, J. (2019). Detecting prairie biodiversity with airborne remote sensing. *Remote Sensing of Environment*, *221*, 38–49. https://doi.org/10.1016/j.rse.2018.10.037

Gitelson, A. A., Merzlyak, M. N., & Chivkunova, O. B. (2001). Optical Properties and Nondestructive Estimation of Anthocyanin Content in Plant Leaves¶. *Photochemistry and Photobiology*, *74*(1), 38. https://doi.org/10.1562/0031-8655(2001)074<0038:opaneo>2.0.co;2

Gitelson, A. A., Viña, A., Verma, S. B., Rundquist, D. C., Arkebauer, T. J., Keydan, G., Leavitt, B., Ciganda, V., Burba, G. G., & Suyker, A. E. (2006). Relationship between gross primary production and chlorophyll content in crops: Implications for the synoptic monitoring of vegetation productivity. *Journal of Geophysical Research Atmospheres*, *111*(8). https://doi.org/10.1029/2005JD006017

Gitelson, A. A., Zur, Y., Chivkunova, O. B., & Merzlyak, M. N. (2002). Assessing Carotenoid Content in Plant Leaves with Reflectance Spectroscopy¶. *Photochemistry and Photobiology*, *75*(3), 272. https://doi.org/10.1562/0031-8655(2002)075<0272:ACCIPL>2.0.CO;2

Gorelick, N., Hancher, M., Dixon, M., Ilyushchenko, S., Thau, D., & Moore, R. (2017a). Google Earth Engine: Planetary-scale geospatial analysis for everyone. *Remote Sensing of Environment*, *202*, 18–27. https://doi.org/10.1016/j.rse.2017.06.031

Gorelick, N., Hancher, M., Dixon, M., Ilyushchenko, S., Thau, D., & Moore, R. (2017b). Google Earth Engine: Planetary-scale geospatial analysis for everyone. *Remote Sensing of Environment*, *202*, 18–27. https://doi.org/10.1016/j.rse.2017.06.031

Grace, J. B., Anderson, T. M., Seabloom, E. W., Borer, E. T., Adler, P. B., Harpole, W. S., Hautier, Y., Hillebrand, H., Lind, E. M., Pärtel, M., Bakker, J. D., Buckley, Y. M., Crawley, M. J., Damschen, E. I., Davies, K. F., Fay, P. A., Firn, J., Gruner, D. S., Hector, A., … Smith, M. D. (2016). Integrative modelling reveals mechanisms linking productivity and plant species richness. *Nature 2016 529:7586*, *529*(7586), 390–393. https://doi.org/10.1038/nature16524

Green, J. L., Bohannan, B. J. M., & Whitaker, R. J. (2008). Microbial biogeography: From taxonomy to traits. *Science*, *320*(5879), 1039–1043. https://doi.org/10.1126/science.1153475

Griffiths, R. I., Thomson, B. C., James, P., Bell, T., Bailey, M., & Whiteley, A. S. (2011). The bacterial biogeography of British soils. *Environmental Microbiology*, *13*(6), 1642–1654. https://doi.org/10.1111/j.1462-2920.2011.02480.x

Griffiths, R. I., Thomson, B. C., Plassart, P., Gweon, H. S., Stone, D., Creamer, R. E., Lemanceau, P., & Bailey, M. J. (2016). Mapping and validating predictions of soil bacterial biodiversity using European and national scale datasets. *Applied Soil Ecology*, *97*, 61–68. https://doi.org/10.1016/j.apsoil.2015.06.018

Grigulis, K., Lavorel, S., Krainer, U., Legay, N., Baxendale, C., Dumont, M., Kastl, E., Arnoldi, C., Bardgett, R. D., Poly, F., Pommier, T., Schloter, M., Tappeiner, U., Bahn, M., & Cl??ment, J. C. (2013). Relative contributions of plant traits and soil microbial properties to mountain grassland ecosystem services. *Journal of Ecology*, *101*(1), 47–57. https://doi.org/10.1111/1365-2745.12014

Grime, J. P. (1998). Benefits of plant diversity to ecosystems: Immediate, filter and founder effects. In *Journal of Ecology* (Vol. 86, Issue 6, pp. 902–910). https://doi.org/10.1046/j.1365-2745.1998.00306.x

Gross, N., Kunstler, G., Liancourt, P., De Bello, F., Suding, K. N., & Lavorel, S. (2009). Linking individual response to biotic interactions with community structure: A trait-based framework. *Functional Ecology*, *23*(6), 1167–1178. https://doi.org/10.1111/j.1365-2435.2009.01591.x

Gross, N., Robson, T. M., Lavorel, S., Albert, C., Le Bagousse-Pinguet, Y., & Guillemin, R. (2008). Plant response traits mediate the effects of subalpine grasslands on soil moisture. *New Phytologist*, *180*(3), 652–662. https://doi.org/10.1111/j.1469-8137.2008.02577.x

Günal, E., Wang, X., Kılıc, O. M., Budak, M., Al Obaid, S., Ansari, M. J., & Brestic, M. (2021). Potential of Landsat 8 OLI for mapping and monitoring of soil salinity in an arid region: A case study in Dushak, Turkmenistan. *PLOS ONE*, *16*(11), e0259695. https://doi.org/10.1371/JOURNAL.PONE.0259695

Guo, Y., Xu, T., Cheng, J., Wei, G., & Lin, Y. (2021). Above- and belowground biodiversity drives soil multifunctionality along a long-term grassland restoration chronosequence. *Science of the Total Environment*, *772*(3), 145010. https://doi.org/10.1016/j.scitotenv.2021.145010

Hacker, P. W., & Coops, N. C. (2022). Using leaf functional traits to remotely detect Cytisus scoparius (Linnaeus) Link in endangered savannahs. *NeoBiota 71: 149-164*, *71*, 149–164. https://doi.org/10.3897/NEOBIOTA.71.76573

Hacker, P. W., Coops, N. C., Laliberté, E., & Michaletz, S. T. (2022). Variations in accuracy of leaf functional trait prediction due to spectral mixing. *Ecological Indicators*, *136*, 108687. https://doi.org/10.1016/J.ECOLIND.2022.108687

Harris, A., & Baird, A. J. (2019). Microtopographic Drivers of Vegetation Patterning in Blanket Peatlands Recovering from Erosion. *Ecosystems*, *22*(5), 1035–1054. https://doi.org/10.1007/s10021-018-0321-6

Hauser, L. T., Timmermans, J., van der Windt, N., Sil, Â. F., César de Sá, N., Soudzilovskaia, N. A., & van Bodegom, P. M. (2021). Explaining discrepancies between spectral and in-situ plant diversity in multispectral satellite earth observation. *Remote Sensing of Environment*, *265*. https://doi.org/10.1016/j.rse.2021.112684

Hautier, Y., Isbell, F., Borer, E. T., Seabloom, E. W., Harpole, W. S., Lind, E. M., MacDougall, A. S., Stevens, C. J., Adler, P. B., Alberti, J., Bakker, J. D., Brudvig, L. A., Buckley, Y. M., Cadotte, M., Caldeira, M. C., Chaneton, E. J., Chu, C., Daleo, P., Dickman, C. R., … Hector, A. (2018). Local loss and spatial homogenization of plant diversity reduce ecosystem

multifunctionality. *Nature Ecology and Evolution*, *2*(1), 50–56. https://doi.org/10.1038/s41559-017-0395-0

Hautier, Y., Seabloom, E. W., Borer, E. T., Adler, P. B., Harpole, W. S., Hillebrand, H., Lind, E. M., MacDougall, A. S., Stevens, C. J., Bakker, J. D., Buckley, Y. M., Chu, C., Collins, S. L., Daleo, P., Damschen, E. I., Davies, K. F., Fay, P. A., Firn, J., Gruner, D. S., … Hector, A. (2014). Eutrophication weakens stabilizing effects of diversity in natural grasslands. *Nature 2014 508:7497*, *508*(7497), 521–525. https://doi.org/10.1038/nature13014

Hautier, Y., Tilman, D., Isbell, F., Seabloom, E. W., Borer, E. T., & Reich, P. B. (2015). Anthropogenic environmental changes affect ecosystem stability via biodiversity. *Science*, *348*(6232), 336–340.

Hayes, P., Turner, B. L., Lambers, H., & Laliberté, E. (2014). Foliar nutrient concentrations and resorption efficiency in plants of contrasting nutrient-acquisition strategies along a 2-million-year dune chronosequence. *Journal of Ecology*, *102*(2), 396–410. https://doi.org/10.1111/1365-2745.12196

He, K. S., Zhang, J., & Zhang, Q. (2009). Linking variability in species composition and MODIS NDVI based on beta diversity measurements. *Acta Oecologica*, *35*(1), 14–21. https://doi.org/10.1016/j.actao.2008.07.006

He, K., & Zhang, J. (2009). Testing the correlation between beta diversity and differences in productivity among global ecoregions, biomes, and biogeographical realms. *Ecological Informatics*, *4*(2), 93–98. https://doi.org/10.1016/j.ecoinf.2009.01.003

He, Y., Yang, J., & Guo, X. (2020). Green Vegetation Cover Dynamics in a Heterogeneous Grassland: Spectral Unmixing of Landsat Time Series from 1999 to 2014. *Remote Sensing 2020, Vol. 12, Page 3826*, *12*(22), 3826. https://doi.org/10.3390/RS12223826

Hector, A., & Bagchi, R. (2007). Biodiversity and ecosystem multifunctionality. *Nature*, *448*(7150), 188–190. https://doi.org/10.1038/nature05947

Hector, A., Hautier, Y., Saner, P., Wacker, L., Bagchi, R., Joshi, J., Scherer-Lorenzen, M., Spehn, E. M., Bazeley-White, E., M.Weilenmann, Caldeira, M. C., Dimitrakopoulos, P. G., Finn, J. A., Huss-Danell, K., Jumpponen, A., & Loreau, M. (2010). General stabilizing effects of plant diversity on grassland productivity through population asynchrony and overyielding. *Ecology*, *91*(8), 2213–2220.

Helfenstein, I. S., Schneider, F. D., Schaepman, M. E., & Morsdorf, F. (2022). Assessing biodiversity from space: Impact of spatial and spectral resolution on trait-based functional diversity. *Remote Sensing of Environment*, *275*(July 2021), 113024. https://doi.org/10.1016/j.rse.2022.113024

Hijmans, R. J., Cameron, S. E., Parra, J. L., Jones, P. G., & Jarvis, A. (2005). Very high resolution interpolated climate surfaces for global land areas. *International Journal of Climatology*, *25*(15), 1965–1978. https://doi.org/10.1002/JOC.1276

Homolová, L., Malenovský, Z., Clevers, J. G. P. W., García-Santos, G., & Schaepman, M. E. (2013a). Review of optical-based remote sensing for plant trait mapping. *Ecological Complexity*, *15*, 1–16. https://doi.org/10.1016/j.ecocom.2013.06.003

Homolová, L., Malenovský, Z., Clevers, J. G. P. W., García-Santos, G., & Schaepman, M. E. (2013b). Review of optical-based remote sensing for plant trait mapping. *Ecological Complexity*, *15*, 1–16. https://doi.org/10.1016/j.ecocom.2013.06.003

Homolova, L., Schaepman, M. E., Lamarque, P., Clevers, J. G. P. W., De Bello, F., Thuiller, W., & Lavorel, S. (2014). Comparison of remote sensing and plant trait-based modelling to predict ecosystem services in subalpine grasslands. *Ecosphere*, *5*(8), 1–29. https://doi.org/10.1890/ES13-00393.1

House, J. I., Archer, S., Breshears, D. D., Scholes, R. J., Coughenour, M. B., Dodd, M. B., Gignoux, J., Hall, D. O., Hanan, N. P., Joffre, R., Le Roux, X., Ludwig, J. A., Menaut, J. C., Montes, R., Parton, W. J., San Jose, J. J., Scanlan, J. C., Scurlock, J. M. O., Simioni, G., & Thorrold, B. (2003). Conundrums in mixed woody-herbaceous plant systems. *Journal of Biogeography*, *30*(11), 1763–1777. https://doi.org/10.1046/j.1365-2699.2003.00873.x

Hu, W., Ran, J., Dong, L., Du, Q., Ji, M., Yao, S., Sun, Y., Gong, C., Hou, Q., Gong, H., Chen, R., Lu, J., Xie, S., Wang, Z., Huang, H., Li, X., Xiong, J., Xia, R., Wei, M., … Deng, J. (2021). Aridity-driven shift in biodiversity–soil multifunctionality relationships. *Nature Communications 2021 12:1*, *12*(1), 1–15. https://doi.org/10.1038/s41467-021-25641-0

Hu, Y., Li, X., Guo, A., Yue, P., Guo, X., Lv, P., Zhao, S., & Zuo, X. (2022). Species diversity is a strong predictor of ecosystem multifunctionality under altered precipitation in desert steppes. *Ecological Indicators*, *137*, 108762. https://doi.org/10.1016/J.ECOLIND.2022.108762

Huete, A. R., & Jackson, R. D. (1988). Soil and Atmosphere Influences on the Spectra of Partial Canopies. *ENVIRONMENT*, *25*, 89–105.

Isbell, F., Calcagno, V., Hector, A., Connolly, J., Harpole, W. S., Reich, P. B., Scherer-Lorenzen, M., Schmid, B., Tilman, D., Van Ruijven, J., Weigelt, A., Wilsey, B. J., Zavaleta, E. S., & Loreau, M. (2011). High plant diversity is needed to maintain ecosystem services. *Nature*, *477*(7363), 199–202. https://doi.org/10.1038/nature10282

Isbell, F., Cowles, J., Dee, L. E., Loreau, M., Reich, P. B., Gonzalez, A., Hector, A., & Schmid, B. (2018). Quantifying effects of biodiversity on ecosystem functioning across times and places. *Ecology Letters*, *21*(6), 763–778. https://doi.org/10.1111/ele.12928

Isbell, F., Craven, D., Connolly, J., Loreau, M., Schmid, B., Beierkuhnlein, C., Bezemer, T. M., Bonin, C., Bruelheide, H., De Luca, E., Ebeling, A., Griffin, J. N., Guo, Q., Hautier, Y., Hector, A., Jentsch, A., Kreyling, J., Lanta, V., Manning, P., … Eisenhauer, N. (2015). Biodiversity increases the resistance of ecosystem productivity to climate extremes. *Nature*, *526*(7574), 574–577. https://doi.org/10.1038/nature15374

Jacquemoud, S., Verhoef, W., Baret, F., Bacour, C., Zarco-Tejada, P. J., Asner, G. P., François, C., & Ustin, S. L. (2009). PROSPECT + SAIL models: A review of use for vegetation characterization. *Remote Sensing of Environment*, *113*(SUPPL. 1), S56–S66. https://doi.org/10.1016/j.rse.2008.01.026

Jetz, W., Cavender-Bares, J., Pavlick, R., Schimel, D., Davis, F. W., Asner, G. P., Guralnick, R., Kattge, J., Latimer, A. M., Moorcroft, P., Schaepman, M. E., Schildhauer, M. P., Schneider, F. D., Schrodt, F., Stahl, U., & Ustin, S. L. (2016). Monitoring plant functional diversity from space. *Nature Plants*, *2*(3), 16024. https://doi.org/10.1038/NPLANTS.2016.24

Jetz, W., McGeoch, M. A., Guralnick, R., Ferrier, S., Beck, J., Costello, M. J., Fernandez, M., Geller, G. N., Keil, P., Merow, C., Meyer, C., Muller-Karger, F. E., Pereira, H. M., Regan, E. C., Schmeller, D. S., & Turak, E. (2019). Essential biodiversity variables for mapping

and monitoring species populations. *Nature Ecology and Evolution*, *3*(4), 539–551. https://doi.org/10.1038/s41559-019-0826-1

Jing, X., Prager, C. M., Borer, E. T., Gotelli, N. J., Gruner, D. S., He, J. S., Kirkman, K., MacDougall, A. S., McCulley, R. L., Prober, S. M., Seabloom, E. W., Stevens, C. J., Classen, A. T., & Sanders, N. J. (2021). Spatial turnover of multiple ecosystem functions is more associated with plant than soil microbial β-diversity. *Ecosphere*, *12*(7). https://doi.org/10.1002/ecs2.3644

Jing, X., Prager, C. M., Classen, A. T., Maestre, F. T., He, J. S., & Sanders, N. J. (2020). Variation in the methods leads to variation in the interpretation of biodiversity–ecosystem multifunctionality relationships. *Journal of Plant Ecology*, *13*(4), 431–441. https://doi.org/10.1093/JPE/RTAA031

Jing, X., Sanders, N. J., Shi, Y., Chu, H., Classen, A. T., Zhao, K., Chen, L., Shi, Y., Jiang, Y., & He, J. S. (2015). The links between ecosystem multifunctionality and above- and belowground biodiversity are mediated by climate. *Nature Communications 2015 6:1*, *6*(1), 1–8. https://doi.org/10.1038/ncomms9159

Jones, M. B., & Donnelly, A. (2004). *Jones_2004_Carbon sequestration in temperate grassland ecosytems and the inlfuence of management,climate and elevated CO2.pdf*. 423–439. https://doi.org/10.1111/j.1469-8137.2004.01201.x

Jönsson, P., & Eklundh, L. (2004). TIMESAT - A program for analyzing time-series of satellite sensor data. *Computers and Geosciences*, *30*(8), 833–845. https://doi.org/10.1016/J.CAGEO.2004.05.006

Jung, M., Koirala, S., Weber, U., Ichii, K., Gans, F., Camps-Valls, G., Papale, D., Schwalm, C., Tramontana, G., & Reichstein, M. (2019). the FLUXCOM ensemble of global land-atmosphere energy fluxes. *Scientific Data*, *6*(74), 1–14. https://doi.org/10.1038/s41597-019-0076-8

Kaisermann, A., de Vries, F. T., Griffiths, R. I., & Bardgett, R. D. (2017). Legacy effects of drought on plant–soil feedbacks and plant–plant interactions. *New Phytologist*, *215*(4), 1413–1424. https://doi.org/10.1111/nph.14661

Kampe, T. U., Johnson, B. R., Kuester, M. A., & Keller, M. (2010). NEON: the first continental-scale ecological observatory with airborne remote sensing of vegetation canopy biochemistry and structure. *Https://Doi.Org/10.1117/1.3361375*, *4*(1), 043510. https://doi.org/10.1117/1.3361375

Kattge, J., Díaz, S., Lavorel, S., Prentice, I. C., Leadley, P., Bönisch, G., Garnier, E., Westoby, M., Reich, P. B., Wright, I. J., Cornelissen, J. H. C., Violle, C., Harrison, S. P., Van Bodegom, P. M., Reichstein, M., Enquist, B. J., Soudzilovskaia, N. A., Ackerly, D. D., Anand, M., … Wirth, C. (2011). TRY - a global database of plant traits. *Global Change Biology*, *17*(9), 2905–2935. https://doi.org/10.1111/j.1365-2486.2011.02451.x

Keller, M., Schimel, D. S., Hargrove, W. W., & Hoffman, F. M. (2008). A continental strategy for the National Ecological Observatory Network. *Frontiers in Ecology and the Environment*, *6*(5), 282–284. https://doi.org/10.1890/1540-9295(2008)6[282:ACSFTN]2.0.CO;2

Klironomos, J. N. (2002). Feedback with soil biota contributes to plant rarity and invasiveness in communities. *Nature*, *417*(May), 1096–1099.

Knapp, A. K., Carroll, C. J. W., & Fahey, T. J. (2014). Patterns and controls of terrestrial primary production in a changing world. In *Ecology and the Environment*. https://doi.org/10.1007/978-1-4614-7501-9_2

Kokaly, R. F., Asner, G. P., Ollinger, S. V., Martin, M. E., & Wessman, C. A. (2009). Characterizing canopy biochemistry from imaging spectroscopy and its application to ecosystem studies. *Remote Sensing of Environment*, *113*(SUPPL. 1), S78–S91. https://doi.org/10.1016/j.rse.2008.10.018

Kothari, S., Beauchamp-Rioux, R., Blanchard, F., Crofts, A. L., Girard, A., Guilbeault-Mayers, X., Hacker, P. W., Pardo, J., Schweiger, A. K., Demers-4 Thibeault, S., Bruneau, A., Coops, N. C., Kalacska, M., Vellend, M., & Laliberté, E. (2023). Predicting leaf traits across functional groups using reflectance spectroscopy. *New Phytologist*, 549–566. https://doi.org/10.1111/nph.18713

Kothari, S., & Schweiger, A. K. (2022). Plant spectra as integrative measures of plant phenotypes. *Journal of Ecology*, *110*(11), 2536–2554. https://doi.org/10.1111/1365-2745.13972

Kozhoridze, G., Orlovsky, N., Orlovsky, L., Blumberg, D. G., & Golan-Goldhirsh, A. (2016). Remote sensing models of structure-related biochemicals and pigments for classification of trees. *Remote Sensing of Environment*, *186*, 184–195. https://doi.org/10.1016/j.rse.2016.08.024

Kulmatiski, A., Beard, K. H., Stevens, J. R., & Cobbold, S. M. (2008). Plant-soil feedbacks: A meta-analytical review. *Ecology Letters*, *11*(9), 980–992. https://doi.org/10.1111/j.1461-0248.2008.01209.x

Kursa, M. B., & Rudnicki, W. R. (2010). Feature Selection with the Boruta Package. *Journal of Statistical Software*, *36*(11), 1–13. https://doi.org/10.18637/JSS.V036.I11

Laliberté, E. (2017). Below-ground frontiers in trait-based plant ecology. *New Phytologist*, *213*(4), 1597–1603. https://doi.org/10.1111/nph.14247

Lange, M., Eisenhauer, N., Sierra, C. A., Bessler, H., Engels, C., Griffiths, R. I., Mellado-Vázquez, P. G., Malik, A. A., Roy, J., Scheu, S., Steinbeiss, S., Thomson, B. C., Trumbore, S. E., & Gleixner, G. (2015). Plant diversity increases soil microbial activity and soil carbon storage. *Nature Communications*, *6*. https://doi.org/10.1038/ncomms7707

Laughlin, D. C. (2011). Nitrification is linked to dominant leaf traits rather than functional diversity. *Journal of Ecology*, *99*(5), 1091–1099. https://doi.org/10.1111/j.1365-2745.2011.01856.x

Lausch, A., Bastian, O., Klotz, S., Leitão, P. J., Jung, A., Rocchini, D., Schaepman, M. E., Skidmore, A. K., Tischendorf, L., & Knapp, S. (2018). Understanding and assessing vegetation health by in situ species and remote-sensing approaches. *Methods in Ecology and Evolution*, *9*(8), 1799–1809. https://doi.org/10.1111/2041-210X.13025

Lausch, A., Erasmi, S., King, D. J., Magdon, P., & Heurich, M. (2016). Understanding forest health with remote sensing-Part I-A review of spectral traits, processes and remote-sensing characteristics. *Remote Sensing*, *8*(12), 1–44. https://doi.org/10.3390/rs8121029

Lavorel, S. (2013). Plant functional effects on ecosystem services. *Journal of Ecology*, *101*(1), 4–8. https://doi.org/10.1111/1365-2745.12031

Lavorel, S., & Grigulis, K. (2012). How fundamental plant functional trait relationships scale-up to trade-offs and synergies in ecosystem services. *Journal of Ecology*, *100*(1), 128–140. https://doi.org/10.1111/j.1365-2745.2011.01914.x

Lavorel, S., Grigulis, K., Lamarque, P., Colace, M. P., Garden, D., Girel, J., Pellet, G., & Douzet, R. (2011). Using plant functional traits to understand the landscape distribution of multiple ecosystem services. *Journal of Ecology*, *99*(1), 135–147. https://doi.org/10.1111/j.1365-2745.2010.01753.x

Leff, J. W., Bardgett, R. D., Wilkinson, A., Jackson, B. G., Pritchard, W. J., De Long, J. R., Oakley, S., Mason, K. E., Ostle, N. J., Johnson, D., Baggs, E. M., & Fierer, N. (2018). Predicting the structure of soil communities from plant community taxonomy, phylogeny, and traits. *ISME Journal*, *12*(7), 1794–1805. https://doi.org/10.1038/s41396-018-0089-x

Leff, J. W., Jones, S. E., Prober, S. M., Barberán, A., Borer, E. T., Firn, J. L., Harpole, W. S., Hobbie, S. E., Hofmockel, K. S., Knops, J. M. H., McCulley, R. L., La Pierre, K., Risch, A. C., Seabloom, E. W., Schütz, M., Steenbock, C., Stevens, C. J., & Fierer, N. (2015). Consistent responses of soil microbial communities to elevated nutrient inputs in grasslands across the globe. *Proceedings of the National Academy of Sciences*, *112*(35), 10967–10972. https://doi.org/10.1073/pnas.1508382112

Legay, N., Baxendale, C., Grigulis, K., Krainer, U., Kastl, E., Schloter, M., Bardgett, R. D., Arnoldi, C., Bahn, M., Dumont, M., Pommier, T., Clément, J. C., & Lavorel, S. (2014). Contribution of above- and below-ground plant traits to the structure and function of grassland soil microbial communities. *Annals of Botany*, *114*(5), 1011–1021. https://doi.org/10.1093/aob/mcu169

Legendre, & Laliberté. (2010). A distance-based framework for measuring functional diversity from multiple traits. *Ecology*, *91*(1), 299–305.

Lepš, J., de Bello, F., Lavorel, S., & Berman, S. (2006). Quantifying and interpreting functional diversity of natural communities: Practical considerations matter. *Preslia*, *78*(4), 481–501.

Li, C., Wulf, H., Schmid, B., He, J. S., & Schaepman, M. E. (2018). Estimating plant traits of alpine grasslands on the qinghai-tibetan plateau using remote sensing. *IEEE Journal of Selected Topics in Applied Earth Observations and Remote Sensing*, *11*(7), 2263–2275. https://doi.org/10.1109/JSTARS.2018.2824901

Liang, M., Baiser, B., Hallett, L. M., Hautier, Y., Jiang, L., Loreau, M., Record, S., Sokol, E. R., Zarnetske, P. L., & Wang, S. (2022). Consistent stabilizing effects of plant diversity across spatial scales and climatic gradients. *Nature Ecology and Evolution*, *6*(11), 1669–1675. https://doi.org/10.1038/s41559-022-01868-y

Liu, J., Lu, S., Liu, C., & Hou, D. (2022). Nutrient reallocation between stem and leaf drives grazed grassland degradation in inner Mongolia, China. *BMC Plant Biology*, *22*(1). https://doi.org/10.1186/s12870-022-03875-4

Liu, Q., Zhang, Q., Jarvie, S., Yan, Y., Han, P., Liu, T., Guo, K., Ren, L., Yue, K., Wu, H., Du, J., Niu, J., & Svenning, J. C. (2021). Ecosystem restoration through aerial seeding: Interacting plant–soil microbiome effects on soil multifunctionality. *Land Degradation & Development*, *32*(18), 5334–5347. https://doi.org/10.1002/LDR.4112

Liu, S., Sun, Y., Dong, Y., Zhao, H., Dong, S., Zhao, S., & Beazley, R. (2019). The spatio-temporal patterns of the topsoil organic carbon density and its influencing factors based

on different estimation models in the grassland of Qinghai-Tibet Plateau. *PLOS ONE*, *14*(12), e0225952. https://doi.org/10.1371/JOURNAL.PONE.0225952

Löfgren, O., Prentice, H. C., Moeckel, T., Schmid, B. C., & Hall, K. (2018). Landscape history confounds the ability of the NDVI to detect fine-scale variation in grassland communities. *Methods in Ecology and Evolution*, *9*(9), 2009–2018. https://doi.org/10.1111/2041-210X.13036

Lohbeck, M., Poorter, L., Martinez-Ramos, M., Bongers, F., & Craft, N. J. B. (2015). Biomass is the main driver of changes in ecosystem process rates during tropical forest succession. *Ecology*, *96*(5), 1242–1252. https://doi.org/10.1890/14-0472.1

Lopes, M., Fauvel, M., Ouin, A., & Girard, S. (2017). Spectro-temporal heterogeneity measures from dense high spatial resolution satellite image time series: Application to grassland species diversity estimation. *Remote Sensing*, *9*(10). https://doi.org/10.3390/rs9100993

López-García, Á., Varela-Cervero, S., Vasar, M., Öpik, M., Barea, J. M., & Azcón-Aguilar, C. (2017). Plant traits determine the phylogenetic structure of arbuscular mycorrhizal fungal communities. *Molecular Ecology*, *26*(24), 6948–6959. https://doi.org/10.1111/mec.14403

Ma, X., Mahecha, M. D., Migliavacca, M., van der Plas, F., Benavides, R., Ratcliffe, S., Kattge, J., Richter, R., Musavi, T., Baeten, L., Barnoaiea, I., Bohn, F. J., Bouriaud, O., Bussotti, F., Coppi, A., Domisch, T., Huth, A., Jaroszewicz, B., Joswig, J., … Wirth, C. (2019). Inferring plant functional diversity from space: the potential of Sentinel-2. *Remote Sensing of Environment*, *233*(July), 111368. https://doi.org/10.1016/j.rse.2019.111368

Madritch, M. D., Kingdon, C. C., Singh, A., Mock, K. E., Lindroth, R. L., & Townsend, P. A. (2014). Imaging spectroscopy links aspen genotype with below-ground processes at landscape scales. *Philosophical Transactions of the Royal Society B: Biological Sciences*, *369*(1643). https://doi.org/10.1098/rstb.2013.0194

Maestre, F. T., Quero, J. L., Gotelli, N. J., Escudero, A., Ochoa, V., Delgado-Baquerizo, M., García-Gómez, M., Bowker, M. A., Soliveres, S., Escolar, C., García-Palacios, P., Berdugo, M., Valencia, E., Gozalo, B., Gallardo, A., Aguilera, L., Arredondo, T., Blones, J., Boeken, B., … Zaady, E. (2012). Plant species richness and ecosystem multifunctionality in global drylands. *Science*, *335*(6065), 214–218. https://doi.org/10.1126/science.1215442

Malik, A. A., Chowdhury, S., Schlager, V., Oliver, A., Puissant, J., Vazquez, P. G. M., Jehmlich, N., von Bergen, M., Griffiths, R. I., & Gleixner, G. (2016). Soil fungal: Bacterial ratios are linked to altered carbon cycling. *Frontiers in Microbiology*, *7*(AUG), 1–11. https://doi.org/10.3389/fmicb.2016.01247

Manning, P., de Vries, F. T., Tallowin, J. R. B., Smith, R., Mortimer, S. R., Pilgrim, E. S., Harrison, K. A., Wright, D. G., Quirk, H., Benson, J., Shipley, B., Cornelissen, J. H. C., Kattge, J., Bönisch, G., Wirth, C., & Bardgett, R. D. (2015). Simple measures of climate, soil properties and plant traits predict national-scale grassland soil carbon stocks. *Journal of Applied Ecology*, *52*(5), 1188–1196. https://doi.org/10.1111/1365-2664.12478

Manning, P., Van Der Plas, F., Soliveres, S., Allan, E., Maestre, F. T., Mace, G., Whittingham, M. J., & Fischer, M. (2018). Redefining ecosystem multifunctionality. *Nature Ecology and Evolution*, *2*(3), 427–436. https://doi.org/10.1038/s41559-017-0461-7

Mao, W., Felton, A. J., Ma, Y., Zhang, T., Sun, Z., Zhao, X., & Smith, M. D. (2018). Relationships between aboveground and belowground trait responses of a dominant

plant species to alterations in watertable depth. *Land Degradation and Development*, *29*(11), 4015–4024. https://doi.org/10.1002/ldr.3159

Mapfumo, R. B., Murwira, A., Masocha, M., & Andriani, R. (2016). The relationship between satellite-derived indices and species diversity across African savanna ecosystems. *International Journal of Applied Earth Observation and Geoinformation*, *52*, 306–317. https://doi.org/10.1016/j.jag.2016.06.025

Mason, C. M., & Donovan, L. A. (2015). Evolution of the leaf economics spectrum in herbs: Evidence from environmental divergences in leaf physiology across Helianthus (Asteraceae). *Evolution*, *69*(10), 2705–2720. https://doi.org/10.1111/evo.12768

Meyer, H., & Pebesma, E. (2022). Machine learning-based global maps of ecological variables and the challenge of assessing them. *Nature Communications 2022 13:1*, *13*(1), 1–4. https://doi.org/10.1038/s41467-022-29838-9

Mibei, E. K., Ambuko, J., Giovannoni, J. J., Onyango, A. N., & Owino, W. O. (2017). Carotenoid profiling of the leaves of selected African eggplant accessions subjected to drought stress. *Food Science and Nutrition*, *5*(1), 113–122. https://doi.org/10.1002/fsn3.370

Millard, P., & Singh, B. K. (2010). Does grassland vegetation drive soil microbial diversity? *Nutrient Cycling in Agroecosystems*, *88*(2), 147–158. https://doi.org/10.1007/s10705-009-9314-3

Moreau, D., Pivato, B., Bru, D., Busset, H., Deau, F., Faivre, C., Matejicek, A., Strbik, F., Philippot, L., & Mougel, C. (2015). Plant traits related to nitrogen uptake influence plant-microbe competition. *Ecology*, *96*(8), 2300–2310. https://doi.org/10.1890/14-1761.1

Moreno-Martínez, Á., Camps-Valls, G., Kattge, J., Robinson, N., Reichstein, M., van Bodegom, P., Kramer, K., Cornelissen, J. H. C., Reich, P., Bahn, M., Niinemets, Ü., Peñuelas, J., Craine, J. M., Cerabolini, B. E. L., Minden, V., Laughlin, D. C., Sack, L., Allred, B., Baraloto, C., … Running, S. W. (2018). A methodology to derive global maps of leaf traits using remote sensing and climate data. *Remote Sensing of Environment*, *218*(August), 69–88. https://doi.org/10.1016/j.rse.2018.09.006

Nerlekar, A. N., & Veldman, J. W. (2020). High plant diversity and slow assembly of old-growth grasslands. *Proceedings of the National Academy of Sciences of the United States of America*, *117*(31), 18550–18556. https://doi.org/10.1073/PNAS.1922266117/SUPPL_FILE/PNAS.1922266117.SD01.XLSX

Nunes, M. H., Davey, M. P., & Coomes, D. A. (2017). On the challenges of using field spectroscopy to measure the impact of soil type on leaf traits. *Biogeosciences*, *14*(13), 3371–3385. https://doi.org/10.5194/bg-14-3371-2017

Obermeier, W. A., Lehnert, L. W., Pohl, M. J., Makowski Gianonni, S., Silva, B., Seibert, R., Laser, H., Moser, G., Müller, C., Luterbacher, J., & Bendix, J. (2019). Grassland ecosystem services in a changing environment: The potential of hyperspectral monitoring. *Remote Sensing of Environment*, *232*(June), 111273. https://doi.org/10.1016/j.rse.2019.111273

Oehri, J., Schmid, B., Schaepman-Strub, G., & Niklaus, P. A. (2017). Biodiversity promotes primary productivity and growing season lengthening at the landscape scale. *Proceedings of the National Academy of Sciences of the United States of America*, *114*(38), 10160–10165. https://doi.org/10.1073/PNAS.1703928114/SUPPL_FILE/PNAS.201703928SI.PDF

Oliveira, B. F., Moore, F. C., & Dong, X. (2022). Biodiversity mediates ecosystem sensitivity to climate variability. *Communications Biology*, *5*(1). https://doi.org/10.1038/s42003-022-03573-9

O'Mara, F. P. (2012). The role of grasslands in food security and climate change. *Annals of Botany*, *110*(6), 1263–1270. https://doi.org/10.1093/aob/mcs209

Orwin, K. H., Buckland, S. M., Johnson, D., Turner, B. L., Smart, S., Oakley, S., & Bardgett, R. D. (2010). Linkages of plant traits to soil properties and the functioning of temperate grassland. *Journal of Ecology*, *98*(5), 1074–1083. https://doi.org/10.1111/j.1365-2745.2010.01679.x

Parnell, J. J., & Blevins, K. (2022). *TOS SCIENCE DESIGN FOR TERRESTRIAL MICROBIAL DIVERSITY PREPARED BY*.

Paruelo, J. M., & Lauenroth, W. K. (1995). Regional patterns of normalized difference vegetation index in North American shrublands and grasslands. *Ecology*, *76*(6), 1888–1898. https://doi.org/10.2307/1940721

Paruelo, J. M., Texeira, M., Staiano, L., Mastrángelo, M., Amdan, L., & Gallego, F. (2016). An integrative index of Ecosystem Services provision based on remotely sensed data. *Ecological Indicators*, *71*, 145–154. https://doi.org/10.1016/j.ecolind.2016.06.054

Pasari, J. R., Levi, T., Zavaleta, E. S., & Tilman, D. (2013). Several scales of biodiversity affect ecosystem multifunctionality. *Proceedings of the National Academy of Sciences of the United States of America*, *110*(25), 10219–10222. https://doi.org/10.1073/pnas.1220333110

Pau, S., Nippert, J. B., Slapikas, R., Griffith, D., Bachle, S., Helliker, B. R., O'Connor, R. C., Riley, W. J., Still, C. J., & Zaricor, M. (2022). Poor relationships between NEON Airborne Observation Platform data and field-based vegetation traits at a mesic grassland. *Ecology*, *103*(2). https://doi.org/10.1002/ECY.3590

Peng, Y., Feng, J., Sang, W., & Axmacher, J. C. (2022). Geographical divergence of species richness and local homogenization of plant assemblages due to climate change in grasslands. *Biodiversity and Conservation*, *0123456789*. https://doi.org/10.1007/s10531-022-02364-2

Pereira, H. M. ;, Ferrier, S., Walters, M., G. N. Geller, R. H. G. Jongman, R. J. S., Bruford, M. W., N. Brummitt, S. H. M. B., Cardoso, A. C., N. C. Coops, E. D., Faith, D. P., Freyhof, J., R. D. Gregory, C. Heip, R. H., G. Hurtt, W. J., D. S. Karp, M. A. M., Obura, D., Onoda, Y., Pettorelli, N., Reyers, B., Sayre, R., J. P. W. Scharlemann, S. N. S., … M. Walpole, M. W. (2013). Essential Biodiversity Variables. *Science*, *339*(January 2013), 277–278.

Pérez-Ramos, I. M., Roumet, C., Cruz, P., Blanchard, A., Autran, P., & Garnier, E. (2012). Evidence for a "plant community economics spectrum" driven by nutrient and water limitations in a Mediterranean rangeland of southern France. *Journal of Ecology*, *100*(6), 1315–1327. https://doi.org/10.1111/1365-2745.12000

Pettorelli, N., Safi, K., & Turner, W. (2014). Satellite remote sensing, biodiversity research and conservation of the future. *Philosophical Transactions of the Royal Society B: Biological Sciences*, *369*(1643). https://doi.org/10.1098/rstb.2013.0190

Pettorelli, N., Schulte to Bühne, H., Tulloch, A., Dubois, G., Macinnis-Ng, C., Queirós, A. M., Keith, D. A., Wegmann, M., Schrodt, F., Stellmes, M., Sonnenschein, R., Geller, G. N., Roy, S., Somers, B., Murray, N., Bland, L., Geijzendorffer, I., Kerr, J. T., Broszeit, S., …

Nicholson, E. (2018a). Satellite remote sensing of ecosystem functions: opportunities, challenges and way forward. *Remote Sensing in Ecology and Conservation*, *4*(2), 71–93. https://doi.org/10.1002/rse2.59

Pettorelli, N., Schulte to Bühne, H., Tulloch, A., Dubois, G., Macinnis-Ng, C., Queirós, A. M., Keith, D. A., Wegmann, M., Schrodt, F., Stellmes, M., Sonnenschein, R., Geller, G. N., Roy, S., Somers, B., Murray, N., Bland, L., Geijzendorffer, I., Kerr, J. T., Broszeit, S., … Nicholson, E. (2018b). Satellite remote sensing of ecosystem functions: opportunities, challenges and way forward. *Remote Sensing in Ecology and Conservation*, *4*(2), 71–93. https://doi.org/10.1002/rse2.59

Pettorelli, N., Vik, J. O., Mysterud, A., Gaillard, J. M., Tucker, C. J., & Stenseth, N. C. (2005). Using the satellite-derived NDVI to assess ecological responses to environmental change. *Trends in Ecology and Evolution*, *20*(9), 503–510. https://doi.org/10.1016/j.tree.2005.05.011

Pierce, S., Ceriani, R. M., De Andreis, R., Luzzaro, A., & Cerabolini, B. (2007). The leaf economics spectrum of Poaceae reflects variation in survival strategies. *Plant Biosystems*, *141*(3), 337–343. https://doi.org/10.1080/11263500701627695

Ploton, P., Mortier, F., Réjou-Méchain, M., Barbier, N., Picard, N., Rossi, V., Dormann, C., Cornu, G., Viennois, G., Bayol, N., Lyapustin, A., Gourlet-Fleury, S., & Pélissier, R. (2020). Spatial validation reveals poor predictive performance of large-scale ecological mapping models. *Nature Communications*, *11*(1). https://doi.org/10.1038/s41467-020-18321-y

Pommier, T., Cantarel, A. A. M., Grigulis, K., Lavorel, S., Legay, N., Baxendale, C., Bardgett, R. D., Bahn, M., Poly, F., & Clément, J. C. (2018). The added value of including key microbial traits to determine nitrogen-related ecosystem services in managed grasslands. *Journal of Applied Ecology*, *55*(1), 49–58. https://doi.org/10.1111/1365-2664.13010

Poorter, H., Lambers, H., & Evans, J. R. (2014). Trait correlation networks: A whole-plant perspective on the recently criticized leaf economic spectrum. *New Phytologist*, *201*(2), 378–382. https://doi.org/10.1111/nph.12547

Porazinska, Dorota L., Farrer, Emily C., Spasojevic , Marko J., C. P. B. de M. S. A. S. J. G. S. C. T. W. A. J. K. K. N. S. S. K. (2018). *Plant diversity and density predict belowground diversity and function in an early successional alpine ecosystem*. *99*(9), 1942–1952. https://doi.org/10.1002/ecy.2420

Punalekar, S. M., Verhoef, A., Quaife, T. L., Humphries, D., Bermingham, L., & Reynolds, C. K. (2018). Application of Sentinel-2A data for pasture biomass monitoring using a physically based radiative transfer model. *Remote Sensing of Environment*, *218*(October 2017), 207–220. https://doi.org/10.1016/j.rse.2018.09.028

Qi, J., Chehbouni, A., Huete, A. R., Kerr, Y. H., & Sorooshian, S. (1994). A modified soil adjusted vegetation index. *Remote Sensing of Environment*, *48*(2), 119–126. https://doi.org/10.1016/0034-4257(94)90134-1

Quideau, S. A., McIntosh, A. C. S., Norris, C. E., Lloret, E., Swallow, M. J. B., & Hannam, K. (2016). Extraction and Analysis of Microbial Phospholipid Fatty Acids in Soils. *Journal of Visualized Experiments*, *114*, 1–9. https://doi.org/10.3791/54360

Radujković, D., Verbruggen, E., Seabloom, E. W., Bahn, M., Biederman, L. A., Borer, E. T., Boughton, E. H., Catford, J. A., Campioli, M., Donohue, I., Ebeling, A., Eskelinen, A., Fay, P. A., Hansart, A., Knops, J. M. H., MacDougall, A. S., Ohlert, T., Olde Venterink, H.,

Raynaud, X., … Vicca, S. (2021). Soil properties as key predictors of global grassland production: Have we overlooked micronutrients? *Ecology Letters*, *24*(12), 2713–2725. https://doi.org/10.1111/ELE.13894

Räsänen, A., Manninen, T., Korkiakoski, M., Lohila, A., & Virtanen, T. (2021). Predicting catchment-scale methane fluxes with multi-source remote sensing. *Landscape Ecology*, *0123456789*. https://doi.org/10.1007/s10980-021-01194-x

Ratajczak, Z., Nippert, J. B., & Collins, S. L. (2012). Woody encroachment decreases diversity across North American grasslands and savannas. *Ecology*, *93*(4), 697–703. https://doi.org/10.1890/11-1199.1

Ratnam, J., Bond, W. J., Fensham, R. J., Hoffmann, W. A., Archibald, S., Lehmann, C. E. R., Anderson, M. T., Higgins, S. I., & Sankaran, M. (2011). When is a 'forest' a savanna, and why does it matter? *Global Ecology and Biogeography*, *20*(5), 653–660. https://doi.org/10.1111/J.1466-8238.2010.00634.X

Reich, P. B. (2014). The world-wide "fast-slow" plant economics spectrum: A traits manifesto. *Journal of Ecology*, *102*(2), 275–301. https://doi.org/10.1111/1365-2745.12211

Reichstein, M., Bahn, M., Mahecha, M. D., Kattge, J., & Baldocchi, D. D. (2014). Linking plant and ecosystem functional biogeography. *Proceedings of the National Academy of Sciences of the United States of America*, *111*(38), 13697–13702. https://doi.org/10.1073/pnas.1216065111

Reinermann, S., Asam, S., & Kuenzer, C. (2020). Remote sensing of grassland production and management-A review. In *Remote Sensing* (Vol. 12, Issue 12). https://doi.org/10.3390/rs12121949

Ren, H., & Feng, G. (2015). Are soil-adjusted vegetation indices better than soil-unadjusted vegetation indices for above-ground green biomass estimation in arid and semi-arid grasslands? *Grass and Forage Science*, *70*(4), 611–619. https://doi.org/10.1111/gfs.12152

Revill, A., Florence, A., MacArthur, A., Hoad, S., Rees, R., & Williams, M. (2019). The Value of Sentinel-2 Spectral Bands for the Assessment of Winter Wheat Growth and Development. *Remote Sensing*, *11*(17), 2050. https://doi.org/10.3390/rs11172050

Risch, A. C., Zimmermann, S., Ochoa-Hueso, R., Schütz, M., Frey, B., Firn, J. L., Fay, P. A., Hagedorn, F., Borer, E. T., Seabloom, E. W., Harpole, W. S., Knops, J. M. H., McCulley, R. L., Broadbent, A. A. D., Stevens, C. J., Silveira, M. L., Adler, P. B., Báez, S., Biederman, L. A., … Moser, B. (2019). Soil net nitrogen mineralisation across global grasslands. *Nature Communications*, *10*(1), 1–10. https://doi.org/10.1038/s41467-019-12948-2

Rivero, R. G., Grunwald, S., Binford, M. W., & Osborne, T. Z. (2009). Integrating spectral indices into prediction models of soil phosphorus in a subtropical wetland. *Remote Sensing of Environment*, *113*(11), 2389–2402. https://doi.org/10.1016/J.RSE.2009.07.015

Rocchini, D., Luque, S., Pettorelli, N., Bastin, L., Doktor, D., Faedi, N., Feilhauer, H., Féret, J. B., Foody, G. M., Gavish, Y., Godinho, S., Kunin, W. E., Lausch, A., Leitão, P. J., Marcantonio, M., Neteler, M., Ricotta, C., Schmidtlein, S., Vihervaara, P., … Nagendra, H. (2018). Measuring β-diversity by remote sensing: A challenge for biodiversity monitoring. *Methods in Ecology and Evolution*, *9*(8), 1787–1798. https://doi.org/10.1111/2041-210X.12941

Rocchini, D., McGlinn, D., Ricotta, C., Neteler, M., & Wohlgemuth, T. (2011). Landscape complexity and spatial scale influence the relationship between remotely sensed spectral diversity and survey-based plant species richness. *Journal of Vegetation Science*, *22*(4), 688–698. https://doi.org/10.1111/j.1654-1103.2010.01250.x

Rocchini, D., Salvatori, N., Beierkuhnlein, C., Chiarucci, A., de Boissieu, F., Förster, M., Garzon-Lopez, C. X., Gillespie, T. W., Hauffe, H. C., He, K. S., Kleinschmit, B., Lenoir, J., Malavasi, M., Moudrý, V., Nagendra, H., Payne, D., Šímová, P., Torresani, M., Wegmann, M., & Féret, J. B. (2021a). From local spectral species to global spectral communities: A benchmark for ecosystem diversity estimate by remote sensing. *Ecological Informatics*, *61*(November 2020). https://doi.org/10.1016/j.ecoinf.2020.101195

Rocchini, D., Salvatori, N., Beierkuhnlein, C., Chiarucci, A., de Boissieu, F., Förster, M., Garzon-Lopez, C. X., Gillespie, T. W., Hauffe, H. C., He, K. S., Kleinschmit, B., Lenoir, J., Malavasi, M., Moudrý, V., Nagendra, H., Payne, D., Šímová, P., Torresani, M., Wegmann, M., & Féret, J. B. (2021b). From local spectral species to global spectral communities: A benchmark for ecosystem diversity estimate by remote sensing. *Ecological Informatics*, *61*(November 2020). https://doi.org/10.1016/j.ecoinf.2020.101195

Rossi, C., Kneubühler, M., Schütz, M., Schaepman, M. E., Haller, R. M., & Risch, A. C. (2020). From local to regional: Functional diversity in differently managed alpine grasslands. *Remote Sensing of Environment*. https://doi.org/10.1016/j.rse.2019.111415

Rossi, C., Kneubühler, M., Schütz, M., Schaepman, M. E., Haller, R. M., & Risch, A. C. (2021). Remote sensing of spectral diversity: A new methodological approach to account for spatio-temporal dissimilarities between plant communities. *Ecological Indicators*, *130*, 108106. https://doi.org/10.1016/j.ecolind.2021.108106

Rossi, C., Kneubühler, M., Schütz, M., Schaepman, M. E., Haller, R. M., & Risch, A. C. (2022). Spatial resolution, spectral metrics and biomass are key aspects in estimating plant species richness from spectral diversity in species-rich grasslands. *Remote Sensing in Ecology and Conservation*, *8*(3), 297–314. https://doi.org/10.1002/rse2.244

Saetre, P., & Bååth, E. (2000). Spatial variation and patterns of soil microbial community structure in a mixed spruce-birch stand. *Soil Biology and Biochemistry*, *32*(7), 909–917. https://doi.org/10.1016/S0038-0717(99)00215-1

Sanchez, G. (2013). *PLS Path Modeling with R*.

Schellberg, J., & Pontes, L. da S. (2012). Plant functional traits and nutrient gradients on grassland. *Grass and Forage Science*, *67*(3), 305–319. https://doi.org/10.1111/J.1365-2494.2012.00867.X

Schimel, D., Pavlick, R., Fisher, J. B., Asner, G. P., Saatchi, S., Townsend, P., Miller, C., Frankenberg, C., Hibbard, K., & Cox, P. (2015). Observing terrestrial ecosystems and the carbon cycle from space. *Global Change Biology*, *21*(5), 1762–1776. https://doi.org/10.1111/gcb.12822

Schirpke, U., Kohler, M., Leitinger, G., Fontana, V., Tasser, E., & Tappeiner, U. (2017). Future impacts of changing land-use and climate on ecosystem services of mountain grassland and their resilience. *Ecosystem Services*, *26*, 79–94. https://doi.org/10.1016/j.ecoser.2017.06.008

Schittko, C., Onandia, G., Bernard-Verdier, M., Heger, T., Jeschke, J. M., Kowarik, I., Maaß, S., & Joshi, J. (2022). Biodiversity maintains soil multifunctionality and soil organic

carbon in novel urban ecosystems. *Journal of Ecology*, *110*(4), 916–934. https://doi.org/10.1111/1365-2745.13852

Schneider, F. D., Morsdorf, F., Schmid, B., Petchey, O. L., Hueni, A., Schimel, D. S., & Schaepman, M. E. (2017). Mapping functional diversity from remotely sensed morphological and physiological forest traits. *Nature Communications*, *8*(1). https://doi.org/10.1038/s41467-017-01530-3

Schweiger, A. K., Cavender-Bares, J., Townsend, P. A., Hobbie, S. E., Madritch, M. D., Wang, R., Tilman, D., & Gamon, J. A. (2018). Plant spectral diversity integrates functional and phylogenetic components of biodiversity and predicts ecosystem function. *Nature Ecology and Evolution*, *2*(6), 976–982. https://doi.org/10.1038/s41559-018-0551-1

Sexton, J. O., Noojipady, P., Song, X. P., Feng, M., Song, D. X., Kim, D. H., Anand, A., Huang, C., Channan, S., Pimm, S. L., & Townshend, J. R. (2015). Conservation policy and the measurement of forests. *Nature Climate Change 2015 6:2*, *6*(2), 192–196. https://doi.org/10.1038/nclimate2816

Shabbir, Z., Sardar, A., Shabbir, A., Abbas, G., Shamshad, S., Khalid, S., Murtaza, G., Dumat, C., & Shahid, M. (2020). *Copper uptake, essentiality, toxicity, detoxification and risk assessment in soil-plant environment*. https://doi.org/10.1016/j.chemosphere.2020.127436

Shao, C., Shuai, Y., Wu, H., Deng, X., Zhang, X., & Xu, A. (2023). Development of a Spectral Index for the Detection of Yellow-Flowering Vegetation. *Remote Sensing 2023, Vol. 15, Page 1725*, *15*(7), 1725. https://doi.org/10.3390/RS15071725

Shipley, B., Lechowicz, M. J., Wright, I., & Reich, P. B. (2006). Fundamental trade-offs generating the worldwide leaf economics spectrum. *Ecology*, *87*(3), 535–541. https://doi.org/10.1890/05-1051

Siefert, A., Violle, C., Chalmandrier, L., Albert, C. H., Taudiere, A., Fajardo, A., Aarssen, L. W., Baraloto, C., Carlucci, M. B., Cianciaruso, M. V., de L. Dantas, V., de Bello, F., Duarte, L. D. S., Fonseca, C. R., Freschet, G. T., Gaucherand, S., Gross, N., Hikosaka, K., Jackson, B., … Wardle, D. A. (2015). A global meta-analysis of the relative extent of intraspecific trait variation in plant communities. In *Ecology Letters* (Vol. 18, Issue 12, pp. 1406–1419). https://doi.org/10.1111/ele.12508

Singh, A., Serbin, S. P., McNeil, B. E., Kingdon, C. C., & Townsend, P. A. (2015). Imaging spectroscopy algorithms for mapping canopy foliar chemical and morphological traits and their uncertainties. *Ecological Applications*, *25*(8), 2180–2197. https://doi.org/10.1890/14-2098.1

Singh, R., Patel, N. R., & Danodia, A. (2022). Deriving Phenological Metrics from Landsat-OLI for Sugarcane Crop Type Mapping: A Case Study in North India. *Journal of the Indian Society of Remote Sensing*, *50*(6), 1021–1030. https://doi.org/10.1007/S12524-022-01515-W/TABLES/1

Soliveres, S., Maestre, F. T., Eldridge, D. J., Delgado-Baquerizo, M., Quero, J. L., Bowker, M. A., & Gallardo, A. (2014). Plant diversity and ecosystem multifunctionality peak at intermediate levels of woody cover in global drylands. *Global Ecology and Biogeography*, *23*(12), 1408–1416. https://doi.org/10.1111/GEB.12215/SUPPINFO

Soliveres, S., Manning, P., Prati, D., Gossner, M. M., Alt, F., Arndt, H., Baumgartner, V., Binkenstein, J., Birkhofer, K., Blaser, S., Blüthgen, N., Boch, S., Böhm, S., Börschig, C., Buscot, F., Diekötter, T., Heinze, J., Hölzel, N., Jung, K., … Allan, E. (2016). Locally rare

species influence grassland ecosystem multifunctionality. *Philosophical Transactions of the Royal Society B: Biological Sciences*, *371*(1694). https://doi.org/10.1098/rstb.2015.0269

Sousa, D., Fisher, J. B., Galvan, F. R., Pavlick, R. P., & Cordell, S. (2021). *Tree Canopies Reflect Mycorrhizal Composition*. 1–9. https://doi.org/10.1029/2021GL092764

Stumpf, F., Schneider, M. K., Keller, A., Mayr, A., Rentschler, T., Meuli, R. G., Schaepman, M., & Liebisch, F. (2020). Spatial monitoring of grassland management using multi-temporal satellite imagery. *Ecological Indicators*, *113*(February), 106201. https://doi.org/10.1016/j.ecolind.2020.106201

Suding, K. N., Golding, D. E., & Hartman, K. M. (2003). RELATIONSHIPS AMONG SPECIES TRAITS: SEPARATING LEVELS OF RESPONSE AND IDENTIFYING LINKAGES TO ABUNDANCE. *Ecology*, *84*(June 2000), 1–16.

Svoray, T., Perevolotsky, A., & Atkinson, P. M. (2013). Ecological sustainability in rangelands: The contribution of remote sensing. *International Journal of Remote Sensing*, *34*(17), 6216–6242. https://doi.org/10.1080/01431161.2013.793867

Tan, X., Shan, Y., Wang, X., Liu, R., & Yao, Y. (2022). Comparison of the predictive ability of spectral indices for commonly used species diversity indices and Hill numbers in wetlands. *Ecological Indicators*, *142*(April), 109233. https://doi.org/10.1016/j.ecolind.2022.109233

Tardy, V., Spor, A., Mathieu, O., Lévèque, J., Terrat, S., Plassart, P., Regnier, T., Bardgett, R. D., van der Putten, W. H., Roggero, P. P., Seddaiu, G., Bagella, S., Lemanceau, P., Ranjard, L., & Maron, P. A. (2015). Shifts in microbial diversity through land use intensity as drivers of carbon mineralization in soil. *Soil Biology and Biochemistry*, *90*, 204–213. https://doi.org/10.1016/j.soilbio.2015.08.010

Thompson, P. L., Isbell, F., Loreau, M., O'connor, M. I., & Gonzalez, A. (2018). The strength of the biodiversity-ecosystem function relationship depends on spatial scale. *Proceedings of the Royal Society B: Biological Sciences*, *285*(1880), 1–9. https://doi.org/10.1098/rspb.2018.0038

Thomson, E. R., Spiegel, M. P., Althuizen, I. H. J., Bass, P., Chen, S., Chmurzynski, A., Halbritter, A. H., Henn, J. J., Jónsdóttir, I. S., Klanderud, K., Li, Y., Maitner, B. S., Michaletz, S. T., Niittynen, P., Roos, R. E., Telford, R. J., Enquist, B. J., Vandvik, V., Macias-Fauria, M., & Malhi, Y. (2021). Multiscale mapping of plant functional groups and plant traits in the High Arctic using field spectroscopy, UAV imagery and Sentinel-2A data. *Environmental Research Letters*, *16*(5). https://doi.org/10.1088/1748-9326/abf464

Thorpe, A. S., Barnett, D. T., Elmendorf, S. C., Hinckley, E. L. S., Hoekman, D., Jones, K. D., Levan, K. E., Meier, C. L., Stanish, L. F., & Thibault, K. M. (2016). Introduction to the sampling designs of the National Ecological Observatory Network Terrestrial Observation System. *Ecosphere*, *7*(12), e01627. https://doi.org/10.1002/ECS2.1627

Thouverai, E., Marcantonio, M., Bacaro, G., Re, D. Da, Iannacito, M., Marchetto, E., Ricotta, C., Tattoni, C., Vicario, S., & Rocchini, D. (2021). Measuring diversity from space: a global view of the free and open source rasterdiv R package under a coding perspective. *Community Ecology*, *22*(1), 1–11. https://doi.org/10.1007/s42974-021-00042-x

Tian, D., Xiang, Y., Seabloom, E., Chen, H. Y. H., Wang, J., Yu, G., Deng, Y., Li, Z., & Niu, S. (2022). Ecosystem restoration and belowground multifunctionality: A network view. *Ecological Applications*. https://doi.org/10.1002/EAP.2575

Tilman, D., Reich, P. B., & Knops, J. M. H. (2006). Biodiversity and ecosystem stability in a decade-long grassland experiment. *Nature*, *441*(7093), 629–632. https://doi.org/10.1038/nature04742

Tuanmu, M. N., & Jetz, W. (2015). A global, remote sensing-based characterization of terrestrial habitat heterogeneity for biodiversity and ecosystem modelling. *Global Ecology and Biogeography*, *24*(11), 1329–1339. https://doi.org/10.1111/geb.12365

Ustin, S. L., Asner, G. P., Gamon, J. A., Fred Huemmrich, K., Jacquemoud, S., Schaepman, M., & Zarco-Tejada, P. (2009). Retrieval of quantitative and qualitative information about plant pigment systems from high resolution spectroscopy. *International Geoscience and Remote Sensing Symposium (IGARSS)*, *113*, 1996–1999. https://doi.org/10.1109/IGARSS.2006.517

Ustin, S. L., Valko, P. G., Kefauver, S. C., Santos, M. J., Zimpfer, J. F., & Smith, S. D. (2009). Remote sensing of biological soil crust under simulated climate change manipulations in the Mojave Desert. *Remote Sensing of Environment*, *113*(2), 317–328. https://doi.org/10.1016/j.rse.2008.09.013

Van Cleemput, E., Vanierschot, L., Fernández-Castilla, B., Honnay, O., & Somers, B. (2018). The functional characterization of grass- and shrubland ecosystems using hyperspectral remote sensing: trends, accuracy and moderating variables. *Remote Sensing of Environment*, *209*(January), 747–763. https://doi.org/10.1016/j.rse.2018.02.030

van den Hoogen, J., Geisen, S., Routh, D., Ferris, H., Traunspurger, W., Wardle, D. A., de Goede, R. G. M., Adams, B. J., Ahmad, W., Andriuzzi, W. S., Bardgett, R. D., Bonkowski, M., Campos-Herrera, R., Cares, J. E., Caruso, T., de Brito Caixeta, L., Chen, X., Costa, S. R., Creamer, R., … Crowther, T. W. (2019). Soil nematode abundance and functional group composition at a global scale. *Nature*, *572*(7768), 194–198. https://doi.org/10.1038/s41586-019-1418-6

Van Der Heijden, M. G. A., Bardgett, R. D., & Van Straalen, N. M. (2008). The unseen majority: Soil microbes as drivers of plant diversity and productivity in terrestrial ecosystems. *Ecology Letters*, *11*(3), 296–310. https://doi.org/10.1111/j.1461-0248.2007.01139.x

van der Putten, W. H., Bradford, M. A., Pernilla Brinkman, E., van de Voorde, T. F. J., & Veen, G. F. (2016). Where, when and how plant–soil feedback matters in a changing world. *Functional Ecology*, *30*(7), 1109–1121. https://doi.org/10.1111/1365-2435.12657

Vazquez, C., de Goede, R. G. M., Rutgers, M., de Koeijer, T. J., & Creamer, R. E. (2021). Assessing multifunctionality of agricultural soils: Reducing the biodiversity trade-off. *European Journal of Soil Science*, *72*(4), 1624–1639. https://doi.org/10.1111/EJSS.13019

Veldman, J. W., Buisson, E., Durigan, G., Fernandes, G. W., Le Stradic, S., Mahy, G., Negreiros, D., Overbeck, G. E., Veldman, R. G., Zaloumis, N. P., Putz, F. E., & Bond, W. J. (2015). Toward an old-growth concept for grasslands, savannas, and woodlands. *Frontiers in Ecology and the Environment*, *13*(3), 154–162. https://doi.org/10.1890/140270

Vermote, E., Justice, C., Claverie, M., & Franch, B. (2016). Preliminary analysis of the performance of the Landsat 8/OLI land surface reflectance product. *Remote Sensing of Environment*, *185*, 46–56. https://doi.org/10.1016/J.RSE.2016.04.008

Violle, C., Enquist, B. J., McGill, B. J., Jiang, L., Albert, C. H., Hulshof, C., Jung, V., & Messier, J. (2012). The return of the variance: Intraspecific variability in community ecology. *Trends in Ecology and Evolution*, *27*(4), 244–252. https://doi.org/10.1016/j.tree.2011.11.014

Wagg, C., Bender, S. F., Widmer, F., & van der Heijden, M. G. A. (2014). Soil biodiversity and soil community composition determine ecosystem multifunctionality. *Proceedings of the National Academy of Sciences*, *111*(14), 5266–5270. https://doi.org/10.1073/pnas.1320054111

Wakeling, I. N., & Morris, J. J. (1993). A test of significance for partial least squares regression. *Journal of Chemometrics*, *7*(4), 291–304. https://doi.org/10.1002/CEM.1180070407

Wall, D. H., Bardgett, R. D., & Kelly, E. (2010). Biodiversity in the dark. In *Nature Geoscience* (Vol. 3, Issue 5, pp. 297–298). Nature Publishing Group. https://doi.org/10.1038/ngeo860

Wallis, C. I. B., Homeier, J., Peña, J., Brandl, R., Farwig, N., & Bendix, J. (2019). Modeling tropical montane forest biomass, productivity and canopy traits with multispectral remote sensing data. *Remote Sensing of Environment*, *225*(January), 77–92. https://doi.org/10.1016/j.rse.2019.02.021

Wang, C., Wang, N., Zhu, J., Liu, Y., Xu, X., Niu, S., Yu, G., Han, X., & He, N. (2018). Soil gross N ammonification and nitrification from tropical to temperate forests in eastern China. *Functional Ecology*, *32*(1), 83–94. https://doi.org/10.1111/1365-2435.13024/SUPPINFO

Wang, R., & Gamon, J. A. (2019). Remote sensing of terrestrial plant biodiversity. *Remote Sensing of Environment*, *231*(December 2018), 111218. https://doi.org/10.1016/j.rse.2019.111218

Wang, R., Gamon, J. A., Emmerton, C. A., Li, H., Nestola, E., Pastorello, G. Z., & Menzer, O. (2016). Integrated analysis of productivity and biodiversity in a southern Alberta prairie. *Remote Sensing*, *8*(3), 1–20. https://doi.org/10.3390/rs8030214

Wang, R., Gamon, J. A., Montgomery, R. A., Townsend, P. A., Zygielbaum, A. I., Bitan, K., Tilman, D., & Cavender-Bares, J. (2016). Seasonal variation in the NDVI-species richness relationship in a prairie grassland experiment (cedar creek). *Remote Sensing*, *8*(2). https://doi.org/10.3390/rs8020128

Wang, R., Gamon, J. A., Schweiger, A. K., Cavender-Bares, J., Townsend, P. A., Zygielbaum, A. I., & Kothari, S. (2018a). Influence of species richness, evenness, and composition on optical diversity: A simulation study. *Remote Sensing of Environment*, *211*(September 2017), 218–228. https://doi.org/10.1016/j.rse.2018.04.010

Wang, R., Gamon, J. A., Schweiger, A. K., Cavender-Bares, J., Townsend, P. A., Zygielbaum, A. I., & Kothari, S. (2018b). Influence of species richness, evenness, and composition on optical diversity: A simulation study. *Remote Sensing of Environment*, *211*(September 2017), 218–228. https://doi.org/10.1016/j.rse.2018.04.010

Wang, Z., Chlus, A., Geygan, R., Ye, Z., Zheng, T., Singh, A., Couture, J. J., Cavender-Bares, J., Kruger, E. L., & Townsend, P. A. (2020). Foliar functional traits from imaging

spectroscopy across biomes in eastern North America. *New Phytologist*. https://doi.org/10.1111/nph.16711

Wang, Z., Townsend, P. A., Schweiger, A. K., Couture, J. J., Singh, A., Hobbie, S. E., & Cavender-Bares, J. (2019). Mapping foliar functional traits and their uncertainties across three years in a grassland experiment. Remote Sensing of Environment. *Remote Sensing of Environment*, *221*(July 2018), 405–416. https://doi.org/10.1016/j.rse.2018.11.016

Wardle David A., Bardgett Richard D., Klironomos John N., Setälä Heikki, van der Putten Wim H., & Wall Diana H. (2004). Ecological Linkages Between Aboveground and Belowground Biota . *Science*, *304*(June), 1629–1633.

Weber, D., Schaepman-Strub, G., & Ecker, K. (2018). Predicting habitat quality of protected dry grasslands using Landsat NDVI phenology. *Ecological Indicators*, *91*(February), 447–460. https://doi.org/10.1016/j.ecolind.2018.03.081

Weintraub, S. (2022). *NEON User Guide to Plant foliar traits (DP1.10026.001) D*.

Westoby, M., Reich, P. B., & Wright, I. J. (2013). Understanding ecological variation across species: Area-based vs mass-based expression of leaf traits. *New Phytologist*, *199*(2), 322–323. https://doi.org/10.1111/nph.12345

White, J. G., & Zasoski, R. J. (1999). Mapping soil micronutrients. *Field Crops Research*, *60*(1–2), 11–26. https://doi.org/10.1016/S0378-4290(98)00130-0

White, R., Murray, S., & Rohweder, M. (2000). *Pilot Analysis of Global Ecosystems - Grassland Ecosystems*. https://doi.org/10.1021/es0032881

Willers, C., Jansen van Rensburg, P. J., & Claassens, S. (2015). Phospholipid fatty acid profiling of microbial communities-a review of interpretations and recent applications. *Journal of Applied Microbiology*, *119*(5), 1207–1218. https://doi.org/10.1111/jam.12902

Wilson, C. H., Caughlin, T. T., Rifai, S. W., Boughton, E. H., Mack, M. C., & Flory, S. L. (2017). Multi-decadal time series of remotely sensed vegetation improves prediction of soil carbon in a subtropical grassland. *Ecological Applications*, *27*(5), 1646–1656. https://doi.org/10.1002/EAP.1557

Wilson, C. H., Strickland, M. S., Hutchings, J. A., Bianchi, T. S., & Flory, S. L. (2018). Grazing enhances belowground carbon allocation, microbial biomass, and soil carbon in a subtropical grassland. *Global Change Biology*, *24*(7), 2997–3009. https://doi.org/10.1111/GCB.14070

Wold, S., Sjöström, M., & Eriksson, L. (2001). PLS-regression: a basic tool of chemometrics. *Chemometrics and Intelligent Laboratory Systems*, *58*(2), 109–130. https://doi.org/10.1016/S0169-7439(01)00155-1

Wright, I. J., Reich, P. B., Ackerly, D. D., Cornelissen, J. H. C., Westoby, M., Baruch, Z., Bongers, F., Cavender-Bares, J., Chapin, T., Diemer, M., & Others. (2004). The worldwide leaf economics spectrum. *Nature*, *428*, 821–827.

Wright, J. P., & Sutton-Grier, A. (2012). Does the leaf economic spectrum hold within local species pools across varying environmental conditions? *Functional Ecology*, *26*(6), 1390–1398. https://doi.org/10.1111/1365-2435.12001

Wulder, M. A., Roy, D. P., Radeloff, V. C., Loveland, T. R., Anderson, M. C., Johnson, D. M., Healey, S., Zhu, Z., Scambos, T. A., Pahlevan, N., Hansen, M., Gorelick, N., Crawford, C. J., Masek, J. G., Hermosilla, T., White, J. C., Belward, A. S., Schaaf, C., Woodcock, C. E.,

... Cook, B. D. (2022). Fifty years of Landsat science and impacts. In *Remote Sensing of Environment* (Vol. 280, Issue April, p. 113195). Elsevier Inc. https://doi.org/10.1016/j.rse.2022.113195

Xu, C., Zeng, Y., Zheng, Z., Zhao, D., Liu, W., Ma, Z., & Wu, B. (2022). Assessing the Impact of Soil on Species Diversity Estimation Based on UAV Imaging Spectroscopy in a Natural Alpine Steppe. *Remote Sensing*, *14*(3). https://doi.org/10.3390/rs14030671

Xu, Y., Dong, K., Jiang, M., Liu, Y., He, L., Wang, J., Zhao, N., & Gao, Y. (2022). Soil moisture and species richness interactively affect multiple ecosystem functions in a microcosm experiment of simulated shrub encroached grasslands. *Science of The Total Environment*, *803*, 149950. https://doi.org/10.1016/J.SCITOTENV.2021.149950

Yan, J., Zhang, G., Ling, H., & Han, F. (2022). Comparison of time-integrated NDVI and annual maximum NDVI for assessing grassland dynamics. *Ecological Indicators*, *136*, 108611. https://doi.org/10.1016/J.ECOLIND.2022.108611

Yan, Y., Zhang, Q., Buyantuev, A., Liu, Q., & Niu, J. (2020). Plant functional β diversity is an important mediator of effects of aridity on soil multifunctionality. *Science of the Total Environment*, *726*. https://doi.org/10.1016/J.SCITOTENV.2020.138529

Yang, F., Wu, J., Zhang, D., Chen, Q., Zhang, Q., & Cheng, X. (2018). Soil bacterial community composition and diversity in relation to edaphic properties and plant traits in grasslands of southern China. *Applied Soil Ecology*, *128*(November 2017), 43–53. https://doi.org/10.1016/j.apsoil.2018.04.001

Zaret, M. M., Kuhs, M. A., Anderson, J. C., Seabloom, E. W., Borer, E. T., & Kinkel, L. L. (2022). Seasonal shifts from plant diversity to consumer control of grassland productivity. In *Ecology Letters* (Vol. 25, Issue 5, pp. 1215–1224). https://doi.org/10.1111/ele.13993

Zemunik, G., Turner, B. L., Lambers, H., & Laliberté, E. (2016). Increasing plant species diversity and extreme species turnover accompany declining soil fertility along a long-term chronosequence in a biodiversity hotspot. *Journal of Ecology*, *104*(3), 792–805. https://doi.org/10.1111/1365-2745.12546

Zhao, W., Xiao, C., Li, M., Xu, L., & He, N. (2022). Variation and adaptation in leaf sulfur content across China. *Journal of Plant Ecology*, *15*(4), 743–755. https://doi.org/10.1093/jpe/rtac021

Zhao, Y., Guirado, E., Gaitan, J. J., & Maestre, F. T. (2022). Aridity Thresholds Determine the Relationships between Ecosystem Functioning and Remotely Sensed Indicators Across Patagonia. *IEEE Transactions on Geoscience and Remote Sensing*, *60*. https://doi.org/10.1109/TGRS.2021.3113594

Zhao, Y., Wang, X., Novillo, C. J., Arrogante-Funes, P., Vázquez-Jiménez, R., & Maestre, F. T. (2018). Albedo estimated from remote sensing correlates with ecosystem multifunctionality in global drylands. *Journal of Arid Environments*, *157*, 116–123. https://doi.org/10.1016/J.JARIDENV.2018.05.010

Zhao, Y., Yin, X., Fu, Y., & Yue, T. (2022). A comparative mapping of plant species diversity using ensemble learning algorithms combined with high accuracy surface modeling. *Environmental Science and Pollution Research*, *29*(12), 17878–17891. https://doi.org/10.1007/s11356-021-16973-x

Zomer, R. J., Xu, J., & Trabucco, A. (2022). Version 3 of the Global Aridity Index and Potential Evapotranspiration Database. *Scientific Data 2022 9:1*, *9*(1), 1–15. https://doi.org/10.1038/s41597-022-01493-1

Zwetsloot, M. J., van Leeuwen, J., Hemerik, L., Martens, H., Simó Josa, I., Van de Broek, M., Debeljak, M., Rutgers, M., Sandén, T., Wall, D. P., Jones, A., & Creamer, R. E. (2021). Soil multifunctionality: Synergies and trade-offs across European climatic zones and land uses. *European Journal of Soil Science*, *72*(4), 1640–1654. https://doi.org/10.1111/EJSS.13051

APPENDIX A

Data availability at the 90 Nutrient Network sites (Chapter 5). Including sampling year, ecosystem properties measured and number and year range of Landsat images available at each sampled site. C = soil carbon, N = soil nitrogen, P = soil phosphorus, K = soil potassium, Zn = soil zinc, Fe = soil iron, OM = soil organic matter, AB = aboveground biomass, LT = litter turnover, IR = invasion resistance, PAR = photosynthetically absorbed radiation, PSR = plant species richness

Site	Sampling year	Field measured ecosystem properties	Number of Landsat images	Landsat timeseries year range
ahth.is	2019	C, N, P, K, Zn, Fe, OM, C:N, N:P, AB, LT, IR, PAR, PSR	1038	1984 - 2019
amcamp.us	2007	C, N, P, K, Zn, Fe, OM, C:N, N:P, AB, LT, IR, PAR, PSR	496	1984 - 2007
arch.us	2015	C, N, P, K, Zn, Fe, OM, C:N, N:P, AB, LT, IR, PAR, PSR	886	1984 - 2015
azi.cn	2007	C, N, P, K, Zn, Fe, OM, C:N, N:P, AB, LT, IR, PAR, PSR	902	1986 - 2007
badlau.de	2015	C, N, P, K, Zn, Fe, OM, C:N, N:P, AB, LT, IR, PAR, PSR	930	1984 - 2015
bari.ar	2015	C, N, P, K, Zn, Fe, OM, C:N, N:P, AB, LT, IR, PAR, PSR	855	1984 - 2015
barta.us	2007	C, N, P, K, Zn, Fe, OM, C:N, N:P, AB, LT, IR, PAR, PSR	1070	1984 - 2007
bldr.us	2011	C, N, P, K, Zn, Fe, OM, C:N, N:P, AB, LT, IR, PAR, PSR	2561	1984 - 2011
bnbt.us	2021	C, N, P, K, Zn, Fe, OM, C:N, N:P, AB, LT, IR, PAR, PSR	3699	1984 - 2021
bnch.us	2016	C, N, P, K, Zn, Fe, OM, C:N, N:P, AB, LT, IR, PAR, PSR	3780	1984 - 2016
bogong.au	2012	C, N, P, K, Zn, Fe, OM, C:N, N:P, AB, LT, IR, PAR, PSR	1172	1986 - 2012
bttr.us	2007	C, N, P, K, Zn, Fe, OM, C:N, N:P, AB, LT, IR, PAR, PSR	1007	1984 - 2007
bunya.au	2013	C, N, P, K, Zn, Fe, OM, C:N, N:P, AB, LT, IR, PSR	634	1987 - 2013
burrawan.au	2016	C, N, P, K, Zn, Fe, OM, C:N, N:P, AB, LT, IR, PAR, PSR	1879	1987 - 2016
burren.ie	2015	C, N, P, K, Zn, Fe, OM, C:N, N:P, AB, LT, IR, PAR, PSR	700	1984 - 2015
cammead.us	2021	C, N, P, K, Zn, Fe, OM, C:N, N:P, AB, LT, IR, PAR, PSR	1675	1984 - 2021
cbgb1.us	2011	C, N, P, K, Zn, Fe, OM, C:N, N:P, AB, LT, IR, PAR	3062	1984 - 2016
cbgb2.us	2016	C, N, P, K, Zn, Fe, OM, C:N, N:P, AB, LT, IR, PAR	2980	1984 - 2016
cbgb3.us	2011	C, N, P, K, Zn, Fe, OM, C:N, N:P, AB, LT, IR, PAR	2971	1984 - 2016
cdcr.us	2016	C, N, P, K, Zn, Fe, OM, C:N, N:P, AB, LT, IR, PAR, PSR	2071	1984 - 2016
cdpt.us	2011	C, N, P, K, Zn, Fe, OM, C:N, N:P, AB, LT, IR, PAR, PSR	3490	1984 - 2011
cereep.fr	2018	C, N, P, K, Zn, Fe, OM, C:N, N:P, AB, IR, PAR, PSR	4144	1984 - 2018
chilcas.ar	2016	C, N, P, K, Zn, Fe, OM, C:N, N:P, AB, LT, IR, PAR, PSR	2228	1984 - 2016
comp.pt	2012	C, N, P, K, Zn, Fe, OM, C:N, N:P, AB, IR, PAR, PSR	543	1984 - 2012
cowi.ca	2016	C, N, P, K, Zn, Fe, OM, C:N, N:P, AB, LT, IR, PAR, PSR	3347	1984 - 2016
derr.au	2007	C, N, P, K, Zn, Fe, OM, C:N, N:P, AB, IR, PAR, PSR	842	1986 - 2007
elliot.us	2016	C, N, P, K, Zn, Fe, OM, C:N, N:P, AB, LT, IR, PAR, PSR	2316	1984 - 2016
ethamc.au	2016	C, N, P, K, Zn, Fe, OM, C:N, N:P, AB, IR, PAR, PSR	2657	1987 - 2016
ethass.au	2016	C, N, P, K, Zn, Fe, OM, C:N, N:P, AB, LT, IR, PAR, PSR	2749	1987 - 2016
fnly.us	2007	C, N, P, K, Zn, Fe, OM, C:N, N:P, AB, LT, IR, PAR, PSR	773	1984 - 2007
frue.ch	2011	C, N, P, K, Zn, Fe, OM, C:N, N:P, AB, IR, PSR	1729	1984 - 2011
gilb.za	2012	C, N, P, K, Zn, Fe, OM, C:N, N:P, AB, IR, PAR, PSR	563	1984 - 2012
glac.us	2007	C, N, P, K, Zn, Fe, OM, C:N, N:P, AB, LT, IR, PAR, PSR	1531	1984 - 2007
glacphr.us	2021	C, N, P, K, Zn, Fe, OM, C:N, N:P, AB, LT, IR, PAR, PSR	2793	1984 - 2021
hall.us	2011	C, N, P, K, Zn, Fe, OM, C:N, N:P, AB, IR, PAR, PSR	1166	1984 - 2011
hart.us	2011	C, N, P, K, Zn, Fe, OM, C:N, N:P, AB, LT, IR, PAR, PSR	2468	1984 - 2011
hnvr.us	2007	C, N, P, K, Zn, Fe, OM, C:N, N:P, AB, LT, IR, PAR, PSR	513	1984 - 2007
hogtwo.us	2017	C, N, P, K, Zn, Fe, OM, C:N, N:P, PSR	887	1984 - 2017
hopl.us	2019	C, N, P, K, Zn, Fe, OM, C:N, N:P, AB, LT, IR, PAR, PSR	1746	1984 - 2019
jena.de	2014	C, N, P, K, Zn, Fe, OM, C:N, N:P, AB, LT, IR, PAR, PSR	1335	1984 - 2014
jorn.us	2013	C, N, P, K, Zn, Fe, OM, C:N, N:P, AB, IR, PAR, PSR	1623	1984 - 2013
kbs.us	2016	C, N, P, K, Zn, Fe, OM, C:N, N:P, AB, LT, IR, PAR, PSR	1828	1984 - 2016

kilp.fi	2016	C, N, P, K, Zn, Fe, OM, C:N, N:P, AB, LT, IR, PAR, PSR	1238	1984 - 2016
kiny.au	2007	C, N, P, K, Zn, Fe, OM, C:N, N:P, AB, LT, IR, PAR, PSR	848	1986 - 2007
koffler.ca	2013	C, N, P, K, Zn, Fe, OM, C:N, N:P, AB, LT, IR, PAR, PSR	1941	1984 - 2013
konz.us	2011	C, N, P, K, Zn, Fe, OM, C:N, N:P, AB, IR, PSR	664	1984 - 2011
lake.us	2015	C, N, P, K, Zn, Fe, OM, C:N, N:P, AB, LT, IR, PAR, PSR	979	1984 - 2015
lancaster.uk	2016	C, N, P, K, Zn, Fe, OM, C:N, N:P, AB, LT, IR, PAR, PSR	2755	1984 - 2016
lead.us	2007	C, N, P, K, Zn, Fe, OM, C:N, N:P, AB, LT, IR, PAR, PSR	688	1984 - 2007
look.us	2016	C, N, P, K, Zn, Fe, OM, C:N, N:P, AB, LT, IR, PAR, PSR	3797	1984 - 2016
lubb.us	2018	C, N, P, K, Zn, Fe, OM, C:N, N:P, AB, LT, IR, PAR, PSR	898	1984 - 2018
marcel.us	2021	C, N, P, K, Zn, Fe, OM, C:N, N:P, AB, LT, IR, PAR, PSR	1927	1984 - 2021
mcdan.us	2018	C, N, P, K, Zn, Fe, OM, C:N, N:P, AB, LT, IR, PAR, PSR	894	1984 - 2018
mcla.us	2019	C, N, P, K, Zn, Fe, OM, C:N, N:P, AB, LT, IR, PAR, PSR	3295	1984 - 2019
meto.us	2017	C, N, P, K, Zn, Fe, OM, C:N, N:P, PSR	887	1984 - 2017
mrapids.us	2021	C, N, P, K, Zn, Fe, OM, C:N, N:P, AB, LT, IR, PAR, PSR	1433	1984 - 2021
msla.us	2021	C, N, P, K, Zn, Fe, OM, C:N, N:P, AB, LT, IR, PAR, PSR	5449	1984 - 2021
msum.us	2016	C, N, P, K, Zn, Fe, OM, C:N, N:P, AB, LT, IR, PAR, PSR	2157	1984 - 2016
mtca.au	2011	C, N, P, K, Zn, Fe, OM, C:N, N:P, AB, IR, PAR, PSR	686	1984 - 2011
nilla.au	2019	C, N, P, K, Zn, Fe, OM, C:N, N:P, AB, LT, IR, PAR, PSR	1720	1987 - 2019
pape.de	2007	C, N, P, K, Zn, Fe, OM, C:N, N:P, AB, LT, IR, PAR, PSR	581	1984 - 2007
ping.au	2013	C, N, P, K, Zn, Fe, OM, C:N, N:P, AB, LT, IR, PAR, PSR	1737	1986 - 2013
pinj.au	2016	C, N, P, K, Zn, Fe, OM, C:N, N:P, AB, LT, IR, PAR, PSR	1365	1987 - 2016
potrok.ar	2015	C, N, P, K, Zn, Fe, OM, C:N, N:P, AB, LT, IR, PAR, PSR	1547	1986 - 2021
saana.fi	2014	C, N, P, K, Zn, Fe, OM, C:N, N:P, AB, LT, IR, PAR, PSR	1536	1984 - 2017
sage.us	2011	C, N, P, K, Zn, Fe, OM, C:N, N:P, AB, LT, IR, PAR, PSR	1342	1984 - 2011
sandhill.us	2019	C, N, P, K, Zn, Fe, OM, C:N, N:P, AB, LT, IR, PAR, PSR	993	1984 - 2019
sava.us	2007	C, N, P, K, Zn, Fe, OM, C:N, N:P, AB, LT, IR, PAR, PSR	576	1984 - 2007
sedg.us	2007	C, N, P, K, Zn, Fe, OM, C:N, N:P, AB, LT, IR, PAR, PSR	598	1984 - 2007
sereng.tz	2008	C, N, P, K, Zn, Fe, OM, C:N, N:P, AB, LT, IR, PAR, PSR	309	1984 - 2008
sevi.us	2007	C, N, P, K, Zn, Fe, OM, C:N, N:P, AB, IR, PAR, PSR	1155	1984 - 2007
sgs.us	2011	C, N, P, K, Zn, Fe, OM, C:N, N:P, AB, LT, IR, PAR, PSR	2526	1984 - 2011
shps.us	2016	C, N, P, K, Zn, Fe, OM, C:N, N:P, IR, PAR, PSR	2230	1984 - 2016
sier.us	2019	C, N, P, K, Zn, Fe, OM, C:N, N:P, AB, LT, IR, PAR, PSR	2324	1984 - 2019
smith.us	2016	C, N, P, K, Zn, Fe, OM, C:N, N:P, AB, LT, IR, PAR, PSR	2802	1984 - 2016
spin.us	2016	C, N, P, K, Zn, Fe, OM, C:N, N:P, AB, IR, PAR, PSR	3760	1984 - 2016
summ.za	2012	C, N, P, K, Zn, Fe, OM, C:N, N:P, AB, IR, PAR, PSR	591	1984 - 2012
sval.no	2016	C, N, P, K, Zn, Fe, OM, C:N, N:P, AB, LT, IR, PAR, PSR	281	1985 - 2016
temple.us	2007	C, N, P, K, Zn, Fe, OM, C:N, N:P, AB, IR, PAR, PSR	1037	1984 - 2007
thth.is	2016	C, N, P, K, Zn, Fe, OM, C:N, N:P, AB, LT, IR, PSR	486	1984 - 2016
tmlr.is	2016	C, N, P, K, Zn, Fe, OM, C:N, N:P, AB, IR, PSR	488	1984 - 2016
trel.us	2011	C, N, P, K, Zn, Fe, OM, C:N, N:P, AB, LT, IR, PAR, PSR	1193	1984 - 2011
tyso.us	2007	C, N, P, K, Zn, Fe, OM, C:N, N:P, AB, LT, IR, PAR, PSR	538	1984 - 2007
ufrec.us	2013	C, N, P, K, Zn, Fe, OM, C:N, N:P, AB, LT, IR, PSR	808	1984 - 2013
ukul.za	2012	C, N, P, K, Zn, Fe, OM, C:N, N:P, AB, IR, PAR, PSR	298	1984 - 2012
unc.us	2011	C, N, P, K, Zn, Fe, OM, C:N, N:P, AB, LT, IR, PAR, PSR	1244	1984 - 2011
valm.ch	2016	C, N, P, K, Zn, Fe, OM, C:N, N:P, AB, LT, IR, PAR, PSR	3863	1984 - 2016
vargrass.no	2018	C, N, P, K, Zn, Fe, OM, C:N, N:P, AB, IR, PAR, PSR	1092	1984 - 2018
veluwe.nl	2017	C, N, P, K, Zn, Fe, OM, C:N, N:P, AB, LT, IR, PAR, PSR	1044	1984 - 2017
yarra.au	2021	C, N, P, K, Zn, Fe, OM, C:N, N:P, AB, IR, PAR, PSR	3314	1987 - 2021

APPENDIX B

Pearson's correlations between individual ecosystem properties and satellite NDVI phenometrics averaged over 3-30 year timeseries.

ecosystem property	metric	result	3-year	6-year	9-year	12-year	15-year	18-year	21-year	24-year	27-year	30-year
biomass_mean	auc	R	0.451	0.489	0.459	0.464	0.460	0.460	0.423	0.422	0.421	0.421
biomass_mean	auc	p	0.000	0.000	0.000	0.000	0.000	0.000	0.000	0.000	0.000	0.000
biomass_mean	cv	R	0.181	0.113	0.120	0.104	0.071	0.057	0.079	0.074	0.070	0.076
biomass_mean	cv	p	0.109	0.314	0.285	0.357	0.522	0.609	0.476	0.504	0.524	0.491
biomass_mean	dec	R	0.415	0.356	0.361	0.332	0.262	0.292	0.290	0.296	0.301	0.308
biomass_mean	dec	p	0.000	0.001	0.001	0.002	0.017	0.007	0.008	0.006	0.005	0.004
biomass_mean	inc	R	0.466	0.333	0.352	0.324	0.352	0.308	0.311	0.306	0.298	0.306
biomass_mean	inc	p	0.000	0.002	0.001	0.003	0.001	0.005	0.004	0.005	0.006	0.005
biomass_mean	len	R	0.172	0.211	0.186	0.219	0.303	0.301	0.262	0.273	0.268	0.273
biomass_mean	len	p	0.128	0.058	0.096	0.049	0.005	0.006	0.016	0.012	0.014	0.012
biomass_mean	max	R	0.498	0.498	0.479	0.465	0.428	0.436	0.425	0.418	0.422	0.422
biomass_mean	max	p	0.000	0.000	0.000	0.000	0.000	0.000	0.000	0.000	0.000	0.000
biomass_mean	mean	R	0.418	0.461	0.447	0.444	0.424	0.428	0.385	0.388	0.391	0.391
biomass_mean	mean	p	0.000	0.000	0.000	0.000	0.000	0.000	0.000	0.000	0.000	0.000
CN_ratio_mean	auc	R	0.111	0.124	0.148	0.143	0.130	0.137	0.167	0.157	0.150	0.149
CN_ratio_mean	auc	p	0.320	0.261	0.179	0.195	0.232	0.209	0.121	0.147	0.165	0.168
CN_ratio_mean	cv	R	-0.175	-0.132	-0.059	-0.044	-0.059	-0.049	-0.090	-0.083	-0.074	-0.066
CN_ratio_mean	cv	p	0.115	0.230	0.591	0.690	0.589	0.657	0.409	0.445	0.496	0.542
CN_ratio_mean	dec	R	-0.024	-0.008	0.012	0.029	0.029	0.047	0.030	0.048	0.051	0.063
CN_ratio_mean	dec	p	0.830	0.939	0.911	0.794	0.789	0.666	0.785	0.657	0.641	0.561
CN_ratio_mean	inc	R	-0.092	-0.071	-0.010	-0.010	0.005	0.014	-0.013	-0.003	0.006	0.008
CN_ratio_mean	inc	p	0.409	0.524	0.925	0.926	0.961	0.895	0.905	0.977	0.953	0.940
CN_ratio_mean	len	R	0.041	0.073	0.104	0.131	0.082	0.100	0.117	0.096	0.085	0.086

CN_ratio_mean	len	p	0.714	0.508	0.346	0.236	0.453	0.357	0.280	0.378	0.432	0.429
CN_ratio_mean	max	R	0.115	0.117	0.132	0.120	0.135	0.135	0.146	0.151	0.145	0.149
CN_ratio_mean	max	p	0.302	0.288	0.231	0.275	0.214	0.215	0.178	0.162	0.179	0.167
CN_ratio_mean	mean	R	0.241	0.213	0.194	0.180	0.182	0.175	0.216	0.209	0.201	0.197
CN_ratio_mean	mean	p	0.029	0.052	0.077	0.101	0.094	0.108	0.044	0.052	0.062	0.067
inv_res_mean	auc	R	-0.137	-0.164	-0.161	-0.174	-0.121	-0.130	-0.133	-0.137	-0.142	-0.141
inv_res_mean	auc	p	0.224	0.142	0.149	0.117	0.272	0.238	0.225	0.210	0.196	0.197
inv_res_mean	cv	R	0.230	0.211	0.232	0.215	0.170	0.152	0.133	0.121	0.119	0.106
inv_res_mean	cv	p	0.039	0.057	0.036	0.052	0.121	0.169	0.224	0.269	0.278	0.333
inv_res_mean	dec	R	0.016	-0.032	0.001	0.006	-0.027	-0.030	-0.027	-0.035	-0.023	-0.029
inv_res_mean	dec	p	0.891	0.778	0.995	0.955	0.807	0.786	0.807	0.754	0.837	0.792
inv_res_mean	inc	R	0.087	0.036	0.036	0.000	0.009	-0.022	-0.036	-0.039	-0.035	-0.038
inv_res_mean	inc	p	0.442	0.749	0.748	0.998	0.937	0.842	0.741	0.722	0.751	0.727
inv_res_mean	len	R	-0.030	-0.026	-0.031	-0.050	-0.003	-0.041	-0.048	-0.070	-0.093	-0.095
inv_res_mean	len	p	0.792	0.818	0.781	0.654	0.980	0.712	0.660	0.524	0.397	0.386
inv_res_mean	max	R	-0.114	-0.180	-0.178	-0.182	-0.165	-0.157	-0.157	-0.152	-0.146	-0.143
inv_res_mean	max	p	0.311	0.106	0.110	0.101	0.134	0.154	0.152	0.166	0.184	0.191
inv_res_mean	mean	R	-0.232	-0.246	-0.269	-0.280	-0.222	-0.223	-0.211	-0.202	-0.196	-0.193
inv_res_mean	mean	p	0.037	0.026	0.015	0.011	0.042	0.041	0.052	0.064	0.072	0.077
litter_turn_mean	auc	R	-0.003	0.022	0.029	0.065	0.048	0.059	0.021	0.011	0.002	0.006
litter_turn_mean	auc	p	0.984	0.862	0.818	0.606	0.701	0.640	0.863	0.928	0.986	0.961
litter_turn_mean	cv	R	-0.051	-0.035	-0.023	-0.032	-0.050	-0.043	0.006	0.012	0.018	0.002
litter_turn_mean	cv	p	0.685	0.782	0.857	0.803	0.690	0.733	0.960	0.925	0.883	0.988
litter_turn_mean	dec	R	0.180	0.107	0.078	0.023	0.012	-0.001	0.003	0.012	0.058	0.061
litter_turn_mean	dec	p	0.152	0.395	0.537	0.857	0.925	0.995	0.983	0.922	0.641	0.625
litter_turn_mean	inc	R	-0.035	-0.111	-0.057	-0.050	-0.032	-0.030	0.013	0.014	0.032	0.034
litter_turn_mean	inc	p	0.785	0.378	0.652	0.690	0.796	0.812	0.917	0.912	0.794	0.787
litter_turn_mean	len	R	-0.119	-0.055	-0.058	0.023	-0.007	0.044	0.022	0.000	-0.012	0.003
litter_turn_mean	len	p	0.344	0.666	0.646	0.854	0.954	0.723	0.862	0.998	0.924	0.979
litter_turn_mean	max	R	0.080	0.069	0.078	0.070	0.063	0.051	0.039	0.030	0.024	0.017

litter_turn_mean	max	p	0.526	0.585	0.535	0.579	0.613	0.682	0.753	0.808	0.845	0.888
litter_turn_mean	mean	R	0.095	0.094	0.090	0.085	0.067	0.059	0.010	0.003	-0.010	-0.006
litter_turn_mean	mean	p	0.452	0.455	0.476	0.500	0.596	0.638	0.936	0.978	0.938	0.961
NP_ratio_mean	auc	R	0.027	0.085	0.090	0.096	0.218	0.225	0.216	0.220	0.218	0.235
NP_ratio_mean	auc	p	0.812	0.440	0.416	0.387	0.044	0.038	0.044	0.041	0.042	0.029
NP_ratio_mean	cv	R	0.094	0.090	0.106	0.088	-0.026	-0.021	-0.010	-0.005	0.008	-0.005
NP_ratio_mean	cv	p	0.402	0.416	0.335	0.429	0.815	0.849	0.927	0.964	0.939	0.966
NP_ratio_mean	dec	R	0.128	0.067	0.152	0.122	0.004	0.007	0.020	0.026	0.053	0.047
NP_ratio_mean	dec	p	0.251	0.546	0.168	0.268	0.968	0.952	0.855	0.809	0.626	0.668
NP_ratio_mean	inc	R	0.044	0.055	0.090	0.069	0.042	0.035	0.039	0.051	0.063	0.079
NP_ratio_mean	inc	p	0.696	0.617	0.417	0.531	0.699	0.750	0.720	0.642	0.561	0.467
NP_ratio_mean	len	R	0.051	0.121	0.105	0.145	0.210	0.213	0.200	0.192	0.176	0.196
NP_ratio_mean	len	p	0.648	0.273	0.344	0.189	0.053	0.049	0.063	0.075	0.102	0.069
NP_ratio_mean	max	R	0.055	0.070	0.088	0.085	0.150	0.164	0.162	0.169	0.178	0.185
NP_ratio_mean	max	p	0.625	0.525	0.428	0.444	0.168	0.132	0.133	0.118	0.099	0.086
NP_ratio_mean	mean	R	-0.003	0.052	0.041	0.029	0.163	0.171	0.156	0.161	0.160	0.175
NP_ratio_mean	mean	p	0.979	0.641	0.709	0.794	0.134	0.116	0.150	0.137	0.140	0.105
OM_mean	auc	R	0.235	0.240	0.210	0.241	0.273	0.289	0.263	0.268	0.264	0.266
OM_mean	auc	p	0.033	0.028	0.056	0.028	0.011	0.007	0.014	0.012	0.013	0.013
OM_mean	cv	R	0.017	0.122	0.212	0.243	0.200	0.206	0.220	0.223	0.228	0.227
OM_mean	cv	p	0.876	0.269	0.053	0.026	0.065	0.057	0.041	0.038	0.034	0.035
OM_mean	dec	R	0.190	0.313	0.384	0.384	0.303	0.314	0.309	0.302	0.325	0.321
OM_mean	dec	p	0.087	0.004	0.000	0.000	0.005	0.003	0.004	0.004	0.002	0.002
OM_mean	inc	R	0.072	0.182	0.248	0.287	0.292	0.287	0.302	0.310	0.319	0.323
OM_mean	inc	p	0.521	0.097	0.023	0.008	0.006	0.007	0.004	0.004	0.003	0.002
OM_mean	len	R	0.128	0.138	0.115	0.144	0.213	0.215	0.184	0.198	0.182	0.192
OM_mean	len	p	0.253	0.211	0.297	0.192	0.049	0.047	0.088	0.066	0.092	0.075
OM_mean	max	R	0.262	0.281	0.289	0.305	0.304	0.317	0.308	0.304	0.309	0.307
OM_mean	max	p	0.018	0.010	0.008	0.005	0.004	0.003	0.004	0.004	0.004	0.004
OM_mean	mean	R	0.265	0.255	0.211	0.203	0.219	0.226	0.196	0.196	0.197	0.194

OM_mean	mean	p	0.016	0.019	0.055	0.063	0.043	0.036	0.069	0.068	0.068	0.072
pct_C_mean	auc	R	0.279	0.273	0.238	0.254	0.272	0.290	0.272	0.275	0.275	0.275
pct_C_mean	auc	p	0.011	0.012	0.029	0.020	0.011	0.007	0.011	0.010	0.010	0.010
pct_C_mean	cv	R	0.113	0.162	0.250	0.266	0.226	0.232	0.253	0.248	0.253	0.254
pct_C_mean	cv	p	0.313	0.140	0.022	0.014	0.036	0.032	0.018	0.020	0.018	0.018
pct_C_mean	dec	R	0.185	0.283	0.360	0.348	0.269	0.265	0.262	0.256	0.269	0.264
pct_C_mean	dec	p	0.095	0.009	0.001	0.001	0.012	0.014	0.014	0.017	0.012	0.014
pct_C_mean	inc	R	0.215	0.283	0.304	0.317	0.332	0.339	0.360	0.355	0.359	0.364
pct_C_mean	inc	p	0.053	0.009	0.005	0.003	0.002	0.001	0.001	0.001	0.001	0.001
pct_C_mean	len	R	0.206	0.187	0.158	0.168	0.212	0.234	0.220	0.232	0.227	0.231
pct_C_mean	len	p	0.063	0.089	0.150	0.128	0.050	0.030	0.041	0.030	0.035	0.031
pct_C_mean	max	R	0.287	0.299	0.306	0.315	0.313	0.322	0.314	0.309	0.312	0.311
pct_C_mean	max	p	0.009	0.006	0.005	0.004	0.003	0.002	0.003	0.004	0.003	0.003
pct_C_mean	mean	R	0.260	0.260	0.218	0.213	0.222	0.229	0.196	0.199	0.199	0.198
pct_C_mean	mean	p	0.018	0.017	0.046	0.052	0.040	0.034	0.069	0.065	0.064	0.067
pct_N_mean	auc	R	0.309	0.296	0.259	0.271	0.283	0.295	0.270	0.274	0.276	0.275
pct_N_mean	auc	p	0.005	0.006	0.017	0.013	0.008	0.006	0.012	0.010	0.010	0.010
pct_N_mean	cv	R	0.177	0.227	0.291	0.304	0.262	0.267	0.286	0.281	0.282	0.287
pct_N_mean	cv	p	0.112	0.037	0.007	0.005	0.015	0.013	0.007	0.008	0.008	0.007
pct_N_mean	dec	R	0.234	0.332	0.381	0.375	0.299	0.301	0.300	0.289	0.295	0.288
pct_N_mean	dec	p	0.034	0.002	0.000	0.000	0.005	0.005	0.005	0.007	0.006	0.007
pct_N_mean	inc	R	0.272	0.353	0.359	0.358	0.365	0.373	0.390	0.384	0.383	0.392
pct_N_mean	inc	p	0.013	0.001	0.001	0.001	0.001	0.000	0.000	0.000	0.000	0.000
pct_N_mean	len	R	0.209	0.190	0.166	0.172	0.230	0.236	0.210	0.227	0.225	0.226
pct_N_mean	len	p	0.059	0.083	0.132	0.118	0.033	0.029	0.051	0.034	0.036	0.035
pct_N_mean	max	R	0.324	0.334	0.329	0.333	0.320	0.333	0.324	0.318	0.322	0.321
pct_N_mean	max	p	0.003	0.002	0.002	0.002	0.003	0.002	0.002	0.003	0.002	0.002
pct_N_mean	mean	R	0.267	0.256	0.220	0.214	0.218	0.225	0.190	0.194	0.197	0.194
pct_N_mean	mean	p	0.015	0.019	0.044	0.050	0.044	0.037	0.078	0.072	0.068	0.071
ppm_Fe_mean	auc	R	-0.063	-0.040	-0.028	-0.018	-0.044	-0.044	-0.065	-0.061	-0.064	-0.065

ppm_Fe_mean	auc	p	0.574	0.721	0.802	0.872	0.687	0.688	0.552	0.577	0.557	0.551
ppm_Fe_mean	cv	R	0.089	0.052	0.071	0.112	0.151	0.163	0.190	0.202	0.205	0.205
ppm_Fe_mean	cv	p	0.429	0.636	0.520	0.311	0.166	0.134	0.078	0.061	0.057	0.056
ppm_Fe_mean	dec	R	0.041	0.016	-0.003	0.018	0.034	0.037	0.054	0.069	0.084	0.096
ppm_Fe_mean	dec	p	0.716	0.888	0.976	0.874	0.753	0.736	0.619	0.525	0.439	0.377
ppm_Fe_mean	inc	R	0.024	-0.009	0.020	0.033	0.076	0.081	0.128	0.147	0.152	0.148
ppm_Fe_mean	inc	p	0.829	0.938	0.858	0.764	0.485	0.457	0.236	0.173	0.161	0.172
ppm_Fe_mean	len	R	-0.117	-0.062	-0.018	-0.003	-0.024	-0.038	-0.076	-0.074	-0.078	-0.076
ppm_Fe_mean	len	p	0.295	0.574	0.874	0.976	0.829	0.726	0.482	0.499	0.473	0.484
ppm_Fe_mean	max	R	0.056	0.042	0.036	0.033	0.022	0.024	0.021	0.025	0.023	0.018
ppm_Fe_mean	max	p	0.619	0.707	0.744	0.763	0.839	0.827	0.848	0.818	0.830	0.868
ppm_Fe_mean	mean	R	-0.014	0.007	0.003	-0.006	-0.039	-0.046	-0.075	-0.076	-0.081	-0.082
ppm_Fe_mean	mean	p	0.904	0.947	0.979	0.954	0.724	0.674	0.493	0.483	0.455	0.452
ppm_K_mean	auc	R	-0.153	-0.135	-0.130	-0.136	-0.133	-0.152	-0.175	-0.173	-0.168	-0.175
ppm_K_mean	auc	p	0.170	0.220	0.238	0.218	0.224	0.163	0.105	0.109	0.120	0.105
ppm_K_mean	cv	R	0.043	-0.011	-0.032	-0.023	-0.008	-0.004	0.012	0.009	0.005	0.012
ppm_K_mean	cv	p	0.699	0.917	0.776	0.835	0.939	0.968	0.916	0.936	0.964	0.912
ppm_K_mean	dec	R	-0.001	0.011	-0.023	-0.043	-0.058	-0.068	-0.047	-0.063	-0.075	-0.075
ppm_K_mean	dec	p	0.991	0.919	0.833	0.696	0.596	0.533	0.669	0.561	0.488	0.487
ppm_K_mean	inc	R	0.037	-0.008	-0.075	-0.087	-0.066	-0.067	-0.050	-0.048	-0.058	-0.055
ppm_K_mean	inc	p	0.739	0.941	0.498	0.434	0.548	0.541	0.642	0.657	0.595	0.614
ppm_K_mean	len	R	-0.141	-0.121	-0.067	-0.078	-0.039	-0.090	-0.128	-0.114	-0.105	-0.118
ppm_K_mean	len	p	0.207	0.272	0.543	0.480	0.721	0.409	0.237	0.293	0.332	0.278
ppm_K_mean	max	R	-0.140	-0.155	-0.166	-0.162	-0.182	-0.175	-0.171	-0.176	-0.176	-0.175
ppm_K_mean	max	p	0.211	0.160	0.132	0.141	0.094	0.108	0.114	0.103	0.104	0.106
ppm_K_mean	mean	R	-0.177	-0.169	-0.170	-0.172	-0.174	-0.181	-0.193	-0.196	-0.191	-0.196
ppm_K_mean	mean	p	0.113	0.125	0.122	0.117	0.110	0.095	0.073	0.069	0.076	0.069
ppm_P_mean	auc	R	0.280	0.298	0.301	0.293	0.218	0.218	0.209	0.200	0.195	0.185
ppm_P_mean	auc	p	0.011	0.006	0.005	0.007	0.044	0.044	0.052	0.063	0.070	0.086
ppm_P_mean	cv	R	-0.105	-0.090	-0.036	-0.031	0.005	0.014	0.016	0.020	0.014	0.035

ppm_P_mean	cv	p	0.349	0.415	0.745	0.778	0.965	0.900	0.881	0.856	0.898	0.748
ppm_P_mean	dec	R	0.019	0.062	0.059	0.110	0.139	0.163	0.162	0.162	0.148	0.154
ppm_P_mean	dec	p	0.867	0.573	0.593	0.321	0.203	0.134	0.134	0.134	0.173	0.156